ISSN 0915-6348

NATIONAL INSTITUTE FOR FUSION SCIENCE

Proceedings of the Symposium on Cryogenic Systems for Large Scale Superconducting Applications

May 27 - 29, 1996
Ceratopia - Toki and NIFS
Toki, Japan

T. Mito (Ed.)

(Received - Sep. 2, 1996)

NIFS-PROC-28 Sep. 1996

RESEARCH REPORT
NIFS-PROC Series

NAGOYA, JAPAN

Proceedings of the Symposium on Cryogenic Systems for Large Scale Superconducting Applications

Edited by Toshiyuki Mito

May 27-29, 1996
Ceratopia-Toki and NIFS
Toki, Japan

Supported by NIFS Symposium
and JSPS-DFG Seminar

Keywords; Cryogenic system, Superconducting Application,
Large Helical Device, Fusion Device,
High Energy Physics

A commemorative Photo of participants on the Symposium
at the evening of the first day (May 27, 1996).

Organizers

Chairman

Junya Yamamoto (NIFS)

Members

Sadao Satoh (NIFS) Toshiyuki Mito (NIFS) Peter Komarek (FZK)

Collaborating Staffs

T. Baba
H. Chikaraishi
M. Iima
S. Imagawa
A. Iwamoto
S. Kato
Y. Kato
R. Maekawa
S. Moriuchi
A. Nishimura
K. Ohba
H. Sekiguchi
M. Shoji
K. Sugiyama
K. Takahata
H. Tamura
S. Yamada
N. Yanagi

PREFACE

It was twenty years ago that a high field superconducting magnet using a novel pressurized superfluid helium cryostat was dramatically reported by a cryogenics group of CEN Grenoble at the Sixth International Cryogenic Engineering Conference in Grenoble, France. This research report verified that cryogenic systems were the key technology for the improvement of the applied superconductivity.

In these twenty years, along with material development and innovation of machine operation engineering, a lot of new technologies in the field of cryogenic engineering had been developed. In the field of fusion research, high energy particle physics and space physics, long time operation of cryogenic system have been achieved. In accordance with the recent high performance of superconductivity and the tendency of research orientation to unreachable parameter region, quite a few big projects using superconductivity have been undertaking.

NIFS symposium "Cryogenic Systems for Large Scale Superconducting Application" was planned to present operation experience of existing apparatus, to show the planning of projects which involve the construction of the cryogenic system for superconducting applications and to give new information of superfluid helium technology, with the limited number of specialist of the field. The symposium was held in Toki-city, where the NIFS (National Institute for Fusion Science) is located, from May 27 to 29, 1996, just after the 16th International Cryogenic Engineering Conference. It was financially supported by NIFS and the Japanese-German Cooperative Science Promotion Program (Japan side sponsor organization is Japan Society for the Promotion of Science - JSPS and Germany side is Deutsche Forschungsgemeinschaft - DFG). Total number of attendants was 97.

The program of the Symposium was composed of 33 oral presentations and 14 poster presentations. The oral presentation was classified into (1)Cryogenic Systems for Experimental Fusion Devices, (2)Test Facilities for Large Scale Superconducting Application, (3)Large Scale Cryogenic System for High Energy Physics, (4)Cryogenic Systems for Large Scale Superconducting Applications, (5)Large Helical Device, (6)Operation Experiences and Research Works on Large Scale Cryogenic Systems, (7)Design and Numerical Simulation of Cryogenic Systems. Details of the Large Helical Device (LHD) was mostly presented in poster sessions at NIFS Main Hall, together with the site tour in NIFS.

Since the Symposium was a single session type and limited in cryogenic systems, we could make the discussion deeper and more fruitful than in large conference. As a symposium planner, I would like to extend my hearty appreciation to all speakers, audience, NIFS staffs, JSPS and DFG.

Junya Yamamoto,
Symposium chairman

Contents

Cryogenic Systems for Large Scale Superconducting Applications (NIFS symposium and JSPS-DFG Seminar)

1. Cryogenic Systems for Experimental Fusion Devices.

2. Test Facilities for Large Scale Superconducting Application.

3. Large Scale Cryogenic System for High Energy Physics.

4a. Cryogenic Systems for Large Scale Superconducting Applications (I).

4b. Cryogenic Systems for Large Scale Superconducting Applications (II).

4c. Cryogenic Systems for Large Scale Superconducting Applications (III).

5. Large Helical Device (LHD).

LHD Poster Sessions at the LHD Experimental Building.

6. Operation Experiences and Research Works on Large Scale Cryogenic Systems.

7. Design and Numerical Simulation of Cryogenic Systems.

Cryogenic Systems for Large Scale Superconducting Applications
(NIFS symposium and JSPS-DFG Seminar)

May 27, 1996		*May 28, 1996*		*May 29, 1996*	
9:00	*Registration*	9:00	4a.Cryogenic Systems for Large Scale Superconducting Applications (I).	9:00	6. Operation Experiences and Research Works on Large Cryogenic Systems.
10:00	1. Cyogenic Systems for Experimental Fusion Devices.	10:30	*Coffee break*	10:55	*Coffee break*
		10:45	4b.Cryogenic Systems for Large Scale Superconducting Applications (II).	11:10	7. Design and Numerical Simulation of Cryogenic Systems.
12:15	*Lunch*	12:15	*Lunch*	13:05	
13:30	2. Test Facilities for Large Scale Superconducting Application.	13:30	4c.Cryogenic Systems for Large Scale Superconducting Applications (III).		
15:30	*Coffee break*	15:00	*Coffee break*		
15:45	3 Large Scale Cryogenic System for High Energy Physics.	15:10	5. Large Helical Device (LHD).		
		16:00	*Transfer from Ceratopia-Toki to NIFS*		
		16:30	LHD Poster Session at NIFS and Tour on the LHD Experimental Building.		
18:15		18:00			
18:30	*The Enkai (Party)*				
20:30					

May 27-29, 1996
Ceratopia-Toki and NIFS
Toki, Japan

Cryogenics in the Large Helical Device

Junya Yamamoto

National Institute for Fusion Science
Oroshi, Toki-shi, Gifu 509-52, Japan

Cryogenics is a key technology for Large Helical Device which composed of superconducting system working at liquid helium temperatures. Estimation of cryogenic mass and heat load is the first step of the cryogenic system. Operating schedule for long term and system design are the important engineering issues in reliable performance. Main R&D, design, and manufacturing process are reported in this "NIFS Symposium on Cryogenic System of Large Scale Superconducting Applications."

1. INTRODUCTION

National Institute for Fusion Science (NIFS) is under constructing the Large Helical Device (LHD) in Toki city, Gifu Prefecture, where is at the geographical center of Japan, about 40 km east of Nagoya City. LHD is the world largest superconducting coils in scale, stored energy, and current.

LHD of NIFS is the world largest superconducting coil system in those which was produced and will be complete in 20 th century. LHD is strongly governed its performance by cryogenics, because the reliability and stability of LTS superconducting properties are dependent on the temperature and its distribution. From the cryogenics side, the LHD is important application and the object of the usefulness of the cryogenics.

This article covers the following scopes. (1) Outline of design and important roles of cryogenic engineering in LHD. (2) Construction schedule of the LHD. (3) Operation schedule of the LHD. (4) Engineering subjects of cryogenics including future improvements. (5) Construction of cryogenics parts of the LHD. (6) Presentation of the LHD in this symposium.

2. OUTLINE OF LHD

The Large Helical Device (LHD) is the first fully superconducting fusion plasma device which strongly depends on superconducting and cryogenic engineering, not only superconducting coils, but also bus lines, mechanical structure materials, a large scale cryogenic helium technology, and so on. Static magnetic field will develop the continuous fusion plasma research. The design basis of the LHD superconducting system is to get high reliability in a long term operation as a fusion plasma devise, however any parts are the first experience in superconducting and cryogenic engineering.

Magnetic field confinement of plasma is done by the helical coil of R=3.9m, r=0.975m, m=10 and l=2. The toroidal field in plasma is 3 T at phase I, and 4 T at phase II. The field is modulated in position and in time by 3 pairs of poloidal coils. Total cryogenic mass is about 850 tons and is mechanically supported by 10 adiabatic legs.

The most of system of LHD is working at cryogenic temperature, so the design in a refrigerator, a coolant distribution control, thermal insulation, and cryogenic stability of superconductor have been important design areas. Materials and structure analysis applicable to electro-magnetic force and thermal stress in LHD have been important design items.

2.1 Helical Coil

The helical coil are fully stabilized pool cooled superconducting coil. The specifications of the coil are tabulated in Table 1. The conductors are not able to withstand the large electromagnetic force by themselves, they are designed to be packed into a thick case (helical-coil can) which is used as a bath for liquid helium and a bobbin for winding. The conductors are directly wound on the can by 450 turns per coil, and the total length was about 36 km. Electrical insulators between conductors are G-FRP and liquid helium.

Table 1 Major parameters of helical coil

Items	Phase I	Phase II
Electromotive force (MA)	5.85	7.8
Coil current density (A/mm2)	40	53
Current (kA)	13.0	17.3
Turn number	450 (150 x 3)	
Maximum field in coil (T)	6.9	9.2
Magnetic stored energy (GJ)	0.92	1.64
Coil temperature (K)	4.4	1.8
Spacer factor (%)	30 -70	
Spacer pitch (mm)	49.2 -64.3	

2.2. Poloidal Coils

There are three pairs of superconducting poloidal coils, that is the inner vertical (IV), the inner shaping (IS), and the outer vertical (OV), which modify the magnetic field. All coils are using a supercritical helium cooled NbTi cable-in-conduit conductors. They are set in the supporting structure to hold electro-magnetic force between coils, however no heat leak between them. Table 2 shows the specification of coils and conductors.

Each coil is composed from 8 double pancakes of a forced cooled conductor filled bare surface 486 (3x3x3x3x6) NbTi strands with 38% void ratio. In pancake manufacturing, pre-formed half of conductor, welding gas inlet port, lower pancake winding, insulation, upper pancake winding, and final insulation in a furnace. Eight pancakes were packed in a coil, superconducting electrical connection each other, and to mount mechanical sleeve.

Table 2. specifications of the poloidal coils

Items	IV	IS	OV
Electro magnetic force (MA)	5.0	-4.5	-4.5
Current radius (m)	1.6	2.8	5.55
Number of turns	15x16=240	13x16=208	9x16=144
Nominal current (kA)	20.8	21.6	31.3
Critical current (kA)	62.4 at 6.5T	64.8 at 5.4T	93.9 at 5.0T
Stored energy (MJ)	68	104	251
Maximum field (T)	6.5	5.4	5.0
Conductor length (km)	2.7	3.7	5.0
Number of flow path	16	16	16
Length of flow path (m)	170	230	314
Critical current (kA)	62.4 at 6.5T	64.8 at 5.4T	93.9 at 5.0T

Conduit dimension (mm)	23.0x27.6	23.0x27.6	27.5x31.8
Conduit thickness (mm)	3.0	3.0	3.5
Void fraction (%)	38	<-	<-

2.3. Superconducting Bus Line

Connecting superconducting coils and power supplies, nine flexible superconducting bus lines will be installed. No quench is allowed to discharge all energy from the coils, specification of the bus lines strongly emphasized in reliability. Helical coil feeders are 6 pairs corresponding 3 blocks in two coils, which is connected to 6 bus lines. On the others, poloidal coil feeders are connected in series of upper and lower coils at the same radial position to 3 bus lines.

Bus line conductor is composed of twisted nine aluminum stabilized NbTi conductors rated 32 kA. The maximum field in a conductor is observed near the LHD. This pair conductor is set in flexible five layers corrugated tube for cooling and insulation. The specification of the bus lines are shown in Table 5.

3. SCHEDULE OF LHD CRYOGENICS

After foundation of NIFS, LHD's superconducting and cryogenics R&D and real machine construction were done as following procedures.

1989 NIFS founded, R&D Superconductor and Coil, R&D Coil: Kyoto-SC Tested.

1990 LHD Project Started, Cryogenic and Superconductivity Laboratories Completed

1991 Applied Superconductivity and Cryogenic R&D Started, R&D Coils: Toki-MC, PF, HC Tested, Poloidal Coil Conductor Developed

1992 Helical Coil Conductor Developed

1993 Poloidal Coil (IV) Completed

1994 LHD Main Hall Completed, Helical Coil Winding Machine Completed, Lower Half of Cryostat and Supporting Structure Completed, Helium Liquefier/Refrigerator Installed

1995 Helical Coil Winding started, Poloidal Coil (IS) Completed, IV-L Coil Tested

1996 Poloidal Coil (OV) Winding Completed, Poloidal Coil (OV-L) Completed, Helical Coil Winding Completed, Liquefier/Refrigerator Test Operation with 1/3 Heat Load, Helical Coil will be Completed, Poloidal Coil (OV-U) will be Completed, Plasma Vacuum Vessel Construction

1997 Total Assembly of LHD

1998 Start Cooling the Device, The First Operation of the Coil System

4. MACHINE OPERATION

Yearly Schedule

Cooling LHD from the room to the operating temperature in 2 weeks.

Continuously 20 weeks in cryogenic temperature for operation.

Raise LHD temperatures to the room temperature within 2 weeks.

Summer Maintenance.

(Refrigerator, Valve Operation, Impurity Gas Filtering, Gas Leakage, Water Supply, Power Supply, Vacuum System, Control System, Coil Diagnostic's, Quench Discrimination Circuit, and Other Maintenance on Superconducting and Cryogenic Machines)

Cooling LHD from the room to the operating temperature in 2 weeks.
Continuously 20 weeks in cryogenic temperature for operation.
Raise LHD temperatures to the room temperature within 2 weeks.
Winter Maintenance.

(Quench Discrimination Circuit, Power Supply, Control System, Vacuum System, Impurity Gas Filtering and so on)

Weekly Schedule
Experiment from Monday to Friday.
Maintenance in Saturday and Sunday.

(Mostly Plasma Diagnostics and Plasma Heating)

Daily Schedule
Experiment from 9 a.m. to 7 p.m.
Charge Coils from 8 a.m., Discharge Coils until 8 p.m.
Maintenance from 8 p.m. to 8 a.m.

(Urgent Repairing)

5. CRYOGENIC SYSTEM DESIGN

In this chapter we summarize the cryogenics parts and requirements to get stable and reliable operation of the LHD.

5.1. Main Parts

5.1.1. Superconducting Helical Coil

Cryogenic stability is obtained by normal liquid He bath cooling method to make sure complex winding formula. Recovery current is enough larger than the operating current in case of mechanical disturbance due to conductor friction, however void ratio is around 18 % in a coil. Liquid helium entered from 5 bottom inlets of each coil, and gas exhausted from 5 outlets of each coil.

5.1.2. Superconducting Poloidal Coil

Supercritical Helium Forced Flow Cooling method is applied to the poloidal coil, due to assuring the electrical insulation and conductor toughness. However this is the first application of forced flow conductor, critical current is more than 3 times of operating current. The coil is cooled by 16 parallel channels of pancakes and sleeves

5.1.3. Superconducting Bus Line

Current feeder lines between power supplies and superconducting coils are connected by flexible paired superconducting bus lines, which is cooled by two phase normal liquid Helium forced flow. critical current is more than 5 times of operating current

5.1.4. Mechanical Supporting Structure

Mechanical structures supporting the electromagnetic force between 8 superconducting coils are made of stainless steel 316, and cooled by normal liquid Helium forced flow. The flow passage is welded on the surface of the structure. This structure is the most difficult one for initial cooling uniform in time and in space.

5.1.5. Radiation Shield

There are the inner radiation shield facing the plasma vacuum vessel at 400 K or more, and the outer radiation shield covering mechanical structure from room temperature radiation. Both shield plates are cooled around 80 K by cold helium gas.

5.1.6. Support Post

Total cryogenic weight is supported by 10 adiabatic post to the base plate of the LHD at 300 K. Active cooling at intermediate plates by cold helium gas around 80 K are achieved.

5.2. Engineering Subjects in LHD Cryogenics

5.2.1. Estimation of Heat Load in operation at Phase I

*To 80 K Shield Plate
Radiation from the Outer Cryostat
Radiation and Conduction from the Plasma Vacuum Vessel
Conduction through the support posts
*To 4.5 K
Radiation from the 80 K Shield Plate
Conduction through the support posts
*To Bus Line
80 K Load
4.5 K Load
*To Current Leads
Liquid He Consumption
*Heat Generation
Conductor Joints
AC Loss

5.2.2. Estimation of Refrigeration Power in Initial Cooling and Its Scenario

Total Heat Capacity to remove (Correspond to 850 tons)
Cooling Time (10 to 12 days)
Allowed Temperature Differences in the mass (50 K)

5.2.3. Impurity Gas Accumulation

Choking CIC Conductor and Piping (P.C.)
Decrease Cooling Surface and Electrical Insulation (H.C.)
Effective Means to Measure ppb Order Impurity
Development to Remove Accumulated Impurities

5.2.4. Fatigue in Welding Parts

Non Destructive Testing of Welding Parts
Remote Repairing in the Cryostat
Construction of Cooling System

5.2.5. Large Scale Refrigerator and Liquefier

5.65 W at 4.4 K, 20.6 kW at 80 K, and 650 L/h
7 Turbines in 2 Cold boxes (above 80 K and below 80 K)
No Liquid Nitrogen required without initial cooldown
8 Screw Compressors
800 m3 at 2 MPa Gas Storage
20000 L Liq. He Reservoir

5.2.6. Cryogenic Transfer Lines and Coolant Control Boxes

Transfer Lines between Cold Boxes, from Cold Box to Liq. He Dewar, Current Leads Cryostat, Helical Coil Valve Box, and Poloidal Coil Valve Box.

5.2.7. Handling of Helium Gas

No Leakage, and no Supply - Refrigerator Mode

5.2.8. Cryogenic System Control

Workstations, VME (Versa Module Europe), Operating Graphic Consoles

5.3. Improvement to Phase II

Specification of LHD is limited by financial reason. Therefore the project is divided to Phase I and II. After initial success of the LHD, we are planning to improve it to Phase II. The followings are its main scheme.

A. Increase Toroidal Field 3T to 4T

Operating Temperature of Helical Coils:

1.8 K (Pressurized He II)

Increase Refrigerator Power and Install HeII Control Box

Operating Temperature of Poloidal Coils:

4.5 K (Same as Phase I)

Use circulating pump

Decrease Temperature on the Inner Radiation Shield

(80 K to around 40 K)

B. Fast Field Change of Poloidal Coil

Increase Power Supply Capacity (high voltage required)

AC Loss in Supporting Structures

Increasing Cooling Capacity

AC Loss in Poloidal Coils

Increase Gas Flow Speed

C. Increase Plasma Heating Power

D. D - D Experiment

6. RELATED PRESENTATION ON LHD IN THE SYMPOSIUM

A. LHD Project

*Large Helical Device Project (O. Motojima)

*Present Status of LHD (T. Satow)

B. LHD Superconducting system

*Helical Coils for LHD (S. Imagawa)

*Quench Analysis of the Helical Coils for LHD (N. Yanagi)

*Poloidal Coils for LHD (K. Takahata)

*Superconducting Current Feeder System for LHD (S. Yamada)

C. Cryogenics and its control

*Cryogenic System for the Large Helical Device (T. Mito)

*Construction and Operation of a 10 kW Class Helium Refrigerator for LHD (S. Satoh)

*Cooling and Excitation Tests of a Single Inner Vertical Poloidal Coil - EXSIV (K. Takahata)

*Design and Experiments on Component Hardware's for LHD Cryogenic System (S. Satoh)

*Design of Central Control System for LHD (H. Yamada)

*Cryogenic Control System for LHD (T. Mito)

*Test Operation of Cryogenic System with a Dummy Heat Load (R. Maekawa)

*Heat Transfer Measurements for the Stability Analyses of the Helical Coil Superconductor (A. Iwamoto)

D.Cryogenic Materials
*Cryogenic Mechanical Test Facilities and Test Results (A. Nishimura)
*Mechanical Test Results for Coil Packs Simulating Superconducting Coils in LHD (H. Tamura)
*Fracture Toughness of Structural Material for LHD (A. Nishimura)
E. Power Supply
*Coil Power Supplies for LHD and Reliability Test of OV Coil Protection System (S. Tanahashi)
*Current Control System for Superconducting Coils of LHD (H. Chikaraishi)

7. CONCLUSION

1) Cryogenics is a key technology to large scale superconducting system.
2) Hardware's of cryogenics made big improvements in these 10 years.
3) System engineering becomes next targets in cryogenics and applied superconductivity.
4) This symposium will give us valuable information to everybody who will engage in an extra large superconducting system

ACKWOLEDGEMENT

This work is a summary of LHD construction group (Leader: Professor Motojima), which is main group of NIFS from more than 50 researchers and technical staffs. For cryogenic R&D, we got a lot of support from Kyoto University, and cooperative researchers in universities, research institutes, and manufacture's engineers. I acknowledge their helpful support from Professor A. Iiyoshi, Director General, and M. Fujiwara, Director of LHD.

10 YEARS OF OPERATION OF THE TORE SUPRA CRYOGENIC SYSTEM

B. GRAVIL - B. JAGER - F. MINOT
Centre d'Etude de Cadarache Association Euratom-CEA sur la Fusion
Departement de Recherches sur la Fusion Controlée
13108 Saint Paul les Durance-France

ABSTRACT

The main innovations of the TORE SUPRA cryogenic system are presented here. The selected technical solutions are described. The problems encountered during the 10 years of operation and evolutions are listed. The operating results are given.

INTRODUCTION

Presentation of the project: The TORE SUPRA Tokamak was built by the EURATOM-CEA association and established at the Cadarache Research Center which is located in the South-East of France. The construction of a high-field superconducting toroidal magnet, from which the experience will be important to future generation Tokamaks, imposed the choice of Nb Ti as superconducting materials. The consequence of this choice was the necessity to cool the conductor with superfluid helium at 1.8 K. The cryogenic system was therefore designed with this imperative in mind, and sometimes required special developments when the usual techniques could not be used. The role of the Service des Basses Températures of Grenoble, because of its experience with superfluid helium techniques, was of utmost importance in this area.
Toroidal magnet: The toroidal magnet consists of 18 superconducting coils. Each winding, is completely enclosed in a tight thin casing making up the enclosure filled with superfluid helium at 1.8 K and 0.125 MPa. Surrounding this enclosure and separated from it by an insulating supporting structure, is a thick stainless steel casing, cooled at about 4.5 K.

REFRIGERATION INSTALLATION

General concepts: The design of the cryogenic system was guided by the following ideas: -Optimization of costs, taking into account investment and operating costs over 10 years.-Savings of energy consumed by a choice of operating modes best-adapted to the operating conditions of the Tokamak. -Long-lasting operation without warming up the Tokamak above 80 K. The choice of components, their redundancy [1] or their maintenance accessibility were determined by this constraint. - The operation of the overall installation must be automatic.

MAIN INNOVATIONS OF CRYOGENIC SYSTEM

Large scale use of pressurized superfluid helium: The use of pressurized superfluid helium for the cooling of magnets gives:- An increase of the critical current of the superconductor material as well as an increase of the maximum acceptable field.- An improvement of the stability of the conductors as well as greater acceptability of power dissipation in the conductor (greater enthalpy).- A decrease of the quantity of the stabilizing material and thus an increase in the current density in the conductor and a decrease of variant field losses.-A greater operating safety of the coils. The total volume of superfluid helium used in the plant is of about 5 m^3, of which 4 m^3 are pressurized superfluid helium.

Thermal buffer: The pulsed operation of a Tokamak is not compatible with the operation of a refrigerator under steady state. For the refrigerator to operate satisfactorily, its load must be as stable as possible. In order to obtain this stability, thermal buffers were installed at levels 1.8 K and 4.5 K. At 1.8 K it is the 4 m^3 of pressurized static superfluid helium which immerse the conductor which play the role of thermal buffers and which limit the temperature increase of the windings to a few hundreds of degrees during plasma discharges. At 4.5 K three volumes of 1 m^3 of liquid helium are installed (one per satellite). They ensure an intermediate energy storage between thick casings and refrigerator.

Divider heat exchangers of cold power: In order to minimize the temperature difference between the 18 coils during cooling down and warming up phases, it is vital to distribute the power in a homogeneous way over the 18 coils. This required the installation of a system of divider heat exchangers of very small temperature differences between coils.

Helium II pumping system.: In view of the power necessary at 1.8 K, the pumping flow rate on the saturated bath is of about 0.015 $kg.s^{-1}$. Low pressure pumping is done by two compressors driven by an electric motor of variable frequency cooled at 80 K and sustained by active magnetic bearings. The warm pumping from about 7000 Pa is ensured by an oil ring pump. This pump alone is able to ensure pumping during idle hour operations.

REFRIGERATION

Description and characteristics: The helium refrigerator [2] built by the Air Liquide company supplies cooling powers which are necessary to the 3 temperature levels required by the superconducting toroidal magnet: P =300 W at T= 1.75 K, for the cooling down of the windings, P = 700 W at T= 4.0 K for the cooling down of the thick casings with a production of 0.003 $kg.s^{-1}$ of liquid helium available for current leads and P = 11 to 32 kW at 80 K for the cooling down of the shields. The power at level 80 K is produced by a turbine and/or liquid nitrogen. The storage volume of liquid nitrogen (100 m^3) was sized to be able to ensure, under normal operation without turbine, an autonomy of about one week. The 4.5 K refrigerator is on Claude cycle at three expander stages. The 1.75 K cycle is supplied by liquid helium at 4.5 K. Final JT heat exchangers are directly placed in the pumping lines at the outlet of the three satellites. The choice of powers installed at levels 4.5 K and 1.8 K was done by taking into consideration the following criteria: Under plasma shot conditions, the recovery time

between two shots must be 4 minutes maximum and in the case of a plasma current disruption, 30 minutes.

SAFETIES AND REDUNDANCIES.

The cryogenic system must operate for long periods at very low temperatures. Specific precautions were taken which mainly concern the risks of pollution of the circuits.
Sub-atmospheric circuits, protection against air leaks: Any air leak can lead to clogging the plant. To avoid this, we installed on all the elements likely to leak, a lock-chamber filled with helium of which the pressure is controlled. Any decrease in pressure of this circuit indicates a leak which can be quickly located. These helium lock-chambers concern :- valves equipped with a double safety system.- all the measurement detectors.- all the safety components such as safety valves or magnetic safety valves. In addition to these systems, the gas from the depressurized circuits is analyzed at the pumping stage discharge. O_2 contents (measurement by 2 cells...) and water content are constantly monitored. Any occurrence violating safety thresholds stops the pumps.
Pressurized circuits: Any helium leak towards the outside must be detected as it can cause air leaks by retrodiffusion effect. A surveillance by He mass spectrometry is performed continuously in the different halls of the plant.

MAIN PROBLEMS ENCOUNTERED [3] AND EVOLUTIONS DURING OPERATION.

"Growing up problems": -After the cool down of all the machine, we noted abnormal losses on the 4.5 K circuits. These losses essentially due to a faulty cooling of the 80 K satellite shields, resulted in a difficulty in supplying the cryostats leads due to the excessive percentage of gas in the liquid helium. A large part of these losses has been corrected. Liquid helium distribution in the satellites was modified by adding a phase separator which supplies the cryostats of current leads with pure liquid helium, while retrieving the enthalpy of the cold vapor in the exchange line of the cold box.
-The shield cooling He which was not purified at 80 K caused partial clogging due to impurities in solid CO and CO2. The circuits were modified in order to eliminate this problem by purifying all the flow rate at 80 K.
Problems encountered during operation : The parts of the magnet at very low temperatures form a cryogenic pump of large pumping capacity. The chamber being perfectly tight, this cryopump essentially accumulates hydrogen coming from the outgassing of stainless steel enclosures. During the shut down of the refrigeration or during a plasma current disruption, the temperature of the thick casings can increase by several degrees. The hydrogen thus liberated causes a pressure increase inducing an increase of exchanges by molecular conduction between the shields and the thick casings. This starts a divergent phenomenon which translated into a rapid increase of the temperatures of the thick casings to above 30 K during a plasma current disruption. In order to avoid this phenomenon, an efficient pumping system was preventively installed. Moreover, during idle hours, the temperature of the thick casings is periodically increased to outgassing the trapped hydrogen.
Problems linked to certain components: The very short life span of the bearings of compressor motors have led us to take a certain number of measures which consisted of :

-Making a complete vibration analysis of the machines and of their support structure which led us to rigidify certain parts so as to limit the effects produced by these vibrations. -Managing the bearings during shut down times in order to avoid the bearing marking phenomenon due to parasite vibrations, either by periodically imposing a rotation of the shaft, or by restraining the shaft to its support structure. Installing vibration measures for all the bearings. These measures are constantly watched and give information on the state of the bearings and on their lubrication. The lubrication period set by the constructor can be shortened according to the indications given by the vibration analysis.

Safety valve tightness: We very quickly encountered problems with the safety valves protecting the cold circuits. A shut down of the system causes their opening and their cooling down often causes leaks on the level of the connections and the non-tightness of the circuits at the set pressure. Several solutions have been found : All the safety valves protecting the cold parts were duplicated and a three-way valve allows to change from one valve to another. On some circuits, we added pressure-controlled cryogenic valves in order to avoid the opening of the safety valves.

OPERATING RESULTS

The cryogenic system has been totally operational for nearly 10 years. The cold operating periods are of about 1 year. The shut down periods at room temperature vary from 2 to 6 months depending on the maintenance programs linked to the Tokamak. Of all the malfunctions causing the unavailability of the machine, the percentage of malfunctions due to the cryogenic system is of **5 %.** The number of cumulated operating hours at $T < T\lambda$ is 22700 h. It is important to point out that no major problem has occurred in the pumping system, whether it be on the cold pumps or on the oil ring pumps.

CONCLUSION

The TS cryogenic system is recognized as being a success throughout the world. It has proven that the ambitious and innovative choices made at the time of its design were the right ones. Other installations, of much larger size, such as CEBAF (USA) or the LHC project CERN (SW) are based on the technology which was used for TORE SUPRA. The success of the TORE SUPRA cryogenic system shows that the technology associated to the 1.8 K, can be used on an industrial scale and that it does not, in any way, penalize the proper operation of a Tokamak.

References list

1 Gravil,B et al.,Back-up Systems of the TS., Cryogenics1994 Vol 34 ICEC 15 Supplement
2 Claudet,G et al.,Design of the cryogenic system for TS Tokamak Cryogenics 26 (1986) 443
3 Bon Mardion, et al.,Initial Operation of the 1.8 K Tore Supra Cryogenic System ICEC 12 (1988) 511

Operation of Nb_3Sn Superconducting Toroidal Magnet System on TRIAM-1M

S. ITOH, K. NAKAMURA , M. SAKAMOTO, K. MAKINO, E. JOTAKI,
Advanced Fusion Research Center
Research Institute for Applied Mechanics
Kyushu University 87
Kasuga 816, JAPAN

ABSTRACT
The high-field superconducting tokamak TRIAM-1M has been well operated since the first operation in June 1986. At the initial stage of plasma experiments, the impurity accumulation were observed in a cryogenic system. In order to take it away, we installed adsorber and thereafter the long-term operation has been continuously demonstrated. And it is confirmed that the plasma disruption dose not cause the quench in the superconducting toroidal magnets in the TRIAM-1M experiments.

INTRODUCTION

The high-field tokamak TRIAM-1M with Nb_3Sn superconducting toroidal field coils (TFC) has been successfully operated for 10 years since its first operation in June 1986[1]. The design of cryogenic system was started in 1979 and the construction of TRIAM-1M was started in 1982. The qualifying tests of the superconducting coil were finished in 1983 with the confirmation of the performance and stability[2,3].

At the initial operation phase, the system was operated well when the TFC were excited only. But during the plasma production, the impurity accumulation was observed in the cryogenic system, especially at the turbine of the refrigerator. This phenomenon obliged us to turn off the refrigerator. Then we installed the adsorber (molecular sieves) in order to take away the impurities.

Plasma experiments were carried out with the maximum filed and it was confirmed that the coils were stable against magnetic field variations in tokamak operation including plasma current disruptions. Moreover in the lower hybrid current drive (LHCD) experiments, TRIAM-1M has successfully demonstrated more than 2-hour steady-state discharge up to now[4].

We introduce the features of the TRIAM-1M superconducting magnet system and its operating scenario. And we also describe the issues of impurity accumulation and the effects of plasma disruption which we have actually experienced.

1 Features of TRIAM-1M Superconducting Magnet System

TRIAM-1M is the high-field superconducting tokamak, which is medium size

(R=0.8m, r=0.12×0.18m) but produces steady state high-field of 8 T at the plasma center. Table 1 shows features of the superconducting TFC. The superconductor is made of Nb_3Sn and their winding configuration is three grade and six double pancakes. The superconducting magnet system has been operated without any quenches at currents up to 6202 A, which produced a maximum field of 11 T at the windings. Table 2 shows the features of cryogenic system and DC power supply for the superconducting magnet system. Power transistor is used for the power supply as the element for feed-back control of constant current

2 Operation Scenario for the Superconducting Magnet System

The superconducting magnet system has been very well operated for ten years. Figure 1 shows the typical operation scenario of a year. There are two experimental terms in a year and one term is about three months. It takes 7-10 days to cool down the system to 4 K before each experimental term and to put it back to room temperature after the term. During the experimental term the superconducting magnets are charged up to 5-8 T before the experiment and it is discharged down to 0 T at the end of experiment every day.

3 Impurity Accumulation in Cryogenic System

In the initial stage in 1986 the superconducting magnet system was operated very well when the superconducting TFC was excited up to 8 T only. But during a series of pulsive plasma production the impurities were generated from the magnets gradually. So we could not continue the experiments longer than 1 week. And we had to put back the system to the room temperature and eliminate the impurities. As the results of impurity analysis of the helium gas it was confirmed that a large amount of CO_2 was contained. This phenomenon resembles "out-gas" in ultra high-vacuum system.

In order to take away the impurities, the room temperature adsorbing system which was made of molecular sieves was settled in March 1987. The adsorbing system has two groups of adsorbers in parallel. They work alternatively and switch every 30 hours. During one group is working, another is activated by baking and evacuation as shown in Fig.2.

After the settlement of the adsorbing system the impurities extremely decreased. Then the superconducting magnet system has been operated very well and successfully demonstrated 100 day continuous operation.

4 Effect of the Plasma Disruptions

The plasma disruption is an important factor for the superconducting magnet system because it may cause the coil quench. Figure 3 shows the example of the disruption in TRIAM-1M. The upper figure shows the variation of the level of liquid helium in the reservoir tank which is set up above the magnets. The lower one is a waveform of plasma current (I_p). The Ip of 355 kA decreases within 2.1 msec abruptly. In this case the consumed liquid helium is 26 ℓ which corresponds to 63 kJ. The relation between the alternative current (AC) loss estimated from the

decrement of the liquid helium and the plasma current just before the disruption is shown in Fig. 4. The open circles and the cross are the AC loss in case of the disruption and no-disruption, respectively. The offset is due to the AC loss of the liquid helium reservoir tank caused by the ohmic heating coil. The difference between the solid line and the broken line is the AC loss due to the disruption. It is found that the AC loss due to the disruption is proportional to the square of the plasma current just before the disruption. This suggest that the constraint is more severe in such higher plasma current as ITER.

SUMMARY

The features and operation scenario of the Nb_3Sn superconducting toroidal magnet system on TRIAM-1M are described. This system has been operated very well and continuously demonstrated the long term operation twice a year. At the initial operation stage, the impurity accumulation was observed in the system during the plasma production. In order to take it away we installed the adsorbing system and thereafter the impurities extremely decreased and the system has successfully demonstrated long term operation more than 100 days.

Although the plasma disruption experiment was carried out, the coil quench has never been observed. It is found that the AC loss due to the disruption is proportional to the square of the plasma current just before the disruption.

REFERENCES

1 ITOH, S. et al., Proc. 11th Int. Conf. on Plasma Physics and Controlled Nuclear Fusion Research, Kyoto,1986, IAEA (1987) **3** 321-331.

2 Nakamura, Y. et al., Bulletin of Research Institute for Applied Mechanics Kyushu University (1984) **60** 319-343 [in Japanese].

3 Nakamura, Y. et al., Proc. 11th Int. Conf. on Magnet Technology (MT-11), Tukuba,1989 767-772.

4 ITOH, S. et al., "Ultra-Long Discharge by Lower Hybrid Current Drive on TRIAM-1M," submitted to the 16th Int. Conf. Fusion Energy, Montreal., October 7-11, 1996.

Table 1 TF coil features

Number of coils	16
Coil bore	0.44 m×0.67 m
Peak field at windings	11 T
Conductor current	6202 A
Critical current at 11 T	9600 A
Stored energy	76 MJ
Conductor material	Nb_3Sn
Helium condition	pool boiling (4.2 K, 1 atm)
Structural material	304 LN
Structure configuration	welded case

Table 2 Features of cryogenic system and DC power supply.

Cryogenic system	
· refrigerator capacity	460 W (at 4.5 K)
· liquefaction rate	210 ℓ /hour
DC power supply	
· power	82.5 kW
· ripple	
at 6200A (current)	$\leqq 5\times10^{-4}$ rms
at 620A (current)	$\leqq 1\times10^{-3}$ rms
at 12.5V (voltage)	$\leqq 1\times10^{-2}$ rms

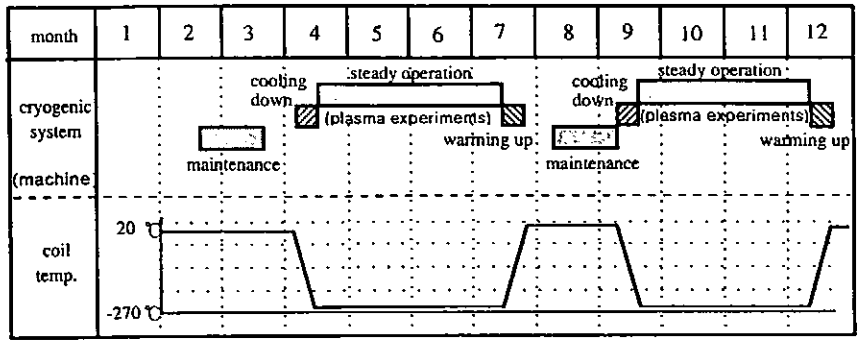

Fig. 1 Operation Scenario of the Year.

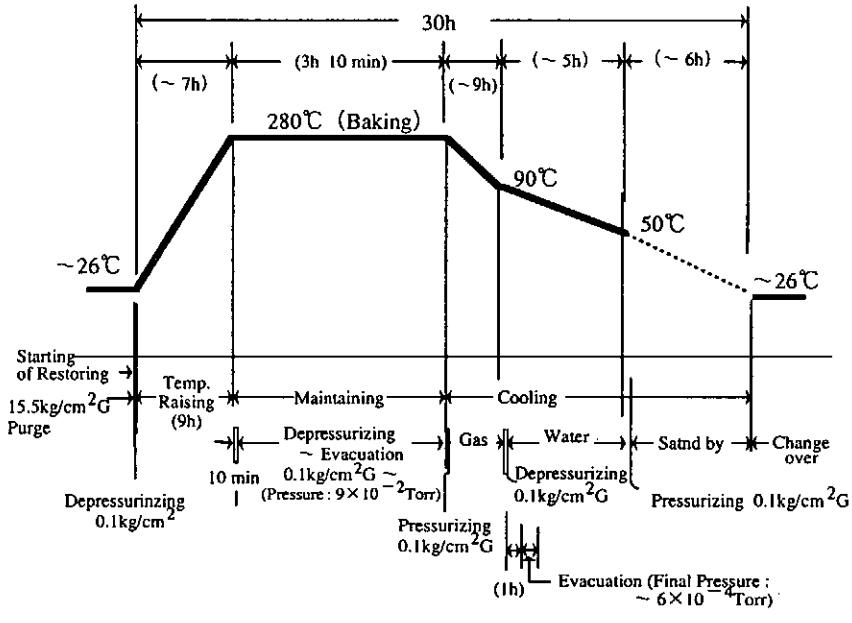

Fig. 2 Activating Scenario of Room-Temperature Adsorber.

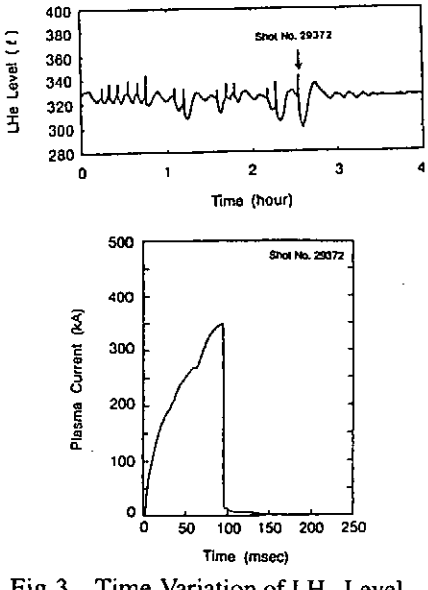

Fig.3 Time Variation of LH_e Level in Case of Plasma Disruption.

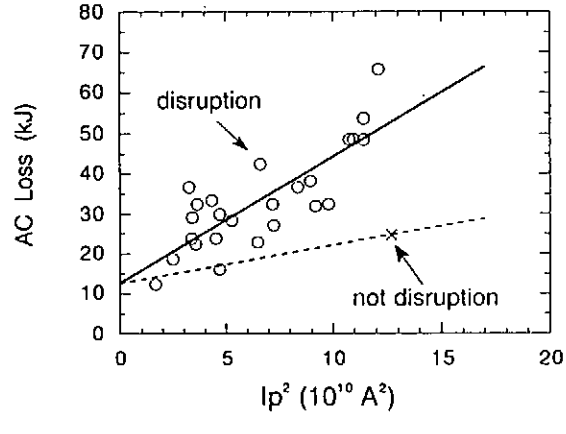

Fig. 4 AC Loss due to Plasma Disruption.

JET EXPERIENCE WITH THE LARGE SCALE CRYOGENIC SYSTEM

W. Obert
JET Joint Undertaking
Abingdon, OXON, OX14 3EA UK

ABSTRACT
JET (Joint European Torus) is the world's largest running experimental device for the study of controlled nuclear fusion. A vital and integral part of JET is an extensive cryogenic system with six large scale cryopump systems which have to handle the process gas used during the fusion experiment. These cryopumps are supplied by two large He refrigerators and a liquid nitrogen storage and distribution plant. Operational experience with the JET cryosystem which has been one of the most reliable subsystems at JET since the beginning of the operation in 1983, will be discussed together with aspects of automatic operation and manpower and maintenance requirements. Stringent design and nuclear manufacturing standards enabled JET to obtain cryopump systems which are practically maintenance free and did not show any failure over 13 years of operation.

INTRODUCTION

The cryosystem of JET represents an investment of >20 M$ and its reliable operation is paramount for the performance of the JET experiment. The system and its components is described in detail elsewhere [1]. The main components are two large liquid helium (LHe) refrigerators, a 110 000 l capacity liquid nitrogen (LN) storage, distribution plant and a series of large scale cryopumps which are integral part of the JET fusion experiment.

THE JET CRYOSYSTEM

Cryopumps

Six large scale cryopump systems (see Fig.1) which handle the process gas from the fusion experiment are the main loads of the JET cryosystem. These cryopumps have to be thermally cycled independently for regeneration on a daily to weekly basis depending on the JET program. All pumps have to operate in a hostile environment (see table1) and in a later stage of the project under a radiation load of 10^{19} neutrons/s. The pumps have also to withstand large eddy current forces caused by magnetic field changes of up to 110 T/s.

Cryopumps	LHCD	Pumped Divertor	Injector
Pumping speed	100 000 l/s	500 000 l/s	8 000 000 l/s
Envir. temperature	450 C	300 C	ambient
Envronment	10 MW RF power	40 MW energ. part.	40 MW energ. part.

Table1: Data of JET cryopumps

As the equipment at the JET torus would have to be maintained by remote control, the cryopumps were designed and built to nuclear quality standards and the design aimed to obtain practically maintenance free systems. The first of our large scale cryopumps have now operated for over 13 years without any failure or maintenance.

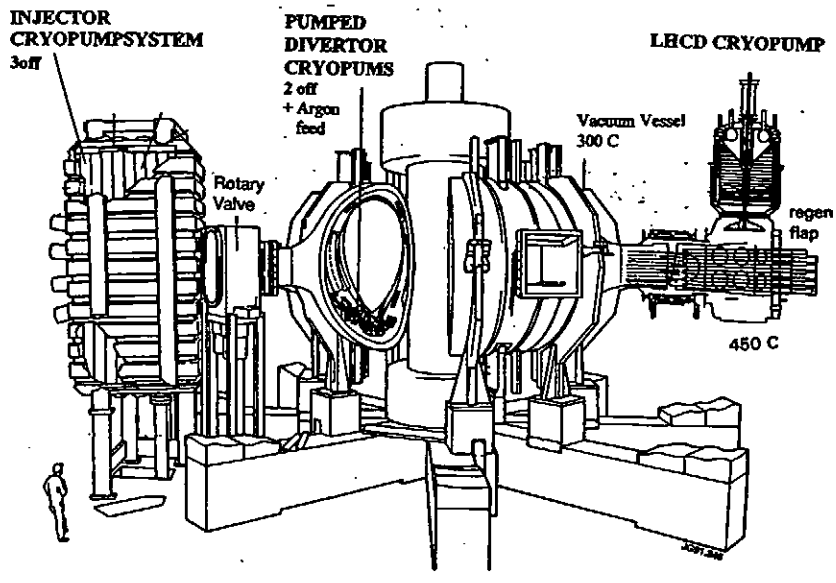

Figure 1: Main cryopump systems at JET

Cryoplant

The cryoplant at JET consists of 2 Sulzer/Linde helium refrigerators/liquefiers with a total power of 1300 kW at 4.4K or 450 l/h liquefaction together with the following peripheral equipment: 15000 litres LHe storage capacity; a gaseous helium recovery system with 160 m^3 medium pressure and 6000m^3 high pressure storage volume, 15g/s 200 bar recovery compressors and 15 g/s purification capacity. A large liquid nitrogen storage and distribution system has a storage capacity of 110000 l for a daily usage of 25000 l and the ability to produce 1500 m^3 /h gaseous nitrogen for venting, water draining gas cooling fire protection and others. There are in addition series of other bulk LHe and LN loads and in total more than 30 individual LHe and LN outlets allow independent supply to different users at the JET machine.

The design of the plant aimed for high redundancy. The main users are supplied by liquid helium via a large LHe buffer capacity of 15000 l which allows to continue operation of the cryoload even at a plant failure. The supply of supercritical He to the PD cryopumps can be switched between the two refrigerators. Two *cold ejectors* are used for the suction to subatmospheric conditions and the circulation of supercritical helium without operating mechanical pumping systems (see Fig. 2).

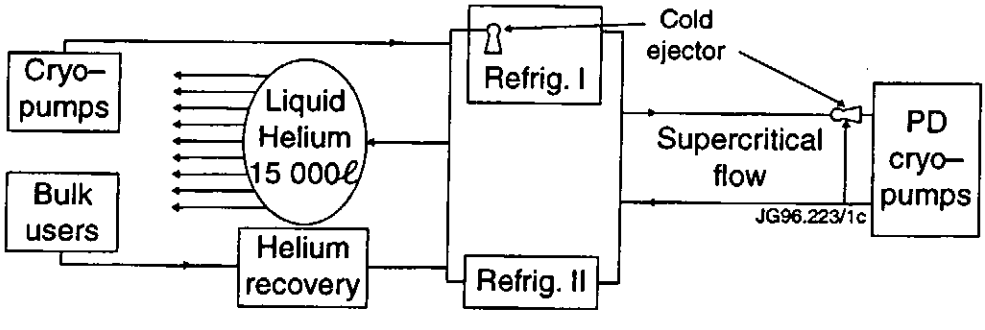

Figure 2: Cryoplant at JET : arrangement of main components

Cryolines

At the JET cryosystem all maintainable parts such as valves and rotating machinery are installed far away from the torus in an area of unrestricted access. This required the use of individual very long transferlines with minimum thermal losses to each cryopump. The good long term experience with these low loss (10mW/m for LHe go line), high pressure stable (> 100 bar go line) flexible transferlines has been reported at the recent ICEC16 [2].

Control System

The plant is fully automatically controlled with its own dedicated control system (see Fig.3). This is based on a PLC (Programmable Logic Controller, AEG-Modicon Quantum with hot-standby) which has a PC supported operator interface which produces mimics, trend and history curves and alarm handling. The operation of all valve sequences is fully automated. A completely independent PLC based interlock loop DPIS (Direct Plant Interlock System) protects the cryoloads and the plant against hazardous conditions. The operation of the plant can be fully monitored from the main control system (CODAS) which also sends the commands to the plant PLC for cryopump operational requests such as cooldown, warm-up or regeneration.

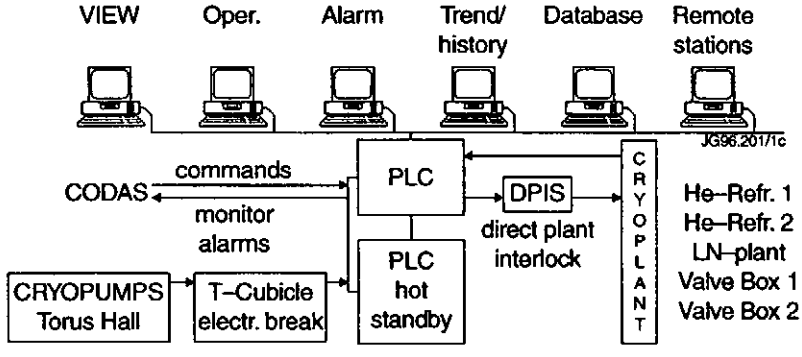

Figure 3: Architecture of JET cryoplant control system

OPERATIONS

JET is operated in two operational shifts and a night shift, where all maintenance and cryopump transients such as regeneration or cooldown take place. The automatic plant control allows operation of the plant; the cryopumps regenerations; cooldowns; warmup and bulk transfer of LHe and LN to various other cryoloads without direct operator involvement. The manpower for operation maintenance and plant improvements/upgrades can be accordingly minimized, the reliability optimized, and operational flexibility maintained.

RELIABILITY/SAFETY

The cryopumps required no remedial work nor maintenance in the period since 1983, neither did the cryolines. However the instrumentation of the early cryopumps was replaced in order to improve performance and to have bakeable sensors which were required for the potential tritium operation of the system. At the cryoplant the mechanical moving components in particular compressors and vacuum pumps are

regularly maintained according to the manufacturers' maintenance schedule which is typically once a year. After a total running period of 14 years the reciprocating Sulzer K160 is still in top shape. A series of problems occurred with the vacuum pumps leading all oil diffusion pumps being replaced by turbomolecular pumps.
During the recent record length 15 months operation campaign (1994/1995) the delays caused by various subsystems of JET were analyzed [3] and once commissioning problems of the new PD cryopump system were omitted the cryosystem was one of the most reliable subsystem of JET. The main reasons for the delays were at the cryosystem blockages in the cryogenic loops from subatmospheric operation and software/control problems caused by problems within the electronics or with the plant instrumentation.

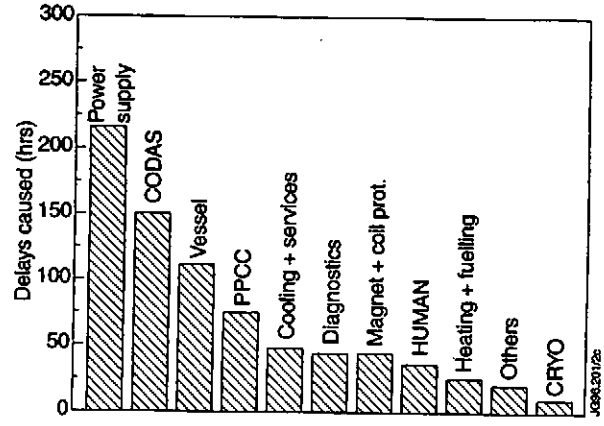

Figure 4: Reliability statistics for various systems of JET, delays caused for JET operation due to various subsystems of JET (integrated over 15 months)

The main reason for the high reliability of the cryosystem can be traced down to:

- Mechanical design
  - design with sufficient safety margin (e.g. thermal stress)
  - application of rigorous quality standards for material selection, welding and surface coating
- Process design
  - decoupling of plant from loads by the large LHe and LN buffer
  - equipment redundancy and spare plant capacity for transient conditions
  - fully automatic plant control with data access for trends, history files and alarms
  - use of passive parts (cold ejectors) instead of mechanical equipment (compressors, vacuum pumps) [1]

The safety record of the cryosystem is very good having no accident reported since 1983 inspite of the daily handling of ~ 30.000 litres of both LHe and LN.

CONCLUSION

The JET cryosystem is very complex and the achievment of high reliability and low manpower requirement has been obtained by applying highest design and manufacturing standards, integrating redundant supply strategies and fully automatic operation.

REFERENCES

1 Obert W. et al.'The JET Cryosystem, Overview and Experience', Advances in Cryogenic Engineering CEC 9 (1993), Vol 39,pp 493-500, Edit. P. Kittel, Plenum Press, NY 1994
2 Obert W., Mayaux C., "Flexible corrugated Cryotransferlines, Long Term Experience at JET and Experience with Supercritical Helium" Proceedings Inten. Cryogenic Eng. Conf. ICEC 16 (1996)
3 J. How et al. "Summary of Physics and Machine Operations 1994-1995", JET-IR(95)07

FZK - Experiences of Cooling Large S.C. Systems

W. Lehmann
Forschungszentrum Karlsruhe, Institut für Technische Physik, Postfach 3640,
D-76021 Karlsruhe, Germany

ABSTRACT

Forschungszentrum Karlsruhe (FZK) has been developing and practicing cryogenics for applied SC-projects for more than 25 years. Suitable cryogenic facilities with He I- and He II-cooling circuits are available. It is reported about operation experiences using different processes for refrigeration and for cooling of the s.c. equipment.

INTRODUCTION

The FZK/ITP Helium Supply and Recovery System presently comprises mainly:

- two refrigerator/liquefier plants:
  the old 1.8 K 300 W Linde plant [1], and the modern Linde He I-2 kW plant [2]
- a purification and recovery system with 12 g/s and 25 g/s capacities, resp.
- Storage tanks for approx. 20 000 ℓ LHe and 15 000 scm gHe.
- Three transfer line systems of 350 m total length, connected to the Fusion Magnet Test Facilities TOSKA and STAR, to the High Field Magnet Experimental Facilities HOMER I and MTA , and to the Cryogenic Test Facility HELITEX.

The principal cooling modes of s.c. magnet systems at FZK/ITP are presently:

- forced-flow-cooling in the fusion magnet applications
- bath cooling with subcooled He II for high-field solenoid systems.

EXPERIENCE GATHERED WITH THE REFRIGERATORS

The fundamental prerequisite of safe s.c. systems cooling is reliable refrigeration. Therefore, operating experience with the two Linde refrigerators will be briefly described. But, first of all, the FZK/ITP typical boundary conditions will be outlined:

- three low-temperature exits at each plant for different users/cooling circuits and LHe supply; refrigerators integrated in the FZK/ITP He-compound system;

- different cooling requirements for different and changing users;
- frequent refrigeration-liquefaction mode or two users at the same time;
- relatively short working time (typically 1 - 6 weeks) → frequent cooldowns and warmups; magnet quenches as one mode of operation;
- unattended standby operation during nights and weekends usual;
- no redundancy of the refrigerator/liquefier machines;

The Linde 1.8 K 300 W refrigerator, equipped with expansion turbines with oil bearings, dry type vertical piston compressor and an eight-stage roots pump unit for He II operation, has been used so far more than 25 years in a total of 20 s.c. experimental facilities. The operating data, the expenditure for maintenance and repair as well as interruptions of refrigerator operation due to malfunctions and damage, respectively, are evident from Fig. 1.

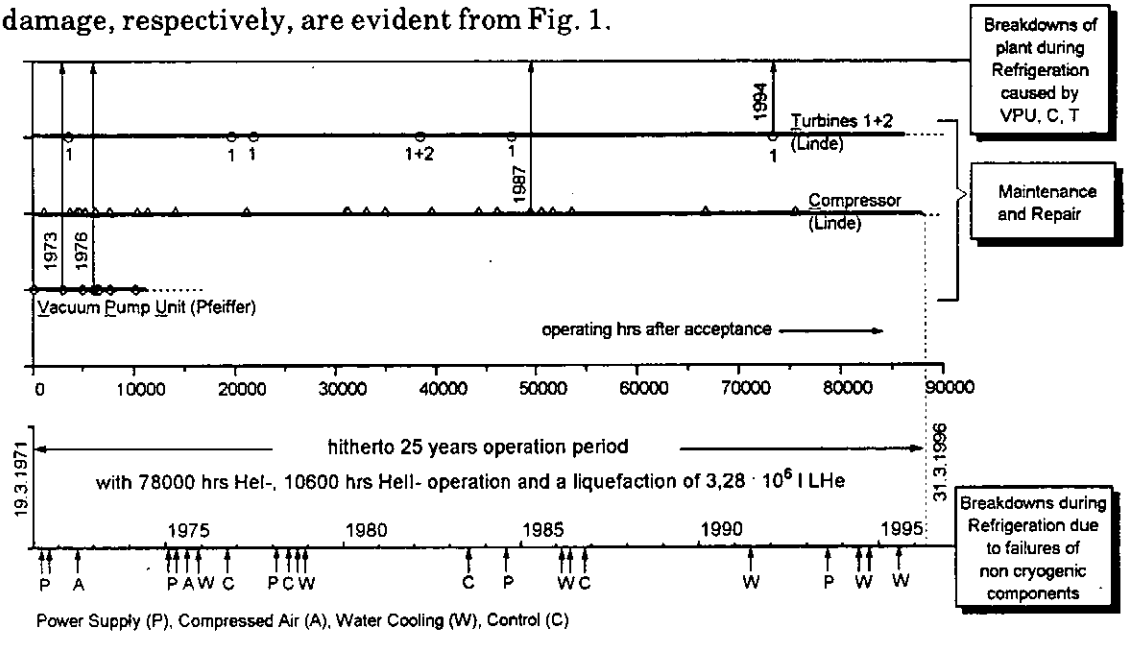

Figure 1 Balance of Linde 1.8 K 300 W refrigerator

Despite the complicated boundary conditions mentioned before, the system has so far worked very reliably. Great damage did neither occur at the machines nor within the cold box. The vacuum pump unit proved to work satisfactorily as a dry pump unit during 11 000 hrs. so far. Having been used for He II bath cooling of s.c. accelerator cavities in the seventies, it is now being used again for 1.8 K forced-flow-cooling of the mechanically reinforced European LCT-NbTi coil installed in the TOSKA test facility.

The modern Linde He I-2 kW refrigerator, equipped with three screw type compressors, a cold box with three expansion turbines with gas bearings, a distributor box with He subcooler, and an industrial process control system, is connected to the Fusion Magnet Test Facilities TOSKA and STAR. It was designed for a combined base refrigeration capacity of 700 W/3.3 K plus 400 W/4.4 K plus

1000 W/80 K plus 4 g/s rate of liquefaction for NET/ITER coil testing, but it can be used in fully automated operation in eight operating modes altogether. First operating experiences have been described in [2]. After acceptance, some smaller modifications and improvements have been made with regard to the compressor slide ring sealing, to the electric insulation of two compressor motors, to some control valve position switches and to software details of the process control system. During first operation of the 2 kW plant with the TOSKA- and STAR test facilities no problems emerged using the new 100 m long transfer line system. Unfortunately, after 7500 operating hours two minor but troublesome problems are not yet settled up to now: a) "noise-problem" at turbine T3 which occurs sometimes, especially under low pressure and low temperature conditions at turbine inlet; b) "slide vane material problem" at the He-blower for adsorber regeneration (incompatibility of material with very dry helium).

EXPERIENCE GATHERED WITH COOLING TECHNIQUES

Forced-Flow-Cooling (ffc) for Fusion Magnets

The advantages of one phase ffc in general and of its application in an autonomous magnet cooling circuit with cold circulator in particular were recognized early [3]:

- Flexibility of operation, characterized, inter alia, by the possible condition $\dot{m}_{Magnet} > \dot{m}_{JT,refrigerator}$.
- Decoupling of the refrigerator circuit from the magnet cooling circuit.

The first advantage had to be utilized already at the time of LCT-EU coil testing at FZK due to the worldwide prevailed assumption that large mass flow rates (>100 g/s) would be needed to stabilize toroidal s.c. coils. Therefore FZK untertook development work together with industrial firms on a three-cylinder and a one-cylinder piston pump for the resulting high pressure drops in the coil (3 ÷ 4 bar) [4], [5].

It has appeared meanwhile that in quite a number of applications lower specific mass flow rates with accordingly lower pumping heads are sufficient in cooling and stabilizing fusion magnets. Therefore, one centrifugal pump each, were installed and tested in both, the HELITEX and TOSKA test facilities.

Our "laboratory scale test operation experiences" with six cold (mechanical) He circulation pumps and 3 different pump types are summarized in table 1.

Stability of Delivery and Mechanical Reliability

The drawbacks of oscillating piston pumps compared with centrifugal pumps are obvious (unsteady delivery and parts subjected to wear). In a closed scr He circuit the (single acting) one-cylinder pump can be operated satisfactorily without damper

elements at low speeds only. When equipped with suitable buffer tanks, it also can be operated at higher speeds due to "decoupling" of the pump pulsations from the cooling circuit [5]. Thanks to the more uniform delivery with smaller pressure amplitudes in absence of buffer tanks, the three-cylinder pumps have proved their worth in various cooling circuit configuration and operating conditions.

Operating Characteristics and Thermohydraulic Behavior

Experiments involving "disturbing thermal loads" have shown, both under conditions of two-phase HeI ffc [3] and scr He ffc [8] that the steepest possible $\Delta p(\dot{m})$ characteristic of the circulator has to be ensured in order to stabilize the flow and to maintain the cooling efficiency in SC coolant channels. Otherwise, sudden thermal loads may cause a dramatic reduction of the passing coolant flow and even reverse flow under certain conditions. The He pumps Nos. 1 ÷ 4 and 5 + 6 in table 1 differ extremely in their delivery characteristics. The centrifugal pumps used react to thermal disturbance in the circuit "very inaptly" compared with the piston pump due to their abnormally flat characteristic curves [8].

The pumps Nos. 3 (PP) and 6 (CP) have been operated under single phase HeI and HeII conditions. Former experience [3] has been confirmed: there is no change in delivery stability and delivery characteristics pumping superfluid helium [9].

Table 1 General View of the Cold Helium Pumps used at FZK/ITP

Pump type	No [Ref]	Producer Year of Constr.	Testfacility (area of appl.)	Design Data $\dot{m}_{max}$ [g/s]	Δp_{max} [bar]	n_{max} [rpm]	Drive	Operating conditions	Operating hours	Number of switchin	Number of cooldown	Parts subjected to wear	Defects / Problems
Piston Pump 3 cyl. (Prototype)	1 [4]	Linde 1980	HELITEX TOSKA B250	150	3	300	3 Phase geared motor 2,2 kW, RT	- Scr. He 4,5 K - dito and subcooled LHeI	5000	> 200	150	stuffing box packings at piston rods (leaking)	- 1 crankshaft bearing worn out - gravity type suction valves /p-, ṁ-instabilities in case of LHe pumping
PP 3 cyl. (Spare)	2	Linde 1983	TOSKA B250	150	3	300	"	Scr. He 4,5 K	500	80	40		gravity type suction valves
PP 3 cyl.	3 [9]	Linde 1990	TOSKA B1000	50	0,7	300	DC geared motor 2 kW, RT	- Scr. He 4,5 K -.Subcooled HeII at 1.8 K	100	60	30		gravity type suction valves
PP 1 cyl. (Prototype)	4 [5]	NTG 1983	HELITEX TOSKA B250 HELITEX	150 60	3 ←	500 ↓ 200	DC geared motor 2 kW, RT	Scr. He 4,5 K	1000	300	50+100	- outlet valve guide box - ball guide box (cross head)	warm piston rod sealing and piston rod gliding surface /oscillations without damper elements at n > 140 rpm in TOSKA
Centrifugal Pump	5 [6,7]	Walther Meissner Institute, Garching 1990	HELITEX	50	0,4	10800	Self-synchronuos motor 30 W Low Temp.	Scr. He 4,5 K	500	70	20	-	- /flat delivery characteristic [8]
CP	6 [6,7]	dito 1990	TOSKA B1000	50	0,4	12000	"	- Scr. He 4,5 K - Subcooled HeII at 1,8 K	100	60	30	-	- /range of instabilities [9]

He II_p Bath Cooling for High Field Solenoids

In this field of application the French cryostat - and cryoprocess - principle with thermal barrier between the subcooled HeII magnet bath and the boiling HeI reservoir and with a "HeII-refrigerator" for subcooling the magnet bath is used.

Comprehensive experiences have been gathered with such systems at FZK / ITP (table 2). Operating experience is highly satisfactory both as regards the efficiency and stability of cooling and the very slow warming up of the magnet bath, in case of interruption of cryosupply, and as regards the reliability of the process components.

Table 2 FZK/ITP Experiences with He II_p Cooled Magnet Cryostats

	HOMER I [10]	MTA [11]	NMR Cryostat [11]	HOMER II
$T_{Magnetbath}$ [K]	1,8	2,17	≤ 2,17	1,8
$P_{Magnetbath, LHeI bath}$ [bar]	1,2	1,2	≈ 1,0	1,2
$\dot{Q}_{Magnetbath, stat.}$ [W]	≤ 10 W	≤ 10 W	0,070	≤ 20
$\dot{Q}_{Magnetbath, max.}$ [W]	10 W	≈15 W	0,8	20
Thermal barrier	GRFP-disk "tight"	GRFP-cushion (convection-barrier)	Insulation vacuum	GRFP-disk "tight"
LHe tank	wide neck	wide neck	2 tanks	wide neck
LHe inventory [ℓ]	max. 200÷300	max. 250	max. 380	max. 300÷400
Magnet mass [kg]	ca. 1700	ca. 1300	ca. 1300	ca. 3400
Stored energy [MJ]	8	4 ÷ 5	4 ÷ 5	18
Operation mode		persistent mode	persistent mode	
Supply of the HeI bath	300 W Linde Refrigerator	300 W Linde Refrigerator	monthly via transport containers	300 W Linde Refrigerator
Beginning of operation	1983	1989	1991	1998
Operating hrs till 1995	10300	5700	>4000 (>30000)	-
RT-LT-cycles	80 ÷ 90	≈ 50	(3)	-

Operating problems used to emerge only in case of impurities and freezing out within filters or needle valves. This is now avoided by careful handling and purging before cooldown, complete warming up prior cryostat dismantling, slight He flow through filters and expansion valves when changing test samples and isolating the cryostat from the quenchgas recovery system during experiment shutdown.

REFERENCES

1 Komarek, P. et al. Cryogenics (1984) 24 603-621
2 Spath, F.K. et al. Adv. Cryog. Eng. (1994) 39 563-570
3 Lehmann, W. Cryogenics and Refrigeration, IAP (1989), 319-327
4 Lehmann, W., Minges, J. Adv. Cryog. Eng. (1984) 29 813-820
5 Hübner, J. et al. Proc. ICEC 10, Helsinki (1984) 574-577
6,7 Berndt, A. et al. Adv. Cryog. Eng. (1988) 33 1147-1152, (1990) 35B 1039-1043
8 Cheng, X, Lehmann, W. Adv. Cryog. Eng. (1994) 39B 1723-1731.
9 Zahn, G. et al. Proc. ICEC 14, Kiev (1992), Cryogenics (1992) 32 100-103
10 Turowski, P., Schneider, Th. Physica B (1990) 164 3-7
11 Komarek, P. et al. KfK-Nachrichten (2/1993) 25 73-82

THERMOMECHANICAL PUMPS FOR COOLING WITH FORCED FLOW OF SUPERFLUID HELIUM.

A. Hofmann

Forschungszentrum Karlsruhe, Institut für Technische Physik,
Postfach 3640, D-76021 Karlsruhe

ABSTRACT
Superfluid helium has excellent features for cooling of superconducting magnets. This is due to its extraordinarily good thermal conductivity and due to its unusual flow behavior. Some applications need cooling by forced convection. Different methods for producing such convections either by use of the external compressor or by additional pumps in secondary loops are considered. Special attention is drawn to the possibilty of using the thermomechanical effect (fountain effect) for driving such convection. The design of such pumps will be described and it will be discussed how they can be applied reasonably.

INTRODUCTION

The extraordinarily high thermal conductivity of subcooled superfluid helium (He II) ensures that no convection is required for bath cooled magnets, but it is not sufficient to remove the heat over the very long distances of internally cooled conductors. Most of such magnet configurations will need forced flow. As to friction loss in such channels, the phenomenon of superfluidity may be ambiguous. Frictionless flow is only apparent in very narrow channels and below certain critical flow velocities. In channels with hydraulic diameters of several millimeters, He-II flow experiences about the same friction loss as single phase He-I. Therefore, most of the conventional pumps can be used to drive He-II flow, and also the option to drive such flow by the external compressor of the refrigerator must be considered. But friction losses at He-II temperatures being more "expensive" than those at higher temperatures, such forced flow loops need more careful design. On the other hand, He-II offers the unique feature of the thermomechanical effect by which it becomes possible to construct pumps working without any mechanically moved components.

THE THERMALLY DRIVEN FOUNTAIN EFFECT PUMP.

Fig. 1 shows schematically how continuous flow of He-II can be driven with a thermomechanical pump (TMP). The main element is the super leak (SF), a porous plug, permeable only for the superfluid component of He-II. Its pore size is less than $1\mu m$. The pressure difference

$$\Delta p = \int_{T_5}^{T_6} \rho s dT \qquad (1)$$

establishes where T_5 and T_6 are the temperatures at both ends (ρ and s are specific density and entropy, resp.). For the low end temperature of $T_5 = 1.8K$, the pressure difference can go up to 0.05 MPa. At the cold end, the plug is anchored to T_0, the temperature of the boiling He-II pool. The warm end is heated by the flow coming from the magnet where the heat load Q has been absorbed. In the heat exchanger WHX, the He flow is cooled down to an intermediate temperature T_6 and in the subsequent heat exchangers HX1 and HX2, the flow is cooled back to the basic temperature. The subcooling system pressure p_0 can be set to arbitrary values. In many cases, atmospheric pressure is convenient. Higher pressures are also allowed, but one should be aware, that the transition

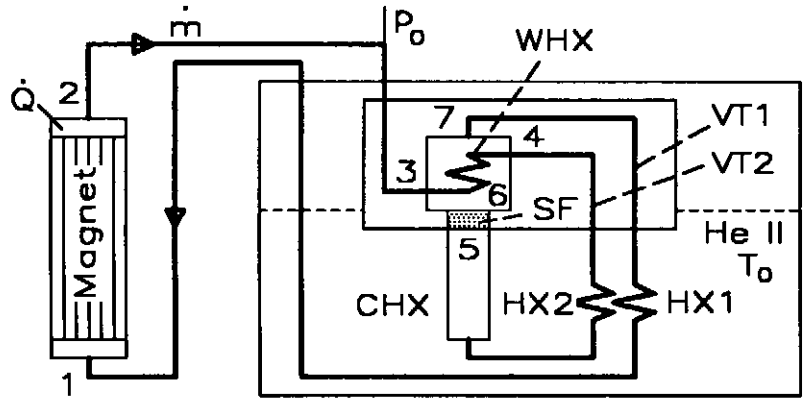

Fig. 1: Schematic of a cooling loop with a self-sustained thermomechanical pump

temperature (λ-line) drops with increasing pressure. No major degradation is found for pressures below 0.5 MPa.

The flow rate depends on the thermal load $\dot{Q}$. This is similar to buoyancy driven thermal convection; but here, the pressure difference is appreciably greater. However, it must be investigated whether it is sufficient for the operation of internally cooled coils.

Layout of cooling loops to be operated with TMPs /1/. The graphs shown in Fig. 2 can be used for analysing the operational state of such systems. The abscissa is a scaled quantity composed of heat load, $\dot{Q}$, and of a factor characterizing the flow resistance. Assuming completely developed turbulent flow in the channels of the magnet which represents the main flow resistance of the whole loop, this factor is given by

$$\beta = \frac{1}{\dot{m}} \sqrt{(\rho \Delta p)} \tag{2}$$

where $\dot{m}$ is the total flow rate going through the pump. This scaling factor results from the onset to describe the pressure drop in a channel with hydraulic diameter D, length L, fluid cross section A, and constant friction factor ξ by

$$\Delta p = \xi \left(\frac{\dot{m}}{A}\right)^2 \frac{L}{2D\rho} \tag{3}$$

By combining the eqns.(2) and (3), we get

$$\beta = \sqrt{(\xi L/(2DA^2))} \tag{4}$$

β can either be derived from the known dimensions of the cooling channel, or from a single measurement of $\dot{m}$ and Δp. This measurement can also be done when the loop is operated with He-I. (This was done for the EURATOM-LCT coil which will be operated next in such a loop). For given value of $\beta\dot{Q}$, the upper graph yields the temperature T_2 establishing at the outlet of the magnet when the inlet temperature is T_0. The middle diagram yields the temperature T_2, at the warm end of the filter. The resultant pumping pressure is plotted in the lower diagram. Ideal conditions for heat exchangers and porous plug have been assumed. The latter means that there is frictionless flow in the filter. This topic will be discussed below.

These diagrams have been used for the design of a TMP suited for the operation of the LCT coil. The total thermal load of the secondary loop will be around $\dot{Q} = 70$ W. Prior tests with He-I yield a friction factor with $\Delta p = 0.1$ bar obtained at 10 g/s of flow. This yields $\beta = 0.87 \times 10^5 \mathrm{m}^{-2}$ and $\beta\dot{Q} = 6.1 \times 10^6$ W/m². With $T_0 = 1.8K$ at the inlet, the expected outlet temperature becomes $T_2 = 2.7$ K. The pump will be operated with $T_6 = 2.1$ K at its warm end, and the resultant pressure head becomes $\Delta p = 0.26$ bar(0.026*MPa*). This will cause $\dot{m} = 23$ g/s of helium flow. The filter of the pump has to be designed such that frictionless flow of this rate is possible when its warm end is operated rather close to T_λ.

Critical flow rates of various materials /2/ are compiled in Fig. 3. We used the sintered Al_2O_3 ceramics type KPM P80 for the fabrication of the pump. Totally, the filter is composed of 27 elements with 25 mm length and 15 mm diameter. They are glued in bores of a stainless steel flange.

Other important components are the different heat exchangers at cold (CHX) and warm end (WHX), respectively, and the back coolers (HX1, HX2). The respective analysis shows that about 75 % of the total heat load $\dot{Q}$ can be transferred to the warm end pool (WHX) where it is converted into work by a process with Carnot efficiency. The resultant overall efficiency, $\varepsilon = \dot{Q}/W$, will be typically in the range of 0.07. All other heat exchangers (CHX, HX1 and HX2) experience about $\dot{Q}/3$ of thermal load. Also the so-called vortex tubes (VT1 and VT2) are rather critical components. Their dimensions have to be optimized with respect to sufficiently small thermal conductance of the internal He-II column, and to tolerable pressure drop /1/. The design of the pump is shown in Fig. 4. It has been tested in a loop where the magnet was simulated by a heater and a throttling valve /3/. The specified data have been verified. The installation of the 1.8 K test of the LCT coil is in progress.

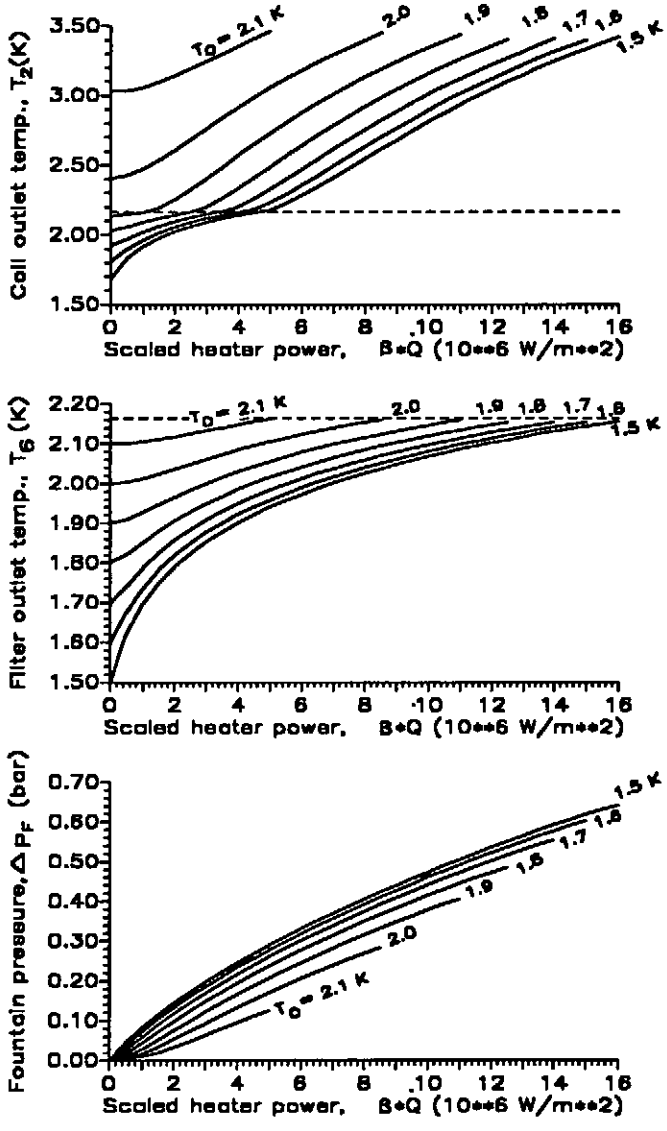

Fig. 2: Operational diagrams of a TMP coolant loops operated at different base temperatures T_0. (flow with const. friction factor, i.e. $\beta = \sqrt{(\rho \Delta p)}\,/\dot{m}$) a) Coil outlet temperature T_2, b) Temperature T_6 at the warm end of the filter, c) Pressure difference caused by the thermomechanical effect.

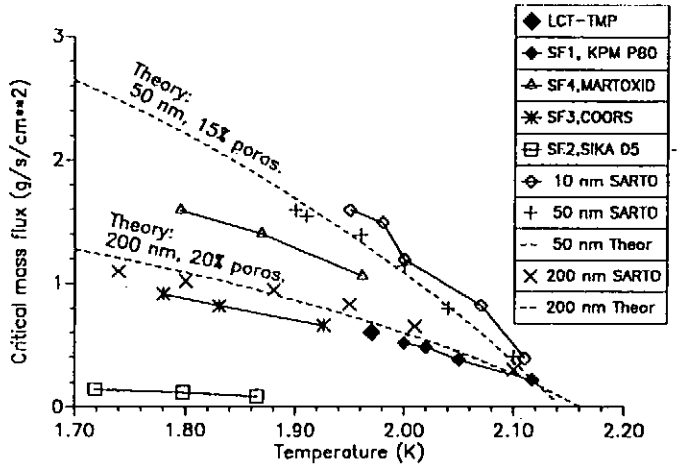

Fig. 3: Critical mass flux of He-II in different filter materials

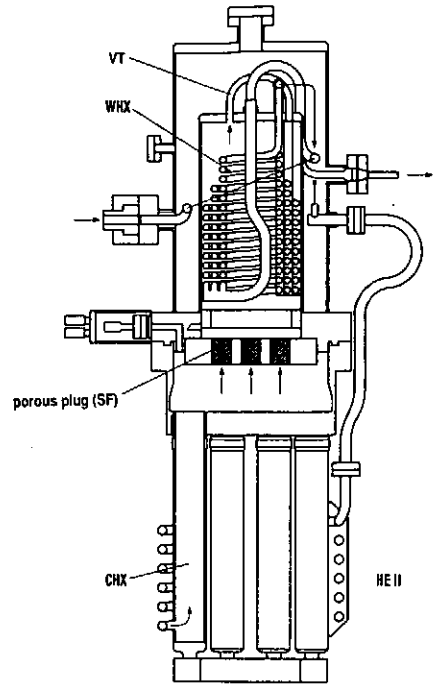

Fig. 4: Design of a TMP for EURATOM/LCT operation

CONCLUSIONS

Thermomechanical pumps prove to be suitable for operating large superconducting coils with internally cooled conductors. When operated in self driven mode, i.e. convection is driven by the heat losses to be removed from the magnet, one should be aware that a temperature difference ("onset temperature") will adjust automatically between inlet and outlet of the pump. For 1.8 K basic temperature, the coil outlet temperature will always be above 2 K (Fig. 2a). For high heat load ($\beta\dot{Q}$) it can go up to 3.5 K. Due to this effect, the "self driven TMP" cooling mode is most suitable for double pancake winding configurations with He-II supply in the high field region. The He outlet being at rather low magnetic field, high outlet temperatures (even in He-I range) can be tolerated. This is of great advantage for the magnet design. No major modification of the He-I internally flow cooled design is required. The electrical insulation of the conductor proves to provide sufficient thermal insulation even when the coil is operated at 1.8 K in the innermost layers and at about 4 K in the coil case /4/. A carefull check of applicability of this concept, however, is necessary when this cooling mode has to be transferred to other configurations such as magnets with layer windings or accellerator magnet configurations.

REFERENCES

/1/ A. Hofmann, "Design of a Fountain effect pump for operating the EURATOM/LCT coil with forced flow of helium II", Adv. in Cryogenic Eng., Vol. 37 (1992), 139

/2/ A. Hofmann, "Critical flow rate of He II in porous plugs operated with warm end temperatures close to T_λ ", Proc. of the 1st Internat. Workshop on Quantum Vorticity and Turbulence in He II Flows, Bericht 2/94 des MPI Göttingen (1994) ISSN 0436-1190, p. 94

/3/ G. Zahn et al., "Test of three different pumps for circulating He I and He II", Cryogenics 32 (1992) 100

/4/ A. Hofmann, "A Study on Nuclear Heat Load Tolerable for NET/TF Coils Cooled by Internal Flow of He-II", KfK-Report, No. 4365 (1988)

21 T Superconducting Magnet System with Saturated Superfluid Helium Cooling

T. Kiyoshi, M. Kosuge, F. Matsumoto, H. Nagai, A. Sato, K. Inoue, H. Maeda* and H. Wada

Tsukuba Magnet Laboratories, National Research Institute for Metals
Tsukuba, Ibaraki 305, Japan
* Present address: Institute for Material Research, Tohoku University
Sendai, Miyagi 980-77, Japan

ABSTRACT

A 21 T superconducting magnet system has operated at NRIM. Saturated superfluid helium cooling was applied for this system in spite of its large stored energy of 45 MJ. By installing a liquid helium tank in a coil vessel, major disadvantages of saturated superfluid helium cooling could be overcome. Two years have passed since this magnet was combined with a helium refrigerator. We briefly report its cryostat design, the total refrigeration system and operation results.

INTRODUCTION

A 21 T superconducting magnet system (21 T SM) has been developed and improved at the Tsukuba Magnet Laboratories of the National Research Institute for Metals (NRIM). This magnet can generate the highest field of 21.5 T in a 61 mm clear bore [1]. In February 1996, it recorded a field of 22.8 T in a 13 mm clear bore by inserting a Bi-2212/Ag coil [2]. This is the highest field generated in a fully superconducting coil system.

One of the characteristics of this system is saturated superfluid helium cooling. Although it is often used for small superconducting magnets, this system is the first trial in large magnet systems. The magnet had operated for four years without a helium refrigerator. Its cooling system and operation results of those days are reported in [3]. In 1994, it was combined with a helium refrigerator and operation procedure has been established until now. In this paper, we report its cryostat design, the refrigeration system and some of its operation experiences.

CRYOSTAT DESIGN

Its cryostat is separated into two chambers as shown in Fig.1. The outer chamber contains two outer NbTi and $(Nb,Ti)_3Sn$ coils that can generate 15 T at 4717 A. As their stored energy amounts to 45 MJ, the outer chamber is thermally insulated from the inner one, which is often used as experimental space. Normally two $(Nb,Ti)_3Sn$ coils are inserted in the inner chamber. The magnet was designed to generate only modest voltages

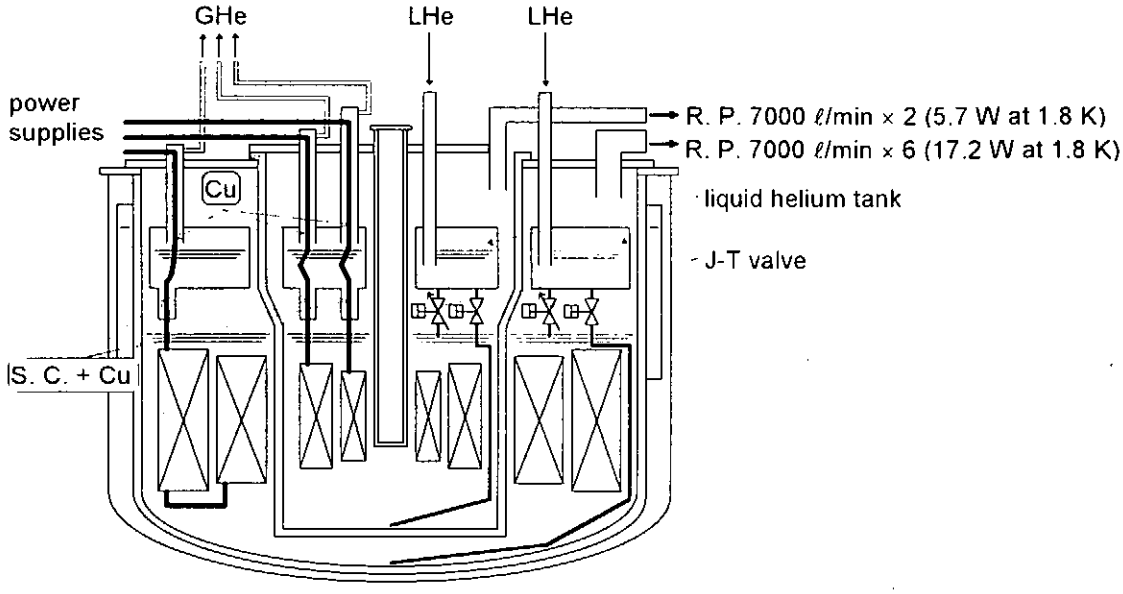

Figure 1 A schematic drawing of the cryostat of the 21 T superconducting magnet.

during quenching, by employing high-current conductors. This made it possible to choose saturated superfluid helium cooling.

Each chamber includes a liquid helium tank over the coils. Liquid helium is introduced into this tank from the refrigerator and supplied into a coil vessel through a J-T valve. A by-pass pipe is installed from the tank to the bottom of the coil vessel. It is used for cooling down from room temperature and for storing liquid helium.

A risk with saturated helium is its low breakdown voltage, especially in the gaseous state. It was overcome with the installation of the liquid helium tanks. Copper parts of current leads are also introduced into the tanks from power supplies. They are cooled with helium vapor and liquid helium at atmospheric pressure. The insulation for this part was designed to satisfy the same condition for a common magnet operated at 4.2 K. It is unavoidable that current leads pass in reduced helium pressure region from the liquid helium tank to the coil. In order to suppress an electric discharge in this region, electrically insulated superconductors are used for current leads. We measured dielectric strengths of the coils in helium vapor and liquid under saturated condition to assure safety of the operation [4].

Safety valves are attached only at the top plates and heat exchangers can be omitted from the system.

REFRIGERATION SYSTEM

The magnet now constitutes a helium closed circuit together with the helium refrigerator and a superconducting part of a 40 T class hybrid magnet system (40 T HM) as reported in [5]. Figure 2 shows a schematic flow diagram of the whole refrigeration system. All the evacuated gas from the rotary pumps is recovered with the compressor. We omitted an extra purification unit by replacing oil for the rotary pumps with that for the compressor. Cooling down of the 21 T SM is often carried out in parallel with regular

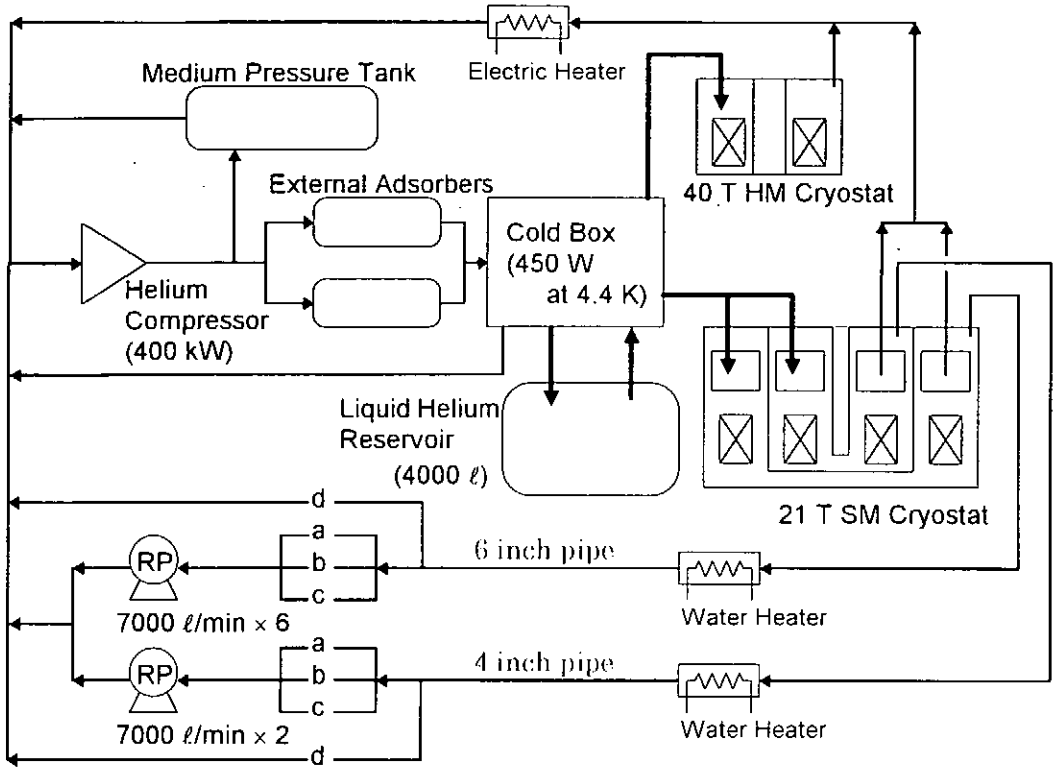

Figure 2 A schematic flow diagram of the refrigeration system including the 21 T SM and the superconducting part of the 40 T HM.

operation of the 40 T HM.

The pumping line for each chamber branches in three just before the rotary pumps. A line (a) is a combination of a needle valve and a narrow pipe. A line (b) is composed of the same size valve and pipes as those of the main pumping line. A line (c) includes a pressure control valve operating below 2700 Pa (20 Torr). Cooling down from 4.3 K to 1.8 K is automatically performed as follows;

1. All the rotary pumps operate. The coil vessel is evacuated only with the line (a) to reduce a load of the compressor.
2. Below 27000 Pa (200 Torr), the valve in the line (b) opens.
3. Below 2700 Pa, the valve in the line (c) starts to function.
4. At 2000 Pa, the line (a) and (b) close. Pressure control begins using the valve in the line (c).

OPERATION RESULTS

Examples of the cooling down curves of the 21 T SM are shown in [5]. Here we report its summaries.

From room temperature, it took 180 h to store liquid helium of 900 ℓ for the outer chamber whose cold mass was 12.2 t. In case of the cryostat of the 40 T HM, it took 150 h for the cold mass of 17.2 t. It was supposed that heat exchange occurred between the inside and the outside of the liquid helium tank. All coolant was introduced into the liquid helium tank first and then transported to the coil vessel. Coolant in the liquid helium tank was warmed from the outside during cooling down operation. On the

contrary, while the magnet operated in steady state at 1.8 K, it was observed that helium in the liquid helium tank was sub-cooled. We prepared the large liquid helium tank as a buffer of liquid helium but should have designed more compact one to reduce the surface area.

With the above mentioned procedure, it took 10 h and 4 h to cool down from 4.3 K to 1.8 K for the outer and the inner chambers, respectively. The lowest temperatures of less than 1.6 K were obtained in both of the chambers by opening the line (b). In the pressure controlled condition, the temperatures were maintained in the range of 1.8 ± 0.05 K.

As we stopped liquid helium supply from the refrigerator for the night, level of superfluid helium was increased by opening the by-pass valves in the morning. Liquid helium consumption rate in the refrigeration system was estimated to be 125 ℓ/h during the 21 T SM operation. This was an average value every operation day. This value might also be decreased by improving the liquid helium tank design to reduce heat leak from the top plates.

Failures of the power supply caused a DC shutdown process of the outer coils twice at the current of 4000A. Its pressure increments in the coil vessel were less than 0.106 MPa (800 Torr) and no gas was released from the system. Little pressure increase was observed for any DC shutdown process of the two inner coils because 98 % of the magnetic energy was stored in the outer coils.

CONCLUSION

The 21 T SM has operated to measure high-field properties of superconductors up to 21 T at NRIM. This system demonstrates usefulness of saturated superfluid helium cooling to low inductive magnet systems. By installing the liquid helium tank in the coil vessel, the problems of current lead cooling and of an electric discharge were overcome. The large size of the liquid helium tank is considered the cause of long cooling down time and of large helium consumption. Liquid helium tank design should be optimized to the next application.

REFERENCES

1. Kiyoshi, T., et al. Generation of Magnetic Fields over 21 T in a 61 mm Clear Bore Using Low Copper Ratio $(Nb,Ti)_3Sn$ Conductors to be published in IEEE Trans. on Magn.
2. Okada, M. et al. Bi-2212/Ag Superconducting Insert Magnet for High Magnetic Field Generation over 22 T to be published in JJAP
3. Oshikiri, M. et al. 21.1 T Superconducting Magnet with 50 mm Clear Bore Physica B (1994) 201 521-525
4. Kiyoshi, T. et al. Development of 20 T Class Superconducting Magnet with Large Bore, IEEE Trans. Magn. (1992) 28 497-500
5. Matsumoto, F. et al. Refrigeration System for Superfluid-Cooled 21 T Magnet and 40 T Hybrid Magnets at TML Physica B (1996) 216 412-416

Cryogenic System for CS Test Facility

Takashi Kato, Kazuya Hamada, Katsumi Kawano, Kunihiro Matsui, Tadao Hiyama, Tadaaki Honda, Kazuhiko Nishida, Shuich Sekiguchi, Kiich Ootsu, and Hiroshi Tsuji

Department of Fusion Engineering Research, Naka Fusion Research Establishment, Japan Atomic Energy Research Institute, 801-1, Mukaiyama, Naka-machi, Naka-gun, Ibaraki-ken, 311-01, Japan

ABSTRACT

Japan Atomic Energy Research Institute has successfully constructed a cryogenic system for the ITER CS model coil, which has verified to have the capacity of more than 5-kW refrigeration or 920-liter/h liquefaction. The newly developed helium compressor system and turbines are adopted, having attained good performances; the isothermal compression of 64% and the isentropic expansion efficiency of 85%, respectively.

INTRODUCTION

An international program on a fusion reactor development, so called Engineering Design Activity (EDA) of International Thermonuclear Experimental Reactor (ITER), has been continuously carried out. Central Solenoid (CS) Model Coil program[1] is now going on as one of the key R&D activities to demonstrate the ITER construction technology. The CS model coil is under developing and it will demonstrate to achieve its designed current of 46 kA and magnetic field of 13 T with pulse operation of more than 0.5 T/s. To implement the coil test, Japan Atomic Energy Research Institute (JAERI) has prepared the CS model coil test facility[2] which has included a newly developed large scale helium cryogenic system. This paper introduces the cryogenic system of the CS model coil test facility.

SYSTEM LAYOUT

Cooling requirements and system specification

The model coil adopts a forced-flow cooled coil applied to a Nb_3Sn cable-in-conduit conductor. The typical cooling requirements are; (1) circulation of supercritical helium (SHe) with 4.5 K, 0.6 MPa, and 350 g/s, (2) cooldown within 20 days for the total weight of around 180 tons, and (3) the maximum heat load of 3 kW at 4.5 K plus 380 liter/h where the conduction and emission heat load, the AC loss during pulse operation, the cryogenic circulation pump work, and the contingency are involved and the liquefaction requirement is for liquid helium (LHe) consumption for two sets of a 50-kA vapor-cooled current lead. The cryogenic system capacity was designed as a 5-kW refrigeration or a 800-liter/h liquefaction[3] to satisfy the maximum heat load condition. In addition, the capacity is considered to cool the coil down in 4-K region within 20 days. Cryogenic pump unit is also installed to generate and circulate SHe through the coil system. The cryogenic pump has advantages for SHe control, transient heat load, and refrigeration efficiency in case of the pump efficiency of more than 0.6 compared to the conventional room-temperature pump unit[4]. The cryogenic system is composed of the following components; helium compressor system, cold box, helium gas holder (gas buffer tank), helium gas recovery system, helium gas purifier, liquid helium storage tank, liquid nitrogen (LN_2) storage tank, and cryogenic pump unit. Their specifications are listed in Table 1 and their flow diagram is shown in Fig. 1, respectively.

Table 1 Specification of the system components

Component	Specification
Helium compressor system	Four units of an oil-injection screw compressor Total mass flow rate: 750 g/s at 1.8 MPa
Cold box	Claude cycle with LN_2 cooling and two-series turbines 5.0 kW at 4.5 K or 800 liter/h
Helium gas holder*	Helium inventory: 14000 m^3 at 2.0 MPa
Helium recovery system*	
Recovery gas tank	Helium inventory: 1900 x 2 m^3 at 1.9 MPa
Recovery compressor	Mass flow rate: 21 g/s at 1.8 MPa
Gas bag	Inventory: 200 x 2 m^3 at 0.105 MPa
Helium purifier*	Mass flow capacity: 21 g/s at 1.9 MPa
Air reduction	Inlet: 1000 ppm, Outlet: less than 1 ppm
Dew point	Inlet: Saturation, Outlet: less than 2.5 ppm
Liquid helium tank*	Inventory: 20,000 liters, Boil-off: less than 0.3 %/day
Liquid nitrogen tank	Inventory: 100,000 liter, Boil-off: less than 0.2 %/day
Cryogenic pump system*	SHe circulation capacity: 100 - 500 g/s Circulation SHe pressure: 0.4 - 1.0 MPa Supply SHe temperature: 4.0 - 5.0 K

*: These components are re-installed from the existing test facility.

NEWLY DEVELOPED COMPONENTS

Cold Box

Claude cycle is adopted, which is composed of eight units of heat exchanger, LN_2 precooling, series arrangement of two turbines, and double joule-Thomson (JT) valves. The cycle is well-experienced, conventional one, expecting reliability and easy investigation of the operation performance.

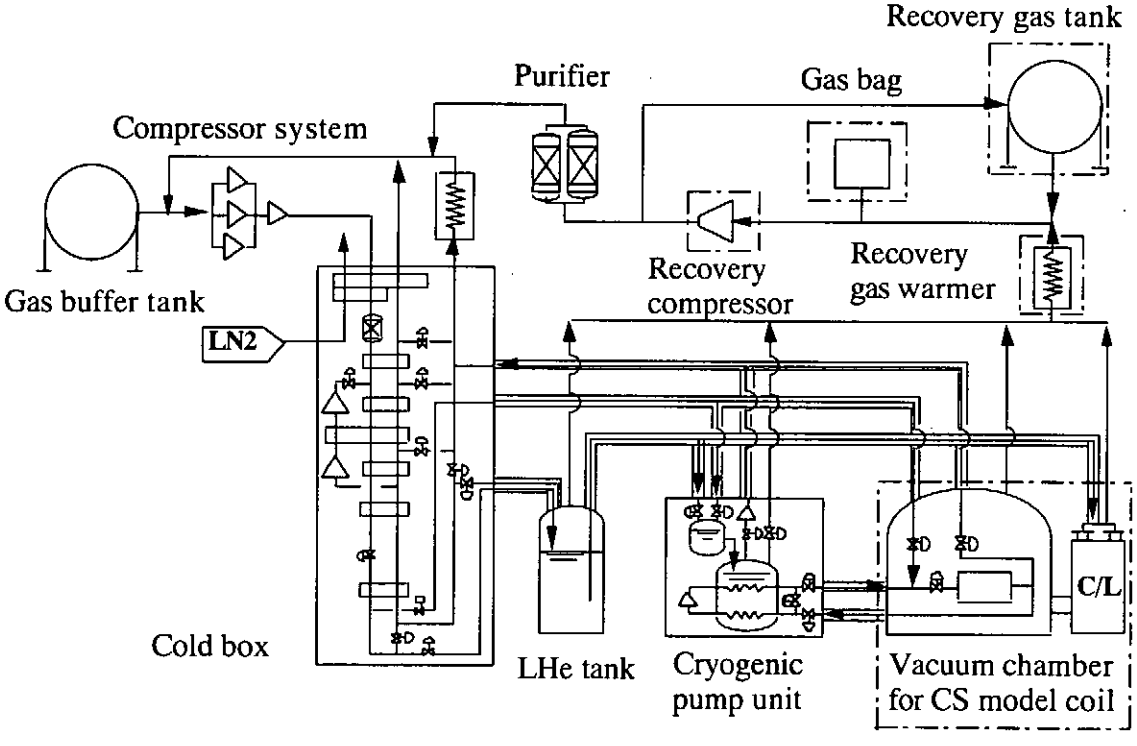

Fig. 1 Cryogenic system flow diagram

Table 2. Measured performance of the compressor system

Performance item	Designed	Measured
Mass flow rate (g/s)	750	786-796
Inlet pressure (MPa)	0.104	0.107
Medium pressure (MPa)	0.3	0.3
Outlet pressure (MPa)	1.8	1.8
Electric consumption (kW)	2450	2190
Isothermal efficiency	~60	63-64

Compressor system

Two-stage compressor system is adopted, arranging three units for the first stage (0.102-0.91 MPa) and one unit for the second stage (9.1-1.8 MPa). Oil injection screw type is used. A compound compressor where the two stages are operated by common shaft driven by one motor is developed for the first stage compressor. Then, the compressor system is substantially three stages, expecting to achieve high isothermal compression efficiency and to avoid contamination generation due to decomposition of oil. The each first stage unit has the mass flow capacity of 250 g/s and the second stage is 750 g/s as the design. The isothermal compression efficiency of around 60% at 800 g/s has been attained at the rated condition in the commissioning test as shown in Table 2.

Turbine

Both the first and the second turbines have been developed that their design specifications should be agreed with their required process conditions. The turbines adopt three-dimensional radial inward-flow impeller with shroud cover. Titanium alloy is selected as a material of the turbine rotor and the impeller to reduce bearing load and thermal conduction from the hot temperature region. Both journal and thrust bearings use a gas bearing system; On the thrust bearing, a compound gas bearing, called a pump-in type spiral grooved bearing, is adopted where the static gas bearing functions till 1,000 rps and the dynamic gas bearing start at more than 1,000 rps when static gas bearing is stopped. The journal bearing adopts a tilting pad type self-acting gas bearing. The turbine performance tests were carried out for both turbines by using the practical cold box. The first and the second turbine shown the isentropic efficiency of around 80% and 85% at the jet-blade speed ratio (U/C_0) of 0.6, respectively, which were higher than the design expectations. The comparison of both the measured and the expected efficiency are listed in Table 2.

ACHIEVED LIQUEFACTION/REFRIGERATION PERFORMANCE

Liquefaction and refrigeration capacities were observed to measure the LHe level change in the LHe tank when controlling the electric heater power. Measured capacities are plotted in the liquefaction-refrigeration diagram as shown in Fig. 2. The capacities depend on the first turbine inlet pressure and the opening of the valve located between the turbines. The specified capacities are sufficiently satisfied and furthermore the liquefaction rate at the pressure of 1.62 MPa shows 920 liter/h. However, the practical operation time of the system is only a few hundred hours. Increasing the operation experience, JAERI intends

Table 3. Comparison of measured and designed turbine efficiency

	Fist turbine		Second turbine	
	Measured	Expected	Measured	Expected
U/C_0	0.60	0.62	0.60	0.64
Isentropic efficiency (%)	~80	75	~85	80

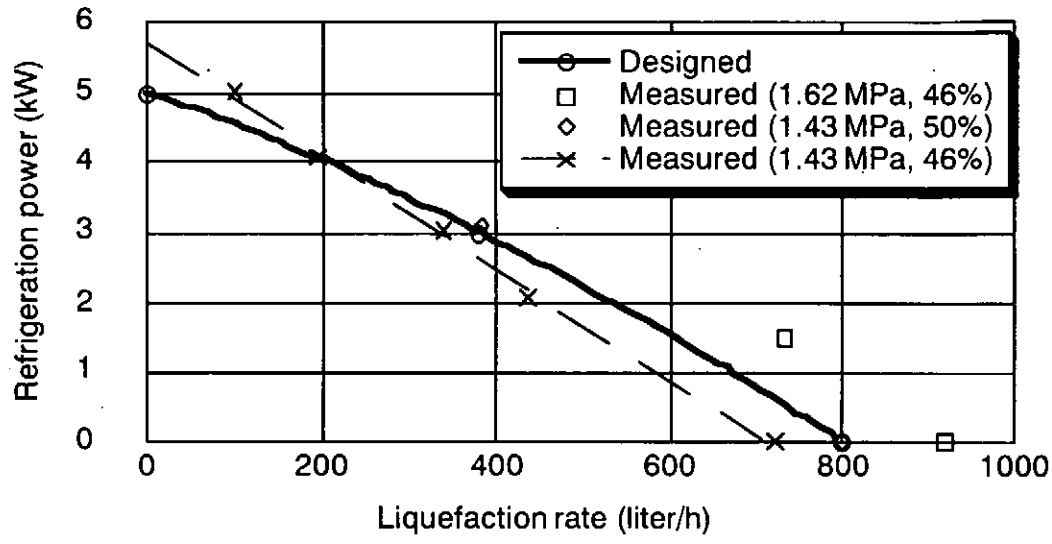

Fig. 2 Measured liquefaction and refrigeration performance as the several parameters

to accumulate the data that can evaluate the system reliability and more detail performance study will be continuously carried out to establish the data base for the ITER cryogenic system.

CONCLUSION

A large helium cryogenic system has been successfully constructed at JAERI, adopting newly developed compressor system and turbines that have attained a good performance such as the isothermal compression efficiency of 64% at 800 g/s and the isentropic expansion efficiency of 85% at U/C_0 of 0.6, respectively. One of the design data base for the ITER cryogenic system is obtained.

ACKNOWLEDGMENTS

Authors would like to thank Drs. S. Shimamoto, M. Ohta, S. Matsuda, and T. Nagashima for their continuous encouragement and support this work. The fabricator work from Kobe Steel Ltd. is gratefully acknowledged.

REFERENCE

1 Okuno, K., Model coil for the International Thermonuclear Experimental Reactor (ITER) magnet system, IEEE Trans. Magn. (1994), Vol. 30, No. 4, 1621-1626
2 Shimamoto, S. et al., Construction of ITER common test facility for CS model coil, Proc. ICEC 14, Tempera, Finland (1995)
3 Hamada, K., et al., Final design of a cryogenic system for ITER CS model coil, Cryogenics (1994) 34 65-68
4 Kato, T., Cryogenic helium pump system for the development of superconducting magnet in a fusion experimental reactor, Fusion Technol. (1992) 887-891

CRYOGENIC SYSTEM FOR TRISTAN RF CAVITIES

K. Hosoyama*, K. Hara*, A. Kabe*, Y. Kojima*, T. Ogitsu*, Y. Morita*,
Y. Sakamoto*, H. Nakai*, T. Fujita**, and T. Kanekiyo**

* KEK, National Laboratory for High Energy Physics Tsukuba, Ibaraki, 305 Japan
** Hitachi Ltd., Kudamatsu, Yamaguchi, Japan

ABSTRACT

A large scale helium refrigeration system was constructed and operated for about 7 years for superconducting RF accelerating cavities (SCC) in TRISTAN electron-positron collider at National Laboratory for High Energy Physics (KEK). The 32 x 5 cell 508 MHz SCC in 16 cryostats were installed in TRISTAN electron-positron collider at KEK for further upgrading of the beam energy, from 27 GeV to 32 GeV. A short description of the main components of the cryogenic system will be given together with the operating experience gained during the commissioning and 7 years operation.

INTRODUCTION

Installation of SCC in the TRISTAN was proposed for further upgrading of the beam energy and authorized as two years project in April 1986[1]. The design study of the cryogenic system[2] was started in August 1986 and the construction was started end of 1987. The operational and upgrading histories of the cryogenic system are shown in Fig. 1. In October 1988 the first cool down test of the cryogenic system with 4 kW refrigeration power (2 turbo-expanders and liquid nitrogen precooling) and 16 x 5-cell SCC in 8 cryostats was performed successfully[3]. Commissioning of SCC to TRISTAN electron-positron collider was started in November 1988. After 6 months operation additional 16 x 5-cell SCC in 8 cryostat was installed to increase the beam energy to 32 GeV and the helium refrigerator was upgraded to increase the cooling capacity from 4 kW to 8 kW and to reduce the consumption of liquid nitrogen by adding a supercritical turbo-expander, two 80 K turbo-expanders respectively[4]. The operation of the cryogenic system with full 32 x 5 cell SCC was started in October 1988 and

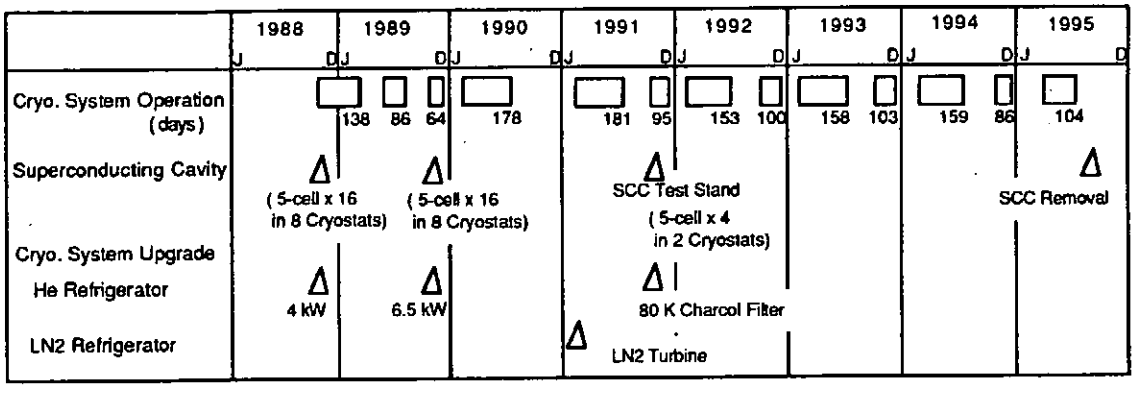

Fig. 1 Operational history of the cryogenic system for TRISTAN RF cavities

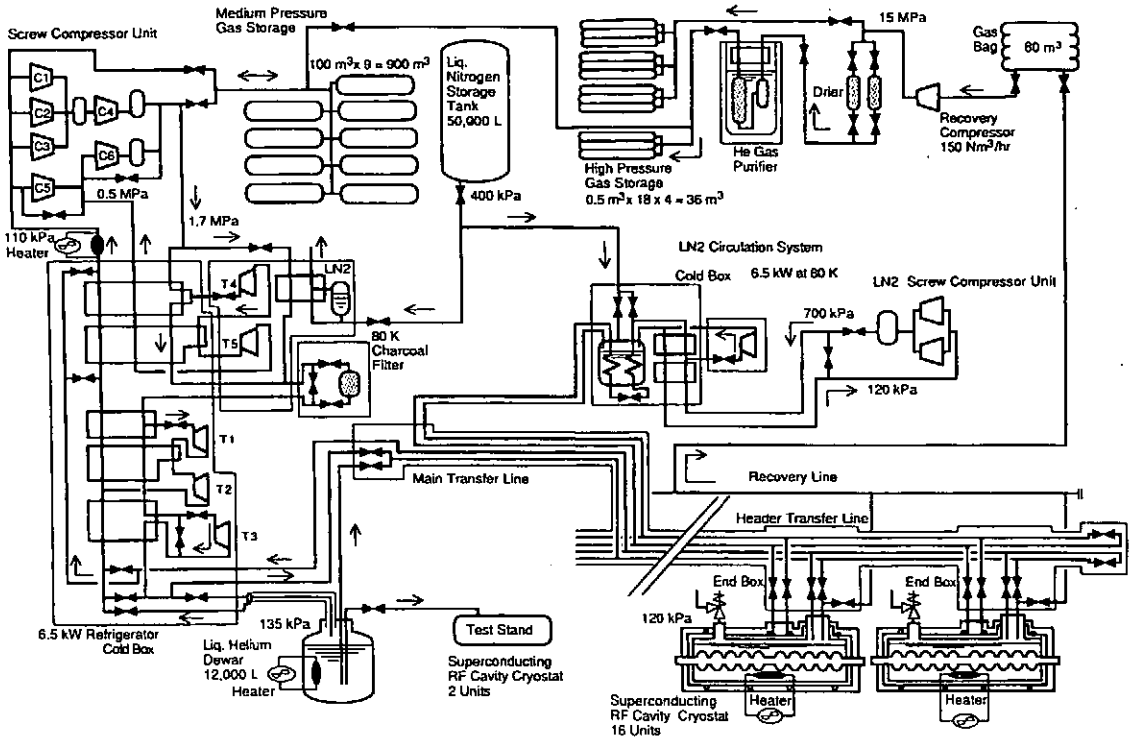

Fig. 2 Flow diagram of the cryogenic system for TRISTAN RF cavities.

continued until end of the TRISTAN physics run in June 1995. The total operation time of the cryogenic system is abut 38,000 hours.

SYSTEM OVERVIEW

The flow diagram of the cryogenic system is shown in Fig. 2. The helium refrigerator with 5 turbo-expanders (T1- T5) has cooling capacity 8 kW at 4.4 K without liquid nitrogen precooling. The total required electic power is 2.6 MW including 130 kW for cooling water and oil pumps. The supercritical turbo-expander T3 was installed just before J-T valve to increase the cooling capacity from 4 kW to 8 kW. The helium compressor unit consists of 6 oil flooded screw compressors and 4 stage oil filters. Liquid helium produced in a 12,000 L liquid helium dewar is distributed to 16 SCC cryostats installed in about 200 m long straight section of underground TRISTAN tunnel through large size about 250 m long multi-channel transfer line. The liquid helium is also supplied to SCC test stand where we could cool down and test the spare SCC in 2 cryostats. Each cryostat contains two 5-cell 508 MHz SCC made of about 2mm thick pure niobium sheet. The cold mass and amount of liquid helium stored in a cryostat are about 1,000 kg and about 830 L respectively. The total amount of liquid helium handled in the system is about 16,500 L. For the helium gas recovery 9 x 100 m^3 medium pressure (1.9 MPa) helium gas storage tanks are connected to the system. A 6.5 kW at 80 K liquid nitrogen circulation system with a turbo-expander and 2 screw compressors in parallel supply liquid nitrogen to 80 K thermal shield in the 16 cryostats in parallel through muti-channel transfer line. A off-line helium gas recovery system consists of a 5 stage air-cooled oil lubricated reciprocating compressor (15 MPa, 150 Nm^3/hr), high pressure low temperature purifiers (80 K, 15 MPa, 150 Nm^3/hr), and high pressure storage vessels (4 x 1350 Nm^3). The whole cryogenic system is controlled by means of a process control computer system.

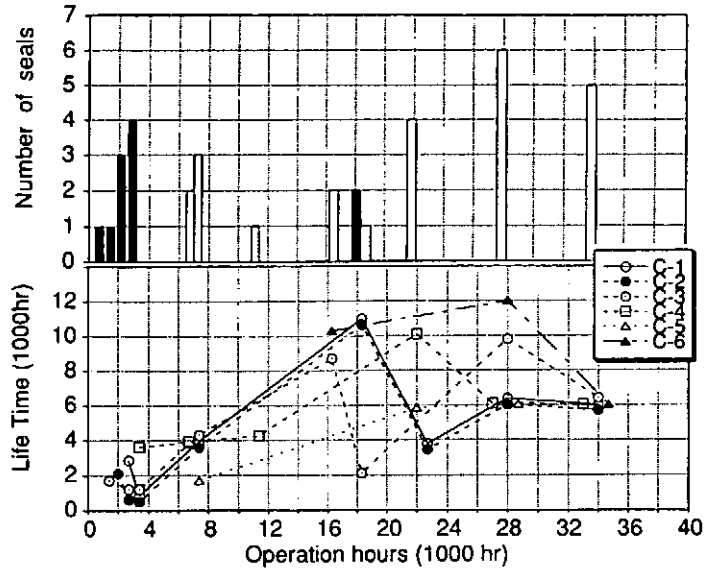

Fig. 3 Replacement and Lifetime of screw compressor's shaft seals

MAINTENANCE

The inspection and maintenance of the cryogenic system were performed regularly once a year during summer shut down of the system. The cryogenic system is obligated to inspect the gas tightness of the system, to measure the thickness of the vessel and pipe walls, to check the operation of safety valves and to correct pressure gauges and thermometers once a year by high pressure regulation law. During this period mechanical machines with wearing parts, such as the compressors, including the air compressors, motors, oil pumps, turbines and valves were inspected carefully and repaired if necessary. The charcoal adsorber of the main helium compressor unit was also changed. In addition the maintenance of the process control computer system were carried out.

Compressors

Figure 3 shows the history of the replacement and the lifetime of the mechanical shaft seals of the compressors. At an early stage in the operation the mechanical seals of the compressors had to be replaced due to leakage of oil from it. These replacements are shown by black bars in Fig. 3. The oil leakage was caused by worn out of pins used for fixed the seal by the mechanical vibration of the compressors. These failures were overcome by improving the hardness of the pins. After the adoption of new type pins lifetime of the seals increased more than 5,000 hours as shown in Fig. 3. The mechanical shaft seals of the main compressors were replaced at annual regular maintenance for precaution. These replacements are shown by white bars. The compressors of the 2nd stage were send to the factory for detailed inspection including the bearing every three years. The checks revealed no damage. The adosorber of the main compressor unit is filled with 1580 L of charcoal and 400 L of molecular sieve. The charcoal adosober had to be changed every year (about 6,000 to 7,000 hours intervals), because the guaranteed lifetime of the charcoal adosorber is 8,000 hours. The replaced new charcoal filter was activated by removing the water using 120 °C dry nitrogen gas.

FAILURES OF THE CRYOGENIC SYSTEM

The total number of failures in the cryogenic system during about 7 years operation was

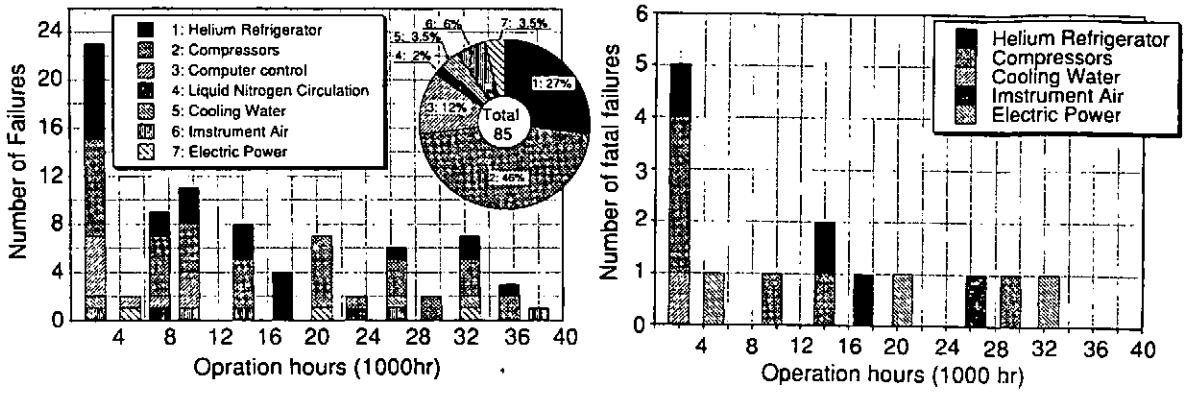

Fig. 4 Statistics of the failures and fatal failures during 7 years operation of the system

85. This number includes 71 failures which did not interrupt the operation of the system and 14 fatal failures which caused the whole system stop. Figure 4 shows the statistics of failures and fatal failures as the function of the operation hours. We classified the failures into seven categories : 1) helium refrigerator (coldbox, turbo-expanders, distribution system), 2) compressors (mechanical seals, oil pump, oil valves etc.), 3) computer control system, 4) liquid nitrogen circulation system, 5) cooling water, 6) instrument air, 7) electric power (main power failure by thunderstorm etc.). The total down time and recovery time of the cryogenic system, during 38,000 hours operation in 7 years, are 24 hours and 197 hours respectively.

SUMMARY

The cryogenic system for the TRISATN superconducting RF cavity was operated very stably and reliably for about 38,000 hours in 7 years. The experience in long operation of the large cryogenic system shows the compressor is the key component and the regular maintenance of the system including utilities is essential to attain the system reliability.

ACKNOWLEDGMENT

The authors wish thanks Professors S. Kurokawa and Y. Kimura for thier continuous support and encouragement and the operation crew, the staff of the superconducting cavity group and Mr. M. Noguchi of Mayekawa for their devoted support and many helpful discussions.

REFERENCES

1. Y. Kimura, TRISTAN project and KEK activities, in: Proc.XIII the International conference on high energy accelerators", Novosibirsk, U.S.S.R., (1986)
2. K. Hara et al., Cryogenic system for TRISTAN superconducting RF cavity, in: "Advances in Cryogenic Engineering", Vol.33, Plenum Press, New York (1988),p.615
3. K. Hosoyama et al., Cryogenic system for the TRISTAN superconducting RF cavities: performance test and present status, in: "Advances in Cryogenic Engineering", Vol.35, Plenum Press, New York, (1990) p.933
4. K. Hosoyama et al., Cryogenic system for TRISTAN superconducting RF cavities: upgrading and present status, to be published in: "Advances in Cryogenic Engineering", Vol.37, Plenum Press, New York,(1992)

The HERA Cryogenic System as an Example for a Large Scale Cryogenic System with High Availability and Reliability

H. Lierl
Deutsches Elektronen-Synchrotron, DESY-MKS1, Notkestrasse 85,
D 22607 Hamburg, Germany

ABSTRACT

The central cryogenic plant of the 6.3 km long HERA superconducting proton accelerator ring at DESY in Hamburg, Germany, cooles 422 main dipoles, 224 main quadrupoles, correction magnets, s.c. cavities and experiment magnets with helium at 4.4 K. It consists of three identical cold boxes with a total cooling capacity of 3 times 6500 Watts at 4.4 K and 3 times 20 kW for the shield cooling around 60 K. For about 43,000 operating hours the cooling system has nearly continuously run at 4.4 K. It operates very stable, reliable and with an availability of more than 98%. Besides operating and maintenance experience this paper shows an analysis of failures and discusses reasons for the good performance of this large scale system. Information about operating costs, helium losses, liquid nitrogen and electrical power consumption are also given.

INTRODUCTION

The HERA cryogenic plant[1,2] started to get into operation in 1987. Together with the system for the helium distribution along the 6.3 km long ring tunnel the whole system[3] was completed in 1990. Besides some other components it cools the 646 main dipoles and quadrupoles which represent a cold mass of 3450 t. Since the start of the accelerator operation in 1991 a continuous, stable and reliable cryogenic supply was mandatory. After a short description of the system this paper describes the operating experience, the reliability and availability of the system, the failure statistics, maintenance experience and the costs and organisation of the operation over several years.

THE CRYOGENIC SYSTEM

There is a central cryogenic plant[4] with three coldboxes and a total of 14 oil lubricated screw compressors which produce the cooling power needed to cool the accelerator ring magnets as indicated in Fig. 1. The helium is compressed in two steps up to 18 bar by a group of four compressors. It is cleaned by a gas purification system in front of each cold box. Before the cold helium leaves the cryogenic hall it is precooled to 4.4 K in two liquid helium storage dewars. Through a big valve box it is directed into two strings of a 4 fold cryogenic transfer line, each supplying one half of the HERA magnet ring. All magnet octants in the ring tunnel, which consist of 623 m long strings of 53 dipoles and 26 quadrupoles, are cooled in parallel. There is a 4.4 K precooler box in front of each octant. Helium supply and end boxes with valves, current leads, sensors and measuring devices at both ends of each octant are used for the different operating modes like cool down, warm up, stationary operation and quench recovery. Experiment magnets, two reference magnets and 16 superconducting cavities are also supplied from the transfer line. The magnets are cooled by supercritical single phase helium at 4.4 K and by a shield cooling circuit between 40 K and 80 K. There is a 300 K high pressure warm up line in the tunnel and a quench gas line which collects the exhausted gas from the magnets after a quench and which directs the helium

to big buffer tanks in front of the cryogenic hall from where it is compressed and reliquified. The main parameters of a coldbox are shown in table 1.

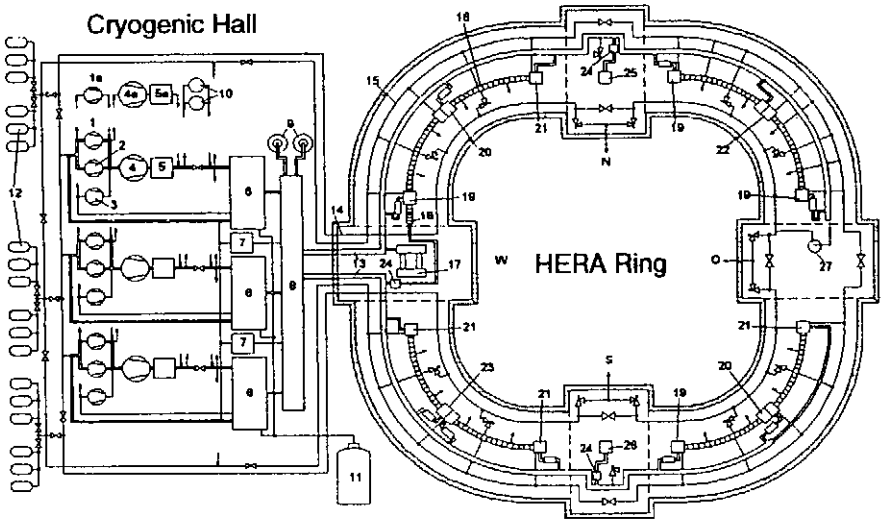

Figure 1 Schematic Layout of the Cryogenic System

1,2,3,1a: *Compressors (low pressure: 1 → 4 bar)*; **4,4a**: *Compressors (high pressure 4 → 18 bar)*; **5,5a**: *Helium Purification System*; **6**: *Coldboxes*; **7**: *Helium Warmers*; **8**: *Helium Distribution Valve Box*; **9**: *Liquid Helium Storage Dewars (2 x 10 m³)*; **10**: *LN_2 cooled purifiers*; **11**: *LN_2 Dewar (150 m³)*; **12**: *Helium Gas Storage Tanks (18 x 267 m³, 20 bar)*; **13**: *Transfer Lines with 4 Process Tubes*; **14**: *Quenchgas Collection Line*; **15**: *Warm, High Pressure Helium Line (300 K, 18 bar)*; **16**: *Superconducting Magnets*; **17**: *Two superconducting Reference Dipoles*; **18**: *16 Superconducting Cavities (Elektron Ring)*; **19**: *Precoolers and Helium Feed Boxes*; **20, 22, 23**: *Middleboxes (Kombination of Feedbox and/or Endbox)*; **21**: *Endboxes with Joule-Thomson-Valve*, **24**: *Detector-Supply Boxes*; **25**: *"H 1"-Detector*; **26**: *"ZEUS"-Detector*,

Table 1: Main parameters of a HERA coldbox

Refrigeration at 4.4 K	6500 W	Total mass flow rate	871 g/s
Refrigeration at 40/80 K	20000 W	Primary power consumption	2845 KW
Current leads cooling at 4.4K	20.5 g/s	Specific power consumption	281 W (300 K)/ W (4.4 K)

REDUNDANCY

The amount of redundancy within the cryogenic system defines the grade of maintenance and uninterrupted cryogenic supply which can be achieved during continuous operation of the system. The HERA cryogenic system was specified with the following high grade of redundancy: There are three cold boxes whereas for normal operation only two of them are needed, one for each half ring. The third coldbox is in standby and serves as redundancy or can be used to supply additional test stands in a magnet test hall. It takes about 1 or 10 hours to switch to a spare coldbox being in cold or warm standby respectively. Even more redundancy exists for the compressors: normally only the two compressor groups in front of the corresponding active coldboxes are in operation. The third compressor group can be switched to each of the other coldboxes (Fig. 1). In addition there exist for each group of the two compression stages a single redundant low pressure and a redundant high pressure machine which can be switched to each position within the other three compressor groups to replace a faulty machine. A similar amount of redundancy exists also for the helium purification systems: behind each compressor group there are oil seperators, oil coalescence filters, pairs of interchangeable helium dryers and charcoal oil adsorber units. Also the single redundant compressor units have their own dryer pair and oil adsorber. A pair of interchangeable liquid nitrogen cooled low temperature purifiers, specified to clean the total helium flow rate of each compressor group can be switched into the helium stream to each coldbox. The process control computer system[5] uses seperate control computers for all main components like compressors, coldboxes, the helium distribution system, cavities etc.. The most critical ones have a redundant back up computer running in "hot stand by". They are all linked to a redundant communication ring. The display computers

driving the operator consoles and a redundant host are also linked to this ring and to the local area network. For the layout of the system an additional safety of 50 % for the 4.4 K cooling power, 10% for the schield cooling circuit and a factor of 2.5 for the current leads cooling was applied to the expected heat loads. During normal operation the HERA cryogenic system runs at about 66 % maximum load of the cold box at 4.4 K and at about 80 % load at the shield circuit.

OPERATIONAL EXPERIENCE

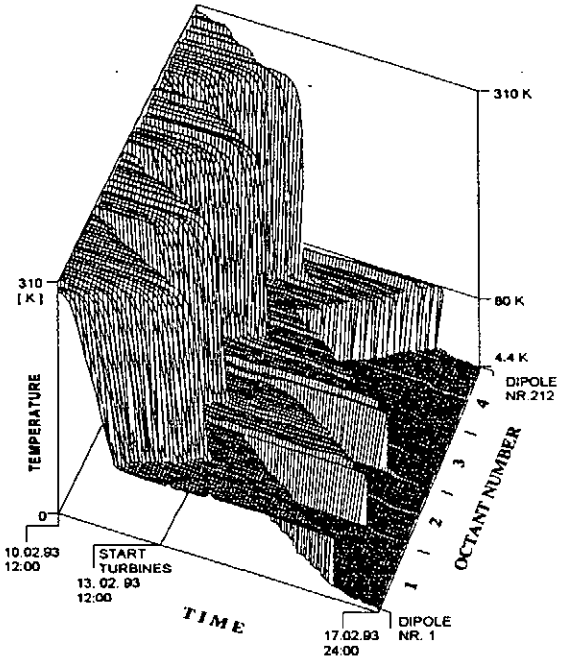

Figure 2 Cool Down of a HERA Halfring in 3 Steps:Temperature Map of the HERA Dipoles

Since 1990 the cryogenic system was running continuously at 4.4 K [6], interrupted only by regular shut down periods of the accelerator. The average annual running time is about 7000 hours. Besides some local warm ups of single octants, which were necessary for repair work at the magnets [7], the whole system saw seven cool down / warm up cycles within 43,000 operating hours. The redundant coldbox is used about 600 hours per year. In total it ran 20,000 hours. For a cool down or warm up ten days are needed. A maximum temperature gradient of 20 K/h is allowed. The cool down is performed in three steps: from 300 K to 80K, to 10 K and down to 4.4 K (Fig. 2). In the first step the helium is cooled only by liquid nitrogen, in the last two steps the turbo expanders in the coldboxes and an additional Joule-Thomson expansion at the end of the magnet octant are used respectively. During steady state operation the temperature in the magnets is stable within about 20 mK and varies along an octant not more than 100 mK. The flow rates are normally 31 g/s at 4.4 K and 12 g/s at 40 K and in total 10 g/s liquifaction rate for all power leads. There are no problems with oscillations of pressure, temperature or massflow rates in the system. In 1995 there were 50 quench alarms detected: 36 of them were induced by beam losses, four were test quenches and three were fake quenches from the electronics or were initiated by a general power failure. Only for 10 quenches the necessary restabilisation of the cryogenic supply produced some accelerator downtime. It takes 20 minutes to empty the quench gas line and half an hour to recool the magnets which reach about 20 K after a quench. Reliquifying, filling of the magnets and establishing again steady state cooling conditions take another one to two hours depending on the size of the quench. The cryogenic system is run by two to three operators in three shifts a day. The producer of the cryogenic plant has a contract to operate the plant which includes all the maintenance and repair work and which led to a very reliable operation.

AVAILABILITY, RELIABILITY AND MAINTENANCE EXPERIENCE

The HERA cryogenic supply has a very high availability with an average value of more than 98 % over several years, Fig.3. This good result is due to the high grade of redundancy of the system. It is always possible to switch over to a spare compressor group or coldbox in case of problems. Thus a careful maintenance of the machines is possible without interruption of the cryogenic supply. Maintenance is necessary for components like compressors, motors, oilpumps, valves, filters, adsorbers, purifiers, power supplies, switches, electrical contacts and electronic components in the control system. After 25,000 operating hours there is a general overhaul of the compressors. The shaft seals of compressors and oil pumps are replaced at oil leakrates >5 l/1000h. Their average

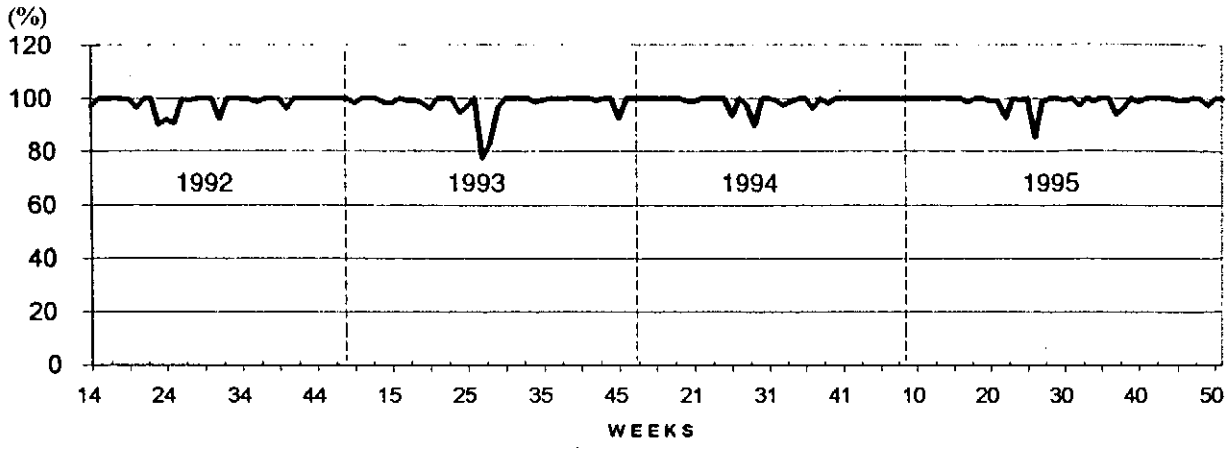

Figure 3 Availability of the Cryogenic System 1992-1995

lifetime is about 2500 hours with a big variation. Once a year the quality of the compressor oil is checked. Up to now no change of oil was necessary. The turbines of the coldboxes don't need any maintenance. But most of the 5 µm turbinefilters in front of it have to be changed nearly every 1400 hours because of aluminium dust coming from the heat exchangers. For some turbines this can be done without interruption of the cryogenic supply. Gas contaminations are maintained at levels less than 1 vpm for H2, O2, N2. Impurities at the outlet of the low temperature purifiers are less than 1 ppm. Their regeneration time is 16 hours after 24 hours of operation. The power transformers for the compressors are serviced once a year, the power supplies every two years whereas the cooling water components and the air compressors are cleaned four and twelf times a year respectively.

FAILURES

Despite the extensive and continuous maintenance there are still failures which are summarised for different categories in Fig.4. Because of a fast correction of failures by the operators and because of the existing redundancy not each failure produces a downtime of the cryogenic supply. Whereas the failure rate of the cryogenic system itself became negligable the main sources are still power interruptions by i.e. thunderstorms and failures within the control computer system.

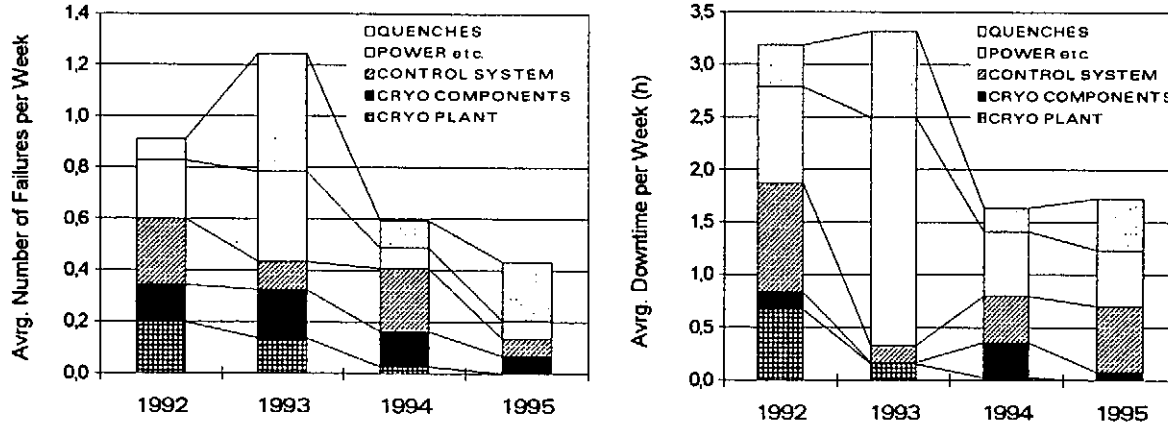

Figure 4 Statistics of failures and downtime of the cryogenic supply 1992-1995

We have identified the most critical failures in the system which will interrupt the cryogenic supply if there will be no reaction by the system itself or by the operators within the indicated time (table 2).

Table 2 Critical failures which can close down the cryogenic supply

Component	Device	Origin of failure	Frequency of failures (# per month)	Critical reaction TIME (minutes)
Cryo Plant	Compressors/ Oilpumps	Main power failures	2	150ms, >300ms
		Oil coolers	1	5-10
		Cooling water	3 per year	15-30
		Slide valves	1	hours
		Shaft seals	2	days
		Break of oil tubes	<1 per year	0
		Computer/PLC Failures	1	0
	Coldboxes	Turbines	2 in 9 years	0
		Turbine filters blocked (Contaminations or dust from heat exchangers)	1	1 h. - 10 days
		Adsorber seals	2 per year	hours
		Pressure bumps	4	5
Total Cryo System	Cryo Control System	Valves (AO,DO)	2-3 per year	1-5
		Measuring points (AI)	2-3 per year	2-?
		Cooling of computers	2-3 per year	30
		Power failure	2	0-20
		Elektronic power supplies	1	0-?
		Data network	1	0-?
	Sensors	Measuring capllaries (p, m)	2-3	2-?
		Temperatures	4 per year	uncritical
		Level sensors	0-1 per year	10
	Valves	Friction	2-3 per year	1-5
		Control air	1 per year	0-30
		Valve cone	1 per year	0
	Heaters	control electronics/ leads	0-1 per year	10
	Insulation vacuum	Leaks / failure of pumps	0-1 per year	0-?

OPERATING COSTS

Besides the costs for the operating contract which covers all the maintenance, repairs and risks and besides personnel costs the main contributions are costs for electrical power and LN2 consumption for the cool down which amounts to 1.5 million liters per year. From the 16 t helium inventory we have to compensate about 40 % losses per year. Fig. 5 shows the break up of annual operational costs for the cryogenic system.

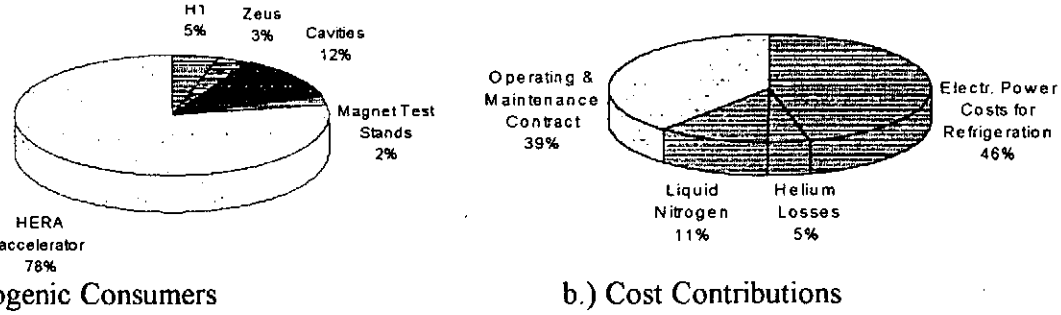

a.) Cryogenic Consumers b.) Cost Contributions

Fig. 5 Operational Costs of the Cryogenic System

SUMMARY

The HERA cryogenic system is an example for a large scale cryogenic system with very high reliability and availability. Operational experience over several years shows that there a no principal problems to operate a large scale system reliably but a lot of small and sometimes critical failures have to be managed by experienced personnel in order not to produce downtime of the cryogenic supply. Enough redundancy in the system is very essential and helps a lot because it opens the possibility to perform permanent maintenance and repairs even during continuous cryogenic operation of the whole system.

REFERENCES

1 Barton jr. H. R., Clausen M., Horlitz G., Lierl H., Central Refrigeration System for the Superconducting HERA Proton Magnet Ring, Proceedings ICFA Workshop on Superconducting Magnets and Cryogenics, Brookhaven Nat. Lab., Upton, N.Y., May 12-16, 1986.

2 Barton jr. H.R et al., The Refrigeration System for the Superconducting Proton Ring of the Electron Proton Collider HERA, Adv. in Cryog. Eng., Plenum Press, N.Y.,1986, 31, 634

3 Lierl H.,Wolff S., Superconducting Magnet and Cryogenic System of HERA. Review Article in Japanese Cryogenic Engineering (TEION KOGAKU), to be published.

4 Main contactor of the *cryoplant*: Sulzer AG, Winterthur, now: Linde Kryotechnik AG, Pfungen, Switzerland. *Compressors*: Aerzener Maschinenfabrik, Aerzen, Germany. Liquid helium storage *dewars*: L'Air Liquide, Sassenage, France. *Transfer lines*: Linde A.G., Munich; Deutsche Babcock A.G., Oberhausen, Germany; DeMaCo, Heerhugowaard, Holland.

5 Clausen M. et al., Experience with a Process Control System for Large Scale Cryogenic systems, Adv. in Cryog. Eng., Plenum Press, New York, 1988, Vol. 33, p. 1113

6 Clausen M., Herzog H., Horlitz G., Knopf U., Lange R., Lierl H., Cryogenic Test and Operation of the Superconducting Magnet System in the HERA Proton Storage Ring, Adv. in Cryog. Eng., Plenum Press, New York, 1992, Vol. 37A, p. 653

7 Wolff S., Operational Experience with Large Superconducting Magnet Systems, Applied Superconductivity, Pergamon Press, 1993, Vol. 1, Nos. 10-12, p. 1457

Helium Cryogenic Systems for the LEP2 and LHC Projects at CERN

Ph. Lebrun *on behalf of* The CERN Accelerator Cryogenics Group
LHC Division, CERN, CH-1211 Geneva 23, Switzerland

ABSTRACT

CERN is presently operating a large distributed 4.5 K helium cryogenic system (48 kW@4.5 K equivalent) for cooling the superconducting acceleration cavities of the 26.7 km circumference LEP2 lepton collider. This also constitutes the first part of the 1.8 K cryogenic system (about 150 kW@4.5 K equivalent) for the future Large Hadron Collider (LHC), the high-field superconducting magnets of which will operate in superfluid helium. We briefly describe the main features of each system, and review the progress of their development, construction and operation.

INTRODUCTION

Particle physics has *volens nolens* become a prime user of large-capacity helium cryogenics, through the generalized use of superconducting devices for accelerating, guiding and focusing high-energy particles in recent accelerators and colliders [1, 2]. The specific requirements, both qualitative and quantitative, set by advanced projects have represented a strong driving force to stimulate technological development in the field and push helium cryogenics out of the laboratory into industrial-scale systems routinely operating with high reliability and high efficiency. At CERN, the European Laboratory for Particle Physics, this evolution took place in the last decade [3], with the superconducting quadrupoles of the LEP high-luminosity insertions, the LEP energy upgrade (LEP2) using superconducting acceleration cavities in large numbers, and the Large Hadron Collider (LHC) project based on high-field superconducting magnets and superfluid helium cryogenics on an unprecedented scale (Figure 1).

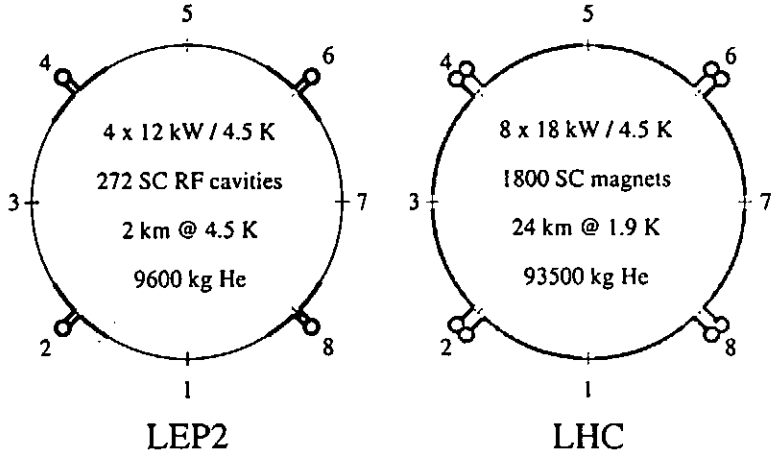

Figure 1 Overview of cryogenics for LEP2 and LHC

ACCELERATING HIGH-ENERGY LEPTONS IN SUPERCONDUCTING CAVITIES: THE LEP2 PROGRAMME

CERN has been operating since 1989 the LEP facility, a high-energy circular electron-positron collider installed in a 26.7 km circumference underground tunnel in the vicinity of Geneva, Switzerland. This machine was primarily built to perform precision studies of the vector bosons which mediate the electroweak interaction. In order to limit the loss of energy by synchrotron radiation from the circulating leptons, LEP has a large radius of curvature and uses low-field, resistive electromagnets for beam guidance. To increase the beam energy of LEP from 45 to 96 GeV and thus open the way for production of W^+W^- pairs (the LEP2 programme), up to 272 superconducting acceleration cavities, operating at 352 MHz with a total active length of about 400 m, are being installed at four equidistant locations in long straight sections around the tunnel, and at depths of up to 150 m below ground level [4]. The four-cell cavities are assembled in strings of four inside common cryomodules, cooled in a bath of saturated (boiling) helium at 1.25 bar [5]. Operation of the cavities at their nominal accelerating gradient of 6 MV/m requires large-power refrigeration at 4.5 K (Table 1).

Table 1 Refrigeration loads of a LEP2 four-cavity cryomodule

Isothermal @ 4.5 K, Static	80	W
Isothermal @ 4.5 K, Dynamic	250	W
Liquefaction 4.5-290 K	0.8	g/s

Refrigeration is provided by four cryogenic plants producing each 12 kW@4.5 K equivalent, and ultimately capable, after upgrading, of 18 kW@4.5 K (Table 2). These plants, designed and constructed by two European suppliers, are of split-coldbox, compact design. The upper coldboxes, located at the surface, operate between 290 and 20 K, and are connected by vertical interconnecting lines to 20-to-4.5 K lower cold boxes installed in caverns at tunnel level [6]. As a consequence of commercial incentives in the procurement contracts and sound technical competition between vendors, the thermodynamic cycles feature high efficiency, with a measured coefficient of performance of 225 W/W@4.5 K. A set of gas-shielded transfer lines, extending 250 m on either side of the lower coldboxes, distributes liquid helium to, and recovers saturated vapour from the cryomodules in the tunnel. Fully automatic operation of the whole system is achieved by means of an industrial, multiprocessor-based process control system running object-oriented software [7]. The 2400 kg helium inventory at each of the four LEP2 sites can be stored in gaseous form at 2 MPa and ambient temperature. The general layout of cryogenic equipment at a LEP2 site is sketched in Figure 2.

Table 2 Refrigeration capacity of LEP2 cryoplants

Isothermal @ 4.5 K	10	kW
Non-isothermal @ 50-75 K	6.7	kW
Liquefaction 4.5-290 K	0.8	g/s

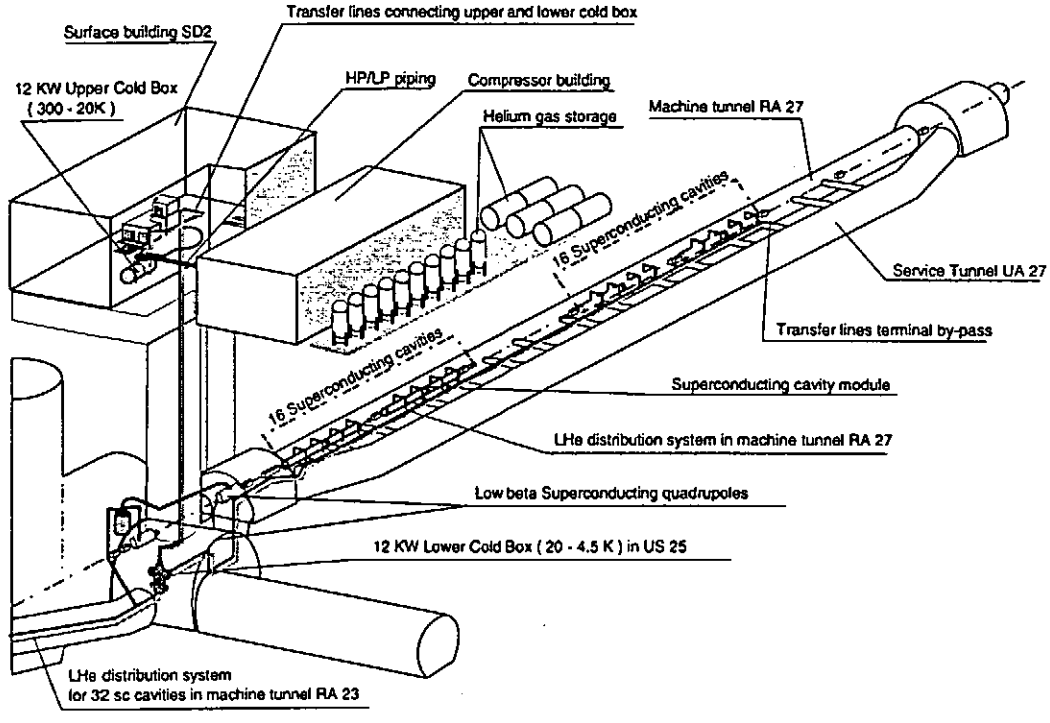

Figure 2 Overall view of cryogenics on a LEP2 site

All plants have been procured, installed and commissioned between 1990 and 1994 [8]. LEP is now currently operating with increasing numbers of superconducting cavities, gradually installed during programmed machine shutdowns [9]. The LEP2 programme is expected to be completed by 1998, and will produce physics until the end of the decade.

COLLIDING HADRONS GUIDED BY HIGH-FIELD SUPERCONDUCTING MAGNETS OPERATING IN SUPERFLUID HELIUM: THE LHC PROJECT

At the end of 1994, the CERN Council approved the construction of the Large Hadron Collider (LHC) project, a proton and ion collider with center-of-mass energy in the TeV-per-constituent range. This machine, to be installed in the LEP tunnel at the end of LEP2 operation, will allow to probe the fine structure of matter at the unexplored scale of 10^{-19} m, by recreating in the laboratory conditions of "temperature" which prevailed in the very early universe. To guide and focus its stiff hadron beams, the LHC will make use of high-field superconducting magnets with a bending field of 8.4 T, operating in pressurized superfluid helium at 1.9 K, over most of the circumference [10, 11]. The LHC cryogenic system, unprecedented in size and complexity [12], will make use of the four LEP2 refrigeration plants, adequately modified and upgraded, as well as of four new plants of similar capacity. At their lower-temperature end, eight additional coldboxes will generate a total of about 20 kW@1.8 K, using multiple-stage, low-pressure cryogenic compressors. The cryogenic power requirements of the LHC sector cryoplants [13] are given in Table 3. Depending upon the particular insertion magnets and equipment to be cooled in each of the eight sectors, four cryogenic plants will feed high-load sectors, and the other four, low-load sectors. Although comparable in entropic

capacity with the upgraded LEP2 refrigerators, the LHC cryogenic plants mostly provide non-isothermal cooling, which will require substantial modifications to cycles and equipment.

Table 3 Refrigeration capacity demands of LHC sector cryoplants

	50-75 K [kW]	4.5-20 K [kW]	4.7 K [kW]	1.8 K [kW]	20-290 K (*) [g/s]
High-load	31	4.3	0.80	2.80	35
Low-load	30	4.3	0.65	2.45	23

(*) For cooling the resistive upper section of HTS current leads

A cryogenic distribution system exploiting the specific properties of superfluid helium, will maintain the furthest magnets within 0.1 K of the temperature at the cryogenic plants, over the 3.3 km length of each sector (Figure 3). Efficient cryostats, with multiple shielding and heat interception, will limit heat loads and contribute to contain refrigeration budgets within technically acceptable limits (Table 4).

Table 4 Distributed heat loads in LHC arcs [W/m]

	50-75 K	4.5-20 K	1.9 K
Heat inleak	6.38	0.13	0.27
Resistive heating	0.04	-	0.11
Beam-induced (ultimate)	-	1.35	0.05
Total	6.42	1.48	0.43

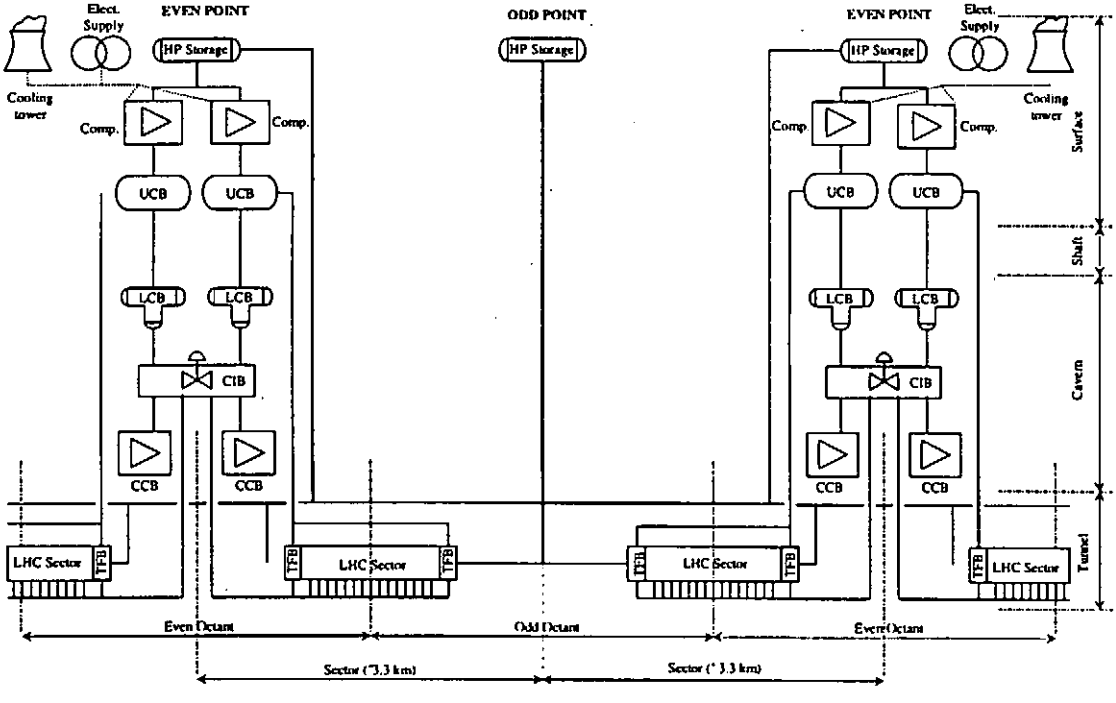

Figure 3 General architecture of LHC cryogenics

A vigorous development programme, conducted in collaboration with national laboratories and industry, has permitted to validate design choices for LHC cryogenics on prototype components, particularly as concerns cryostat design and performance [14], thermohydraulics of two-phase superfluid helium [15], cryogenic centrifugal compressors [16, 17] and complete system tests on a magnet string [18]. The project is now in the beginning of its construction phase, and is expected to start producing physics at full energy in 2005.

CONCLUSION : MEGASCIENCE AS MOTOR OF TECHNICAL DEVELOPMENT

Large projects in particle physics have stimulated the development of helium cryogenics on an industrial scale, and created a reservoir of know-how and experience in the field. Besides providing immediate returns to the work in progress, both actions may be seen as long-term investments opening the way for the increased use of applied superconductivity in science, technology and society.

REFERENCES

1 Horlitz, G., Refrigeration of Large-Scale Superconducting Systems for High-Energy Accelerators, Cryogenics (1992) 32 ICEC Supplement 44-51

2 Lebrun, Ph., Large-scale Cryogenics for Particle Accelerators, Proc. XXVI Int. Conf. on High-Energy Physics, AIP (1993) 2000-2007

3 Lebrun, Ph. *on behalf of* The CERN Cryogenics Group, Cryogenics in CERN Accelerators, Proc. Kryogenika'94 Usti nad Labem (1994) 96-100

4 The LEP2 Team, LEP Design Report Volume 3 LEP2, Wyss, C. ed., CERN/AC/96-01(LEP2) (1996)

5 Güsewell, D., Barranco-Luque, M., Claudet, S., Erdt, W.K., Frandsen, P.K., Gayet, Ph., Schmid, J., Solheim, N.O., Titcomb, Ch. & Winkler, G., Cryogenics for the LEP2 Superconducting Cavities at CERN, Proc. PAC'93 (1993) 4 2956-2958

6 Claudet, S., Erdt, W.K., Frandsen, P.K., Gayet, Ph., Solheim, N.O., Titcomb, Ch. & Winkler, G., Four 12 kW / 4.5 K Cryoplants at CERN, Cryogenics (1994) 34 ICEC Supplement 99-102

7 Gayet, Ph., Claudet, S., Frandsen, P.K., Juillerat, A., Kuhn, H.K., Solheim, N.O., Titcomb, Ch., Winkler, G., Wolles, J.C. & Vergult, P., Architecture of the LEP2 Cryogenics Control System: Conception, Status and Evaluation, Cryogenics (1994) 34 ICEC Supplement 83-86

8 Barranco-Luque, M., Claudet, S., Dauvergne, J.P., Erdt, W.K., Frandsen, P.K., Gayet, Ph., Güsewell, D., Lebrun, Ph., Schmid, J., Solheim, N.O., Titcomb, Ch., Wagner, U. & Winkler, G., Conclusions from Procuring, Installing and Commissioning Six Large-Scale Helium Refrigerators at CERN, presented at CEC'95 Columbus (1995)

9 Barranco-Luque, M., Claudet, S., Gayet, Ph., Solheim, N.O. & Winkler, G., Operation of the Cryogenic System for Superconducting Cavities in LEP, presented at ICEC16 Kitakyushu (1996)

10 The LHC Study Group, The Large Hadron Collider, Conceptual Design, Lefèvre, P. & Pettersson, T. eds., CERN/AC/95-05(LHC) (1995)

11 Evans, L.R., The Large Hadron Collider Project, invited paper at ICEC16 Kitakyushu (1996)
12 Lebrun, Ph., Superfluid Helium Cryogenics for the Large Hadron Collider Project at CERN, Cryogenics (1994) 34 ICEC Supplement 1-8
13 Lebrun, Ph., Riddone, G., Tavian, L. & Wagner, U., Demands in Refrigeration Capacity for the Large Hadron Collider, presented at ICEC16 Kitakyushu (1996)
14 Benda, V., Dufay, L., Ferlin, G., Lebrun, Ph., Rieubland, J.M., Riddone, G., Szeless, B., Tavian, L. & Williams, L.R., Measurement and Analysis of Thermal Performance of LHC Prototype Dipole Cryostats, presented at CEC'95 Columbus (1995)
15 Rousset, B., Investigation of the Cooling Scheme for the LHC Superconducting Magnets, presented at this symposium
16 Lebrun, Ph., Tavian, L. & Claudet, G., Development of Large-Capacity Refrigeration at 1.8 K for the Large Hadron Collider at CERN, Proc. Kryogenika'96 Praha (1996) 54-59
17 Decker, L., Löhlein, K., Schustr, P., Vins, M., Brunovsky, I., Tucek, L., Lebrun, Ph. & Tavian, L., A Cryogenic Axial-Centrifugal Compressor for Superfluid Helium Refrigeration, presented at ICEC16 Kitakyushu (1996)
18 Bézaguet, A., Casas-Cubillos, J., Guinaudeau, H., Hilbert, B., Lebrun, Ph., Serio, L., Suraci, A. & van Weelderen, R., Cryogenic Operation and Testing of the Extended LHC Prototype Magnet String, presented at ICEC16 Kitakyushu (1996)

Cryogenic System for the Tevatron

M.G. Geynisman, B.L. Norris, J.N. Makara, J.C. Theilacker
Fermi National Accelerator Laboratory*
Batavia, Illinois, 60510, USA

Supporting the world's highest energy proton/antiproton collider in high energy physics research, the Fermilab Tevatron cryogenic system consists of a hybrid system of a Central Helium Liquefier feeding twenty-four 1 kW satellite refrigerators through a 6.5 km transfer line and supplying the liquid helium for the superconducting magnets of the accelerator and liquid nitrogen for the thermal shielding. Tevatron upgrades have been completed by 1996 and resulted in more than doubling the CHL liquefaction capacity, potential decrease of magnet operating temperatures from 4.9°K to 3.9°K, and proven increase of Tevatron energy from 900 GeV to 990 GeV without loosing operational stability.

SYSTEM OVERVIEW

The cryogenic system (see Fig.1) for the Fermilab's superconducting Tevatron accelerator has reached its 13th year of operation. The original design [1] of the Tevatron 6.5 km superconducting ring provided for 777 dipoles, 216 quads, 204 correction elements, and 86 specialty components located in a 2.1 m diameter concrete tunnel buried 6.0 m below ground, distributed refrigeration system located in 24 satellite refrigerator and 6 compressor buildings around the ring above ground, and liquefaction system of the Central Helium Liquefier (CHL) feeding satellite refrigerators through a 6.5 km co-axial transfer line supplying the liquid helium (LHe) for the superconducting magnets of the accelerator and liquid nitrogen (LN_2) for the thermo shielding. The original distributed refrigeration system had a capacity of 23.2 kW at 5°K, plus 1000 liters/hour of LHe to cool the magnet power leads. The original CHL helium liquefaction capacity was 4000 liters/hour. The helium inventory of the cold refrigeration system is 20000 liters, plus additional 10000 liters in the Tevatron transfer line. Losses of the helium inventory are made up via the 60000 liters liquid helium storage at CHL. Gas helium inventory transient control is available via 13 tanks (total volume of 1500 m^3, 1.7 MPa at room temperature). A Nitrogen Reliquefier (NRL), rated at 4680 liters/hour with three stages of compression, Refrigerant 22 precooling, and 151000 liters of liquid nitrogen storage were added to the system in 1985 [2]. NRL provides 80% of the LN_2 consumed for precool during normal 900 GeV operations with the remaining needs supplied from local LN_2 vendors.

Multiple modifications and additions have been made through the years to increase reliability of the cryogenic system, but major upgrades were incorporated in 90s to increase the particle energy in the Tevatron accelerator from 900 GeV to 1 TeV [3]. That has been accomplished through a) modification to the satellite refrigeration system to lower the temperature down by 1°K [4]; b) upgrade of the CHL [5]; c) upgrade of the refrigeration control system [6]. By 1995 all listed above upgrades have been completed, the system has been tested, and proven to be reliably functional at 3.93°K, thus providing for an increase of Tevatron energy up to 990 GeV without loosing an operational stability [7].

---

* *Work supported by U.S. Department of Energy under contract No. DE-AC02-76CH03000*

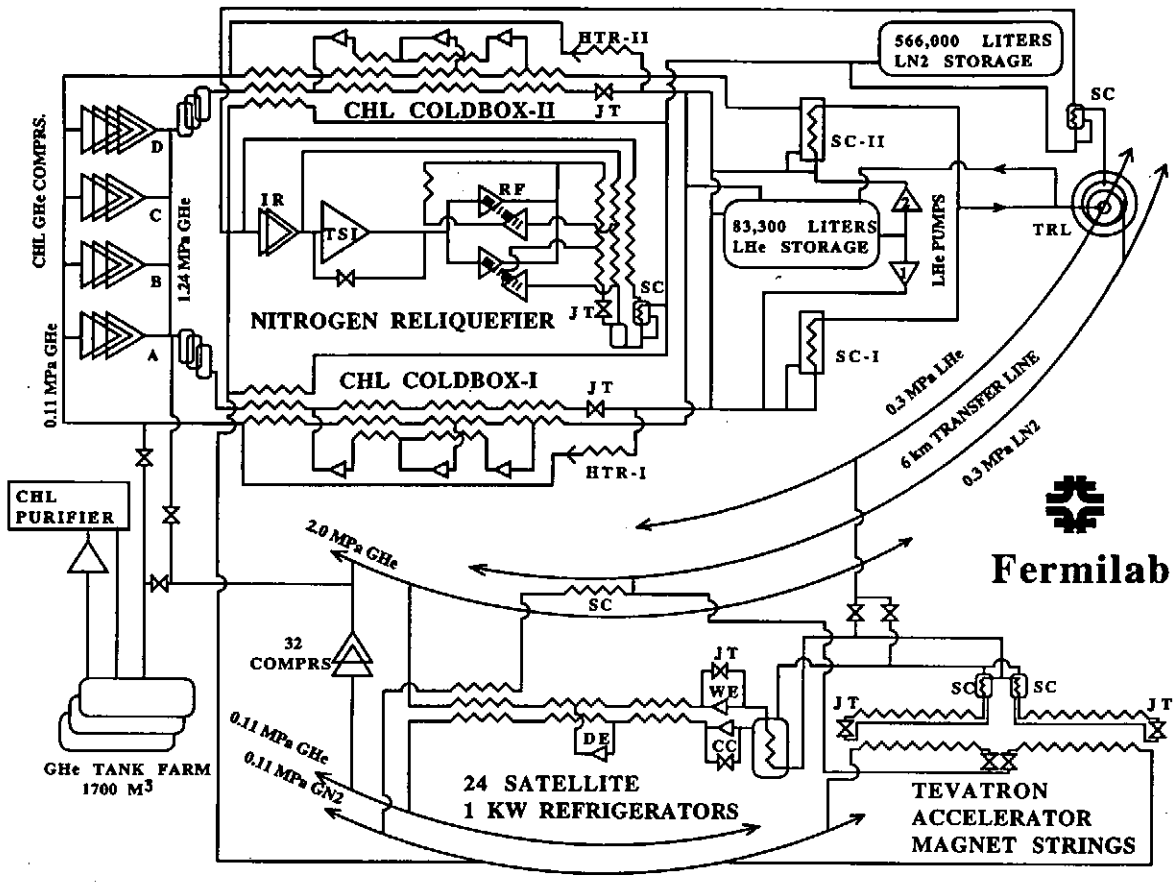

Figure 1 Cryogenic System for the Tevatron

DISTRIBUTED REFRIGERATION SYSTEM

The refrigeration system is divided into six sectors, each consisting of four refrigerators located above ground, ~1 km magnet string in the tunnel, and a compressor building. The system includes eight compressor buildings with total of 32 Mycom 2-stage 300 kW screw compressors which supply high pressure gas helium (2.03 MPa) to the satellite refrigerators coldboxes via a common 75 mm header. The refrigerators use counter flow heat exchangers to cool the high pressure helium flow from room temperature to 5.5°K at the inlet of 5.6 kW "wet" expander. The "wet" expander is controlled with AC variable frequency drive with Mitsubishi regenerative unit. The output of the "wet" expander is routed through a 130 liter subcooling dewar and return flow subcooler to the magnets strings. At the design 4.6°K magnet temperature each refrigerator has a capacity of 625 watts in a standalone mode (using 1.5 kW "dry" expander controlled with a regenerative DC motor/generator) and 966 watts consuming LHe from CHL in satellite mode. The current satellite refrigerator utilizes a new valve box with a 130 liter dewar serving as a phase separator for a "cold" compressor manufactured by Ishikawajima-Harima Heavy Industries Co., Ltd. (IHI). Each "cold" compressor pumps on a dewar to maintain the two-

phase pressure as low as 50.7 kPa (0.5 atm) producing 3.56°K helium in the dewar and magnet strings. The "cold" compressor is driven by 1.25 kW induction motor controlled with a Toshiba inverter controller incorporated into IHI control package. All two-phase to atmospheric connections have been "hardened" for reliable subatmospheric operation. The superconducting magnet coils are cooled by subcooled LHe that is continuously counter heat exchanged with two-phase flow. The advantage of a two-phase system is the possibility for uniform temperature over a long distance. There are forty-eight 125 m long magnet strings associated with the Tevatron. Typical temperature for the two-phase is 4.45°K for 900 GeV operations. The superconducting coils operate 10 to 400 mK higher due to heat leak and AC losses.

CENTRAL HELIUM LIQUEFIER

The inceptive design of the Tevatron cryogenic system envisioned redundancy of accelerator operations on either the CHL assisted satellite mode or stand-alone mode with twenty four dry expanders and LN2 precooling of the satellite system in periods when the CHL was off-line due to failure or trip. However, the refrigeration loads of the accelerator magnet system increased beyond the capacity of the stand-alone mode of the twenty four independent satellite refrigerators, thus making the CHL system vital for normal accelerator operations. The present CHL helium plant consists of: a) four parallel reciprocating compressors (three of 540 g/s, plus one of 750 g/s) rated at 5.1 MW total power; b) hydrocarbon removal system; c) two independent Claude cycle cold boxes rated at 4000 liters/hour and 5400 liters/hour with LN_2 precool; d) helium distribution and storage system; e) helium purification system. Both coldboxes have almost identical design with the plate fin heat exchangers from Altec International Inc., and are tied in parallel to the common compressor suction and discharge headers. Coldbox-I has three oil bearing turbo-expanders (42 kW, 23 kW, 9.5 kW) from Sulzer Brothers Ltd. Coldbox-II has three oil bearing turbo-expanders (58.3 kW, 32.2 kW, 13.2 kW) from Atlas Copco Rotoflow Inc. The equivalent refrigeration capacity can be assessed as 9.6 kW (coldbox-I), plus 12.5 kW (coldbox-II) at 4.6°K. The actual available capacity of the coldbox-I was determined in March 1996 experimentally as 3775 liters/hour (131 g/s) at 1214 g/s inlet flow, and the actual available capacity of the coldbox-II as 5220 liters/hour (181 g/s) at 1500 g/s inlet flow. Two distribution valve boxes and liquid helium pumps are installed in parallel allowing independent operations of either system. The option to operate both systems concurrently exists, thus allowing cool downs and engineering runs with the available compressors. The liquid helium inventory is being increased up to 83300 liters, and gas helium inventory up to 1700 m^3. Also, a reliable supply of liquid nitrogen has proven to be vital for accelerator operation, thus making necessary to increase its total inventory to assure 120 hours of LN_2 backup supply in the event of normal LN_2 production and delivery are interrupted. Therefore the CHL nitrogen inventory is being expanded from 151000 liters to 566000 liters of liquid nitrogen.

NEW CRYOGENIC CONTROL SYSTEM

The Tevatron cryogenic control system is designed to control 24 satellite refrigerators and eight compressor buildings. Data acquisition (~700 data points per refrigerators) is required at the rate of 1 Hz for all data. The new control system is based on a Multibus II platform using Intel 32 bit, 80386 microprocessor. Token ring is used as the link between 6 primary crates (one crate per Tevatron sector) while Arcnet is used as a LAN between the primary

crate and individual I/O crates located at each refrigerator or compressor building. New control system features include: processor to processor communications, fast event driven circular buffer, hierarchical alarm system, higher level language support, and more elaborate controlling algorithms with a capability of on-line calculations. Each refrigerator has a cryo thermometry I/O subsystem and cryo device I/O subsystem. Each subsystem I/O uses Intel 16 MHz, 80C186 processor to control all the activity such as settings and readings. Thermometry I/O subsystem provides support for 96 channels of pulsed current, resistance thermometry, and acts as a link to Tevatron quench protection system. The cryo device I/O provides support for transducer input, valve actuator controls, power leads digital controls, vacuum gauge readback, and various motor driven devices, such as expansion engines and compressors. PID loops are easily modified by the operator at a console level. Cooldown of refrigerators and magnets from room temperature, or recovery after a quench are done automatically via specialized finite state machine software.

The CHL control system consists of nine Texas Instrument (now Siemens) PM550 process controllers to implement control, alarm, and interlocks functions for nine major subsystems. The NRL control system is being upgraded to Siemens SIMATIC TI505 process controller and IBM PC-based Wonderware InTouch 5 graphical interface.

HIGH ENERGY TEST

Initial high energy testing took place in December, 1993 and January, 1994. During that time, the Tevatron was uniformly tuned for 75.8 kPa (3.93 K) with cold compressor operation. The ultimate ramp-to-quench energy achieved was 998 GeV. The second major testing sequence took place in July, 1995. Again, the entire Tevatron was tuned for a uniform cold compressor temperature of 3.93 K. An attempt was made to uniformly tune the cold compressor temperatures down to 58.6 kPa (3.69 K) to investigate the increase in quench energy, but the steady state operation were not possible due to capacity limits of CHL coldbox-II. Finally, the recent testing in October, 1995, was to determine the quench energy of the Tevatron while individually tuning the operating temperature of each satellite system until a lower temperature limit was reached in the quench limiting house. A maximum quenching energy of 1010 GeV was achieved. The quenching magnets will need to be replaced in order to proceed to a higher energy, with a goal being 1000 GeV operation for Collider Run-II.

REFERENCES

1. Rode, C.H., Tevatron Cryogenic System, 12th International Conference of High Energy Accelerators (1983)
2. Mulholland, G.T., Design and Performance of a 90,800 kg/day Nitrogen Reliquefier for Fermilab Energy Saver, Advances in Cryogenic Engineering (1986), 31 1087-1094
3. Theilacker, J.C., Upgrade of the Tevatron Cryogenic System, Advances in Cryogenic Engineering (1994), 39A 517-522
4. Norris, B.L., Initial Performance of Upgraded Tevatron Cryogenic Systems, Advances in Cryogenic Engineering (1996), 40
5. Makara, J.N., et al, Fermilab Central Helium Liquefier Upgrade, Advances in Cryogenic Engineering (1994), 39A 523-529
6. Norris, B.L., et al, New Cryogenic Control for the Tevatron Low Temperature Upgrade, Advances in Cryogenic Engineering (1994), 39B 1185-1192
7. Theilacker, J.C., Tevatron High Energy Testing, Fermilab TM (1995), EXP#-190

Cryogenic System for the Muon g-2 Superconducting Magnet

Lin Xiang Jia, Gerry Bunce, James R. Cullen, Michael A. Green,* Chien-ih Pai, Louis P. Snydstrup, and Thomas Tallerico

Brookhaven National Laboratory, Upton, NY 11973, U.S.A.
* E. O. Lawrence Berkeley National Laboratory, University of California, Berkeley, CA 94720, U.S.A.

A cryogenic system for the Muon g-2 Superconducting Magnet was built at Brookhaven National Laboratory, U.S.A.. The g-2 magnet consists of four large superconducting solenoids which are up to 15.1 meters in diameter with a total cold mass of 6.2 tons. The superconducting solenoids are indirectly cooled by using forced two-phase helium in tubes which are up to 200 meters in length. The J-T circuit of a refrigerator is capable of delivering 625 W at 4.5 K. The solenoids are powered through a pair of 5300A multi-tube gas-cooled electrical leads.

INTRODUCTION

A cryogenic system for the 3.1 GeV muon storage ring of the g-2 experiment at Brookhaven National Laboratory, U.S.A. began its commissioning run in December 1995. The magnet consists of four large superconducting solenoids which are built into three continuous cryostat rings that are up to 15.1 meters in diameter with a total cold mass of 6.2 tons. The superconducting solenoids are indirectly cooled using forced two-phase helium in tubes which are up to 200 meters in length. The J-T circuit of a refrigerator is capable of delivering 625 W at 4.5 K. The two-phase helium flows from the refrigerator J-T circuit through a heat exchanger in a liquid helium control dewar and an interconnect to three cryostats. The cooling loop for the three cryostats can be either in parallel or in series and each of the cryostats can be cooled individually. The cool-down time is about ten days. The solenoids are powered through a pair of 5300A multi-tube gas-cooled electrical current leads. This paper describes the muon g-2 cryogenic system.

SYSTEM DESCRIPTION

The g-2 cryogenic system is composed of three main solenoid cryostats, one beam inflector solenoid cryostat, two pairs of gas-cooled electrical current leads, a refrigerator plant, a two-phase flow control dewar, and a cryostat interconnect.

Solenoid Cryostats

Four large superconducting solenoids are built into three large ring cryostats. The two outer solenoids, 24 turns of conductors on each and 15.1 meters in diameter, share a common cryostat. The two inner solenoids, 24 turns of conductors on each and 13.4 meters in diameter, are built into separate cryostats. Cooling of the superconductors in each cryostat is accomplished indirectly via thermal conduction between cooling tubes and the solenoid mandrels. Two-phase helium flows in these cooling tubes, which has a rectangular cross section with a hydraulic diameter of 16.2 mm. Two cooling tubes are welded on the aluminum outer mandrel and one cooling tube is on each of the two aluminum inner mandrels. The cooling loop for the outer mandrel may start at a point on the lower portion of the mandrel, travel clockwise around the mandrel, move vertically to the upper portion of the mandrel, then returns counter clockwise to the starting azimuth on the mandrel. On inner solenoid mandrels the fluid enters, loops around once and exits. The length of cooling tube is 96 meters in the outer cryostat and 42 meters in each of the two inner cryostats. There is an additional 40 meters of cooling tubes for the superconductor leads for the interconnections of the four solenoids.

Current Leads

There are two pairs of electrical current leads in the system. One pair of 5300 A for the ring solenoids and one pair of 2850 A for the inflector magnet. They are cooled by forced single-phase helium gas flow drawn from the main two-phase flow circuit. The current leads are located in the vacuum insulated interconnect chambers, which do not require liquid helium vessels. Each of the leads consists of a bundle of multi-tube sets. Each of the multi-tube sets is made of four nested phosphorous deoxidized copper tubes, which are 10~20 mm in diameters, with annual flow passages between the tubes. These multi-tube sets reduce the current density of each lead, enhance the heat transfer, and reduce the pressure drop. A pair of the 5300 A ring solenoid leads is made to fit in a vacuum space of 300 mm in diameter by 600 mm in length.

Heat Loads

The heat load at 4.5 K for two-phase helium cooling flow in the three cryostats is approximately 180 watts. In addition, 42 watt refrigeration is required for a separated superconducting inflector magnet. Two pairs of gas cooled power leads for the storage ring and the inflector solenoids require 114 watts of equivalent refrigeration. The heat load in the distribution system of two-phase helium requires approximately 80 watts, which include a cryogenic interconnect for three cryostats, control valve boxes, a control dewar, and cold transfer lines. The total heat load at 4.5 K in the g-2 magnet system is, therefore, approximately 416 watts.

Refrigerator Capacity

A liquid nitrogen precooled Claude cycle refrigerator with six heat exchangers, a dual piston reciprocating expander, and a J-T valve is used. The cold box is fed with two screw compressors with total of 100 grams per second helium flow at 2 MPa. It can provide 625 watts of refrigeration at 4.5 K to the g-2 magnets. The contingency allowance ratio of the available refrigeration to the refrigeration required is about 1.5.

Control Dewar

The cryogenic system uses a control dewar with a built-in heat exchanger to sub-cool the helium from a refrigerator J-T flow circuit before it goes into the magnet cryostats. It provides low quality liquid helium with higher pressure and lower temperature. It acts as a thermal subcooler, oscillation dumper for helium supply for the three solenoid cryostats, as well as a phase separator for helium returning from the cryostats. The function of the control dewar is important for long cooling channels like that in the g-2 solenoid mandrel cooling circuit, because the pressure drop along the flow channel is high and the transport capacity of the system is limited by excessive pressure drop. The heat exchanger in the control dewar shifts the phase of the helium from the gas side of the two-phase dome to the liquid side. The liquid temperature in the control dewar pool is lower than that in heat exchanger while liquid temperature in the heat exchanger is the saturation temperature at control dewar pressure. Therefore, the outgoing helium from the heat exchanger will be the subcooled. One J-T valve and other six cryogenic valves are installed in a valve box which is located at the top of the control dewar.

Cryostat Interconnect

The three solenoid cryostats are cold-linked together through a C shaped cryogenic interconnect chamber of 18.1 meters in length and 0.25 meters in diameter. It is a vacuum insulated chamber with liquid nitrogen heat shield. At each section of the interconnect there are two superconductor cable leads, which electrically connect four superconducting solenoids. There are four helium cooling tubes at each section. Two of them are thermally attached to the superconductor cable, and the other two establish the flow loops among the three cryostats. Two control valve boxes are built in the interconnect so that the three cryostats can be cooled either in series flow or in parallel flow. The pressure drop is reduced in parallel flow, which does not only increase the helium mass flow rate but also reduce the differential temperature around the ring solenoid conductors azimuthally.

System Control

An industrial computer with a modular set of software and programmable logic controllers (PLC) through their input/output ports and data highway network to temperature sensors, pressure transducers, liquid level probe, flow meters, and valve actuators. A 4~20 mA analog input format and a 0~10 volts analog output are used for the PLC modules. The cryogenic software provides operator interface, real-time supervisory control, and data acquisition and logging in both graphic and text formats. It also sends the status reports on the cryogenic system for remote communications through an Ethernet interface.

Temperature Uniformity

Control of the temperature distribution along the large diameter superconducting solenoid ring is critical when using forced two-phase helium cooling approach. The pressure drop along the cooling path was about 10.6 kPa if the three solenoids were cooled in parallel, which resulted in a temperature difference of 0.1 K between the inlet and the outlet of two-phase helium flows. For the series cooling, temperature difference could be higher than 0.2 K. The parallel approach was used during the normal operation. Once the mass flow was set up for a steady flow, no further adjustment was needed. The actual temperature difference of the solenoid mandrels was smaller than the above numbers because both the inlet and the outlet of cooling paths are located at the same portion of the continuous solenoid mandrel.

Power-on Tests

The excitation tests were carried out at current charging rates from 1 A/sec to 6 A/sec. A ramping rate which was higher than 6 A/sec will cause the temperature to increase from 0.1K to 0.2 K due to eddy current heating through the solenoid mandrel rings. Additional helium mass flow rates were required for each solenoid mandrel cooling when one increased the ramping rate above 6 A/sec.

The magnet was powered through a pair of multi-tube electrical current leads. The mass flow rate through the leads was adjusted according to the temperatures at the bottoms of the leads. The voltage drops across each leads were used as the secondary control parameters. The multi-tube leads were designed to be cooled by forced convective gas flow. Its operation was not so sensitive as to require a constant flow adjustment. From zero current to the half current (2450 A for the main solenoids) one did not have to increase helium mass flow rate. Meanwhile, there was no frost formed at the warm-side of the leads and superconducting temperature was maintained at the cold ends of the leads. The liquid helium consumption at 4.2 K was 0.07 g/sec per thousand amperes. These current leads could be overcooled, which often happens in practice as long as there is enough cooling power available or the frost at the warm-ends does not cause any problem, such as condensing moisture between electrodes.

Switch-off Tests

A series of energy extraction tests was attempted at 100 A, 1500 A, and 2450 A in order to study the temperature rise due to the quench-back by the eddy current heating in the solenoid mandrels. It has been observed that the system has a desirable capability for a fast quench recovery. Quenched gas in the solenoid cooling tubes was purged out to helium gas storage through two quench control valves, which was preset to open at 2.0 bar and 3.1 bar. When the outer solenoids quenched at 2450 A during the energy extraction, the temperature increased to 20 K in 100 seconds and dropped down to 4.5 K in another ten minutes. The corresponding maximum pressure peak was 2.62 bar and was settled in two minutes. The system was recovered automatically and no maned operation was needed in the half current quench.

CONCLUSION

The cryogenic system for the Muon g-2 Magnet has been successfully constructed and tested. The magnet was cooled and excited up to 50% of the full current by the time this report was written. The forced two-phase flow scheme was capable to cool-down the three 15-meter-in-diameter superconducting solenoids in ten days and maintained at 4.5 K of the operation temperature within 0.1 K temperature differentials around the solenoid rings.

ACCEPTANCE TESTS

The first commissioning run of the g-2 cryogenic system began in December 1995 and continued for two months. The magnet was powered in early January 1996.

Cool-down and Warm-up

One of the import characteristics of large diameter superconducting solenoids is the substantial thermal contraction of the cold members in the cryostats. Each of the internal components of the cryostat, such as the solenoid mandrel and liquid nitrogen heat shield requires their own space for confined-free thermal contraction. The three cryostat rings have an average diameter of 15 meters. When they are cooled from

room temperature to liquid helium temperature (liquid nitrogen temperature for heat shield), thermal shrinkage of the solenoid mandrel can be 31 mm radially. Although it is impossible to cool every internal component of the cryostat uniformly, certain clearance between solenoid mandrel and heat shield as well as the clearance between the heat shield and cryostat shell must be maintained in order to avoid any mechanical collision during cool-down and warm-up. The differential temperature control bands between the helium mandrels and nitrogen shields at different temperature range have been strictly followed by throttling the helium and nitrogen flows in each cooling circuits. It took ten days for each of the cool-downs or warm-ups. The largest temperature difference between the warm and the cold spots in each cryostat was maintained less than 60 K. The warm and cold spots appeared at flow inlet position and at the position of 180° away from the inlet.

ACKNOWLEDGMENTS

This project was performed in the Department of AGS of the Brookhaven National Laboratory and supported by Office of the Energy Research, Office of High Energy and Nuclear Physics, High Energy Physics Division, United States Department of Energy under Contract No. DE-AC02-76CH00016.

REFERENCES

1 E821 Collaboration, Muon g-2 design report, BNL AGS E821, A new precision measurement of the muon (g-2) value at the level of 0.35 ppm Brookhaven National Laboratory Report (1994).

2 The g-2 Collaboration, The g-2 storage ring superconducting magnet system, IEEE Transactions on Magnetics MAG-30, No. 4, p 2423 (1994)

3 Green, M., et al. The g-2 superconducting magnet system, 13th ICMT, Victoria, B.C. (1993)

4 Jia, L. X., et al. Cryogenics for the muon g-2 superconducting magnet system, Cryogenics, Vol. 34, ICEC Supplement, p 87-90 (1994)

5 Jia, L. X., et al. Design parameters for gas cooled electrical leads of the g-2 magnets Cryogenics, Vol. 34, ICEC Supplement, p 631-634 (1994)

6 Bunce, G., et al. A progress report on the g-2 storage ring magnet system, 14th ICMT Tampere, Finland (1995)

7 Jia, L. X., et al. Cryogenic tests of the g-2 superconducting solenoid magnet system CEC-ICEC 95, Columbus, Ohio (1995)

8 Bunce, G., et al. The large superconducting solenoids for the g-2 ring, IEEE Transactions on Applied Superconductivity 5, No. 2 (1995)

Cooling System for Wendelstein 7-X

Felix Schauer
Max-Planck-Institut f. Plasmaphysik, Boltzmannstr. 2, D-80801 Garching, Germany

ABSTRACT

Cooling requirements and operating scenarios of the Wendelstein 7-X superconducting magnet system as well as of auxiliary equipment are described. A first basic layout of the cooling system is presented. All data given are input for the currently starting refrigeration plant design studies.

INTRODUCTION

The superconducting magnet system of the stellarator Wendelstein 7-X (W7-X) contains 50 nonplanar main field (MF) and 20 planar ancillary field (AF) coils with diameters of 2.7 m and 3.2 m, respectively, arranged toroidally at an average large diameter of 11 m. There are seven coil types, and all 10 coils of one type are series connected electrically and regularly distributed over the torus. Since each such coil group is joined to one current supply, a total of 14 current leads is needed. The nominal coil current is 16 kA, the stored magnetic energy 600 MJ, the axis field 3 T, and the coil field maximum 6 T.

All coils are wound from an 11.5 mm cable-in-conduit conductor with ≈250 NbTi-Cu strands, and a 16x16 mm² Al-alloy conduit. The MF and AF coils are subdivided into six double layers with average lengths of 172 m, and three double layers with 110 m, respectively. The coolant is supercritical He with an inlet temperature of 3.8 K.

Each winding pack is embedded within a separately cooled massive steel housing which in turn is supported against its neighbours by a steel vault structure. The coil system including the vault is attached to a ring-shaped steel weight support structure.

The coils and structure elements add up to a total cold mass of around 350 tons which have to be cooled down to and operated at ≈4 K. To this end six principal cooling loops are required: one each for the MF and AF coil conductors, the coil housings including the vault, the weight support structure, the current leads, and the heat radiation shield. Additional duties of the plant are refrigeration and LHe supply for W7-X auxiliary equipment like cryovacuum pumps, ECRH superconducting gyratron magnets, pellet injection, diagnostic instruments, and for other LHe users of the institute.

Many options for the cooling system design have to be considered. Besides the numerous variants available for the refrigerator system proper - made up basically of the cold box, compressors, purifier, storage and distribution system, and controls - one has several possibilities to further subdivide the basic W7-X circuits. Moreover, one can drive the He streams by pumps at low, ambient, or some intermediate temperature, and one has to decide between a warm or cold vacuum pump for the 3.8 K subcooler. The distribution box as well as the subcooler might be installed either near the cold box or next to the W7-X torus which is installed in a distance of ≈40 m from the cold box.

In order to base the specification of the whole W7-X cooling system on as much expertise and practical experience as possible, it is intended to order two design studies by companies working in this field. In this paper the cooling demands, the operation conditions, and a first general plant layout are described.

W7-X COOLING REQUIREMENTS

Table 1 gives a summary of stationary cooling requirements for the six principal circuits. The data within one column (=one circuit) do not necessarily belong to one single operation condition. Circulation pump losses up to ≈ 1000 W at 4 K might have to be added to the quoted ones. The cooling circuits are described below.

Table 1 W7-X stationary operation refrigerator requirements

		MF-coils	AF-coils	housing & vault	support rings	current leads	radiation screen*
No. of parallel channels		300	60	70	5	14	5
T_{in}	(K)	3.8	3.8	3.8	4.3	4.3	60
T_{out}	(K)	4.3	4.3	4.2	4.5	300	75
$\dot{m}_{total}$	(g/s)	400	80	350	75	20	50
Δp	(bar)	3.5	2.1	$20 \cdot 10^{-3}$	0.1	$5 \cdot 10^{-3}$	1
total losses	(W)	350	40	400	50	2000**	4000

* values for plasma vessel baking at 150 C.

** corresponding to 4 K temperature level, or equivalent to ≈580 l/h liquefaction rate

MF and AF Cois

One conductor double layer is one cooling length, and all of them are operated in parallel - i.e. at the same pressure drop. Considering the connections between the coils of a group, the layer positions within a coil, and the coil positions within the torus, a maximal cooling length difference of ≈20 % is expected. This leads to a ≈10 % mass flow rate difference. Since the flow optimum for minimal temperature increase is rather flat [1], the influence of this difference on the cooling conditions is small. One can set the flow such that the short lengths lying in the high field regions are cooled best.

Important parameters which determine the helium flow requirements within the cables are losses and flow cross section, i. e. the cable void fraction. Both are not known yet exactly, so the cooling has to be designed for a suitable value range: for losses up to 6 mW/m and a void fraction value range of 35 % to 39 %.

Coil Casing and Magnetic Force Support Vault

This circuit carries the main burden at machine cooldown. The coil casings are covered by a copper sheet each which in turn is cooled by one channel soldered on top of it. The copper has to be split at least once between the He connections in order to avoid a closed low-resistance current loop, and to reduce heat flow from the return to go streams. Copper covers also the vault support structure between the coils, it is thermally coupled to the housing circuits. The return streams of the latter are further used to cool both attachment points per coil at the weight support structure.

The housing cooling loops are connected in parallel. The average AF coil perimeter is larger by about 18 % with respect to the corresponding MF values. The dif-

ferences can be compensated by choosing suitable channel diameters. Control valves for the He streams are probably not necessary; however, this question is being investigated.

Other housing cooling designs are discussed too. The final decision which system will be applied will be taken after experiments with the currently built coil and cryostat prototypes. A change of the circuit by addition of parallel loops does not influence the plant design significantly. Since the pressure drop is small, additional loops might be supplied simply by installing additional commercially available turbine pumps.

Weight Support Structure

All 70 coils, together with the vault, are supported by a double-ring-shaped structure situated at the torus inboard side. This structure, resting on 3 feet per module, is cooled by the return streams of both coil cooling circuits and the housing cooling, and by a separate cooling loop which is mainly used for cooldown. Since the attachment points of the coils are cooled anyway by the housing cooling return streams, the temperature requirements on this extra circuit are relaxed (s. Table).

Current Leads

The largest loss contribution will come from the 14 current leads of the seven coil groups. Highly variable He streams corresponding to different magnet load conditions have to be provided. The helium returns at ambient temperature to the refrigerator, the 4 K equivalent losses are ≤ 2 kW.

By the time when the current leads are needed there might be high temperature superconductor feedthroughs available. This option will be considered during refrigerator system design.

Heat Radiation Shield

All cryostat inside walls - these are the inside of the outer vessel and the outsides of the plasma vessel as well as diagnostic port walls - are covered by superinsulation layers and a copper heat radiation shield. Its optimal temperature lies around 60 K. During normal operation it will by cooled by a He gas stream with entrance and exit temperatures of $\approx$60 K and $\approx$70 K, respectively. During baking the plasma vessel for UHV purposes at 150 C, the shield losses increase such that the exit temperature reaches $\approx$75 K.

Other Refrigeration and Liquid Helium Users

The most important additional refrigeration power consumers are cryo-vacuum pumps for divertors and neutral beam injection heating. Both systems are not yet specified, the following data are rough estimates only: For the divertor pumps a He-stream of ≤ 50 g/s, $T_{in} \leq 4$ K, $T_{out} \leq 4.4$ K, and for the NI heating around 80 l/h LHe at ≈ 3.8 K will be needed if the W7-X plasma is on. For the cyclic pump operation appropriate provisions have to be made for fast cooldown and He vapour management.

The plant will have to provide additional 2000 l LHe per week for other users.

OPERATING SCENARIOS

Normal and Standby Operation

There will be somwhere between 100 and 150 operation days per year with the magnet system being switched on in the morning and off at evening. The system will be kept at

4 K or somewhat above that during short operation breaks of one to a few days, like nights and weekends. For longer interruption periods of the order of a week up to a few months the system will be warmed up for standby operation at ≈80 K.

Cooldown

The cooldown from room to operating temperature shall last about two weeks at most while never exceeding a temperature difference of ≈40 K anywhere within the coils or cold structure. The last cooling step from 80 K to 4 K, as well as from standby to normal operation temperature, should be possible within less than one day.

Coil Quench and Emergency Switch-off

In an emergency situation the coil system will be switched off with a time constant of five seconds. If one coil quenches, the others remain superconducting during discharge. The refrigerator system has to handle the expulsion of about 15 kg He automatically and, if there is no damage detected, should continue cooling. In the unprobable case of a simultaneous quench of all coils, up to 1000 kg He gas need to be warmed up and stored away immediately. If some defect was the reason of that quench a controlled switch-off has to be initiated. Otherwise, the system has to go automatically into the standby-mode.

BASIC SYSTEM LAYOUT

Fig. 1 shows the basic plant layout. It shall be pointed to the fact that the cold gas distribution system design is strongly dependent on the decision where to place the subcooler. The latter is starting point of most W7-X cooling circuits. The position of the subcooler will heavily influence layout and costs of the ≈40 m transfer lines.

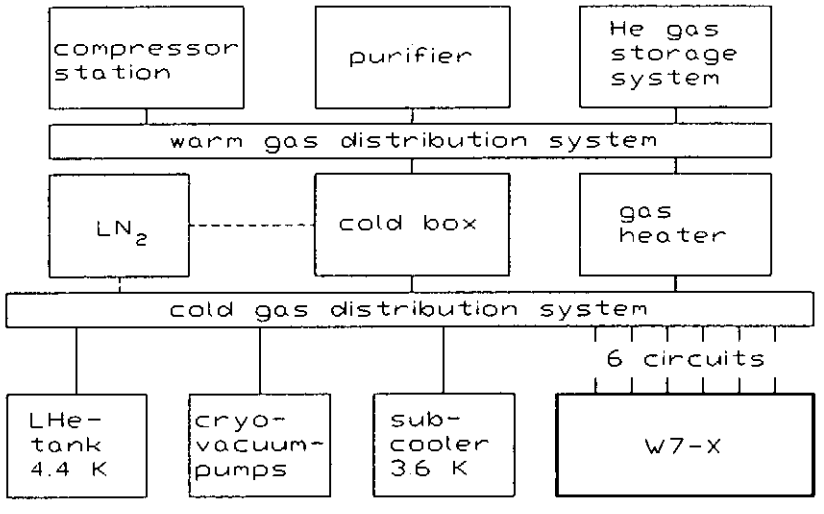

Figure 1 Basic refrigeration system layout

REFERENCES

1 Schauer, F., Optimization and stability of a cable-in-conduit superconductor 14th Int. Conf. on Magn. Techn., 11-16 June 1995, Tampere, Finland, paper E16

Investigation of the Superfluid Helium Cooling Scheme for the LHC Superconducting Magnets

Rousset Bernard
CEA-Grenoble/DRFMC/SBT, 17 rue des Martyrs, 38054 Grenoble Cedex 09, France

The LHC cooling scheme will consist of a static pressurized bath containing the superconducting magnets, cooled by a two-phase flow of saturated helium II. A 40 mm I.D., 90 m long heated tube with a slope of 1.4% has been built in Grenoble to characterize this scheme. At the tube outlet, the flow is visualized in a 0.2 m long Pyrex tube thanks to a CMOS video camera cooled at nitrogen temperature. We present here pressure drop, heat exchange and video picture obtained for flow rates up to 0.0063 Kg/s and temperatures ranging from 1.8 to 2 K.

INTRODUCTION

In collaboration since 1988 with the CERN cryogenics team on the LHC cryogenic system, we have studied and experimented various potential cooling schemes. In all cases, the superconducting magnets of the LHC will operate in static baths of pressurized helium II at 1.9 K and about 0.1 MPa, cooled by different methods.
Preliminary work had explored cooling scheme exploiting thermal conduction[1] and forced convection[2] in pressurized superfluid helium, with periodic recooling by saturated bath in lumped heat exchangers. The first scheme is barely sufficient to match the increased cooling requirements of the project. A special loop has been built at Grenoble in order to characterize large scale pressurized Helium II forced convection. A predictive time dependent code was implemented and compared to experiments with very good accuracy. But this cooling scheme required a helium II circulating pump and an extra heat exchanger between the forced flow and the cold source compared to the final solution.
This retained solution[3] will consist of a helium II two-phase flow directly connected to the cold source. Inside the tube, a flow of saturated helium II absorbs the heat loads by gradual vaporization of the liquid phase. Provided the tube is made of a good thermal conductor, and its inner surface properly wetted by liquid, the applied heat load can be extracted across a small temperature difference (in the order of a few mK). The length of such a scheme is limited by the pressure drop in the two phase flow, which raises the inlet saturation temperature, as well as by the decrease of the inner tube wetted perimeter, which raises the temperature difference between saturated and pressurized bath. A series of experiments was performed in order to investigate the efficiency of this cooling scheme and also to develop a predictive model of thermohydraulic two phase helium II behaviour.

EXPERIMENTAL FACILITIES

All measurements were performed at Grenoble on the previously described[2;4] Superfluid Helium Test Facility.

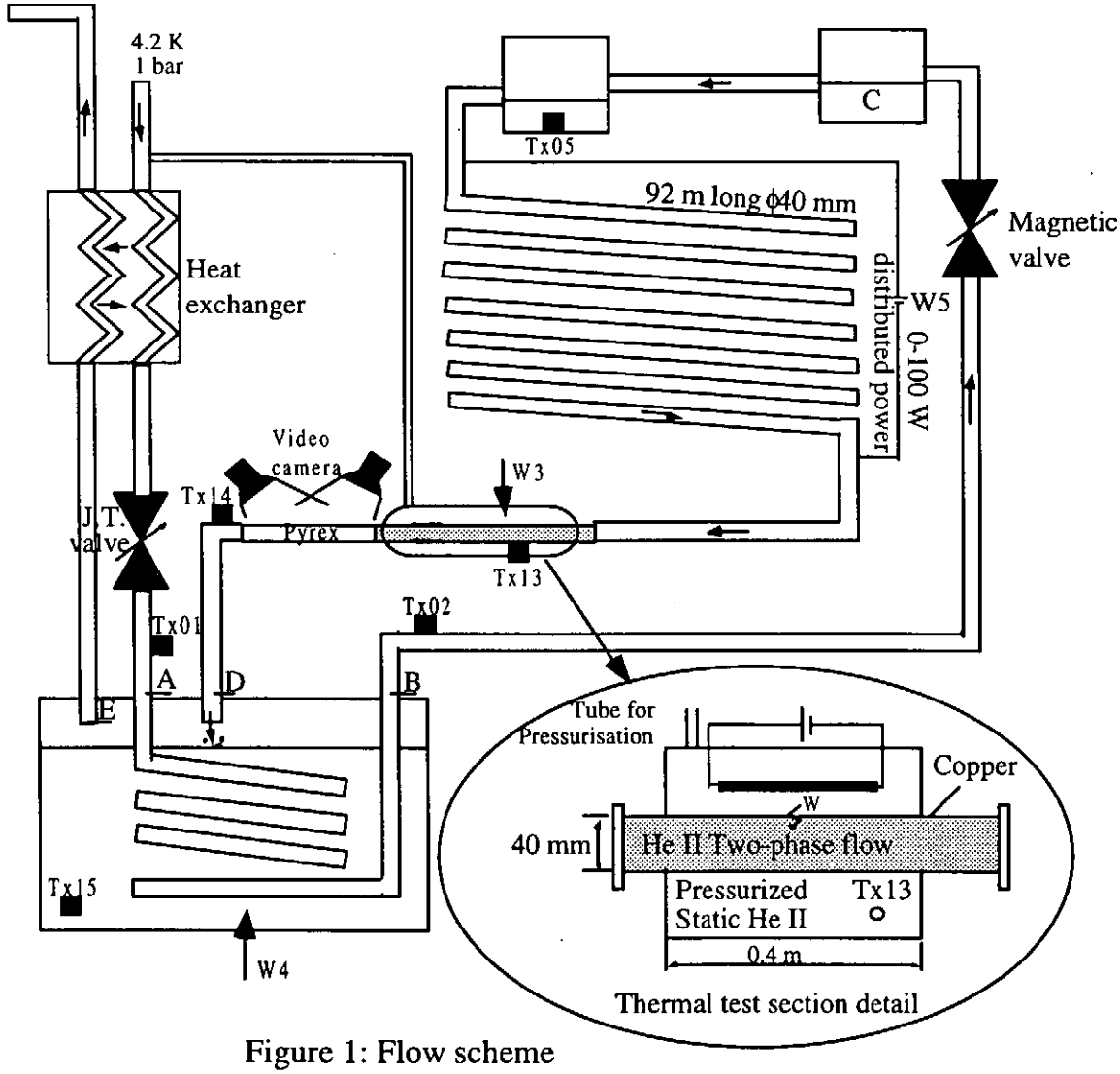

Figure 1: Flow scheme

Following path ABCDEFG, the flow scheme, shown in Figure 1, consists of a J.T. valve, a subcooler between A and B, the test loop between C and D, and finally a saturated bath from which the mass flow rate exits at point E at 100% saturated vapour. The experimental loop contains immersed thermometers (Tx05 and Tx15) at the extremities of the 40 mm I.D. 92 m long line, a heater W5 which is use to vary the quality along the line, a visual observation section and a thermal test section (which serves as LHC magnet heat transfer model). Total mass flow rate ($\dot{m}_{tot}$) is measured at room temperature by means of venturi and gas flowmeter.

Measurements

In order to avoid any temperature errors due to possible thermal gradient, we used immersed thermometers (Tx05 and Tx15) located in boxes at the extremities of the heated line to measure the saturated flow temperature. An *in situ* re-calibration allows an accuracy better than 1 mK for relative measurements between the two thermometers. Using the vapour pressure curve, it is straightforward to calculate the pressure drop along the line.

Analysis

A calculation of the flow pattern map[5] applied to the whole range of our experiments indicates that the flow would remain always stratified, owing to the large ratio between saturated liquid and gas densities. This is experimentally confirmed for low qualities, the video pictures showing horizontal interfaces (figure 2). For these reasons, a complete diabatic two-phase flow model was developed with the assumption of separate flows and horizontal interface. Mass, momentum and energy balances are written and for each phase assuming themodynamical equilibrium and the resulting system is solved numerically. On figure 3, all experimental pressure drop for qualities and temperatures ranging respectively between 0.1 and 0.9, 1.8 and 2 K are displayed and compared to the model. The model is in good agreement with the experiments, but nevertheless always lower than its. Possible reasons for this are extremity effects which are not taken into account in the code or possible vapour superheat effects during the experiments.

Fig 2: Video picture for m=6 g/s T=1.9 K and heat load about 14 W

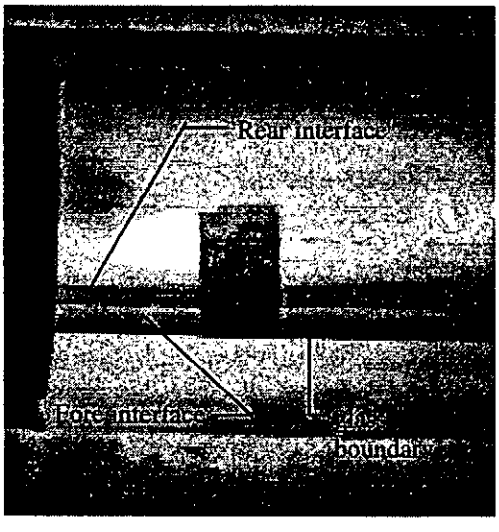

Fig 3: Pressure drop along a 40 mm I.D., 90 m long heated tube for mtot=6.3 g/s

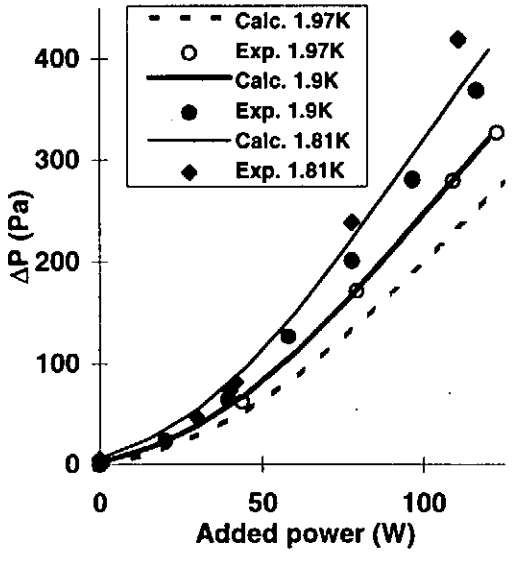

THERMAL BEHAVIOUR OF A DIABATIC TWO-PHASE FLOW

Thermal measurements were performed by means of the pressurized Helium II chamber. Calibration of the thermal heat exchange between pressurized and saturated bath was

obtained in a separate cryostat with the internal tube wetted over its full surface. Assuming heat flux being transported by liquid alone, the wetted surface fraction can be calculated from the thermal heat exchange calibration. Figure 5 indicates a drastic increase of wetted perimeter for high superficial gas velocities. This unexpected good heat exchange does not appear to be explained by fully stratified flow. Other experiments are planned to discriminate between various possible flow patterns: horizontal stratified and mist two-phase flow, horizontal stratified plus thin films on wall two-phase flow, semi-annular two-phase flow...

Fig4: Temperature difference between He II pressurized bath and He II saturated flow for a 3 W/m input power

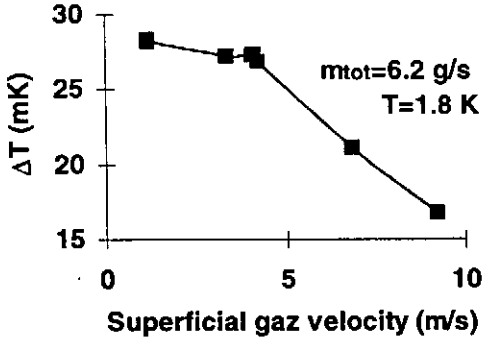

Fig5: Comparison of wetted perimeter deduced from thermal measurements and from model using an horizontal interface

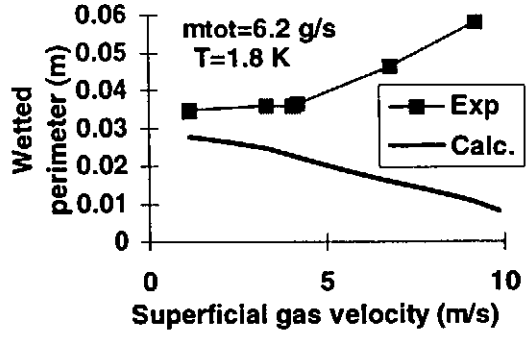

CONCLUSION

We have developped a model which predicts the diabatic two-phase flow pressure drop with an accuracy better than 15% in the range of our experiments. The video pictures seems indicate flat horizontal interface but for high gas velocities, thermal measurements show unexpected good heat exchange which does not appear to be explained by fully stratified flow. In the range studied, we haven't found any limitations for this cooling scheme.

REFERENCES

1 Claudet, G. and al, Preliminary study of a superfluid helium cryogenic system for the Large Hadron Collider Proc. workshop on superconducting magnets and cryogenics (1986) 270-275

2 Rousset, B. and al, Pressure drop and transient heat transport in forced flow of single-phase helium II at high Reynolds numbers Cryogenics (1994) 34 317-320

3 Lebrun, P., Superfluid helium cryogenics for the Large Hadron collider project at CERN Cryogenics (1994) 34 1-8

4 Rousset, B. and al, Thermohydraulic behaviour of he II in stratified co-current two-phase flow to be presented at ICEC16

5 Taitel, Y. and Dukler, A. E., A model for predicting flow regime transitions in horizontal and near horizontal gas-liquid flow AIChE Journal (1976) 22 47-55

The Cryogenic System for the NHMFL Hybrid Magnet*

S.W. Van Sciver, K. Bartholomew and S.J. Welton
National High Magnetic Field Laboratory
1800 E. Paul Dirac Drive
Tallahassee, FL 32310

ABSTRACT

The present paper describes the cryogenic system for the National High Magnetic Field Laboratory Hybrid superconducting magnet system. This system employs an innovative design primarily driven by the requirements that the magnet be reliable and easily accessable to the users. To achieve these requirements, the magnet is being built from highly stable cable-in-conduit conductors operating at 1.8 K and internally cooled with static He II. The superconducting magnet is supported in its own cryostat on a thermally optimized stainless steel column. All connections to the cryogenic system and power supplies occur at the supply cryostat. The magnet and supply cryostats are connected by means of a services duct that carries the cryogenc and current bus. This approach allows the magnet cryostat to be free of penetrations.

INTRODUCTION

The National High Magnetic Field Laboratory (NHMFL) is developing a new hybrid magnet system which will, when complete, provide the world's highest steady magnetic fields to the physics and materials research community.[1] This system consists of two separate magnets: a 14 T, 616 mm warm bore superconducting outsert magnet and a 31 T, 33 mm bore resistive insert. The superconducting magnet is supported by a cryogenic system operating at 1.8 K with static, pressurized He II. Various aspects of the design and development of the NHMFL Hybrid cryogenic system have been previously published.[2.3] The present paper further describes progress on this development with emphasis on results of recent thermal performance tests.

CRYOSTAT DESIGN

He II was selected as the coolent for the NHMFL Hybrid to allow improved performance and better thermal stability for the conductor. The hybrid cryogenic system was designed in collaboration with CVI Inc. for indirect cooling to permit remote operation of the magnet. The resulting system consists of an arrangement connecting the magnet cryostat to the supply cryostat by a services duct filled with static He II. All connections to the outside world are through the supply cryostat allowing the magnet user free access to the bore.

The magnet cryostat in its final configuration is shown in cross-section in Fig. 1. All conductors are cable-in-conduit type with helium supplied to each layer or pancake in a parallel flow configuration. In addition , the magnet vessel contains a static bath of He II. This increased helium reservoir is needed for transient stability of the magnet.

The helium is supplied to the magnet from the supply cryostat, shown in cross-section in Fig. 2. The supply cryostat contains all the cryogenic and magnet peripheral equipment included in this vessel: a pair of 11 kA vapor cooled current leads, two JT heat exchangers, a weight loaded relief valve which opens during cooldown and in the event of a magnet quench, a three-way valve which serves to either supply helium directly to the magnet during cooldown or permit counterflow heat transport between the magnet and supply cryostat, and finally an instrumentation probe for measurement of fluid conditions in both the upper and lower reservoir. All these components have similar conical seats to seal between the upper and lower reservoirs.

The cryogenic system is supplied using a pair of PSI 1630 refrigerator/liquifiers with associated perfierals. The table below displays the performance of these refrigerators.

Table 1: Performance characteristics of refrigerators for NHMFL Hybrid

	Mode 1	Mode 2	Mode 3
Liquifaction Rate	60 l/h	56 l/h	70 l/h
5 K Refrigeration		20 W (1.6 g/s)	
20 K Refrigeration	60 W (1.8 g/s)		

In addition, a pair of Kinney vacuum pumps supply 1000 l/s of pumping capacity at 10 Torr for the main refrigera tion of the He II.

He II temperatures are achieved in the lower reservoir of the supply cryostat by pumping on the liquid in the saturated bath heat exchanger. A schematic of the He II heat exchanger is shown in Fig. 3. The lower reservoir of the end heat exchanger consists of a copper tube of 100mm OD and length about 0.9 m. Seven closed end reentrant copper tubes penetrate from the lower end to increase the surface area of this component. The vapor-He I heat exchanger on the return side is a tube-screen type device. Each heat exchanger is capable of delivering 16.5 watts of cooling with an outside bath temperature of 1.8 K, limited by pumping capacity. Under these conditions the inside reservoir is maintained at 1.77 K. The temperature drop between the two reservoirs is almost entirely due to the Kapitza conductance of the copper tubes.

CRYOSTAT TEST RESULTS

We have conducted several tests of the NHMFL hybrid cryostat to confirm its performance characteristics. In advance of receiving the superconductivity magnet, the magnet cryostat was equipped with a dummy load which completes the hydraulic circuit and allows thermal loading tests to be performed. The dummy load consists of an aluminum tubular manifold system that occupies the magnet location top of the support column. In this configuration, the cryostat can fully test all operational characteristics with the exception of the thermal mass.

For the initial cooldown of the cryostat, the entire system is supplied a forced circulation of two phase helium directly from the refrigerator/liquidifer. The liquid passes through the magnet cryostat and collects in the bottom of the supply cryostat. Once the supply cryostat is filled, the three-way valve is switched to normal position and pumping is initiated on the JT heat exchangers. Since the liquid is now static, the magnet cryostat begins to warm from the background heat leak vaporizing the contained helium ultimately reaching about 25 K. This condition continues for several hours until the He II counterflow process within the conduit condenses the vapor in the magnet cryostat. Cooling then continues until the entire system reaches 1.8 K.

The steady state heat load for the entire cryostat has been measured to be 16.5 W @ 1.8 K. This heat leak is considerably higher than the calculated value of 6.7 W. We are continuing to test the system to define the source of the additional heat leak. Heat leaks at 20 K and 80 K are all within specification.

We have tested the hybrid cryostat for recovery from a transient disturbance in the magnet cryostat. Such a process might represent a small quench of the superconducting magnet or an insert resistive magnet trip. The disturbance is accomplished by powering a heater located in the dummy load manifold. A typical trace of the such a test is shown in Fig. 4, corresponding to a 500 kJ pulse. Note that although the temperature of the dummy load in the magnet cryostat goes to a high value, approximately 50 K, the lower reservoir of the same cryostat remains below 2 K and therefore full of He II. Thus, after the heat source is extinguished, recovery to a normal operating conditions is rather rapid, of order xx hours in the present case.

CONCLUSION

The NHMFL Hybrid cryostat has been developed and tested for supporting the 14-T superconducting outsert magnet. The cryostat is now operational at the Laboratory and testing continues in advance of installation and acceptance of the magnet system.

ACKNOWLEDGMENT

This work is based upon research conducted at the National High Magnetic Field Laboratory (NHMFL), which is supported by the National Science Foundation, under Award No. DMR-9527035.

REFERENCES

1. Miller, J.R. et.al., An Overview of the 45-T Hybrid Magnet System for the New National High Magnetic Field Laboratory, IEEE Trans. on Magnetics (1994) 30 1563-70
2. S.W. Van Sciver, et. al. Design, Development and Testing of the Cryogenic System for the 45-T Hybrid, Adv. Cryog. Engn. (1996) 41 to be published
3. S.J. Welton, et. al. Design, Development and Testing of the JT Heat Exchangers for the 45-T Hybrid Magnet, Adv. Cryog. Engn. (1996) 41 to be published

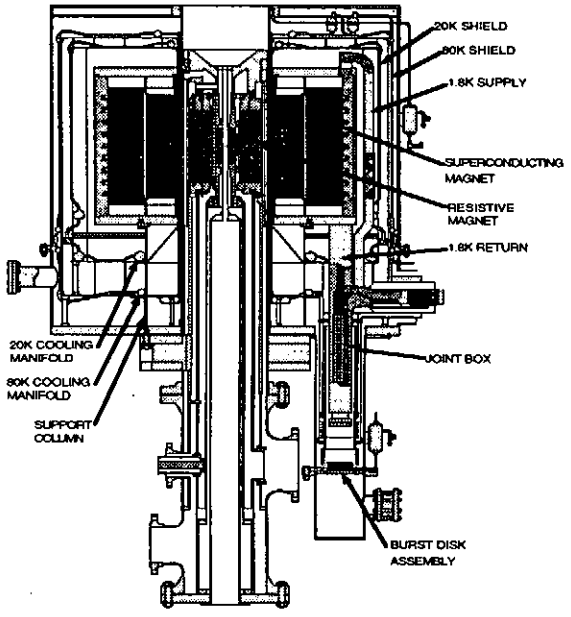

Fig. 1: Cross section of Magnet Cryostat

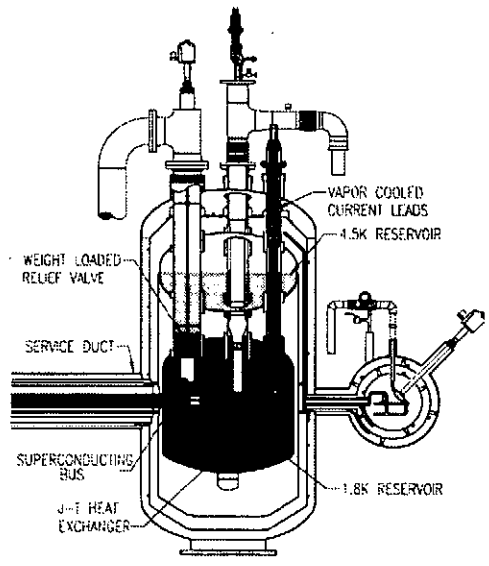

Fig. 2: Cross section of the Supply Cryostat

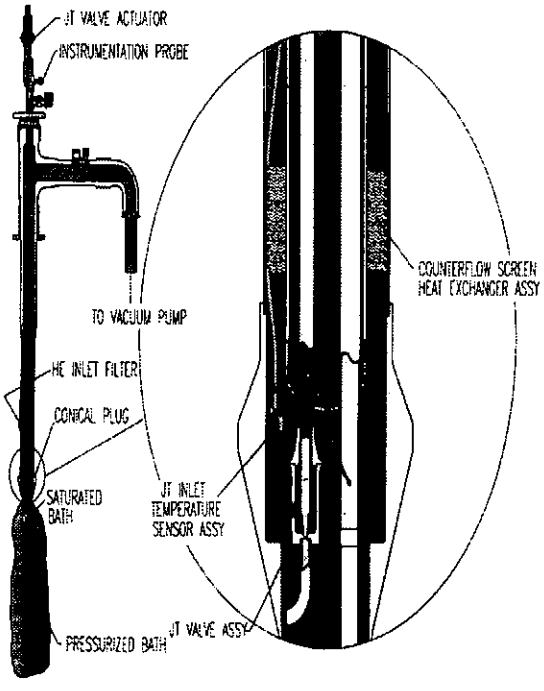

Fig. 3: Cross section of JT Heat Exchanger

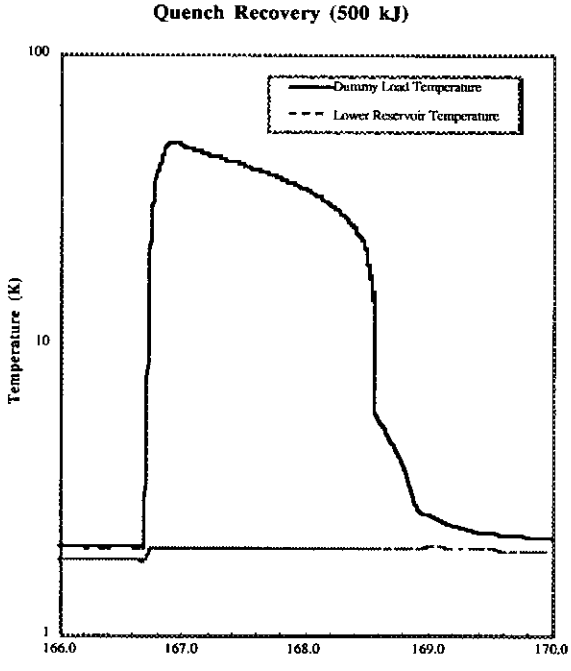

Fig. 4: Quench recovery curve after 500 kJ pulse in Dummy Load

Cryogenic Design of 70MW Class Superconducting Generators

Tatsumi Ichikawa
Super-GM, 5-14-10 Nishi-tenma, Kita-ku, Osaka, 530 Japan

This paper describes outline of the cryogenic designs for 70MW class superconducting generators and their helium refrigeration system developed in a 11 year R&D project, which has been commissioned from NEDO as a part of the New Sunshine Program of AIST of MITI. The verification test of the generators is scheduled to be started in October 1996.

INTRODUCTION

Since 1988, Super-GM (Engineering Research Association for Superconductive Generation Equipment and Materials) has been conducting an 11 year R&D project on application of superconductive technology to electric power apparatuses, which has been commissioned from NEDO (New Energy and Industrial Technology Development Organization) as a part of the New Sunshine Program of AIST (Agency of Industrial Science and Technology) of MITI (the Ministry of International Trade and Industry)[1].

One of the major objects of the R&D is to establish technologies for design and manufacture of 200MW class pilot generator, by developing three types of 70MW class model SCG (called the model machine) and testing the model machine to verify their performances and reliability. Another object of the R&D is to establish technologies for high reliable helium refrigeration system for superconducting power apparatuses including SCG.

TECHNOLOGIES TO BE DEVELOPED FOR SCG SYSTEM VIEWED FROM CRYOGENIC DESIGN

Figure 1 shows a typical configuration of SCG, in which superconducting field windings are used. A field winding composed of superconduting wires can generate stronger magnetic field and be smaller size as compared with that for conventional generators. This results not only in reduction of generator loss and size, but also in enhancement of stability of generator.

To realize SCG which has the above merits, the following technologies should be developed from a view-point of cryogenic design; technologies for reducing heat transfer from the rotor surface and the rotor shafts to the rotating helium vessel in the rotor, for reducing heat generation in various components of the rotor, including superconductor, mainly due to change in magnetic field not only caused by AC stator current but also the field current changing in generator excitation control, and for supplying liquid helium to rotating vessel and extracting gas helium from the vessel.

Super-GM has been developing three types of model machines to develope and verify these technologies. The major specifications of the model machines are shown in Table 1.

Moreover, refrigeration system for SCG should be reliable for long-term operation of SCG (typically, one year). Super-GM has been developing and testing a high-reliable helium refrigeration system (rated liquefaction capacity: 100 L/h, allowable impurities capacity in helium gas: less than 0.1 ppm, long-term operability: over 10,000 hr).

RECENT PROGRESS IN R&D

Model machines

Various fundamental techniques were developed early stage in the project and verified by various partial models in middle stage of the project. Since then, three generator rotor each for the three types of the model machines and one generator stator to be commonly used for each rotor have been designed, manufactured and tested at factories[2].

As for the slow response excitation type A model machine, the rotor combined with the stator is now under synthetic performance test at factory (Figure 2). Figure 3 shows the temperature profile of the field winding at cool-down test.

As for the slow response excitation type B model machine, a large-scaled partial rotor model was manufactured and tested to verify the designing and manufacturing techniques for the rotor. For example, as shown in Figure 4, the soundness of the partial rotor model against quench condition by forced increase of the field excitation current was verified. The rotor for the model machine is under synthetic performance test at factory.

As for the quick response excitation type model machine, a large-scaled partial rotor model was manufactured and tested at factory. For example, it was confirmed that the partial rotor model was successfully operated against a current changing rate of 5000A/sec (Figure 5) which corresponds the maximum changing rate required in quick response excitation control. The winding support shaft of the rotor for the model machine was finished machining as shown in Figure 6 and superconductor is being wound into the shaft.

Refrigeration system

Figure 7 shows the refrigeration system diagram for the model machines. The system was already manufactured, utilizing fundamental techniques developed early stage in the project. The performance test of the system was carried out at factory, using a simplified dummy load apparatus which simulated heat load of the model machine[3].

It was confirmed that the system was fulfilled the rated liquefaction capacity of 100 L/h and the allowable impurities capacity in the helium gas to less than 0.1 ppm. Furthermore, its operating performance as to liquefaction rate control (Figure 8) and as to liquid helium supply to the model machine were clarified.

Verification test facility

Various tests are planned at a verification test facility for the model machines and the refrigeration system. These tests are classified into four categories as shown in Table 2; basic tests for synchronous generator, basic tests for SCG, load tests for SCG, and severe tests for SCG. These tests contain more than 40 types of tests.

The test facility is under construction and almost completed in the site of Osaka Power Station, Kansai Electric Power Company (Figure 9). The refrigeration system was already installed at the facility and is now under adjustment test prior to verification test combining the model machine. Figure 10 shows the simplified system configuration of the test facility.

Each of three 70MW class model machines is planned to be sequentially tested using a motor-generator (M-G) method. The model machine is not connected to outside power system. The test method is especially suitable for the severe tests.

CONCLUSION

The verification test on performance and reliability of the model machines and the refrigeration system is one of the major items in the latter half of the project. The test of the first model machine is scheduled to be started in October 1996. Various technologies for design and manufacture of 200MW class pilot generator will be established through the verification study which is performed not only by analysis of various test results at factories and at the test facility, but also by analysis with computer codes utilizing the test results.

Super-GM will actively conduct the R&D for practical use of superconductive technology in electric power field not only with cooperation and support from the utility companies, the manufacturers in Japan as well as university and national research organizations but also with international cooperation and information exchange.

REFERENCES

1.Ageta,T., Ichikawa,T., Tunoda,Y., Kazumori,M., Taniguchi,H., Yagi,Y., Ueda,A. and Kitajima,T., Recent development progress of 70MW class superconducting generators (part1), No.11-102, 1994 CIGRE Session, Aug.28-Sept.3, 1994, Paris, France.

2.Yamaguchi,K., Suzuki,K., Miyaike,K., Toyoda,K. and Ichikawa,T. , Development of 70MW class superconducting generators, ICEC16, May 20-24, 1996, Kitakyushu, Japan

3.Yanagi,H., Ikeuchi,M., Machida,A., Ikeda,Y., Development of helium refrigeration systems for 70MW class superconducting generators, ICEC16, May 20-24, 1996, Kitakyushu, Japan

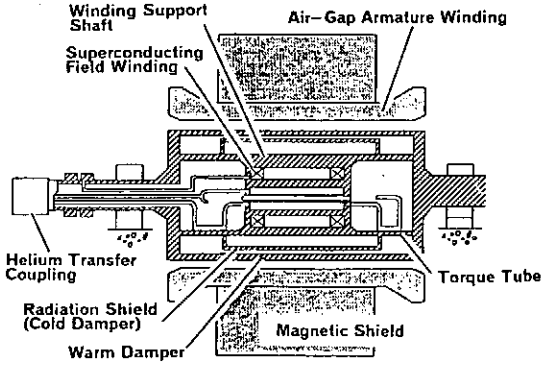

Fig.1 Typical configuration of SCG

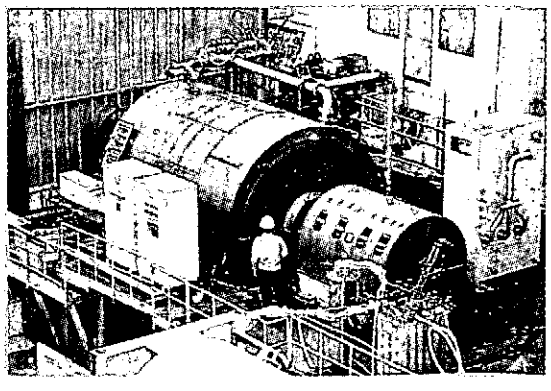

Fig.2 Outer view of factory test (slow response type A)

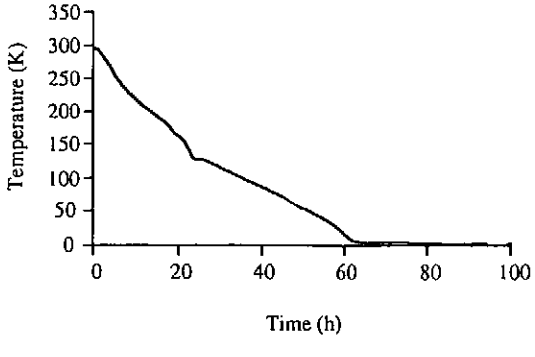

Fig.3 Cool down profile of winding support shaft (slow response type A)

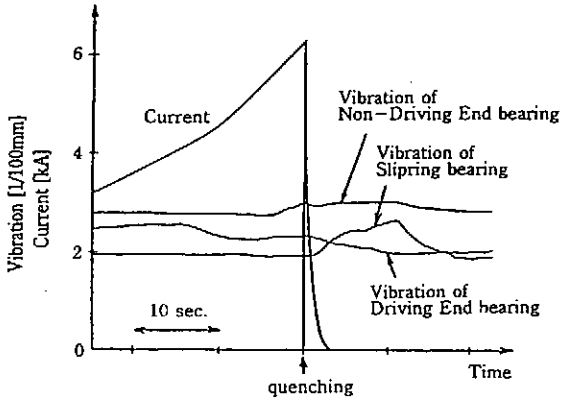

Fig.4 Vibration characteristics of current quench test (slow response type B partial rotor model)

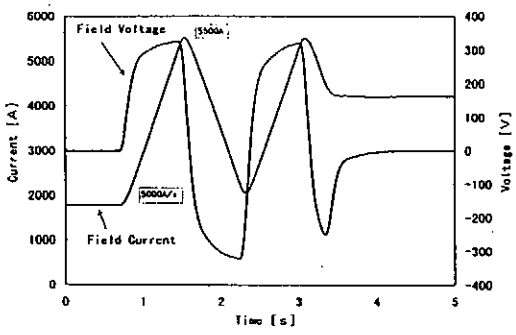

Fig.5 Result of pulsed-excitation test

(quick response type partial rotor model)

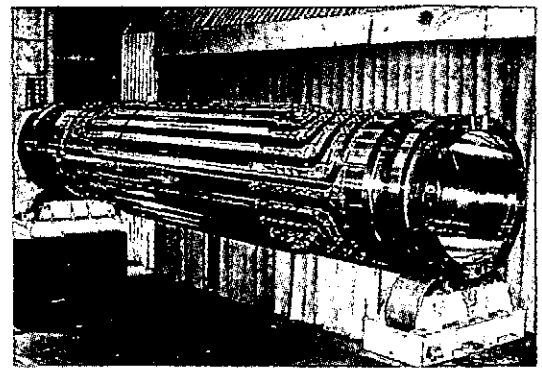

Fig.6 Winding support shaft for quick response excitation type rotor

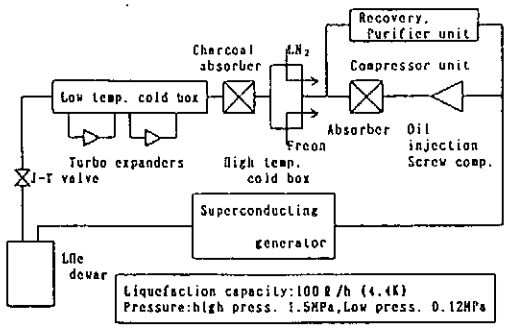

Fig.7 Refrigeration system diagram for

70MW class model machine

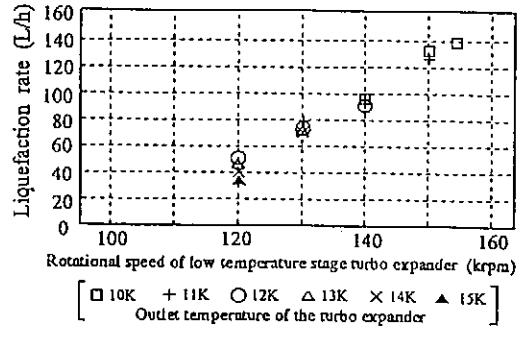

Fig.8 Liquefaction test result

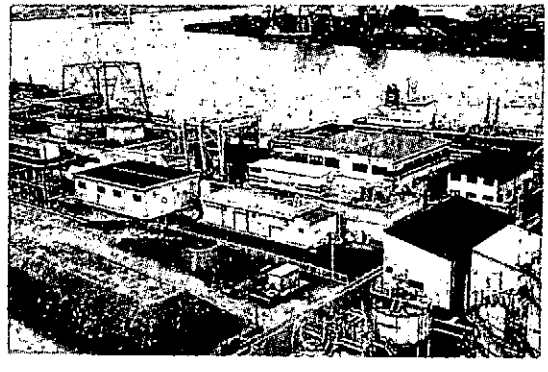

Fig.9 Test facility under construction

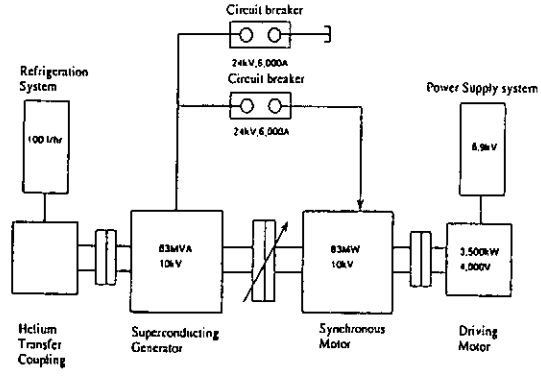

Fig.10 Test system for model machine

Table 1 Major specifications of model machines

Item		Slow response type A	Slow response type B	Quick response type
Specifications				
Capacity	MVA	83	83	73
Voltage	kV	10	10	10
Current	A	4,792	4,792	4,215
Power Factor		0.9	0.9	0.9
Rotation speed	r.p.m.	3,600	3,600	3,600
Synchronous reactance	p.u.	0.35	0.35	0.45
Field current				
Rated	A	3,000	3,000	3,200
Maximum	A	3,600	3,600	4,500
Rotor structure				
Warm damper		Single layer type	Squired cage type	Three layer type
Cold damper/Radiation shield		Three layer type	Single layer type	Single layer type
Thermal contraction mechanism		Double bearing	Flexible disc	Flexible support
Property of superconductor		High stability	High current density	Low AC loss
Stator structure		Air gap winding Double transposed conductor Water cooling		

Table 2 Major verification tests

1. Basic testes for synchronous machine
· No-load saturation curve, short-circuit characteristic
· Sudden short circuit test
· Efficiency test etc.
2. Basic tests for superconducting generator
· Static exitation test
· Field current test
· Dumper test
· Vibration test
· Cool-down and warm-up test etc.
3. Load tests
· P-Q characteristic test
· Longterm reliability test
· Excitation system voltage response test
· Daily Stop and Start test
· Load rejection test etc.
4. Sever tests
· Overspeed test
· 3-phase sudden short circuit test
· Quenching test
· Excessive negative-phase-sequence current test

CRYOGENICS FOR MAGNETIC LEVITATING TRAIN

Hiroshi NAKASHIMA
Maglev System Development Division, Railway Technical Research Institute, 2-8-38 Hikari cho Kokubunji shi Tokyo 185, JAPAN

ABSTRACT

Magnetically levitatited (Maglev) vehicle using on-board superconducting magnets have been development for the past 25 years in Japan.
These vehicles can be levitated magnetically as much as 100 mm above the guideway surface, and propelled by synchronous motors using the superconducting magnets.
The target speed in the commercial service of this system is 500 km/h, which will be able to connect Tokyo and Osaka in one hour.
The current state of the development of Maglev system, especially on the development of the superconducting magnets will be reviewed.

INTRODUCTION

The development of the Maglev system in Japan was started as early as in 1969 to study its feasibility as the high speed ground transportation system.

After several years of basic tests and developments, a 7 km test track was constructed in Miyazaki prefecture in 1977. Using the 1st test vehicle ML-500 a world speed record of 517 km/h was attained in 1979. Also, this test track has served to yield important data for the development of the Maglev system these 19 years.

In 1990 the project of a new test line was decided as a steady step to realization of the revenue service using the the Maglev system. Now, this new test line (Yamanashi test line) is being constructed in Yamanashi prefecture.

The running test will be started soon after the completion of the new test line for a maximum target speed of 550km/h.

Two sets of trains are designed and will be used for the running tests. The first set of train with 3 cars (fig.1) is already completed and was carried to the car depot last July. All kinds of test including riding comfort at high speed and confirmation of durability are planned.

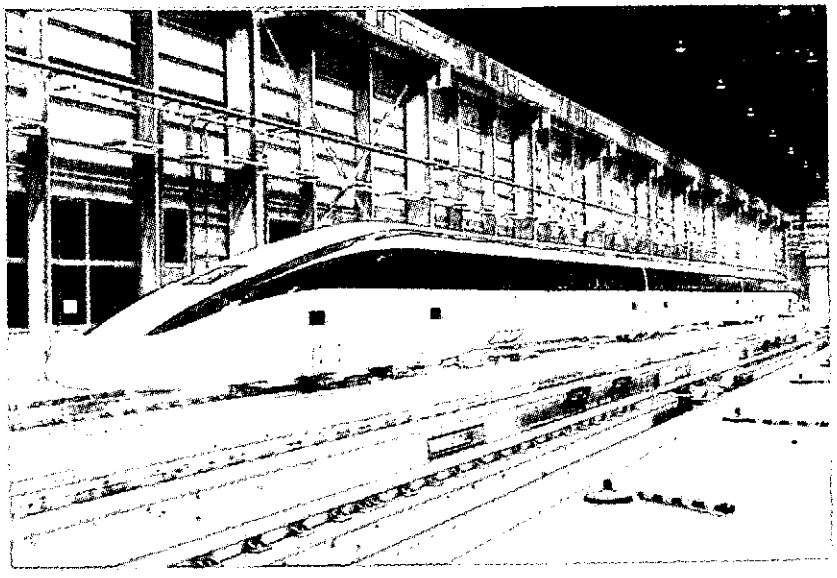

Fig. 1 Test vehicle for Yamanashi Test Line.

SUPERCONDUCTING MAGNET

The superconducting magnet is one of the most important parts of Maglev system. They have to stand strong forces levitating, propelling or guiding the vehicle. Also, they have to work stably in severe circumstances such as flux fluctuation from the ground coils and mechanical vibration.

Fig.2 and 3 show an image of the superconducting magnet and the superconducting

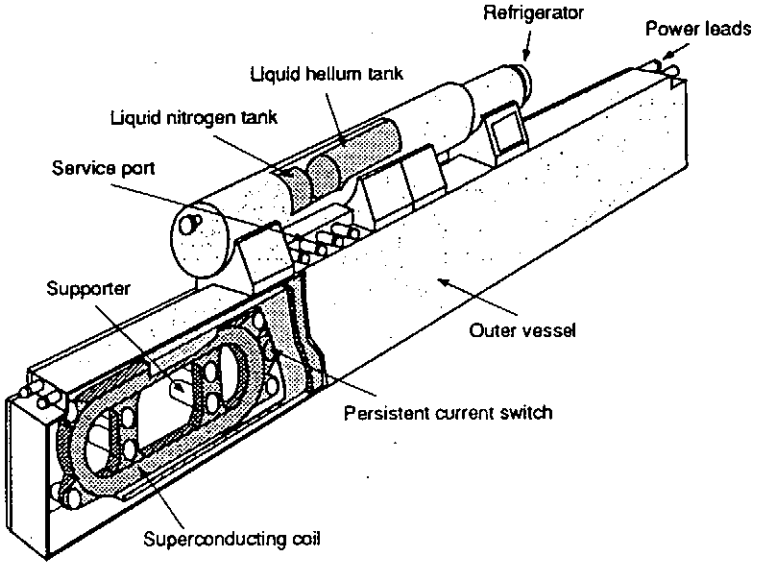

Fig. 2 Image of the superconducting magnet.

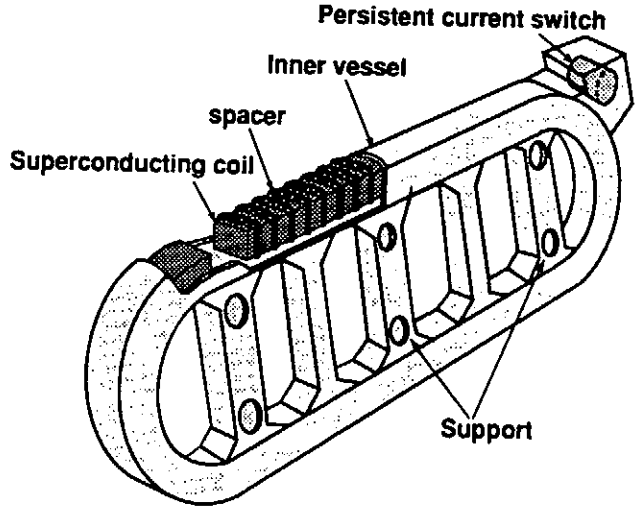

Fig. 3 Image of the superconducting coil.

coil.

Table 1 gives the basic characteristics of the superconducting magnet in one of the models for the Yamanashi test vehicle.

The superconducting coils installed in the test vehicle MLU002(1987 - 1991) suffered so many quenching troubles. This fact promoted an improvement on the stability characteristics of the superconducting coils.

They are practically implemented in the designing of the superconducting magnets for Yamanashi new test line under construction.

Table 1 Basic characteristics of the superconducting magnet.

Items	Specifications
Dimensions of SCM	5.32 m(L) × 1.17 m(H)
Weight of SCM	1500 kg
Magnetomotive force	700 kA
Number of coils	4
Pole pitch	1350 mm
Maximum empirical magnetic field	4.23 T
Heat leakage to inner vessel	4 W
Levitative force per magnet	98 kN
Refrigeration capacity	8W at 4.3K

ON BOARD REFRIGERATOR

The on board refrigerator has 8W of cooling capacity at 4.3K with about 8kW of input power.

Three types of refrigerator were developed for this on board refrigerator. One is

the Cloude cycle, the second is the stirling cycle refrigerator and the third is the Gifford Mcmahon cycle refrigerator.
The regenerator type refrigerator have been so much improved recently using a new kind of regenerator at cryogenic temperature. On this reason the latter two type of the refrigerator are used for the test vehicle of Yamanashi test line.
These refrigerator can not only keep the liquid Helium in the cryostat, but also increase the liquid Helium on necessity.

CONCLUDING REMARKS

The running tests on Yamanashi Test Line will be started on spring of 1997. The test results will prove the superiority of the superconducting Maglev system for high speed ground transportation.
One of the remaining tasks to be solved is the confirmation of the reliability of the total system. This will be one of the important roles to be played by the new test line.
The development of the superconducting magnets for Maglev system has been subsidized by the Ministry of Transportation of Japan.

REFERENCES

[1] H.Nakashima, The Superconducting Magnet for the Maglev Transport System, IEEE, Transactions on Magnetics, VOL.30,No.4,July 1994, pp.1572 - 1578
[2] H.Tsuchishima, T.Herai, Superconducting Magnet and Onboard Refrigeration System on Japanese Maglev Vehicle, IEEE, Transactions on Magnetics, Vol.27,No.2,March 1991, pp.2272 - 2275
[3] H.Tsuruga, Superconducting Maglev System on the Yamanashi Maglev Test Line, Future Transportation Technology Conference and Exposition, Costa Nesa, California, August 1992

A CRYOGENIC SYSTEM FOR HT-7 TOKAMAK

Yanfang Bi and Cryogenic Group
Institute of Plasma Physics, Academia Sinica, Hefei 230031, China

The superconducting toroidal magnet of tokamak HT-7 is cooled with supercritical/two-phase helium flow. A 500W/4.5K refrigerator with four piston expanders supplies the mass flow. The HT-7 cryogenic system was complete in July 1994. Since then the tokamak has been cooled down five times successfully for the primary test, engineering tests and normal plasma physics experiments. The last operation status confirmed that the system has some capacity margin to back up the magnet steady operation at the toroidal fields of 1.5-2.0 T range for a long term. A plasma current of 140kA amplitude and 1.3s pulse duration was achieved in March 1996.

INTRODUCTION

The tokamak HT-7 is a reconstructed device from the tokamak T-7 [1]. It has the same major radius of 122cm and minor radius of 35cm , but HT-7 has much more and larger ports for heating and diagnosing plasma. In order to add 26 new larger ports the superconducting toroidal magnet (STM) was rearranged to symmetry distribution of 24 two-double-pancake coils, and the plasma chamber, coil cases, 80K shields and cryostat shell had to be modified or rebuilt. So that the heat load at 4.6K zone increases to 130W.

The STM is cooled with supercritical/two-phase helium flow. The NbTi/Cu superconductor of the coils contains nine 2mm-diameter channels. 48 double pancake coils are connected in series electrically and in parallel hydraulically. All LHe and LN_2 tube lines in the cryostat were renewed and junction leak on the lines must be low enough. A primary cryogenic test for the cryostat vacuum and STM performance check was carried out before final welding the two halves of plasma chamber in July 1994. From the end of 1994 till the March 1995 the engineering tests to obtain plasma was performed. Plasma currents of 160kA amplitude and 250ms pulse duration were achieved. But the cryogenic system could back up STM current below 3 kA only because of helium leak in the cryostat section for the current leads. After a leaking ceramic electrical insulator on the downstream tube line was detected and changed, the vacuum in cryostat was improved up to $4x10^{-4}$Pa and tenfold better than before. To minimize the mass flow required for STM current leads (maximum design current of 7 kA) a couple of initial leads which require 2g/s mass flow were renewed and achieved the optimized performance. The transfer lines between the

refrigerator and tokamak were improved into simple and short. During normal plasma physics experiments in March 1996 the system can provide enough refrigeration and mass flow for STM running at higher than 3 kA (toroidal field >1.5T) due to the heat loads much reduced.

SYSTEM DESCRIPTION

The cryogenic system for HT-7 tokamak is equipped with two similar 500W/4.5K refrigerators/liquefiers having four piston expanders each and three piston compressors (one 6Nm³/min and two 20Nm³/min, the maximum outlet pressure of 3 MPa). For normal tokamak operation one refrigerator and one big compressor or adding a small one is required. The rest are as the spare machines. The refrigerators are located 80m far away from the compressors, but only 6m distance from the HT-7 current lead unit.

The flow diagram of refrigerator No.1 is shown in Fig.1. The refrigerator has flexible running modes: two or three stages of engine expansion, one or two J-T expansions, using injector 1 to reduce the supply helium temperature and using injector 2 to enhance the mass flow cooling the tokamak. During STM cool down the four expanders work in two stages at a return helium temperature range of 100-40K. In the range of 40-4.6K the three-stage expansion can get much fast cooldown speed. If refrigerator No.1 is operated in liquefaction mode, the liquefying rate of three-stage engine expansion increases up to 160L/hr about 26% higher than that in the two-stage expansion. While STM charging the mass flow >35g/s is required. Using injector 2 can increase mass flow up to 40g/s. If injector 1 is on line, pressure in the subcooler may decrease to 0.05MPa, the temperature of outlet helium flow fall to 3.6K, but the mass flow through STM has to be reduced. According to our experience large mass flow is more effective for HT-7 STM stability than supplying lower temperature helium flow.

The 80K copper shields in cryostat are cooled with LN_2 fed from a 1m³ storage vessel. The vessel altitude is 2m above the tokamak. For plasma baking regime the LN_2 is driven by a pump. According to the LN_2 consumption rate the shield heat load is about 3.5kW/80K.

COOLDOWN

The HT-7 STM (~14000kg weight) has been cooled down five times successfully for the primary test, engineering tests and normal plasma experiments. It takes total 90-100 hours from room temperature to 4.6K. The cooldown speed is limited by the three factors: the helium flow temperature difference between STM outlet and inlet < 70K to avoid mechanical stress damage in STM, the supply helium pressure <1MPa to ensure the electrical insulator safety on the helium supply tube lines in the cryostat, and the refrigeration capacity. When the return flow temperature above 200K the maximum mass flow less than 17g/s is driven by a small compressor, and below 200K a big compressor

instead of the small one. A LN_2 pre-cooler in the refrigerator provides refrigeration until return gas temperature down to 120K. When the return flow temperature reaches 120K four expanders start and cool the heat exchangers in refrigerator. While the mass flow temperature falls to <100K the expanders provide refrigeration and make supply gas temperature <80K. From 80K to 4.6K it takes 7 hours only. When the return flow temperature reaches 6K the flow enters a LHe vessel (250L volume) in the refrigerator. Then LHe from the tokamak will accumulate more and more in the vessel within a few hours that STM is cooled down completely and ready for charging.

The thermal radiation shields (~8000kg) in cryostat is pre-cooled with cold nitrogen gas until the maximum temperature of the shields falls to 120K, then LN_2 is supplied to continue cooling. The shield cooldown speed must be similar with STM and be carefully controlled. Fig.2 shows a cooldown process of STM and shields in March 1996.

HEAT LOAD AND MASS FLOW REQUIRED

When STM is cooled down to 4.6K the vacuum in cryostat should reached ~4×10^{-4}Pa if the leak level is normal. The total heat load of STM is about 130W/4.6K. To cool a couple of 7kA current leads 0.7g/s mass flow from the return line is required. The heat loss on the transfer line between the refrigerator and current lead block is estimated total 20W including 12m-length transfer tube, five bayonet connections and a bypass valve.

Because the 48 NbTi/Cu superconducting strands embedded in HT-7 conductors are parallel arrangement without twist. When toroidal field changing the coupled length of a coil is 190m (full conductor length), the eddy currents can cause STM premature transition to the normal state. So to ensure STM steady operation a mass flow of 35-40g/s is required and the current ramping speed is limited while the toroidal field >0.5T. Running two expanders and a big compressor can back up the tokamak steady operation at the toroidal field <1.6T. Injector 2 on line is necessary to increase mass flow. When the toroidal field >1.6T a small compressor must run to enhance mass flow. At the mass flow of 35-40g/s the inlet pressures are 0.24-0.26MPa, and the return pressure is 0.13-0.135MPa. So the upstream flow is supercritical and the downstream is two-phase flow. Fig.3 illustrated a T-S diagram for the steady-state operation mode of refrigerator No.1. The parameters of pressure, temperature and mass flow are marked in the diagram.

CONCLUSION

The low leak rate of cryostat, short and low heat loss transferline and the optimum current leads minimize the heat load effectively. The last tokamak operation status has confirmed that the capacity of HT-7 cryogenic system has some margin for the superconducting toroidal magnet cooldown and steady operation at 1.5-2.0T toroidal fields for a term longer than one month.

REFERENCE

1 Ivanov D. P. et al., Some results from the T-7 tokamak superconducting magnet test program IEEE Trans. On Magnetics (1979) MAG-15 550-553

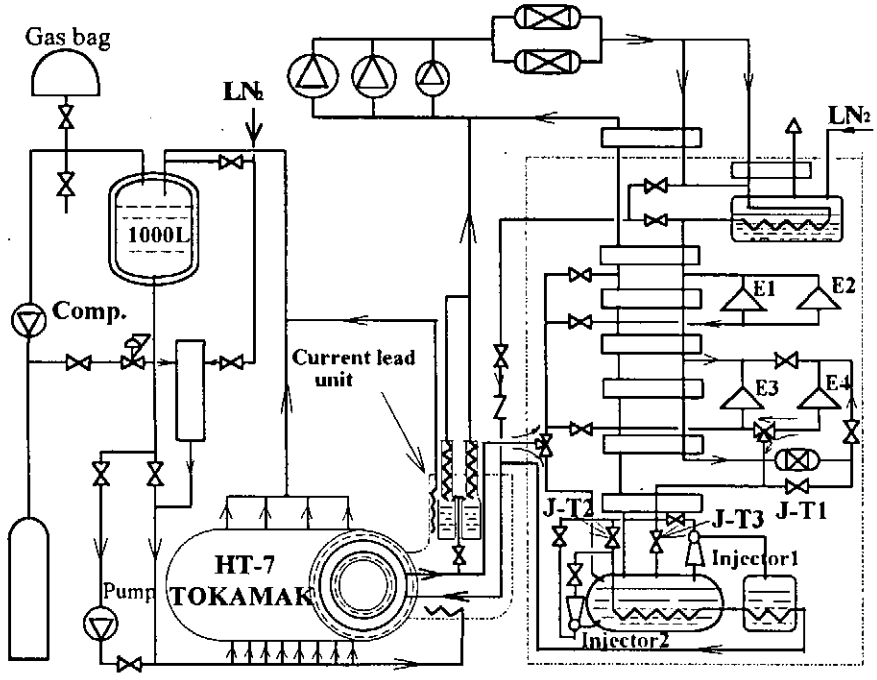

Fig. 1 Flow diagram

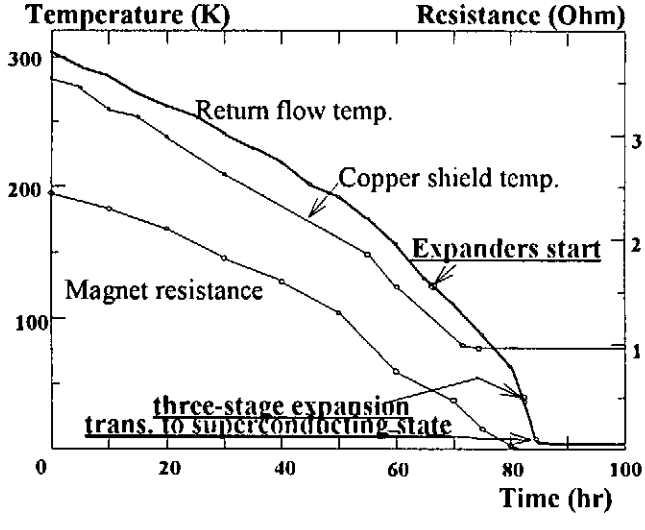

Fig. 2 Cooldown of STM and shield

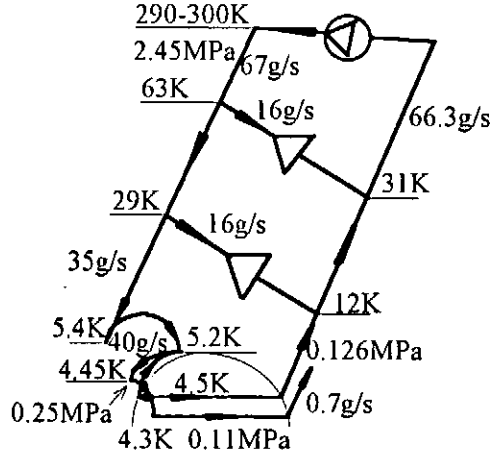

Fig. 3 T-S diagram

The Cryogenic System for the Superconducting e^+ e^- Linear Collider TESLA

G. Horlitz
DESY, Notkestraße 85, 22607 Hamburg (Germany)

ABSTRACT

The superconducting electron/positron collider TESLA (center of mass energy 500 GeV) requires a cryogenic supply system of total estimated cooling capacities of 33 kW at 2.0 K, 36 kW at 4.5 K, 243 kW at 40/80 K and current lead cooling flowrate (liquefaction power) of 0.2 kg/s. The system is spread over a linear range of about 30 km. A new layout is presented in this paper (reduction of HF - pulse rate from 10/s to 5/s results in reduced heat loads, lower numbers of cryo halls with refrigerators and increased subunit lengths).

INTRODUCTION

The TESLA project is under investigation by an international study group from different institutes and universities. Preliminary versions of the cryogenic system have been published recently [1]. Two linacs of about 14 km length, producing 250 GeV electrons and positrons respectively, will be installed collinearly, separated by a ca. 2 km long interaction zone (fig. 1). The cryogenic system, maintaining the operating temperature of 2 K, will be described. A special layout of the first ca 5 km long section will be proposed in order to enable an enlarged range of applications such as increased intensity electron beams of lower energy for nuclear physics experiments , γ - production in a free electron laser (FEL) or electron/proton collisions at HERA (which is one of the options for the final site location for TESLA).

GENERAL LAYOUT

Cavities

Basic elements of the linac are cavities, consisting of nine cell high purity niobium RF-resonators, welded into cylindrical containers of titanium [2]. The desired operating temperature of ≤ 2 K is maintained by superfluid liquid He (He II).

Modules

8 cavities, together with 1 quadrupole (operated at 4.5 K), beam monitors and RF-absorbers are assembled and heat radiation protected by 2 concentric shields (4,5 K; 40/80 K) in a module of 12,2 m length.

Strings

12 modules are arranged in a string. Adjacend strings are interconnected by string connection boxes (SCB) of 2.6 m length (fig. 2, Detail A). The total length of a string including one half SCB at each end, amounts to 149 m.

Subunits

An assembly of 16 strings is a subunit of 2384 m length (fig. 2). Every subunit will be supplied by an individual refrigerator.

The machine structure

Based on an accelerating gradient of 25 MV/m, for an end energy of 250 GeV, for each linac a number of 6 subunits , providing an active length of 10000 m is required. The cold boxes for two adjacent subunits are installed in a common above ground cryo hall (fig. 1). In the tunnel the subunits are connected by unit connection boxes of different types (UCB and UCL).

An operation at HERA requires an inclination of -5 mrad for the first two subunits (fig.1) (the layout of the end sections may be different for other site conditions).The increased beam intensity for these two subunits requires different types of refrigerators with increased cooling capacities (the high capacity at the 2 K level may be easier handled by subdivision into 2 cold boxes per subunit).

The length of one half linac, including boxes, amounts to 14398 m which results in a filling factor of 0.7. The total length of TESLA, including 2 km of interaction region amounts to 30.656 m.

HEAT LOADS

Table 1. TESLA heat loads

Temperature	2 K		4.5 K		40/80 K		
	stat	tot	stat	tot	stat	tot	W
Subunit n	695	2480	2746	2948	15243	19505	W
d	1025	3720	4119	4420	22865	29260	W
in	695	4266	2746	3149	15243	23768	W
id	1025	6400	4119	4725	22865	35650	W
TESLA n	8340	33332	32952	35778	182914	242587	W
d	12300	50000	49428	53667	274371	363881	W

(n = normally expected values; d = design values (safety factor 1.5); in, id = nominal and design values for the increased heat load in the first 2 subunits; stat = HF-power off; tot = HF-power on)

Table 2. TESLA ambient temperature electrical power input in mega watt

Temperature	2 K		4.5 K		40/80 K		Σ input	
	stat	tot	stat	tot	stat	tot	stat	tot
Subunit n	0.56	1.99	0.69	0.74	0.38	0.49	1.6	3.2
d	0.83	3.01	1.03	1.11	0.57	0.73	2.4	4.9
in	0.57	3.47	0.69	0.79	0.38	0.59	1.6	4.9
id	0.87	5.43	1.03	1.18	0.57	0.89	2.5	7.5
TESLA n	6.74	26.84	8.24	8.94	4.57	6.06	19.6	41.8
d	10.04	40.96	12.36	13.42	6.86	9.10	29.3	63.5

The equivalent room temperature power inputs have been listed in Table 2. Conversion factors are: 800; 250; 25 W/W for T = 2.0; 4.5; 60 K respectively.The 2 K factors have been corrected for the load dependent minimum temperatures (1.885 K<T<and 2 .0 K).

THE CRYOGENIC SYSTEM

Supercritical helium (4.4 K / 5 bar) from a refrigerator coldbox is injected into the subunit at point 3 (fig. 2). After having passed the 4.5 K quadrupole/shield circuit the mass flow is split at point 5, one fraction is further cooled down in HX 6 to 2.2 K, the remainder is expanded into the bath precooler (HX 5). The 2.2 K helium is locally expanded through individual JT-valves into the strings. In a 0.3 m diameter return tube both liquid and vapor flow back to HX 6 with decreasing/increasing mass flow rates respectively. All heat from the cavities (which are completely filled with liquid He II) is transported by internal superfluidal heat conduction through vertical connection tubes to the liquid phase in the return tube, where a corresponding amount of liquid is evaporated locally. In steady state operation all liquid has been evaporated completely at the end of each string, the vapor flows through all strings. At the warm end of HX 6 (ca. 3.5 K) the low pressure of the return gas (ca. 28 mbar) is established by a cascade of cold compressors [3].
Flow conditions in the return tube have been investigated theoretically [4]. The behavior of pressures, liquid levels and temperatures is presented in fig. 3 for dessign values of heatloads both in the horizontal standard subunits and in the inclined ones with increased load.
The cooling stream for the 40/80 K shield circuit is deviated from the 40 K point in the upper part of the cold box (point 6, fig. 2). It returns at 80 K and is recycled into the circuit through point 7.

Cool down/warm up procedures
From room temperature to 150 K all cavities will be cooled in parallel through a special cooling gas distribution system (fig. 2, Detail A). Between ca. 150 K and 75 K a rapid cooling speed of about 20 K/min. is required in order to avoid hydrogen diffusion problems in the niobium. A sequential cooling of string after string is applied in this region.

SUMMARY

A possible cooling scheme for TESLA has been worked out and is proposed here. Although many requirements are unique, the limits of the present state of the art are certainly reached, but not exceeded. For future optimisation of the system, experiences from CEBAF, LEP 2, LHC and especially from TTF (the TESLA test facility at DESY) will be of essential value.

REFERENCES

1. Horlitz, G.; Peterson, T.; Trines, D. The TESLA 500 System Layout, TESLA-report No. 95-21 and *
2. Nicol, T. TESLA Test Facility Cryostat Design, TESLA-report No. 95-21 and *
3. Kauschke, M.; Haberstroh, C.; Quack, H. Safe and Efficient Operation of Multistage Cold Compressor Systems, TESLA-report No. 95-21 and *
4. Horlitz, G. A study of pressures, temperatures and liquid levels in the 2 Kelvin refrigeration circuit of a 1830 m TESLA subunit under different conditions and system configurations, TESLA-Report No. 94-17, updated Nov. 1995

* Proc. 16. Intern. Cryog. Eng. Conf. Columbus, Ohio 1995, to be published

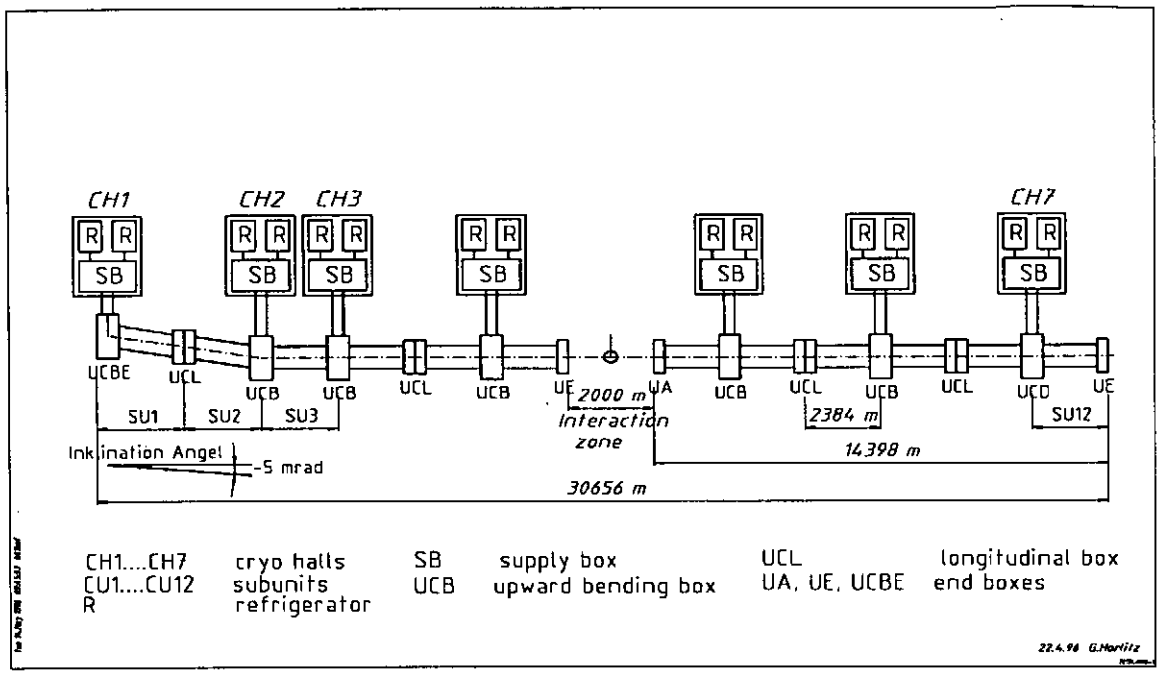

Figure 1 The TESLA refrigerator arrangement

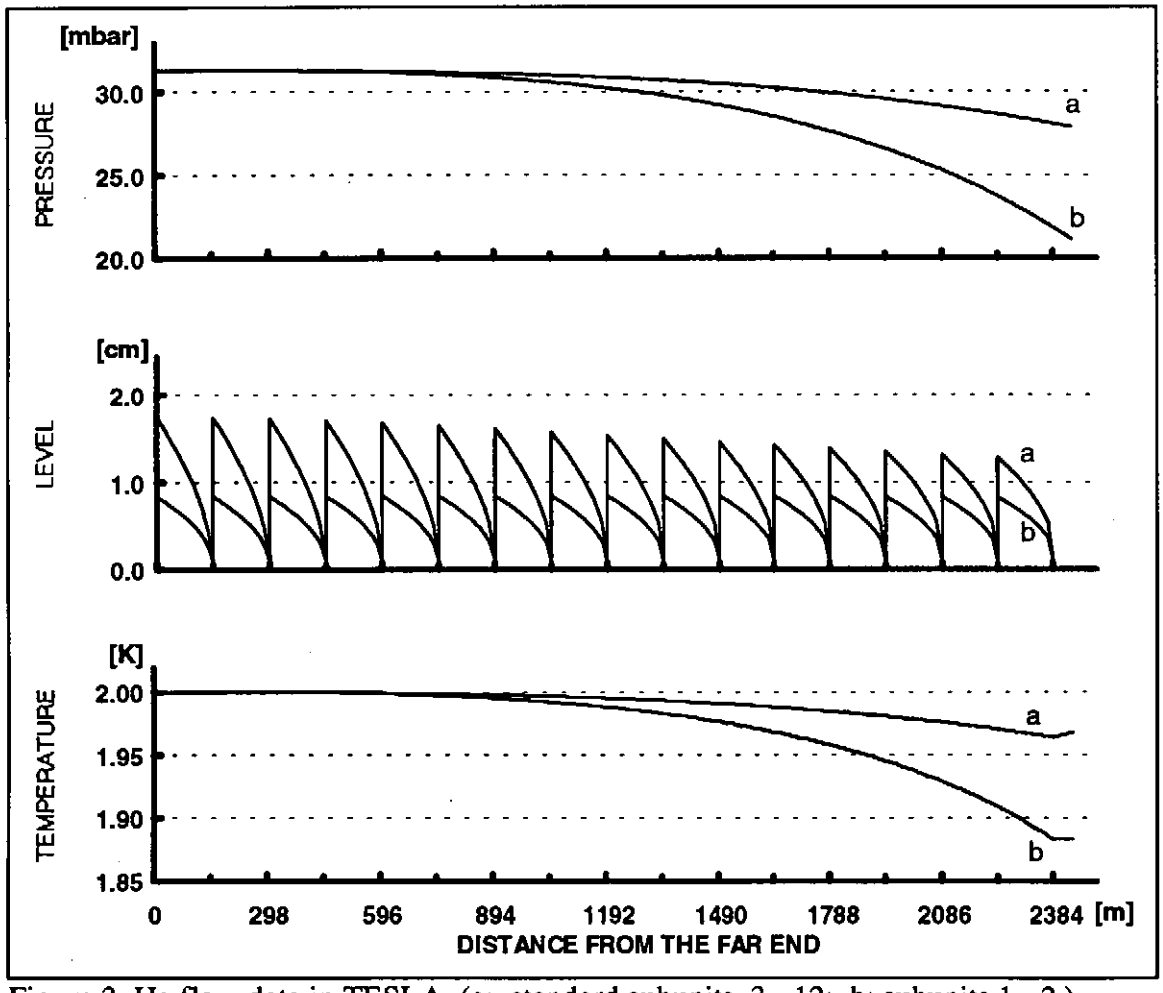

Figure 3 He flow data in TESLA (a: standard subunits 3 - 12; b: subunits 1 - 2).

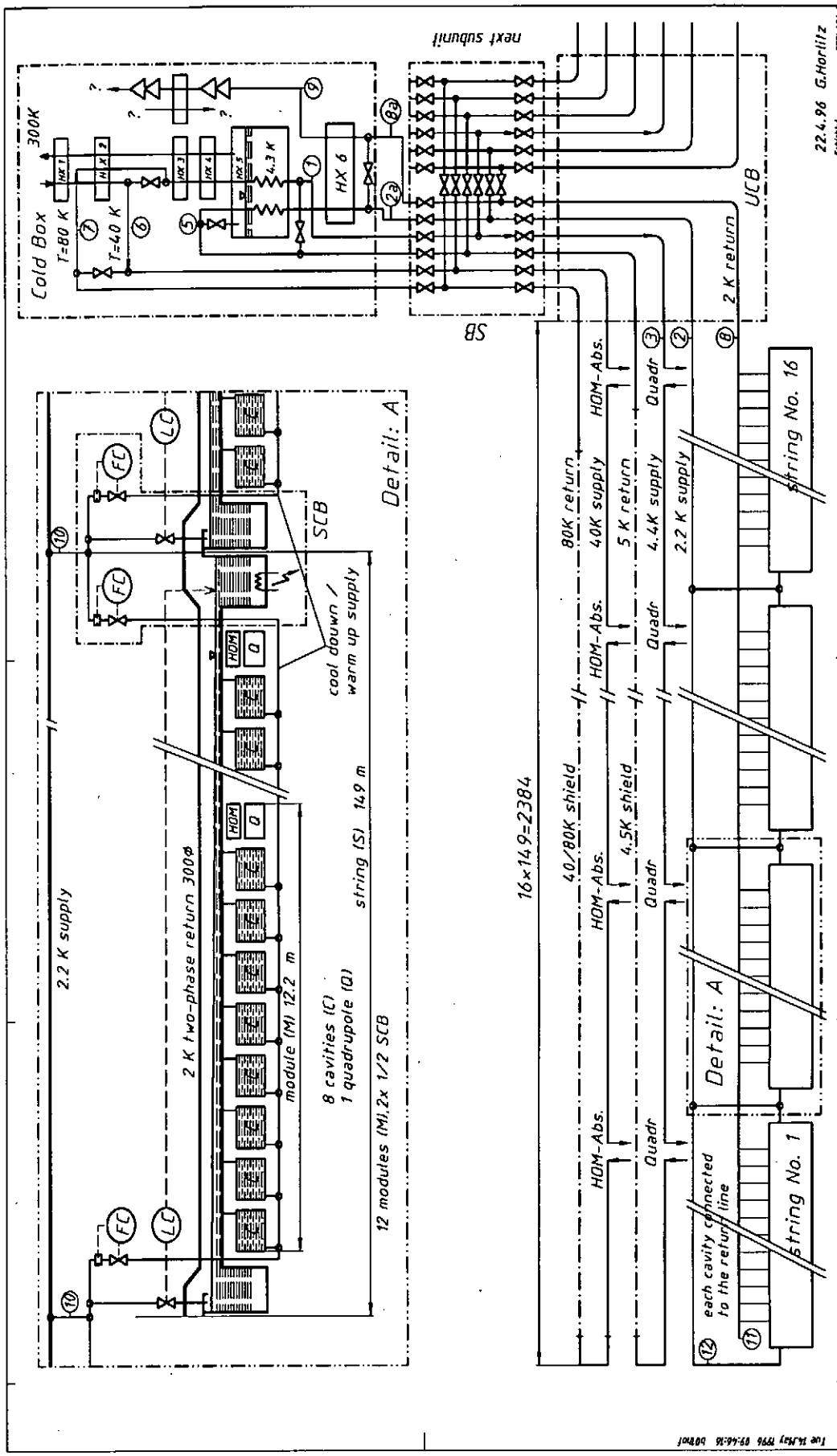

Figure 2 The TESLA subunit cooling system flow scheme

REFERENCE DESIGN OF THE TESLA REFRIGERATORS

H. Quack, M. Kauschke, Ch. Haberstroh
TU Dresden, D-01062 Dresden, Germany

INTRODUCTION

In the preceding contribution to this Symposium [1] the presently valid assumptions about the cooling requirements of the TESLA accelerator at the different temperature levels has been described. Given the total length of 30 km of the cryostats, which have to be cooled, it is obvious that the production of refrigeration has to occur in a distributed manner along the length of the accelerator. The present system design (Fig.1 of [1]) assumes 7 refrigeration feed-in points. Each feed-in point receives its refrigeration from two refrigerators of equal size.
Even though some parameters may change in the further development of the TESLA project, it is important to investigate at this stage, whether all requirements can be fulfilled technically and in a cost effective manner. For this purpose a Reference Design is being worked out. It will be used to identify weaknesses, bottle necks and cost drivers, which then hopefully will be removed in the further progress of the project. The Reference Design is also intended to raise the interest of industrial companies to motivate them to participate in the search for the best technical and commercial solution.

REFERENCE REFRIGERATOR FLOW DIAGRAM

The largest presently operating 2 K helium refrigerator is the Central Helium Refrigerator of the CEBAF project in Newport News, USA [2]. The CEBAF refrigerator contains four cold compressors in series, which compress helium from about 30 mbar to 1200 mbar with a suction temperature of the first stage of about 3.5 K. The exhaust of the fourth stage is mixed at 1.2 bar with the stream coming from 4.4 K users at a temperature level of about 30 K. The CEBAF refrigerator, even though it is running quite reliable now, has two weaknesses, associated with the strong coupling between pressure ratio and volumetric flow rate of turbocompressors:

- the starting of the cold compressors is a rather delicate process and
- the refrigerator can only run full load at 2 K. If the accelerator needs less refrigeration than full capacity of the refrigerator, electrical heaters in the 2 K system have to be switched on. While this electric heating might be a justifiable method for load stabilisation, it is not acceptable for long term operation with a large system like TESLA. Here efficient part load operation is mandatory.

For the Reference Design of the TESLA refrigerators (Fig.1), we have proposed to overcome the CEBAF weaknesses by the introduction of three new features [3]:

- A heat exchanger HX A, allowing heat transfer between the high pressure flow of the main cycle and the cold compressor stream is located between the second and third stage of the cold compressors, about at the 10 K temperature level.
- The heat exchangers downstream of the fourth stage of compression will have a separate flow passage for the stream coming from the cold compressors.
- A separate ambient temperature compression system for the handling of the cold compressor stream is foreseen.

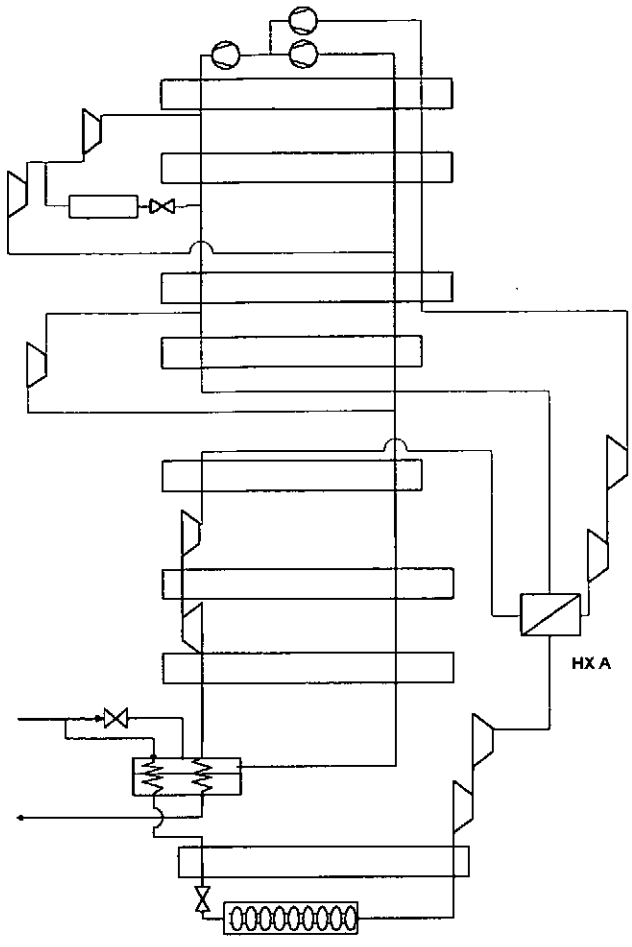

The cycle and the cold compressor staging will be designed in a way, that nearly no heat is transferred in HX A at the most probable operating condition, which may be somewhat smaller than the maximum capacity of the refrigerator.

HX A fulfils three purposes:

- **During startup** of the cold compressor train, when the cryostats are already filled with 4.4 K liquid, the fourth stage is the first machine to start. At CEBAF (without HX A) it has to start with a suction temperature of 4.4 K, which is far away from its normal operating suction temperature of about 20 K. With HX A present, the initial suction temperature will be held at 10 K, which makes the starting much easier.

Fig.1 Flow Diagram of Reference Design

- **At higher mass flow rates** than design, the first two cold compressors will have to increase their speed, providing a higher pressure ratio than normal, but also a higher outlet temperature of the second stage. Without HX A, an increased input power would also be required from stages 3 and 4. But these two stages are probably input power limited. With HX A, the inlet temperature to the third stage will be reduced to 10 K and the driving power will stay closer to its normal value.
- **At lower mass flow rates** than design, the first two cold compressors will have to decrease their speed, providing a smaller pressure ratio, but also a lower outlet temperature of the second stage. Without HX A, stages 3 and 4 would also have to reduce their speed, so the total pressure ratio of the four stages would be greatly reduced. With HX A, the inlet temperature to the third stage will be increased to 10 K, allowing a higher speed and thus a higher pressure ratio of stages 3 and 4. But this will probably not be enough for the exhaust pressure of the fourth stage to reach the design value of 1.2 bar.

Now it helps that the cold compressor stream has its own passages in the following heat exchangers and its own dedicated ambient temperature compressor, which is able to work with suction pressures between say 0.5 bar and 1.5 bar, always matching the mass flow/pressure combinations, which the cold compressors would exhaust.

So the new features allow a reliable, flexible and efficient operation of the cold compressors under all foreseeable operating conditions. Of course it has to be investigated, whether the introduction of HX A could cause new unexpected problems. The temperature level of 10 K has been chosen for HX A, because it is a rather stable temperature in the main refrigeration cycle due to the high specific heat of the high

pressure stream at 10 K. Nevertheless one has to be prepared for the case that this temperature might change or fluctuate, causing disturbances for the cold compressor system. It is mandatory that such non-stationary situations are investigated by numerical simulation [4], before the design is frozen in.

FIELDS FOR DEVELOPMENTS AND COST REDUCTIONS

The Reference Design has been given to industry for comments. Suggestions for improvements are welcome. In addition industry is asked to give budgetary prices, which will be taken into account in the overall TESLA project budget. Also fields for R+D should be suggested. For an expensive project like TESLA, it is imperative that all possibilities for cost reductions are being exploited. The time schedule of the TESLA project will allow to work on technical developments and project handling procedures, which have a potential to reduce first cost and operating costs, without compromising on reliability, of course. It may be allowed to speculate on the fields, where progress may be possible in the foreseeable future:

Safety Margins

The first cost will depend to a certain degree on the overcapacity, which is designed into the system. DESY [1] has had in the past good experience with a safety factor of 1.5. So this is used in the Reference Design. Recently CERN [5] has presented a more sophisticated approach, distinguishing between capacity reserves for unforeseen requirements on one hand and additional equipment (redundancy) to cover against perceived unreliability on the other hand.

Power Cost

The operating costs will be dominated by the power cost: Assuming an input power of 50 MW, 6000 hours per year of full capacity operation and an electricity cost of 100$/MWh (0.15 DM/kWh), one arrives at a yearly power cost of the 14 refrigerators of 30 Mio $. What could be done to reduce the power cost?

New refrigeration cycles

In the last years large scale 4.4 K refrigerators have seen a remarkable improvement in cycle efficiency, mainly by the introduction of expanders in the supercritical region of helium. But these 4.4 K cycles are not directly applicable to 2 K refrigeration with cold compressors which need essentially refrigeration between 5 and 30 K.

-Maybe we will soon see expanders on the right side of the vapour dome, e.g. with 1.2 bar and 5 K outlet, which so far have not been used in helium refrigerators.

- Maybe we will see a rise in the maximum process pressure from today's 18 bar to e.g. 25 bar.

Ambient temperature heat removal

Today's systems depend widely on open cooling water systems with the consequence of

- the necessity for water treatment installations and corrosion problems
- operating conditions changing between summer and winter, day and night.
- relatively high suction temperature of the screw compressors, leading to high compression end temperatures.

Maybe a closed refrigeration system, e.g. with R 134a as refrigerant, with dry air cooled condensers and an evaporation temperature all year around of e.g. 5°C, cooling the oil and the high pressure stream, could provide overall power savings, smaller or less screw compressors and easier operational conditions for the screw compressors.

Efficiency of screw compressors.

The thermodynamic efficiency of helium refrigerators can be derived from the product of the exergy efficiency of the cycle and the isothermal efficiency of the compression:

$$\eta_{Total} = \eta_{Cycle} * \eta_{Compressor}$$

Today's best large helium refrigerators have an efficiency of:

$$\eta_{Total} = 0.6 * 0.55 = 0.33$$

The total efficiency of 0.33 is equivalent to a power factor of 210 W/W.

Indeed, the cryogenic cycle including all its expanders and heat exchangers is more efficient than the rather conventional ambient temperature compressors. The reason is that the presently used screw compressors have not yet been optimised for the compression of helium.

Helium is of course a difficult gas to compress because of its low viscosity, high specific heat ratio and high velocity of sound. But on the other hand, cryogenic refrigerators provide an ultra-pure gas at relatively constant suction pressures and temperatures. Also there is no danger of condensation of water or refrigerant inside the compressor. And when there are multiple parallel units, we may not need slide valves for capacity control on all machines: Maybe speed control on just a few machines would be the right way for capacity control

If these special conditions can be communicated to the compressor manufacturers, they may be able to go to smaller clearances, less viscous oils, better strategies for oil injection, maybe different oil temperatures for the oil streams for bearings and sealings respectively. And if no slide valves are needed, the compressors might even get cheaper. The goal should be to come to an overall isothermal efficiency well above 60% for a two-stage compression from one to 25 bar.

Of course, we can not compromise on the level of reliability. But by standardisation of skids one may even come to groups with less vibrations and e.g. better shaft seals.

Procedures

Today, each major cryogenic refrigeration system has its own approach to computarised control. The consequence is that on several new systems, large cost overruns in hardware and man hours have occurred, as well on the user as on the manufacturer side. What is needed is that all users and manufacturers of large cryogenic systems get together and standardise their procedures for design and execution of control systems.

Plant Simulation

Development of control logic and operator training should be performed using dynamic simulation of the total refrigeration system [4].

REFERENCES

[1] Horlitz, G.: The Cryogenic System for the Superconducting e+e- Linear Collider TESLA, This Symposium

[2] Gistau, G.: High Power Refrigeration at Temperatures around 2.0 K, ICEC16/ICMC, Kitakyushu 1996, Paper OB7-1

[3] Kauschke, M.; Haberstroh, C.; Quack, H.: Safe and Efficient Operation of Multistage Cold Compressor Systems, CEC Columbus, Ohio 1995, Paper WE-B1-1

[4] Kauschke, M.; Quack, H.: Numerical Simulation of Transient States of Large Cryogenic Systems, This Symposium

[5] Riddone, G.; Tavian, L.; Wagner, U.: Demands in Refrigeration Capacity for the Large Hadron Collider, ICEC16/ICMC, Kitakyushu 1996, Paper OB7-3

CRYOGENIC SYSTEM OF THE ELBE LINAC IN DRESDEN

Ch. Haberstroh, H. Quack
Technische Universität Dresden
Institut für Energiemaschinen und Maschinenlabor
Lehrstuhl für Kälte- und Kryotechnik
01062 Dresden, Germany

ABSTRACT
At the Forschungszentrum Rossendorf near Dresden a project for installation of a small superconducting LINAC has been started (project „ELBE-Quelle"). By acceleration with three niobium cavities, placed in two separate cryostats, a 20 MeV electron beam will be provided for nuclear research and FEL experiments.
For operation of the accelerator a cooling power of 200 W at 1.8 K is required. For the 1.8 K cryogenic system different schemes have been worked out which will be discussed in the presentation. Due to the relative low cooling power in the given situation we recommend here a system based on a standard 4.4 K helium refrigerator plant with two additional cold boxes for additional heat exchangers and cryogenic valves. Pumping down to 1.8 K will be done by a multistage warm compressor unit.

INTRODUCTION

The scientific facility Forschungszentrum Rossendorf near Dresden was founded about 40 years ago and represented the central nuclear research center of East-Germany. With the reorganization in 1992 the scientific priorities have been modified. Whereas in former times research work was focused on nuclear power plant technology, today new priorities are put on ion beam material characterization, fabrication of radio-pharmaceutica, MRI and PET-examinations, as well as safety technology for existing power plants.

In the course of the technological reorganization of the Rossendorf Research Center it was decided to have a linear accelerator for electrons installed as a new equipment for basic research. It is planned to end up with a maximum electron energy of 250 MeV in the final state of the project („ELBE" - Electron Linac of high Brilliance and low Emittance). For this 250 MeV accelerator a cooling capacity of 1000 W at 1.8 K would be required resulting in a large scale helium system using cold compression. Time schedule and realization of this project are still open.
A project like the one described above implies a lot of demands, qualifications and risks. It was decided therefore to start with the installation of a 20 MeV linac first (projected under the name „ELBE-Quelle" - ELBE-source). This 20 MeV facility could be used as pre-accelerator stage for the 250 MeV linac if realized later.

Besides introducing the technologies needed for the installation of a linac operating at 1.8 K, experimental work is planned with the 20 MeV electron beam mainly in the field of basic nuclear research, FEL-operation and neutron generation for basic fusion research. The use of two different electron guns will allow operation both in pulsed mode and cw-mode.

CRYOGENIC DEMANDS

For acceleration with a gradient of 10 MV/m high purity niobium cavities will be used, operating at 1.3 GHz and 1.8 K. A 2-cell resonator will serve as capture cavity, further acceleration is done with two 9-cell cavities of about 1 m length each (fig. 1).
To maintain 1.8 K working temperature, bath cooling will be necessary. For the capture cavity a simple bath cryostat is provided. The 9-cell cavities are surrounded by a helium tank with approximately 25 l liquid inventory each, connected with a common two-phase-tube. It is requested to have separate cryostats for the capture cavity on the one hand and for the 9-cell resonator system on the other hand, to be flexible for possible accelerator modification at a later date. Furthermore there is a demand for quick cooldown of the cavities especially in the temperature range from 150 K to 80 K in order to avoid degradation due to hydrogen diffusion („Q-disease"). As the accelerator cavities are extremely sensitive to microphonics, there is a strong demand to avoid any vibration input to the accelerator system.

Being aware of the high thermodynamic loads, heat inputs at 1.8 K will be minimized by means of good thermal insulation and shields at the 80 K temperature level. Due to the high dissipation connected with the cw-regime, the heat load at 1.8 K nevertheless totals in 113 W. Additional 150 W at 80 K are required.
It is extremely expensive to upgrade an existing cryogenic system later. Therefore it was decided to specify 200 W at 1.8 K and 200 W at 80 K respectively.

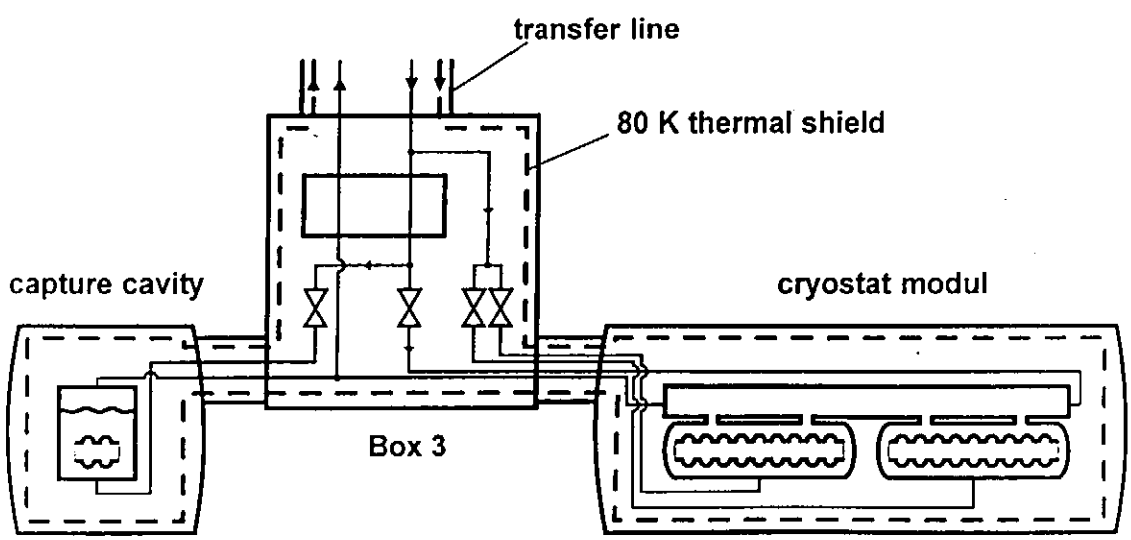

Figure 1 Cryostats for RF cavities with cryogenic supply system

FLOW SCHEMES FOR 1.8 K REFRIGERATION

The 1.8 K operation temperature corresponds to a helium vapour pressure of 1.6 kPa. Due to additional pressure drop in helium lines and heat exchangers we end up with a pressure ratio of nearly 100 to reach atmospheric pressure.
Much emphasis is being put on the question for an optimum 1.8 K helium process. In order to comply with the increasing demand for 1.8 K helium plants in recent years a lot of work has been done e. g. in the field of cold compressor development.

For the layout of the helium system both investment costs and working expenses must be kept in mind. Most important criteria for the choice of an adequate solution is the cooling power required at 1.8 K.

For small heat loads below 120 W at 1.8 K the situation is dominated by the purchase costs only. Therefore a helium cycle consisting of liquefier, Joule-Thomson unit, heater and warm compressor unit is recommended (fig. 2a). Despite exergetic losses it turns out best to warm up the low pressure helium from about 5 K to ambient temperature by means of an electric heater.

Going to higher heat loads (80 - 300 W roughly) a more sophisticated solution is justified, presented in fig. 2b. In addition to the process shown first, further heat exchangers are introduced, and a part of the high pressure helium mass flow is branched off before entering the liquefier unit. The additional heat exchangers allow to warm up the low pressure helium gas almost to ambient temperature. Limits for this solution are given by the low density of the low pressure helium gas resulting in huge heat exchanger and cold box volumes.

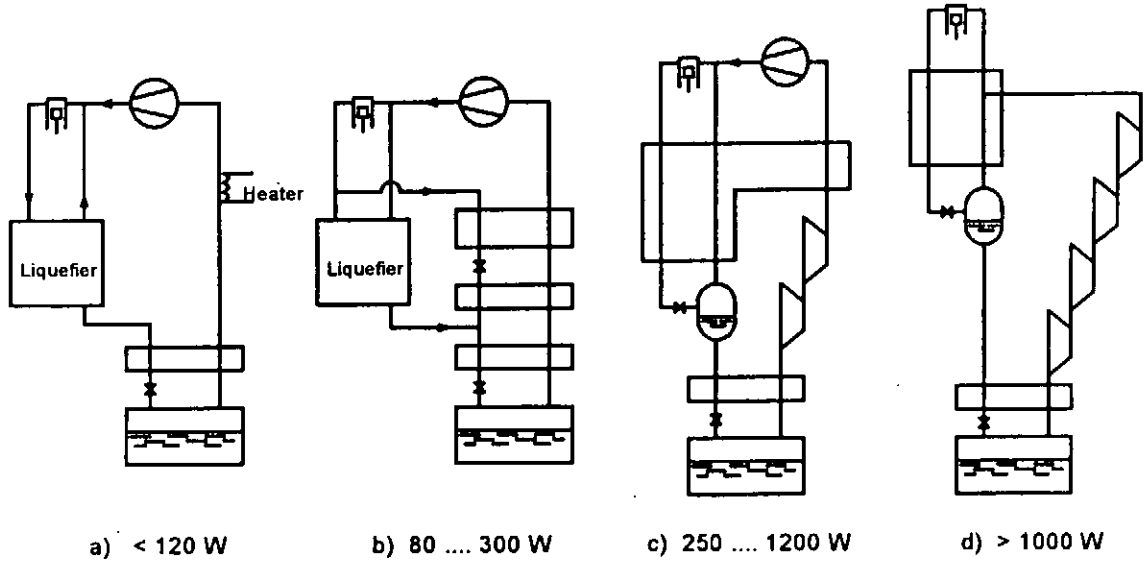

Figure 2 Schemes for 1.8 K Refrigeration

Therefore with further increase of the heat load the use of cold compressors is favorable. In Fig. 2c a configuration with cold compressors is shown, suggested for the range from about 250 W to 1200 W. After a small heat exchanger which subcools the liquid stream a two stage cold compression up to a medium pressure level is introduced. The warming up to ambient temperature can be done by a moderately sized heat exchanger, followed by warm compression up to 0.1 MPa.

The exclusive use of cold compression is suggested for heat loads exceeding 1000 W at 1.8 K. A simplified flow scheme is sketched in fig. 2d. Due to the limited pressure ratio achievable in one centrifugal machine, a multistage arrangement consisting of at least four cold compressors in series is necessary to reach atmospheric pressure. Attention has to be focused on problems caused by the limited operating range of the single stages and on the loss of efficiency while operating not at the design point or on adaptation to variable flow rates. A possible flow scheme using a dampening heat exchanger between compressor stage two and three was presented earlier [1].

SUGGESTED CRYOGENIC SYSTEM FOR THE PROJECT ELBE-QUELLE

The solution suggested to meet the particular cryogenic demands in the given situation are based on the following points:
The layout of the helium system should be according to the flow diagram given in fig. 2b, i. e. after warming the low pressure helium in large Hampson-type heat exchangers compression will be done with a set of roots and rotary vane pumps in series.
The components should be installed in three independent cold boxes. Cold box I is identical with a standard helium liquefier, thus allowing to go for a relatively cheap commercial helium plant. Cold box II is containing the large heat exchangers representing the extension to an 1.8 K system. This cold box has to be designed and manufactured exactly according to the specific demands here. In order to avoid vibrational interference these two units together with all compressors and auxiliary units will be placed in a separate building with own foundations close to the accelerator hall.
Directly beneath the two cavity cryostats a third cold box will be placed containing the last heat exchanger at the 1.8 K temperature level and a set of cryogenic valves. In the cooldown regime the subcooling heat exchanger is bypassed. In order to achieve high cooldown rates it is possible to concentrate the cooling capacity of the whole refrigerator on a single cavity.

[1] M. Kauschke, Ch. Haberstroh and H. Quack, Safe and efficient operation of multistage cold compressor units, paper presented at CEC '95, Columbus

Large Helical Device Project for SC Steady-State Fusion Experiment

O.Motojima

National Institute for Fusion Science
322-6 Oroshicho, Toki 509-52, Japan

The Large Helical Device, a heliotron-type apparatus, is a superconducting toroidal device for the fusion research and has a maximum stored energy of 1.6 GJoule (4 Tesla at the plasma center). The LHD has $\ell/m=2/10$ SC helical coils and three sets of poloidal coils. The plasma performance is simply expressed using an equivalent Q value (fusion out put/heating power) from 0.1 to 0.35. Since the LHD plasma is currentless, it provides a useful and reliable set of data with the characteristic property of the steady-state operation without any danger of current disruptions in Tokamaks. SC is a key technology issue in this project.

1. INTRODUCTION

The Large Helical Device project is now successfully executing 7th year program of 8 years construction. Engineering Research and Development for the LHD have been almost completed, and we have now accomplished more than 75% of the tough and long construction schedule. The schematic view and the specification of the LHD is shown in Fig.1 and Table 1.

The main objectives and target parameters of the LHD[1][2][3] are (1) confinement studies and the demonstration of high temperature plasmas such as the density $\langle n\rangle=10^{20}m^{-3}$ and the temperature $\langle T\rangle$=3-4keV, or $\langle n\rangle=2\times10^{19}m^{-3}$ and T(0)=10keV under an input heating power of 20MW, (2) MHD studies and the realization of high beta plasmas $\langle\beta\rangle \geq 5\%$ (plasma pressure/magnetic pressure), (3) Studies on confinement improvement and steady-state experiments by a divertor, and (4) developments on physics and technologies for fusion reactor. The target of the confinement time is shown in Fig. 2 against the international Stellarator empirical scaling law[4]. In this figure, the data points on Tokamaks L-mode are shown at the same time. From this figure, it becomes clear that the LHD aims at the regime of existing big Tokamaks like as TFTR and therefore, the H-mode production by a divertor is very important for the confinement improvement.

The LHD, a Heliotron-type apparatus, is a superconducting toroidal device with a major radius of 3.9m. It has a maximum stored energy of 1.6 GJoule (4 Tesla at the plasma center). It has $\ell/m=2/10$ SC helical coils and three sets of SC poloidal coils, of which coil currents are 7.8 MA, 5.0 MA, -4.5 MA, and -4.5 MA, respectively. The major goal of the LHD project is to demonstrate a high potentiality of the Heliotron-type device producing currentless-steady-state plasmas with an enough large Lawson parameter and without any danger of a plasma current disruption. It is expected to provide a useful and reliable set of data making it possible to project a fusion reactor precisely. SC is the major technological issue of the LHD project. In Table 2, the parameters of the LHD SC coils are listed. Both of helical and OV poloidal coils are the world biggest SC coils among the existing fusion devices.

Here, it is thought worthwhile to explain the location of the LHD project in the long ranged fusion developing strategy in Japan[5]. This is illustrated in Fig. 3. Our project is positioned as an alternative approach to a demo-reactor belonging to the

Ministry of Education (MOE). It has a role on the more basic exploitation of physics and technology researches than applications. Another is a tokamak approach of JAERI governed by STA (Science and Technology Agency). It is well known that the ITER is a big ongoing project in the world. Since the intrinsic problems concerned with the existence of the huge plasma current of tokamaks, i.e., hazardous disruption, and comprehensive current profile control and required technique for the current drive with a high circulating power, etc., it is a reasonable understanding to develop simultaneously a project of the currentless system. Therefore, the design optimization for the LHD has been intensively executed to produce a high performance of the plasmas close to the break even condition (Fig. 2), and it has been conducted around the machine size of the major radius of R=4m and the magnetic field strength of B=4Tesla. Obviously, the adoption of SC magnet system to ascertain the steady operation was the necessary condition for the LHD. Our definition of steady-state condition is more than 1,000sec which provides the equilibration of the inductive and thermal phenomena. This is also adopted in the ITER project.

Table 1. Specifications of LHD

Major Radius	3.9 m
Coil Minor Radius	0.975 m
Averaged Plasma Radius	0.5～0.65m
ℓ, m	2, 10
Magnetic Field	3(4) T
Helical Coil Current	5.85(7.8) MA
LHe Temperature	4.4(1.8) K
Poloidal Coil Current	
Inner Vertical Coil	5.0 MA
Inner Shaping Coil	-4.5 MA
Outer Vertical Coil	-4.5 MA
LHe Temperature	4.5 K
Plasma Volume	20～30 m^3
Heating Power	40 MW
Coil Energy	0.9(1.6) GJ
Refrigeration Power	9(～15) kW

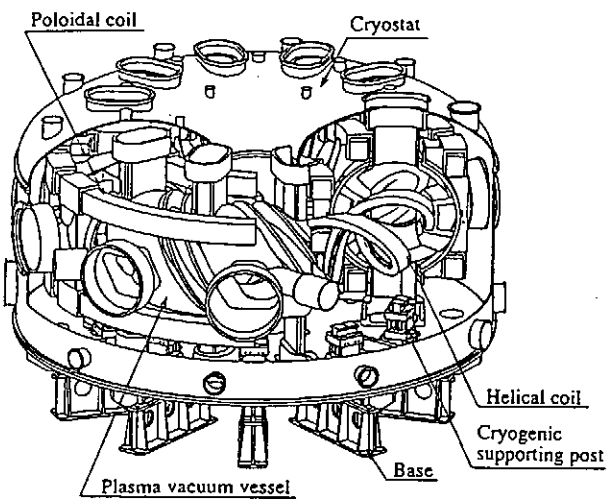

Fig. 1 LHD Device

The realization of the steady-state operation requires a large extent of engineering innovations, primarily in the areas of superconducting technology, plasma facing materials and water cooling systems, and heating systems. It also contributes to build up the engineering scenario required for a long pulse regulated plasma operation. In this paper, we generally review the major progress of the LHD project, i.e., the present status of construction, recent results of SC R&D obtained, and the fabrication technology newly developed for the huge and reliable SC magnet system. These are the necessary goal of the LHD project and are expected to contribute to a future experimental reactor in the next decade.

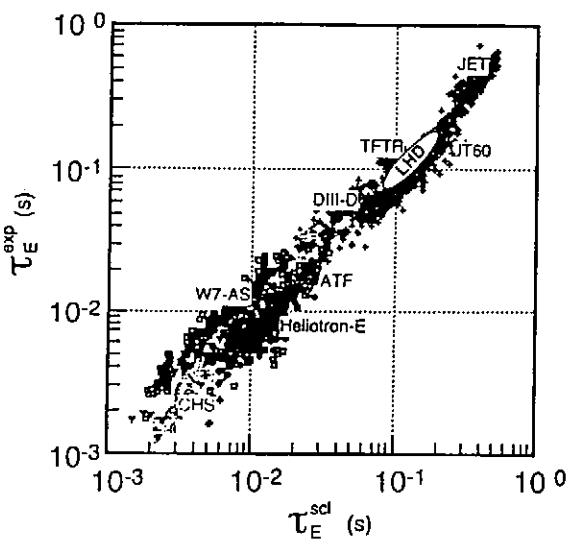

$$\tau_E^{scl} = 0.08\, a^{2.21} R^{0.65} P^{-0.59} n^{0.51} B^{0.83} \iota_{2/3}^{0.40}$$

Fig. 2 Objective of LHD

Table 2 List of Coil Parameters

Items	Helical coil	IV coil	IS coil	OV coil
Superconductor	NbTi/Cu	<--	<--	<--
Conductor type	Compacted strands	CICC	<--	<--
Cooling method	Pool-cooled	Forced flow	<--	<--
Major Radius	3.9 m	1.80	2.82	5.55
Weight per coil	120 ton	16	25	50
Maximum field in coil	9.2 T	6.5	5.4	5.0
Stored energy	1.6 GJ	0.16	0.22	0.61
Nominal current	17.3 kA	20.8	21.6	31.3
Coil current density	53 A/mm2	29.8	31.5	33.0
Magnetomotive force	7.8 MA	5.0	-4.5	-4.5
Hoop force	356 MN (*1)	262	116	263
Up-down force	240 MN	-60.2	95.6	72.2

(*1) When the HC only are excited. In the experimental mode, this force become compressive (~60 MN).

2. PRESENT STATUS OF CONSTRUCTION

The number of major components which are under construction is rapidly increasing. They are (1) poloidal coils IV (1992), IS (1994), OV (1996) (2) lower half of cryostat (1994), (3) helical coil fabrication machine (1994), (4) helical coil conductor (1995), (5) helical coil (1996), (6) liquid helium refrigerator (1994), (7) power supplies of poloidal coil (1994) and helical coil (1996), (8) water cooling system (1994). The year indicated in the bracket means the time of the completion. These major components except coils have been fabricated as several separated sections in the factories. They have been gradually transferred to the institute after the completion of the main experimental hall building in summer 1994. Now, the on-site fabrication of major components is kept going for (1) vacuum chamber, (2) cryostat, (3) magnetic force structural support, etc. Now a day, the coil winding process has successfully completed.

In Fig. 4, we show the present view of the main experimental hall. The size is 45m x 75m x 40mh, In this room, the on-site fabrication of helical and poloidal coils were carried out simultaneously. An air conditioner keeps the temperatures around 25°C even in summer time and humidity less than 60%. Another important facility required is a crane. There are two 250ton and one 30ton cranes which make it possible to execute the necessary assembly process of the major components with the mass of 1,500ton in total. In the photograph, the construction area for the helical coil, the poloidal coil, and the huge SUS magnetic supporting structure are seen.

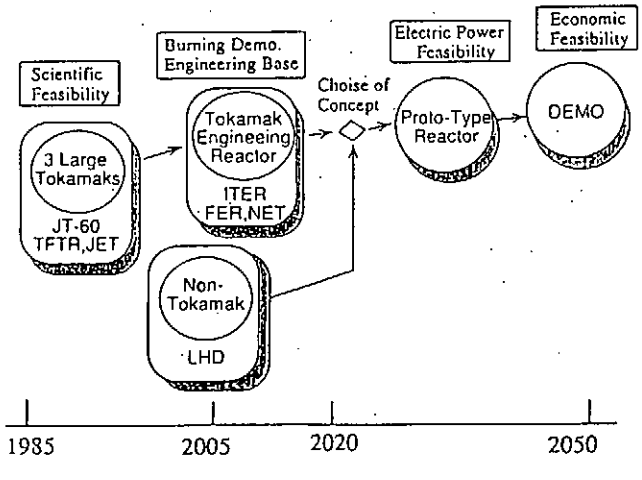

Fig. 3 Fusion Research in Japan

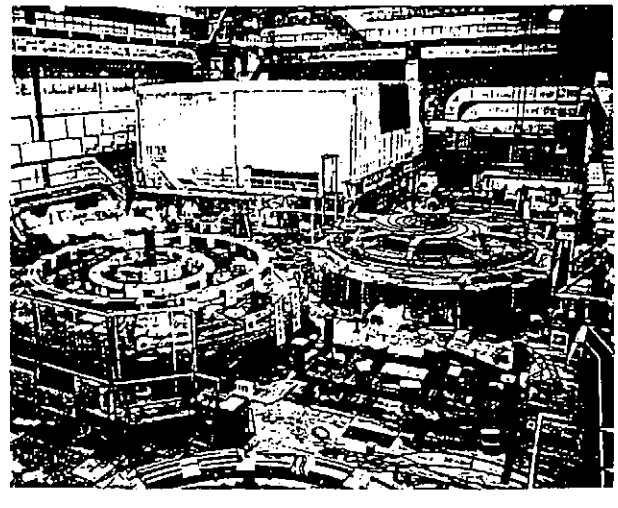

Fig. 4 Present View of Main Experimental Hall

Heating devices are also under construction[6]. An ECH system uses 168GHz gyrotron of CPD type in addition to 84GHz because of the efficient heating for the higher density plasma production. The ECH system of 168GHz/5-10MW (10 tubes) is under construction (1994-1995). One of two NBI beam lines is also under construction (1995-1996). The energy of NBI system has been increased from 125keV(H) to 180keV(H) in order to overcome the reduction of ionization loss by hydrogen atoms in the excited states. Total injection power of 15MW is provided at the beginning of experiments. Each beam line has two negative ion sources. Each ion source can deliver a negative hydrogen ion beam of 40A. The 1/3 size of R&D negative ion source with an extracted current of 16A at 125keV is successfully developed. An ICRF system is now under development focusing on the high power/long pulse or steady-state operation. The entire system test including an RF oscillator, a transmission line, a tuner, and antennas has been completed up to 1MW/30min.

Various diagnostic instruments are now under development and these R&D research becomes possible at the new building of TOKI site[7]. An FIR interferrometer of 119μm/CH_3OH Laser is developed taking care of the control method for the power level and stability. Thomson scattering system of 200 spatial points/500Hz repetition rate is developed using 10 Nd:YAG Laser. The prototype system is applied to CHS[8] and the radial electron temperature profile Te(r) was measured in detail. The HIBP of 6MeV Au beam system is studied using a tandem type accelerator. The HIBP system has been already tested in JIPP-TIIU(500 keV, Ti beam)[9] and in CHS(80 keV, Cs beam) to measure the plasma potential.

3. ROLE OF CURRENTLESS STEADY-STATE EXPERIMENT

The major role of the currentless steady-state experiment of the LHD is obviously and well summarized in the following, (1) satisfying the necessary condition of an economical fusion reactor to ensure the self-ignition, possibly taking the advantage of the currentless plasma, (2) understanding the existing issues on fusion science, i.e., increasing the knowledge on plasma boundary phenomena, plasma wall interaction, plasma heating (burning), fueling, particle and impurity control, ash-exhausting and confinement improvement, and (3) developing necessary issues on fusion technology, i.e., SC magnet, high heat flux component, cooling technique and pumping systems.

In recent years, the interest on the steady-state experiment has also grown up in tokamak devices. As the ITER project makes the progress[10], the new proposal to built a big SC tokamak device and to produce a plasma with a duration more than 1,000sec has become aware of the new target. This milestone, the plasma duration of 1,000sec, exceeds the longest time constant of major plasma-wall interaction processes. In Fig. 5, obtained data points and proposed target values are summarized in the diagram between Lawson parameter $nT\tau$ and plasma duration τ pulse. From this figure, it becomes clear that the LHD explores a new parameter regime. The level of the steady (CW) power is 3MW at the beginning and increased to 10MW gradually. We will sustain the plasma with the temperature of more than a few 1,000eV in the medium density region.

To ascertain and realize the above objectives and obligations, the development of SC magnet technology is indispensable. In this process, the typical advantage of the currentless plasma operation was made clear which could avoid the difficulties of tokamaks. This is well illustrated in the design output, i.e. the reduction of AC loss problems in SC magnets, and eddy current problems of the vacuum chamber and the magnetic force supporting structure, which have no toroidal electric breaks.

4. SC MAGNET TECHNOLOGY

In this session, we introduce the new SC magnet technology developed in NIFS to realize the LHD steady-state experiment. The first important outcome of SC R&D is the development of the fully stabilized conductor for helical coils with an aluminum stabilizer. This is a pool boiling type NbTi conductor with a copper casing. It has the cross section of 12.5mm x 18.0mm and is available for the nominal current of 13 kA at 7 Tesla. The critical current and the recovery current of the conductor is more than 22

kA and 13kA, respectively. The current density of the coil package is 53A/mm^2. To avoid the enhancement of the resistance of the stabilizer by the Hall effect between Aluminum and copper, an optimum resistive layer (Cu-2%Ni: 0.4mm layer) is imposed between the copper casing and the aluminium stabilizer to intercept the produced Hall current. The total length of the conductor reaches to 37km, of which unit length is around 1km. We carried out the SC performance test for the individual rod of fabricated conductors before delivering it to the winding process[10].

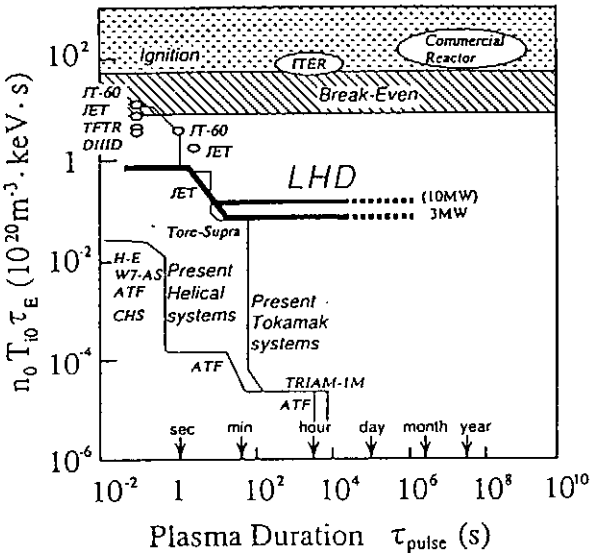

Fig. 5 Summary of Obtained Plasma Data Points and Objective of LHD

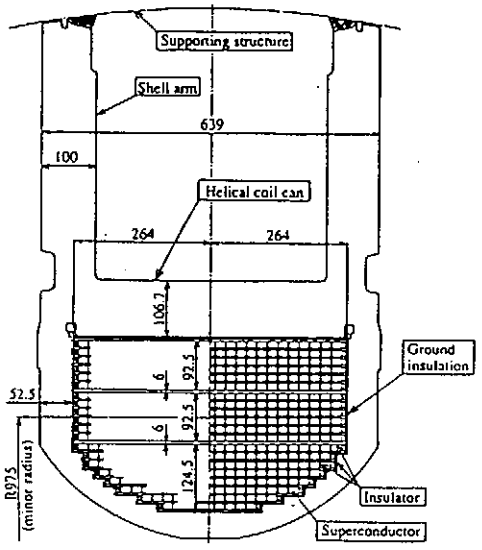

Fig. 6 Cross-section of Helical Coil and Can

We have also spent a large effort to develop an SC poloidal coil system. To fabricate the poloidal coils, a new forced flow helium cooled conductor with a high stability margin (NbTi cable in conduit type, Table 2) has been developed to reduce the AC loss due to the real-time swing of the coil current during the plasma experiments (about 1kA/sec). Cooling-down and current-excitation tests on the smallest poloidal coil (inner vertical coil, IV coil) was a high light of the poloidal coil R&D in 1995[11]. Without the experience of any coil quench, we could reach the nominal current value of 20.8kA. During this test, we accumulated a lot of practical experiences necessary to operate the huge superconducting coils, i.e., the cooling-down scenario, the removal technique of impurities in liquid He, and the monitoring techniques for the temperature and deformation of components, etc.

The executed design and construction tasks of the LHD have typically made a large contribution to the fusion technologies. The mass of the SUS316 supporting structure for the LHD superconducting magnet system is more than 450ton, which sustains the total magnetic force of 40,000ton under the liquid He temperature corresponding to the maximum stress level of 250MPa. Including the coils, the total mass at the liquid He temperature is around 900ton. Due to the requirements for the high rigidity and compactness of this supporting structure, the helical and poloidal coils are attached to a thick and heavy SUS316 cylindrical supporting shell by welding. The thickness and minor radius are 100 mm and 1.8 m, respectively. It is an advantage of the LHD that there is no one-turn electrical break around a torus unlike tokamaks, since the LHD is a currentless-steady device. The helical-coil conductor is wound into a helical-coil-can (Fig. 6) with the mechanical accuracy less than 2 mm and the allotted maximum clearance of 65 μ m between the conductor surface and the insulator. The total number of turns is 450. The helical coil can is welded to the supporting shell with shell-arms. Necessary channels for the He gas void produced is skillfully designed and distributed at the corners of this coil package with a diameter of several millimeters. The method to support the poloidal coils was also carefully decided. The poloidal coils are stiffly fixed to the supporting shell in all directions, which are electrically insulated from the supporting shell. Their mutual displacement is made small enough and symmetrical within $\pm$ 2 mm in any direction, which is quite important to guarantee the

good magnetic surfaces for the plasma confinement.

In the below, we shortly supply more informations on the major progress of SC magnet technology during the LHD construction[1,2]. (1) Helical coil conductor joint; There are 32 joints. We could obtain the enough low value of the resistance of each joint less than 0.7 nano ohm (0.2 W at 17.3 kA). (2) Evaluation of AC loss in helical conductor; The AC loss of helical conductor is evaluated in the cryostat applying a quick swing of the magnetic field. Comparing the measured magnetization change of the conductor from the vacuum, the time constant of 4.3 sec was obtained. (3) Analysis of mechanical rigidity of coils; The helical coil is subject to a high magnetic force above 10 MN/m. Finite element method and mixture principle are utilized to calculate the rigidity of a coil pack which simulates the actual configuration of the helical coil. (4) A superconducting bus line; A flexible SC bus line is developed for a current feed system for the LHD. An aluminum stabilized NbTi/Cu compacted strand cable is used to satisfy the requirement for the fully stabilized condition at a nominal current of 32kA. We will utilize the SC bus line for both helical and poloidal coils. (5) Coil protection; The coil protection circuit for the helical and poloidal coil system is an urgent subject for the LHD operation. A 30 kA range of DC circuit breaker using a power fuse and an AC vacuum breaker is developed for this circuit with a dump resistor. After the demonstration tests using the practical circuit and dummy coils, the operation sequence and the possibility of fault of 10^{-6} are confirmed. (6) Supercritical helium pump for forced flow cooling; A SHe circulating pump for poloidal coils is developed and tested during IV coil test (50gr/s). The mechanical performance with the high pressure drop between inlet and outlet (1atm) was confirmed.

5. SUMMARY

In this year, 1996, the major activity of the LHD construction will move to the finalizing phase at the Toki site. The construction schedule is indicated in Fig. 6. We will keep continuing the necessary tasks for the construction and the assembly of the LHD, which will be completed almost within two years from now, and then the first plasma experiment will start immediately.

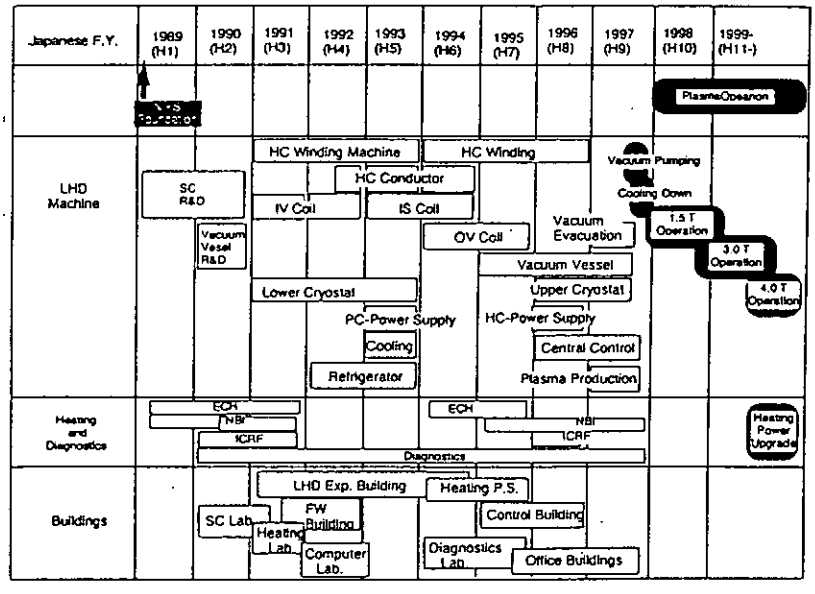

Fig. 6 Construction Schedule of LHD

REFERENCE

(1) O.Motojima, Fusion Technology 26 (1994) 437
(2) O.Motojima, Symposium on Fusion Engineering, Champaign, Ill., Setp.30-Oct.5, 1995, Invited
(3) O.Motojima, et al., Fusion Technology 27 (1995) 123
(4) H.Yamada, et al., To be published in Nuclear Fusion (1996).
(5) A.Iiyoshi, et al., To be published in Fusion Engineering (1996).
(6) T.Watari, et al., Annual Report of NIFS, 1995
(7) Y.Hamada, et al., Annual Report of NIFS, 1995
(8) K.Matsuoka, et al., Annual Report of NIFS, 1995
(9) ITER/JCT Report 1995, San Diego
(10) N.Yanagi, et al., Reported in this conference.
(11) K.Takahata, et al., Reported in this conference.
(12) J.Yamamoto, et al., Annual Report of NIFS, 1995

CRYOGENIC SYSTEM FOR THE LARGE HELICAL DEVICE

T. Mito, S. Satoh, S. Yamada, K. Takahata, N. Yanagi, S. Imagawa,
K. Watanabe, A. Iwamoto, R. Maekawa, T. Baba, S. Moriuchi,
J. Yamamoto, O. Motojima, LHD Group,
(National Institute for Fusion Science, Oroshi, Toki, Gifu 509-52, Japan)

ABSTRACT

The cryogenic system and the cooling schemes for the Large Helical Device (LHD) are described. The cryogenic system for the LHD consists of the helium refrigerator/liquefier, the superconducting helical and poloidal coils and the peripheral equipment, such as superconducting bus-lines, control-valve-boxes and cryogenic transfer-lines. The helium refrigerator/liquefier has cooling capacities of 5.65 kW at 4.4 K, 20.6 kW from 40 K to 80 K and 650 L/h liquefaction. Three different cooling schemes are utilized for each cooling object; a pool boiling for the helical coils (cold mass of 240 tons), a forced flow of supercritical helium for the poloidal coils (182 tons), a forced flow of two phase helium for the coil supporting structure (390 tons) and the superconducting bus-lines (total length of 463 m). The total heat balance and the overall operating scenario of the cryogenic system; such as, a cool-down, a steady-state operation, a warm-up, a power failure and a coil quench, have been discussed.

INTRODUCTION

The Large Helical Device (LHD) is a fully superconducting heliotron type fusion experimental device under construction at the National Institute for Fusion Science (NIFS). The superconducting coils for the LHD consists of two helical coils and three pairs of poloidal coils. The major and minor radii of the helical coils are 3.9 m and 0.975 m, respectively. The magnetic fields at the plasma center and the magnetic stored energies are 3 T and 0.9 GJ in phase I operations and 4 T and 1.6 GJ in phase II operations. The helical coils are cooled by the pool boiling of liquid helium in phase I and are going to be cooled by the superfluid helium in phase II. The poloidal coils are cooled by the forced flow of supercritical helium. The construction of the LHD was started in 1991 and will be completed in 1997.

REQUIREMENTS FOR THE CRYOGENIC SYSTEM

Safety and stable operations of the SC coils should be required because the total magnetic stored energy of the LHD becomes 1.6 GJ in phase II operations. Long term operations are necessary because a warm-up of the total cryogenic system including the SC coils will be done only once or twice per a year. Simple and cost-minimum designs are required for the cryogenic system using commercial or well confirmed components. Short initial cool-down time less than two weeks is required to enable quick start of the plasma experiments. Full automatic control, corresponding to the various cooling modes such as, a cool-down, a steady-state operation, a warm-up, a power failure, a coil quench, is necessary for the cryogenic system to eliminate human errors of the operators due to the complicated cooling schemes of the LHD.

COOLING SCHEMES FOR THE LHD

The LHD cryogenic system consists of the helium refrigerator/liquefier, the LHD cryostat in which the superconducting helical and poloidal coils and the coil supporting structures are installed, and the peripheral equipment, such as superconducting bus-lines, control-valve-boxes and cryogenic transfer-lines.

Figure 1 shows the flow diagram for the cooling objects of the LHD cryogenic system. The conditions of cryogen at the numbered points in the flow diagram are listed in Table 1. In the steady state operation of the LHD, there are four kinds of cryogen; 1) supercritical helium for the poloidal coils, 2) two phase helium for the coil supporting structure and the superconducting bus lines, 3) liquid helium for the helical coils and the current leads, 4) 40K - 80K gaseous helium for the thermal radiation shields of the LHD cryostat, the helical valve box, the poloidal valve box, the current-leads cryostats and the transfer-lines.

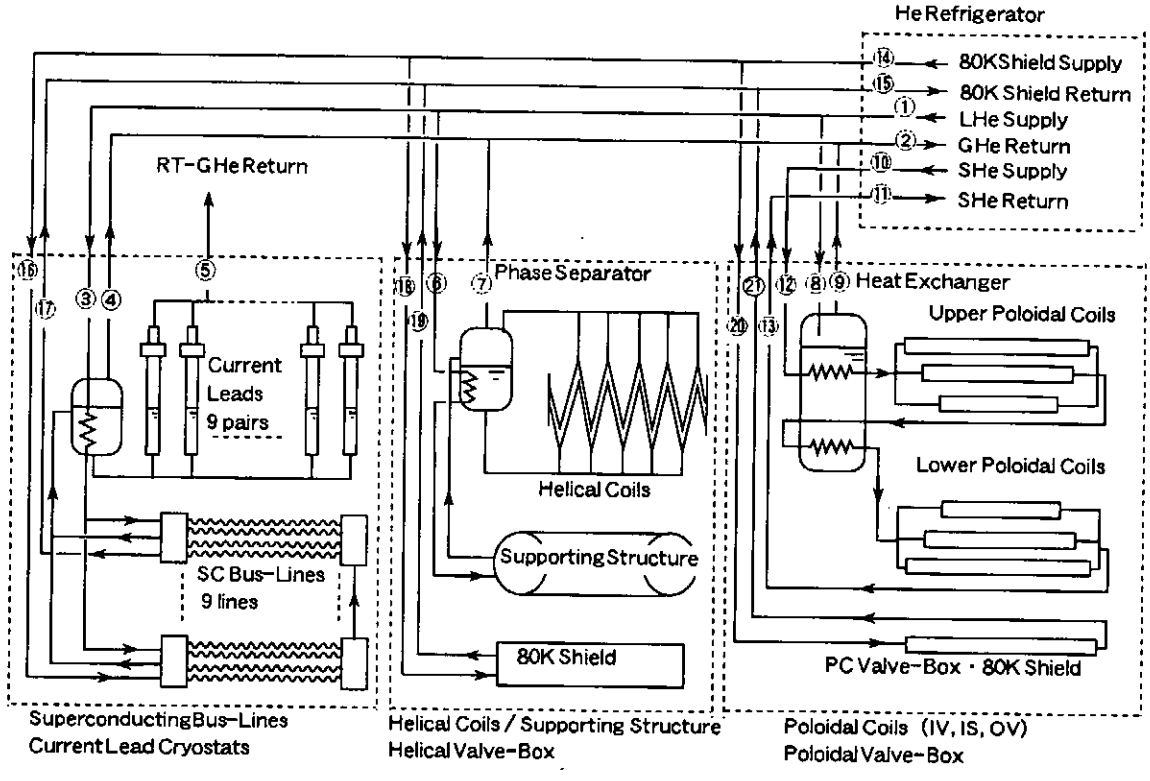

Figure 1. Flow diagram for the cooling objects of the LHD cryogenic system.

Table 1. Conditions of cryogen at the numbered points in the flow diagram (Figure 1).

No.	Kind of He	Press. atm	Temp. K	Flow rate g/s	Enthalpy J/g	Quality	No.	Kind of He	Press. atm	Temp. K	Flow rate g/s	Enthalpy J/g
1	LHe-S	1.6	4.8	334.6	13.1	0.00	12	SHe-S	9.9	5.7	300	19.0
2	GHe-R	1.174	4.7	310.9	32.7	1.00	13	SHe-R	6.8	4.8	300	13.9
3	LHe-S	1.5	4.7	108.8	15.1	0.153	14	80K-S	7.7	40.0	105.2	222.2
4	GHe-R	1.174	4.4	85.1	30.0	1.00	15	80K-R	5.2	80.0	105.2	431.2
5	GHe-R	1.05	300	23.7	1574	-	16	80K-S	7.2	49.5	20.3	272.2
6	LHe-S	1.5	4.7	75.8	15.0	0.149	17	80K-R	5.7	67.5	20.3	366.0
7	GHe-R	1.174	4.4	75.8	30.0	1.00	18	80K-S	7.2	42.5	69.3	235.5
8	LHe-S	1.5	4.7	150.0	14.5	0.094	19	80K-R	5.7	74.4	69.3	402.0
9	GHe-R	1.174	4.4	150.0	30.0	1.00	20	80K-S	7.2	48.5	15.6	267.0
10	SHe-S	10.0	5.5	300	18.1	-	21	80K-R	5.7	67.6	15.6	366.6
11	SHe-R	6.6	4.9	300	14.8	-						

Cooling Scheme of the Poloidal Coils

Three pairs of poloidal coils are named the inner vertical (IV), the inner shaping (IS) and the outer vertical (OV) coils. All poloidal coils are wound with NbTi/Cu cable in conduit conductors (CICC) and are cooled by forced flow of supercritical helium (SHe). Every coils consists of 8 double pancake coils and have 16 parallel cooling paths for the forced flow of SHe. The mass flow rate of the IV, IS and OV coils are 80 g/s, 65.6 g/s and 80 g/s, respectively. The total mass flow rate of six poloidal coils becomes 451.2 g/s. We separate the poloidal coils to two groups; the upper coils and the lower coils and connect them in series to reduce the total mass flow rate to 225.6 g/s. The total mass flow rate of the poloidal coils including the PC sleeves (supporting covers of the poloidal coils which are attached to the supporting structures) is 300 g/s. The inlet and outlet pressures of the upper and lower poloidal coils are 9.85 atm and 8.3 atm, respectively. The pressure drop of each coil is less than 1 atm.

The supercritical helium from the helium refrigerator is supplied to the poloidal valve box, in which it is cooled by a heat exchanger, goes through the upper poloidal coils and returns to the poloidal valve box and is cooled again by a heat exchanger, then is supplied to the lower poloidal coils. Then the supercritical helium returns to the helium refrigerator and liquefies in 20,000 L Dewar through the JT valve.

Cooling Scheme of the Helical Coils

The pool boiling type superconductor is used for the helical coils because of the flexibility for the helical windings. The helical coils, which are covered with the helical coil cans, are cooled with the static pool boiling of liquid helium without any active components for the reliable and safety operation.

The coils are cryogenic stabilized at a nominal current of 13 kA. The coils can be discharged without a quench by fast ramp down (15 min) or fast down (decay tine constant of 5 min), when there are any trouble in the cryogenic system. When the coils quench, the coil currents are shut down with a decay time constant of 20 s, the coils are isolated from the helium refrigerator and the helium gas is released to vent by the three kinds of safety valves.

The liquid helium is supplied from the 20,000 L Dewar to the helical valve box and goes through the cooling pipes of the coil supporting structure as the forced flow of two phase helium, then is separated to liquid and gas at a phase separator in the helical valve box. The helical coils is connected to the phase separator and is cooled by the pool boiling liquid helium.

Cooling Scheme of the Supporting Structure

The supporting structure is cooled by the forced flow of two phase helium because of its complicated structure. The cooling paths of the supporting structure are 80 parallel paths during a cool-down and are reduced to 20 paths in a steady operation. Total mass flow rate of the two phase helium is 75.8 g/s. The two phase helium is separated to liquid and gas at the phase separator in the helical valve-box after cooling the supporting structure. The phase separated liquid helium is used as the pool boiling helium for the helical coils. The cold mass of the supporting structure is 390 ton and the total cold mass is 822 ton.

Cooling Scheme of the Superconducting Bus Lines

The superconducting bus lines are cooled by the forced flow of two phase helium. There are 9 bus lines for H1-I, H1-m, H1-o, H2-I, H2-m, H2-o, IV, IS OV, the total mass flow rate of the bus lines is 109 g/s, and each of them is 12 g/s. The bus lines are from 45 m to 58 m in length and the total length is 463 m. The bus lines require excellent stability and safety exceeding that of superconducting coils themselves because the large magnetic stored energy must be extracted through the bus lines if and when the coils quench. The two phase helium from 20,000 L Dewar is subcooled by a heat exchanger at the current-leads cryostat, then is

supplied to the superconducting bus lines. The returned two phase helium from the bus lines is separated at a phase separator at the current-leads cryostat. The liquid helium baths of the current leads are connected to the phase separator, and the current leads are cooled with helium vapor from the liquid helium baths.

Cryogenic System for the LHD

The cold masses of the LHD are listed in Table 2. The helium refrigerator/liquefier has cooling capacities of 5.65 kW at 4.4 K, 20.6 kW from 40 K to 80 K and 650 L/h liquefaction as listed in Table 2. The corresponding allowable maximum heat loads for each components of the LHD are listed in Table 3.

Table 2. Cold mass of the LHD

Items	Cod mass
Helical coils	240 ton
Poloidal coils	182 ton
IV coils	32 ton
IS coils	50 ton
OV coils	100 ton
Supporting structure	390 ton
Piping etc.	10 ton
Total	822 ton

Table 3. Allowable maximum heat load for the LHD

Items	4.4 K	80 K
Helical coils Supporting Structure HC valve-box 80 K radiation shields	1,135 W	11,540 W
Poloidal coils PC valve-box	800 W	1,560 W
SC bus-lines Current leads	1,165 W +650 L/h	1,900 W
Transfer lines and Others	2,550 W	5,600 W
Total	5,650 W + 650 L/h	20,600 W

SUMMARY

Figure 2 shows construction schedule of the cryogenic system for the LHD. The engineering design and construction of the helium refrigerator/liquefier was started in 1992 and was completed at the end of 1994. We have been conducting test operation of the helium refrigerator/liquefier with a dummy heat load to gather data on cooling characteristics of a large-scale cryogenic system. The assembling of the LHD will be completed at the end of 1997. The first cool-down of the LHD is scheduled at the beginning of 1998.

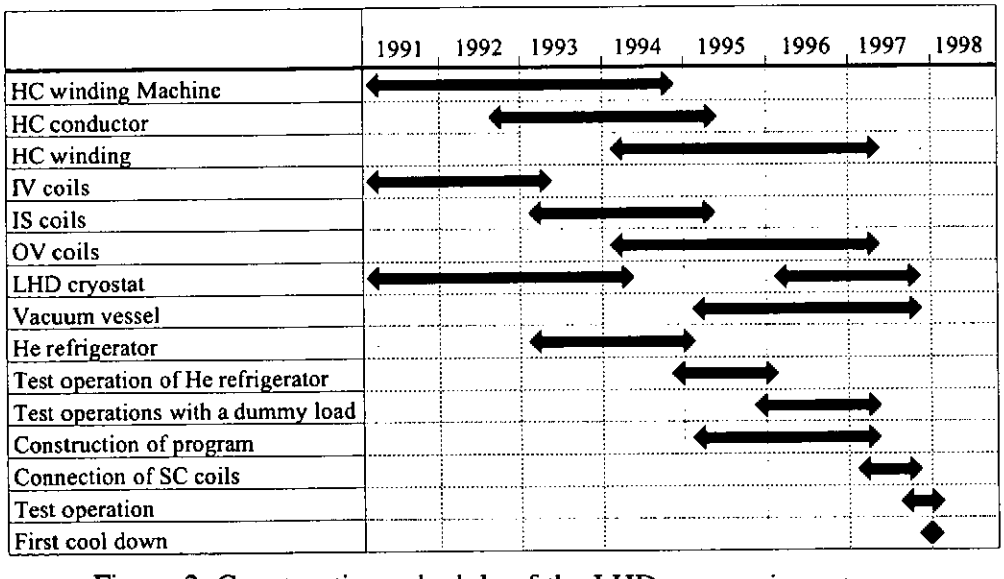

Figure 2. Construction schedule of the LHD cryogenic system

Present Status of the Large Helical Device

T. Satow, J. Yamamoto, K.Takahata, S. Imagawa, N. Yanagi, H. Tamura, S. Yamada, T. Mito, S. Satoh, S. Tanahashi, A. Komori, K. Yamazaki, I. Ohtake, O. Motojima, and LHD Group
National Institute for Fusion Science, Nagoya 464-01, Japan

ABSTRACT
The Large Helical Device (LHD) is now constructed at the Toki site of NIFS. One of inner vertical (IV) coils, IV-L, was cooled down and energized to the rated current of 20.8 kA without a quench. The IV-L, IS-L, and OV-L coils were inserted into individual supporting frames fixed on the lower supporting structure at the end of May. Winding of two helical coils was completed. The LHD superconducting coils, the cryostat, and the plasma vacuum vessel will be assembled in by the end of 1997, and its trial tests will be carried out early in 1998.

INTRODUCTION

The Large Helical Device (LHD) [1] under construction at the National Institute for Fusion Science (NIFS) is a nuclear fusion experimental device consisting of two helical coils wound from aluminum-stabilized composite superconductors, three pairs of poloidal coils wound from cable-in-conduit conductors (CICCs), a cryostat, and a plasma vacuum vessel. The LHD magnets will be cooled down and kept at cryogenic temperatures using a helium refrigeration system, energized by six power supplies through nine pairs of superconducting bus-lines, and various physical quantities will be measured using an LHD control system.

POLOIDAL COILS

One of inner vertical (IV) coils, IV-L, with an outside diameter of 4 m and a stored energy of 68 MJ was cooled down and energized to the rated current of 20.8 kA at the maximum field of 5.2 T without a quench in December 8, 1995. The measured charac-teristic of the IV-L coil and the nominal one of the IV coils are shown in Figure 1. The measured coil current and voltage performances for the IV-L coil are shown in Figure 2.

Another one of IV coils, IV-U, has been preserved in the Cryogenics & Superconductivity Laboratories. One of inner shaping (IS) coils, IS-U, with an outside diameter of 6 m and a stored energy of 104 MJ is kept in the LHD main building.

Winding and assembly of the lower outer vertical (OV-L) coil with an outside diameter of 11.5 m and a stored energy of 251 MJ were completed in the LHD experimental hall. Figure 3 is a photograph of the completed OV-L coil. Each OV coil has 8 double-pancakes wound from CICCs. Electrical joint works between double-pancakes was carried out by the use of the solid-state bonding technique.

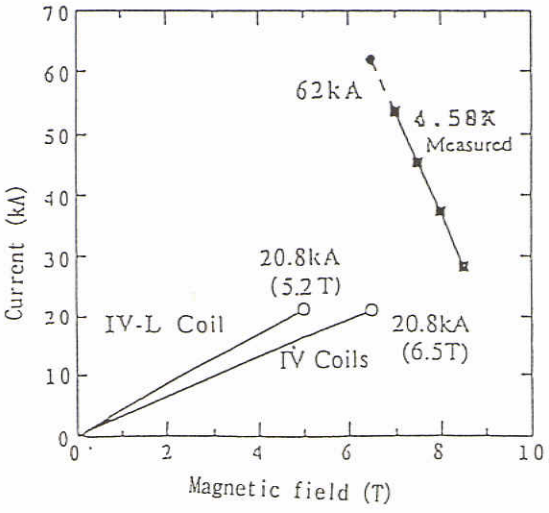

Figure 1 Measured characteristic of the IV-L coil

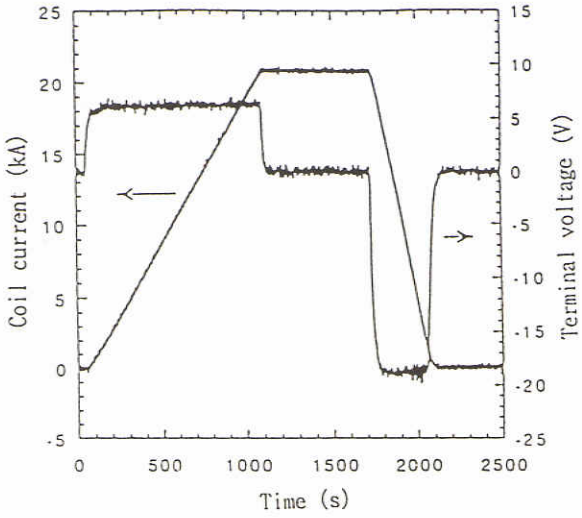

Figure 2 Excitation test results of the IV-L coil

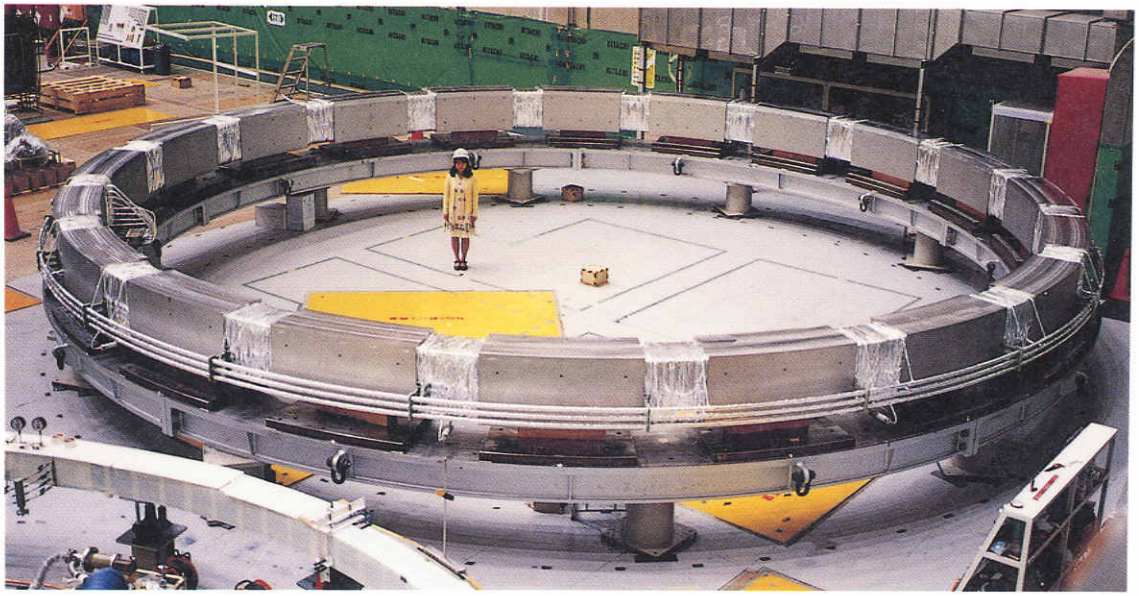

Figure 3 The completed OV-L coil

ASSEMBLY OF THE LOWER POLOIDAL COILS INTO THE LOWER SUPPORTING STRUCTURE

The lower supporting structure has been already assembled as shown in Figure 4. The IV-L, IS-L, and OV-S coils were put on the base vessel of the LHD cryostat (Figure 5). They were inserted into individual supporting frames fixed on the lower supporting structure at the end of May.

The upper supporting structure is in part under construction. Figure 6 shows the final cryogenic supporting structures where three pairs of poloidal coils and a pair of helical coils are assembled [1].

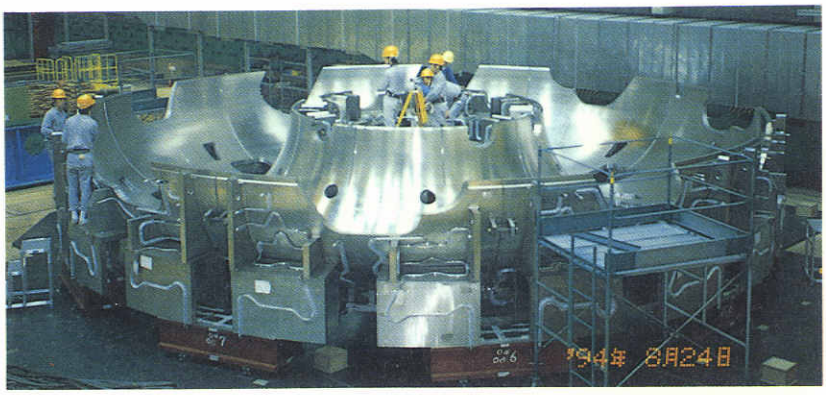

Figure 4 The completed lower supporting structure

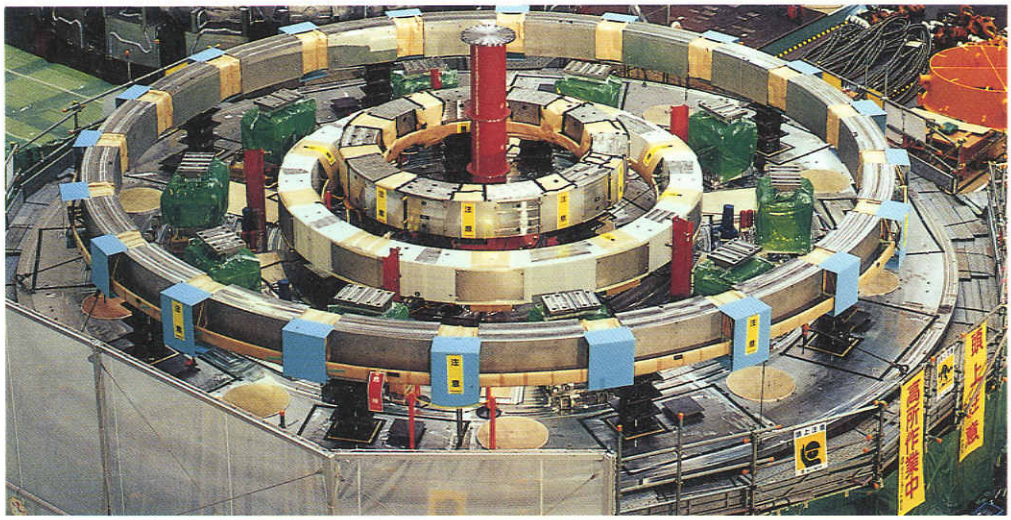

Figure 5 The IV-L, IS-L, and OV-S coils put on the base vessel of the LHD cryostat

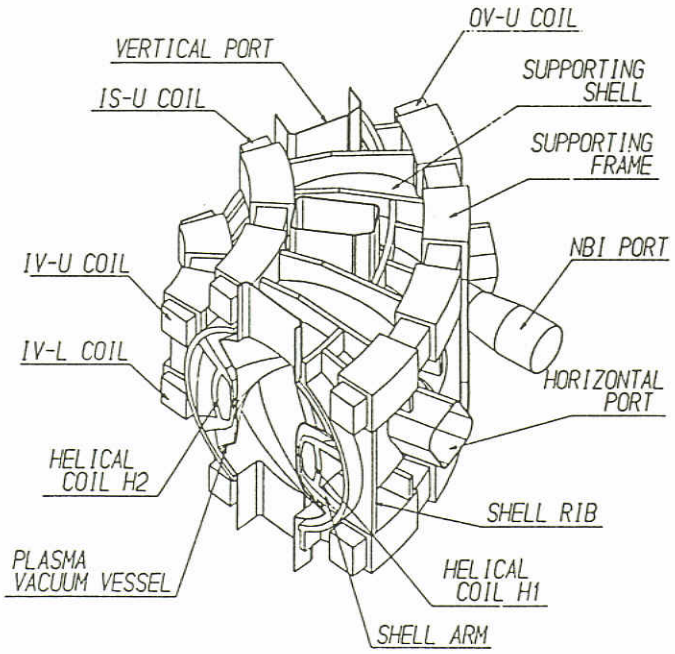

Figure 6 Configuration of the cryogenic supporting structures

HELICAL COILS AND PLASMA VACUUM VESSEL

Each 450-turn-winding of two helical coils was completed at the middle of May (Figure 7). The winding had been carried out in day and night shifts on the special winding machine in the LHD experimental hall. The next work is to weld helium vessel stainless steel lids on the helical coil cases. The helical coils have a combined stored energy of 920 MJ at the rated current of 13 kA in Phasa-I. Part members of the plasma vacuum vessel were fabricated, and are now assembled to many segments at the factory of a company. Inner radiation shields to be attached to the vessel are under fabrication.

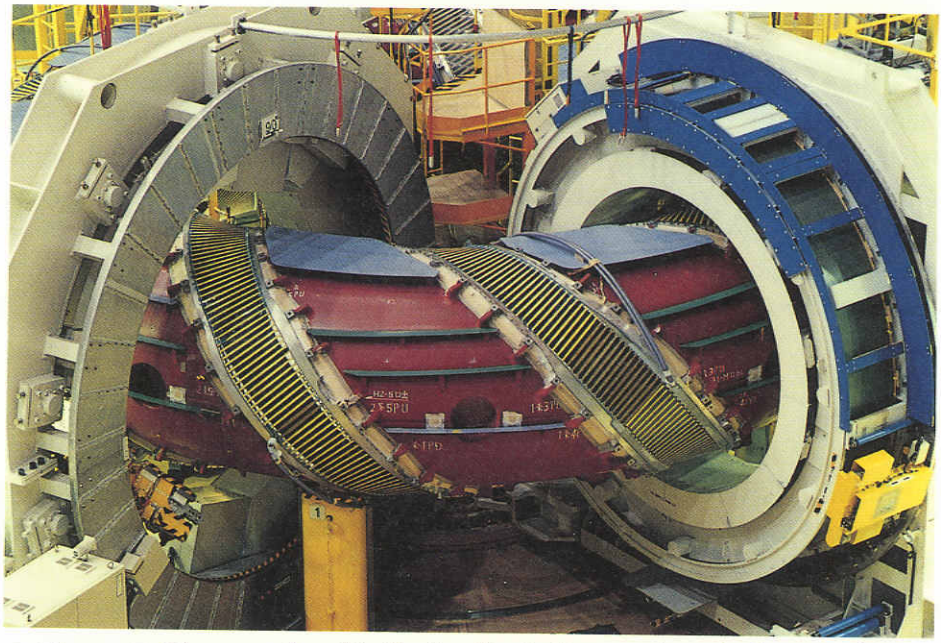

Figure 7 The completed helical coil winding on the winding machine

BUS-LINES, POWER SUPPLIES, CRYOGENIC AND CONTROL SYSTEMS

A pair of flexible superconducting bus-lines were developed as a current feeder system for LHD. They were used for the IV-L tests, and the application to LHD was decided owing to their validity. Four sets of superconducting cables and four cryogenic transfer-tubes have been constructed in FY1995, and the remainders are being made this year. Assembly works of the bus-lines and their current carrying tests will be done in 1997.

Three power supplies for the poloidal coils had been set up and recognized in good quality in the basement of the experimental building. Three power supplies for three blocks of each helical coil are planned to be made this fiscal year. The cryogenic system for LHD had been installed at the Toki site, and tested individually. Its refrigeration capability is 5650 W and 650 L/h at 4.4 K, and 20.6 kW at 80 K. The LHD control system is now under construction.

REFERENCE

1 Satow, T., et al., Present status of design and manufacture of the superconducting magnets for LHD IEEE Trans. Appl. Super. (March 1993) 3, 1 365-368

Helical Coils for LHD

S. Imagawa, S. Masuzaki, N. Yanagi, S. Yamaguchi, T. Satow, J. Yamamoto,
O. Motojima and LHD Group
National Institute for Fusion Science, Furo-cho,Chikusa, Nagoya 464-01 Japan

ABSTRACT

Helical coils for LHD are pool-cooled superconducting coils. In order to produce a fine rational magnetic surface, high accuracy of the position, high current density, and high rigidity are required. Attaining high accurate helical winding, medium size conductors had been selected and were directly wound on high accurate thick cases. The cases are finally supported by a strong outer shell structure to suppress the deformation caused by electromagnetic force. The helical coils are designed to satisfy fully cryostable criterion by grading the wetted surface fraction. On-site winding has finished successfully in May of 1996.

INTRODUCTION

The Large Helical Device (LHD) is a fusion experimental apparatus with a pair of helical coils and three pairs of poloidal coils. Accuracy of the position of coils is very important for magnetic fusion devices to produce a fine rational magnetic surface. In the LHD, accuracy of the position for each coil is required to be within 2 mm that is corresponding to 5×10^{-4} of the major radius. This value is derived to reduce the width of undesirable magnetic islands into one tenth of the plasma minor radius for the most sensitive mode of deformations [1]. Furthermore, high current density is required for the helical coils to keep distance between plasma and the coil. The average current density of a coil was demanded to be higher than 40 A/mm^2 for 4.4 K helium cooling. Deformation of current-center of each coil caused by electromagnetic force is provided to be less than 1.9 mm at central toroidal magnetic field B_0 = 3 T, that is, 3.4 mm at B_0 = 4 T.

Attaining high accurate helical shaping and winding, we selected medium size conductors, which are directly wound on high accurate cases (HC cans). Since the length of the conductor became long, pool-cooling was selected, and a pure aluminum stabilizer was adopted to perform high recovery current. Since it is impossible to withstand large electromagnetic force by the conductors themselves, they are packed into the HC can which are finally supported by an outer shell structure 100 mm thick. The can is used as a bath for liquid helium. Liquid helium is supplied to each bottom, and helium bubble is taken out from each top. There are five inlets and five outlets per coil. Longitudinal cooling channels inside the coils are arranged at the higher ends of each layer and the both top corners, the areas of which are 30 mm^2 and 300 mm^2, respectively. Electrical insulators between conductors are settled at intervals to create transverse cooling channels. The thicknesses of the insulator between turns and layers are 2.0 and 3.5 mm, respectively. The major parameters and cross-sectional view of the helical coil are shown in Table 1 and Fig. 1.

Table 1 Major parameters of the helical coil.

item	Phase I	Phase II
Bath temperature	~ 4.4	~ 1.8 K
Central toroidal field	3	4 T
Maximum field in coil	6.9	9.2 T
Nominal current	13.0	17.3 kA
Critical current	> 22	> 32 kA
Current density of coil	40	53 A/mm^2
Magnetic stored energy	0.92	1.64 GJ
Voltage to earth	±1181	±1574 V
Major / Minor radius	3.9 /0.975 m	
Superconductor	Al stabilized NbTi/Cu	
Surface treatment	Oxidization	
Number of turns	450	
Size of conductor	12.5 × 18.0 mm	

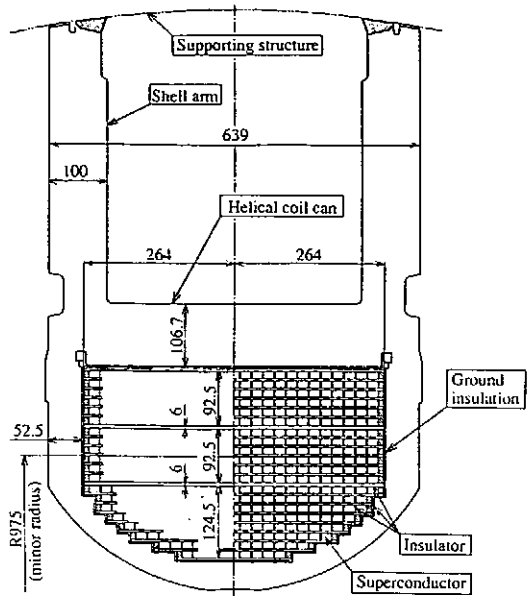

Fig.1 Cross-section of the helical coil.

MECHANICAL DESIGN OF SUPPORTING STRUCTURE

The electromagnetic forces on the helical coil are shown in Fig. 2. The minor radius hoop force is in the order of 10 MN/m. The overturning force in standard operation is almost 1/10 of it, but that in HC only excited mode is comparable to it. Structural analyses were carried out for the supporting structures [2]. The finite element model is shown in Fig. 3. By considering rigidness of poloidal coils, the maximum displacement and stress of the supporting structure are calculated to be 2.39 mm and 264 MPa in 4 T operation modes, respectively. The displacement of the current-center of the helical coil is estimated to be within 3 mm, including own shrinkage of 2 mm, which satisfies our target. The maximum stress intensity appears at the corner of the aperture for outer horizontal port of plasma vacuum vessel. The value is allowable for SUS316 which is main material of the supporting structures.

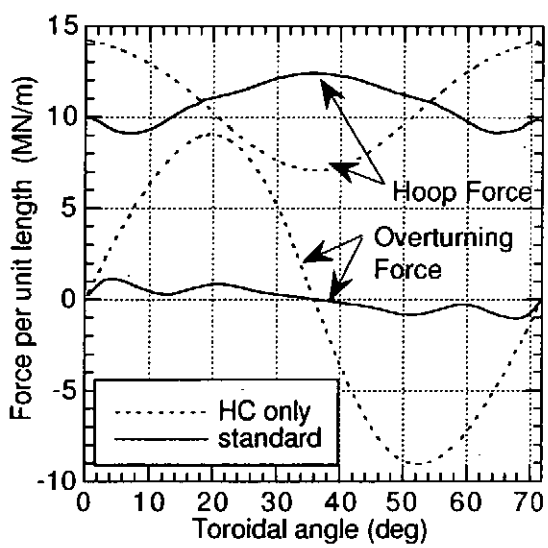

Figure 2 Electromagnetic force on the helical coil at 4 T operation.

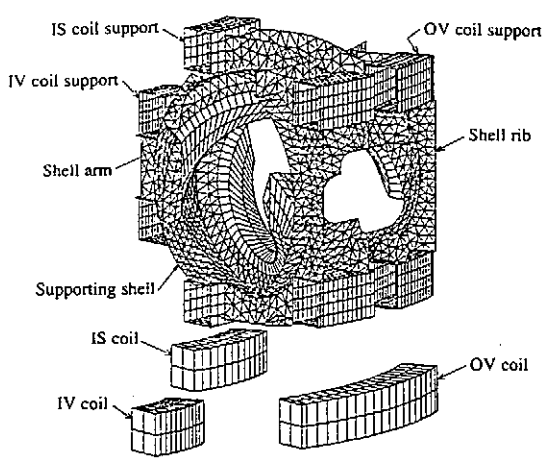

Figure 3 FE model of supporting structure. (Upper half of PCs are shown.)

CRYOGENIC STABILITY OF HELICAL COIL

The transverse component of the magnetic field is the highest at the edge of the helical coil and becomes gradually lower toward the core. On the contrary, the load per unit length on each insulator between the conductors is the largest in the core and becomes smaller towards the edge as shown in Fig. 4. The wetted surface fraction of conductors, therefore, can be enlarged at the edge region in order to enhance the recovery current without enlarging stress on insulators [3]. In actual winding, the dimension of width of each insulator was changed. In considering productivity, the number of steps of width of each layer to layer insulator was limited within three. The averaged wetted surface fraction varies from 0.417 to 0.692, and the smallest recovery current will be 15% higher than that in the case of constant fraction of 0.5, assuming the heat transfer coefficient to be independent on the size of wetted surface. The recovery current of each conductor is calculated as shown in Fig. 5 for the magnetic field of 3 T operation. The minimum value is 13.09 kA, which is almost equal to the nominal current. In this evaluation, heat transfer and magnetoresistance is assumed to have typical values, but both will be varied actually, and some region may exist where the recovery current is less than the nominal current. Still, the helical coil will be operated stably, because almost all the conductors satisfy the cryostable condition.

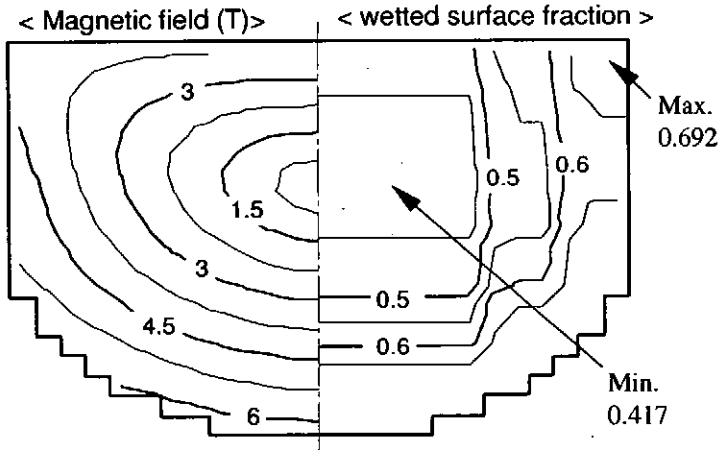

Figure 4 Transverse magnetic field and wetted surface fraction of each conductor

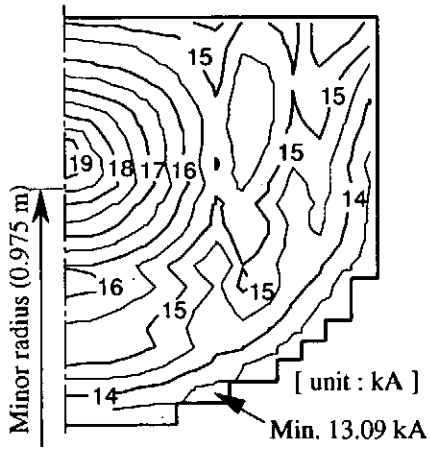

Figure 5 Calculated recovery current of each conductor.

MANUFACTURING HELICAL COIL

Because of the regulation for transportation on road, the helical coils were wound on-site. In order to keep accuracy while winding, we adopted the method to wind the conductors directly on the HC cans which was manufactured with high precision of 1.5 mm. Besides, we developed the winding machine with thirteen numerical controlled driving axes. The average gap between layers was established to be within 65 μm to keep the stress on the conductor under the yield strength [4]. We have developed a method to apply tension up to 50 MPa on the conductor by lateral shifting, and the conductor will be prevented from floating from the lower insulator. The error of the position of the conductor should be kept under 0.5 mm relative to the HC can. The relief by slant of each conductor caused by shaping error is controlled under 0.13 mm in average and 0.30 mm in maximum. By filling

the room-temperature-cured resin under the layer to layer insulator as shown in Fig. 6, the effective residual gap becomes half of the relief by slant. Thus, the average gap between layers should be smaller than 65 μm.

On-site winding was carried out in day and night time since January of 1995, and it finished successfully in May of 1996. The deviations of position of the conductors relative to the HC can were kept within ±0.5 mm as shown in Fig. 7. After winding, top covers of the HC cans with arms will be set on the cans and welded. Next, the entire assembly will be set on the outer supporting shell, and the arms will be welded to the shell. According to the law of propagation of errors, the deformation of the HC cans caused by each welding should be kept under 1 mm to attain the accuracy of 2 mm finally.

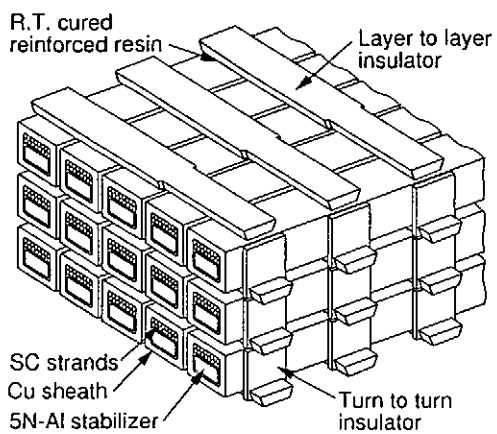

Figure 6 Schematic drawing of a part of the helical coil.

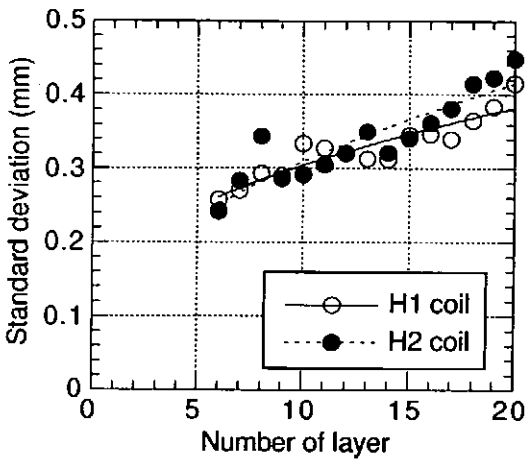

Figure 7 Accuracy of position of each layer in minor radius.

CONCLUSION

Main requirements for the helical coils for LHD are high accurate manufacturing of 2 mm, high current density of 40 A/mm^2, and small deformation against electromagnetic force. By developing a special winding machine and new methods, we finished successfully on-site winding. By optimizing the wetted surface fraction of each conductor, the helical coils will be cryostable at 4.4 K for 3 T operation. From structural analyses, deformation of current-center of the coil was confirmed to satisfy allowable value of 3.4 mm at 4 T operation.

REFERENCES

1 K. Yamazaki, et al., Requirements for accuracy of superconducting coils in the Large Helical Device, Fusion Engrg. Des., 20 (1993) 79-86.

2 S. Imagawa, et al., Design analysis of electromagnetic forces on the Large Helical Device, Fusion Engrg. Des., 20 (1993) 87-95.

3 S. Imagawa, et al., Optimization of Wetted Surface Fraction of Helical Coils for LHD, Cryogenics, 34 ICEC Supplement (1994) 701-704.

4 S. Imagawa, et al., Construction of Helical Coil Winding Machine for LHD and On-site Winding, IEEE Transactions on Magnetics (will be published).

Poloidal Coils for the Large Helical Device (LHD)

K. Takahata, T. Satow, A. Iwamoto, T. Morisaki, S. Imagawa, H. Tamura, K. Yamazaki, T. Mito, J. Yamamoto, O. Motojima and LHD Group
National Institute for Fusion Science, Oroshi, Toki, Gifu 509-52, Japan

ABSTRACT

Poloidal coil system of the Large Helical Device (LHD) consists of three pairs of circular solenoids; Inner Vertical (IV), Inner shaping (IS) and Outer Vertical (OV) coils. Forced flow cooling is adopted as a cooling method of the poloidal coils. The conductors of the poloidal coils are Nb-Ti cable-in-conduit types. Each coil consists of eight double-pancake coils, and coolant flows in parallel from the inner turns to the outer turns. A superconducting joint technique is adopted in the joints among the double-pancake coils. Miniaturized joints and severe quality control bring the reduction of error field.

INTRODUCTION

One of the special features of the LHD is that all magnetic systems, a pair of helical coils and three pairs of poloidal coils, are superconducting. The poloidal coils consist of Inner Vertical (IV), Inner Shaping (IS) and Outer Vertical (OV) coils. The IV and IS coils have been completed and shipped to the institute. One of the OV coils has been finished in April of 1996, and three coils have then been installed into a lower part of the LHD supporting shell. Another OV coil is planning to be completed till the end of 1996. In this paper, we will describe the structure of the conductor, coil and joint. The manufacturing process will also be introduced.

CONDUCTOR AND COIL DESIGN

Specifications of the conductors are listed in Table 1. Nb-Ti cable-in-conduit conductors are adopted because of its high stability. The conductor consists of a cable with 486 strands and a conduit with a thickness of 3 or 3.5 mm and rectangular cross section. The void fraction is 0.38, which is optimized from the viewpoint of a strand movement and an inter-strand coupling loss. To keep the void fraction within an allowance, the strands and conduit were strictly inspected regarding the dimensions. The strand surface is uncoated, which affects current distribution and heat transfer to helium. In the previous research, we confirmed that the bare strand brings high stability margin [1]. To avoid oxidation of the strand surface, pure gas helium was always enclosed into the conduit. The critical current is set to be three times as high as the operating current at the maximum field. Previous research also suggested that stability for partial quenching is

Table 1 Specifications of conductors for the poloidal coils.

	IV	IS	OV
Type	Cable-in-conduit	←	←
Superconducting material	Nb-Ti	←	←
Operating current (kA)	20.8	21.6	31.3
Critical current (kA)	62.4 at 6.5T	64.8 at 5.4T	93.9 at 5.0T
Conduit dimension (mm)	23.0×27.6	23.0×27.6	27.5×31.8
thickness (mm)	3.0	3.0	3.5
Void fraction (%)	38	←	←
Strand diameter	0.76	0.76	0.89
Number of strands	3^4×6=486	←	←
Nb-Ti:Cu	1:2.7	1:3.4	1:4.2
Filament diameter (μm)	15	12	14
Filament twist pitch (mm)	10	8	10
Strand surface	Bare	←	←
Cabling pitch: 1st stage (mm)	60	60	70
2nd	100	100	120
3rd	150	150	170
4th	220	220	250
5th	400	400	400
Inlet helium pressure (MPa)	1.0~0.8	←	←
Inlet helium temperature (K)	4.5	←	←
Flow rate per path (g/s)	5.0	4.1	5.0
Pressure drop per path (MPa)	0.1	←	←

enhanced when the critical current is more than twice as high as the operating one [2].

Figure 1 shows the calculated stability margin. In the analyses, a zero dimensional model is applied, and the magnetic field is fixed to the maximum field of each coil. At the operating current, the conductors have the stability margin of more than 300 mJ/cm^3, which may be high enough for stable operation.

Main parameters of the coils are listed in Table 2. A coil consists of eight double-pancake coils, which corresponds to 16 layers. Because the coolant flows in parallel through each pancake coil, the number of flow paths is also 16. The length of a flow path affects the pressure drop. So, we decrease the turn number of the OV coil to decrease the length of a flow path, which becomes 314 m. The operating current is increased from 20 to 30 kA with decreasing the turn number. Though the OV coil has the largest diameter and operating current, the maximum field is fortunately the lowest. In practice, the IV coil has the severest conditions as regards the conductor stability and stress inside the coil. An important subject of the design and fabrication is to reduce the error field [3]. The required accuracy is 1×10^{-4} at the plasma surface.

Table 2 Main parameters of the poloidal coils.

	IV	IS	OV
Cooling type	Forced flow	←	←
Inner/outer radii* (m)	1.6/2.1	2.7/3.1	5.4/5.8
Height* (m)	0.46	0.46	0.54
Total weight (tons)	16	25	45
Magnetmotiv force (MA)	5.0	4.5	4.5
Number of pancakes	16	16	16
Number of turns	15×16=240	13×16=208	9×16=144
Operating current (kA)	20.8	21.6	31.3
Maximum field (T)	6.5	5.4	5.0
Inductance (H)	0.313	0.445	0.514
Stored energy (MJ)	68	104	251
Conductor length (km)	2.7	3.7	5.0
Number of flow path	16	16	16
Length of a flow path (m)	170	230	314

* including an earth insulation

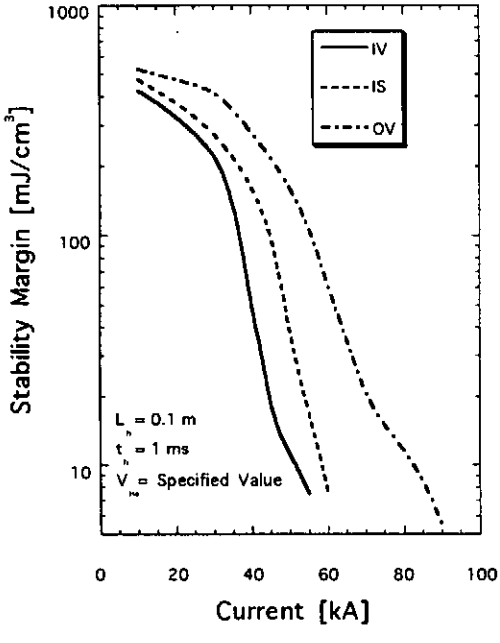

Figure 1 Stability margin calculated by a zero-dimensional model.

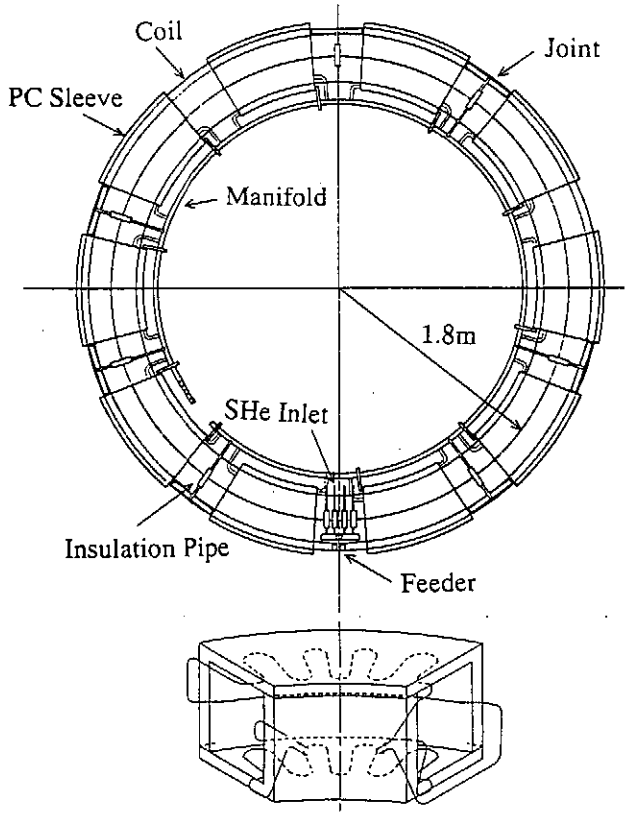

Figure 2 Top view of the IV coil and cooling pipes in the stainless steel sleeve.

COIL FABRICATION

The double-pancake coils were wound with a special winding machine. First, a half conductor was paid out from the conductor bobbin, and the winding started from the middle point of the conductor. The conductor was wrapped with 0.5 mm thick impregnated glass epoxy tape (glass fabric/polyimide/glass fabric laminates). After the winding of a lower pancake, the remaining conductor was wound on the lower pancake and 0.8 mm thick layer insulation. The double-pancake coil was then molded in the special purpose kiln. To minimize the error field, the molded pancakes kept tolerances of ±2 mm for the inner and outer diameters and ±1 mm for the height. The tolerances correspond to extreme accuracy of about 5×10^{-4} for the diameter. The pancakes were then stacked with layer insulation and molded. As for the electric joints between pancakes, a solid state bonding technique was applied. The Nb-Ti filaments were jointed superconductively. Required space for the joint is only 37 mm wide, 50 mm high and 60 mm long. The joint was small enough to reduce the error field. An earth insulation of 4 mm thickness was wound around the molded coil. Finally, the coil was covered with ten fan-shaped stainless steel sleeves of 40 mm thickness. Figure 2 shows the top view of the IV coil and cooling pipes in the sleeve. Their roles are not only to fix the coil into the supporting shell of the LHD but also to shield the heat loss from the shell by installed cooling pipes. Moreover, the coil can be cooled indirectly from the sleeves in initial cooldown [4].

CONCLUSION

Poloidal coil system of the Large Helical Device (LHD) has been fabricated satisfactorily. The conductors, which are Nb-Ti cable-in-conduit types, were designed to have high stability and sufficient low losses. The coils were wound with extreme accuracy of about 5×10^{-4}. This results in high accuracy of the magnetic field. A superconducting joint technique was adopted in the joints among the double-pancake coils. Using this technique, we can miniaturize the joint, which also enables to reduce the error field.

REFERENCES

1. Takahata, K. et al., Stability tests of the Nb-Ti cable-in-conduit superconductor with bare strands for demonstration of the Large Helical Device poloidal field coils IEEE Transactions on Magnetics (1994) 30 1705-1709
2. Takahata, K. et al., Stability of cable-in-conduit superconductors for the Large Helical Device IEEE Transactions on Applied Superconductivity (1993) 3 511-514
3. Nakamoto, K. et al., Design and fabrication of forced-flow superconducting poloidal coils for the Large Helical Device FUSION TECHNOLOGY (1994) 2 909-912
4. Takahata, K. et al., Cooldown performance of an inner vertical field coil for the Large Helical Device, presented at MT-14, Tampere, Finland, June 11-16, 1995

Superconducting Current Feeder System for the LHD

S. Yamada, T. Mito, H. Chikaraishi, S. Tanahashi, R. Maekawa, S. Kitagawa,
K. Nishimura, T. Satow, S. Satoh, J. Yamamoto and O. Motojima
National Institute for Fusion Science, 322-6 Oroshi, Toki, Gifu 509-52, Japan

ABSTRACT

A flexible superconducting (SC) busline was developed as a current feeder system for the fusion experimental device, LHD. An aluminum stabilized NbTi/Cu compacted strand cable was developed to satisfy the fully stabilized requirements at a rated current of 32 kA. A pair of SC cables was electrically insulated and installed in a cryogenic transfer line. Nine sets of SC current feeders with 45.7–58.0 m lengths are installed for LHD. The total heat loads into 80 and 4.2 K levels are estimated to be 2.12 and 1.02 kW, respectively. The SC current feeder system is designed to maintain its rated capacities for 30 minutes, whenever the coolants supplied to the current feeder system are accidentally stopped.

INTRODUCTION

The LHD is a fusion experimental device of the heliotron/torsatron type [1,2]. It consists a pair of helical coils and three sets of poloidal coils with a total stored magnetic energy of 1.6 GJ at phase II operations. Each helical coil includes three block coils that can be excited independently. Therefore, a total number of nine SC buslines is necessary, six for the helical coils and three for the poloidal coils. The distance between the SC coils and their power supply system is 45.7–58.0 m. The merits of using SC buslines are : 1) reduction of the capacity of the power supply system, and 2) simplification of the busline assembly process on site. In the case of LHD, the electrical power consumption exceeds 1.5 MW. Simplification of assembly is possible because a busline can be completely fabricated in a factory like a commercial power cable. To develop such an SC current carrying system for LHD, flexible full scale model of an SC busline of 20 m with basic properties were examined [3-6].
This paper describes the design of an SC current feeder system for LHD. The results of its research and developement are also discussed.

DESIGN CONCEPTS FOR SC CURRENT FEEDER SYSTEM

The design concepts for an SC current feeder system for LHD are as follows. (1) Fully stabilized SC properties should be satisfied when a rated current of 31.3 kA (for OV coil) flows. (2) The breakdown voltage of the current feeder system should be higher than that of the SC coils of the main experimental device. (3) The system should be able to maintain its rated current carrying capacities for 30 minutes, whenever the coolants supplied to the current feeder system are stopped.
The SC current feeder system requires excellent reliability and safety exceeding that of the SC coils of LHD, because the stored magnetic energy of the coils must be extracted through the SC busline when the coils quench. The SC busline should be flexible, because the installation routes from coils to their power supplies have bends. The minimum bend radius is designed to be 1.5 m, because of the legal restrictions on the height, width, and other

Table 1 Specifications of the SC buslines for the LHD.

Items	Specifications
Number of SC busline	9
Rated current	32 kA
Rated withstanding voltage	5.0 kV (in 80 K gas helium)
Minimum bending radius	1.5 m
Length of SC bus line	45.7 - 58.0 m
Heat load into SC busline	0.3 W/m (from 80 to 4.5 K), 3 W/m (from 300 to 80 K)
Type of cryogenic tubes	five corrugated tubes (with thermal shield)

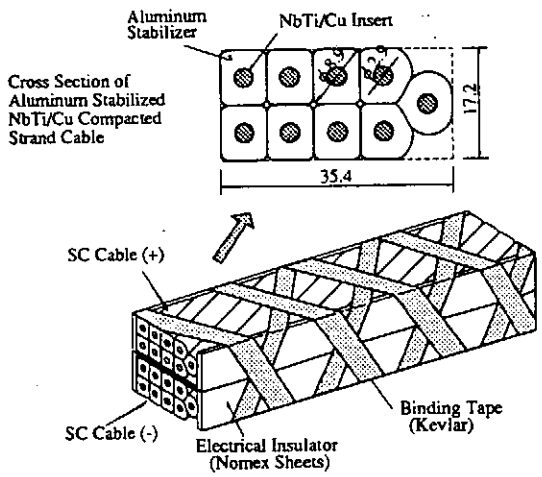

Fig. 1 Aluminum stabilized compacted stranded cables for SC buslines.

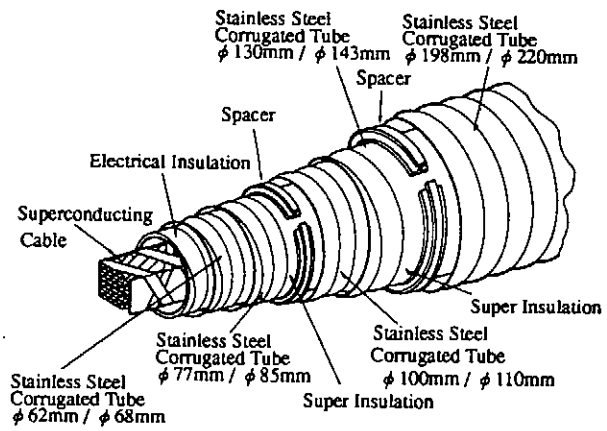

Fig. 2 Configuration of a flexible SC busline for the LHD.

parameters of road freight in Japan. The design specifications for the SC buslines for LHD are listed in Table 1.

RESEARCH AND DEVELOPEMENT FOR SC BUSLINE

The configuration of the SC cable of the full scale model is shown in Fig. 1. An aluminium-stabilized, SC-compacted stranded cable was specially developed to satisfy the high stability and flexibility requirements of a SC busline. Electrical insulation was inserted between a pair of +/- cables. The breakdown voltage between +/- cables was measured with test pieces of R&D SC cables 150 mm in length. Both ends of the test pieces were covered with electrical insulation. Tests were conducted over a wide range of temperatures from 4.2 to 294 K using helium gas. The test results are listed in Table 2. In the coil protection circuits of the actual LHD, maximum induced voltage of the coils is 1.9 kV when de-excitation is rapid and the decay time constant is 20 s. As shown in Table 2, the insulation structure of the SC cables helium gas. The test results are listed in Table 2. In the coil protection circuits of the actual LHD, maximum induced voltage of the coils is 1.9 kV when de-excitation is rapid and the

Table 2 Measured breakdown voltage of short samples.

Conditions	Breakdown voltages
Liquid helium	more than 20 kV
6 - 40 K helium gas	more than 20 kV
75 - 80 K helium gas	8.33 kV
280 - 294 K helium gas	3.21 kV

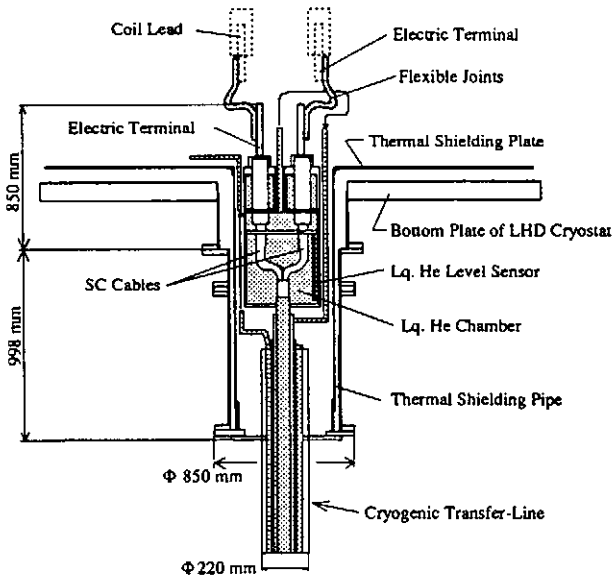

Fig. 3 Structure of the peripheral terminal at the coil side.

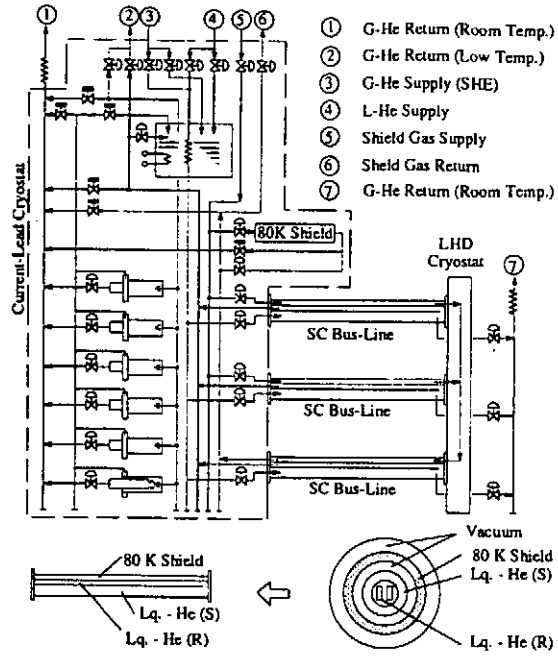

Fig. 4 Helium flow circuit of the current carrying system for the poloidal coil.

decay time constant is 20 s. As shown in Table 2, the insulation structure of the SC cables has a large breakdown voltage margin.

The electromagnetic force on most parts of the SC cables is 9 kN/m. But the maximum magnetic force becomes 34.8 kN/m at the peripheral terminal near the main device, because the leakage magnetic field of 1 T influences the SC cables. Therefore, the SC cables are wrapped together with Kevlar binding tape strong enough to withstand the maximum repelling force. The strength of the Kevlar binding tape was 144 kN/m.

To decrease the heat load into the SC busline, an 80 K helium gas channel is installed as a thermal shield on the actual SC busline for LHD. The overall configuration of the busline is shown in Fig. 2. The vacuum-insulated transfer line consists of five corrugated stainless steel tubes assembled coaxially. A pair of SC cables is covered with insulation layers to satisfy the requirements for electrical insulation between the cables and the surrounding corrugated tubes. Liquid helium flows through the innermost channel to the peripheral terminal and then returns through a second inner channel as two-phase helium. The fourth channel is the 80 K helium gas channel, and the third and fifth channels are vacuum insulation spaces.

Fig. 3 shows the structure of the peripheral terminal on the coil side. The coolants of the SC busline are separated from that of the coil system. Thermal shrinkage of the coil system should be absorbed in the flexible joints between the terminals. SC wires are embedded in both the terminals and the flexible joints to reduce Joule heat losses.

CRYOGENIC DESIGN FOR THE CURRENT FEEDER SYSTEM

Fig. 4 shows the helium flow circuit of the SC current feeder system for the poloidal coils. The cryostat is composed of three pairs of current leads, plates for 80-K thermal shielding, a sub-cooler tank, a heater, and automatic control valves. This flow circuit includes an exhaust line and terminal that were added to an earlier version to eliminate heat transfer. To cool down the SC busline, the cold gas supplied to the innermost channel is taken out at the exhaust terminals. The helium flow circuit for the helical coils consists of the same

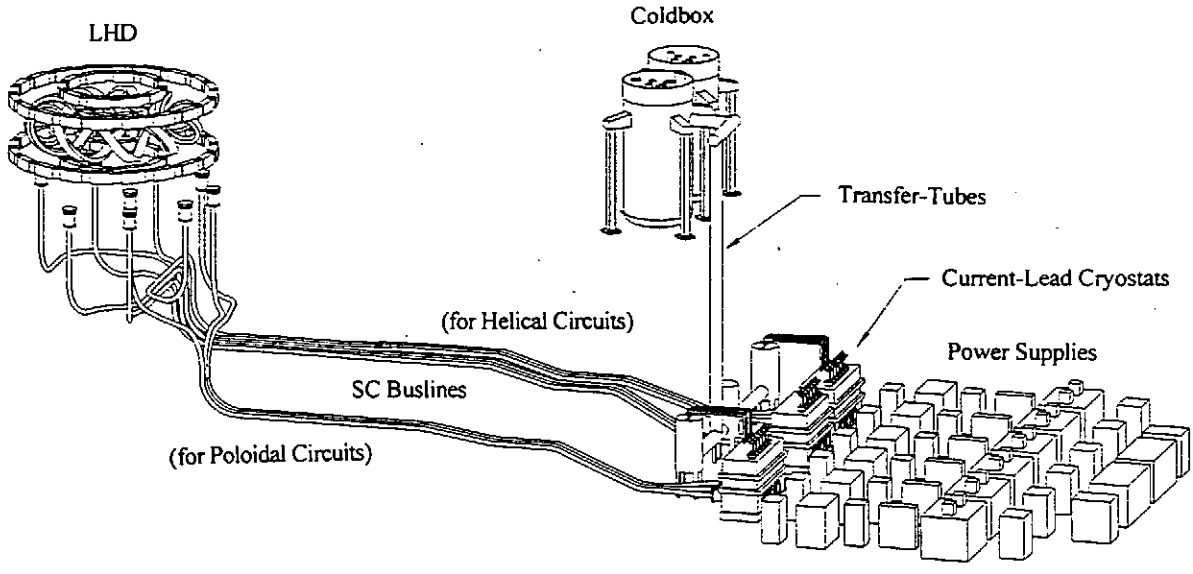

Fig. 5. Bird-eye's view of the SC current feeder system for the LHD.

components used for poloidal coils. The system is designed to be compact by standardizing the components, and also by assembling three sets of current leads in one modular cryostat. Fig. 5 shows a bird-eye's view of the SC current feeder system of LHD. Nine buslines will be installed in the current feeder system. The routes are designed to have no sharp bends. The SC current feeder system should be able to maintaim its rated current capacities for 30 minutes, if the coolant flow is accidentally stopped. The heat balance between the heat inputs and cooling capacities has been investigated [6]. According to scaling laws, the actual current leads are designed to retain liquid helium for 30 minutes. The temperature rise of the thermal shielding channel of the SC busline will be 1.2 degrees. The total heat input to the liquid helium in the SC current feeder system is estimated to be 65 W. It can be cancelled by evaporating 50 l of liquid helium within 30 minutes. The current feeder system is designed to have liquid helium reserves for self-cooling.

CONCLUSION

The design studies for the SC current feeder system for LHD are concluded as follows. (1) A fully stabilized flexible SC cable with a large breakdown voltage was developed for the SC busline. (2) A five-channel transfer-line with an 80 K shielding gas channel is designed to reduce the heat load. (3) The SC current feeder system is designed to maintain its rated current capacities for 30 minutes, whenever flow of the coolants is stopped. (4) The routes of the SC buslines are designed not to have sharp bends.

REFERENCES

[1] O. Motojima et al, Fusion Engin. and Design, Vol. 20, 1993, pp. 3-14.
[2] J. Yamamoto et al, 14th Int. Conf. of Plasma Phys. and Controlled Nucl. Fusion Res., 26 Sept.-1 Oct.,1994, Seville, IAEA-CN-60/F-P-3.
[3] T. Mito et al, IEEE Trans. on Magn., Vol. 30, 1994, pp. 2090-2093.
[4] S. Yamada et al, Proc. of 18th Sympo. on Fusion Technol.,Karlsruhe, 1994, pp.913-916.
[5] T. Mito et al, 1994 Applied Superconductivity Conf., 16-21 Oct., 1994, Boston, LQC-2.
[6] T. Mito et al, Fusion Engin. and Design, Vol. 20, 1993, pp. 217-222.

Coil Power Supplies for LHD and Reliability Test of OV Coil Protection System

Shugo Tanahashi, Hirotaka Chikaraishi, Shuichi Yamada, Shiro Kitagawa,
Junya Yamammoto and Osamu Motojima
National Institute for Fusion Science, Oroshi-cho, Toki, Gifu 509-52, Japan

The Large Helical Device (LHD) has three sets of superconducting helical coils and three sets of superconducting poloidal coils. Three power supplies for poloidal field coils are constructed and three power supplies for helical field coils are under installation. In this paper, specifications and structures of power supplies are described. Next, an reliability test for a quench protection system that uses a new type of dc current breaker is described.

INTRODUCTION

The Large Helical Device (LHD) that is under construction at the Toki site of the National Institute for Fusion Science (NIFS) is a fusion test facility using superconducting coils. This machine has three sets of superconducting helical coils and three sets of superconducting poloidal coils that form the magnetic field to confinement a plasma. The strength of magnetic field becomes 4 T at a plasma center and amount of stored energy becomes over 1.6 GJ in the second stage of project.
Regarding to the power supplies to excite coils, low voltage power supplies for steady state excitation of poloidal coils are constructed and set in the main experimental building in 1994. The steady state power supplies for helical coils are made in 1995 and are under installation. In these power supplies, new type of 30kA class dc opening switch, that consists of a small vacuum breaker and power fuses, is used for quench protection circuit. The prototype of this switch is tested and confirmed its operation but there may be difference between actual system and prototype switch in such as large current system. Therefore a reliability tests using actual OV quench protection system is executed in 1995. In following sections, first we will introduce the supplies, they consist of thyristor rectifiers and quench protection systems. Next, the result of reliability test of protection system is described.

POWER SUPPLIES FOR LHD SUPERCONDUCTING COILS

Figure 1 shows a diagram of dc power supplies for steady state excitation of poloidal field coils. Also the same type power supplies excite helical field coils. This figure contains thyristor rectifiers, dc filters, quench protection subsystems and polarity change units.
As table 1 shows operation currents of LHD in second phase. It shows that the coil currents flow in uni-direction expect the IS coil, so the power supplies are based on single rectifier. For the IS coil, the current reverses in mode 1-a only and mode change to these does not so often. Therefore, we decide to use a mechanical cross switch after the power supply to reverse a current in mode 1-a.
Table 2 shows specifications of power supplies for steady state excitation of LHD superconducting coils. In this table, poloidal field power supplies are de-rated into 3T operation of LHD, which is the first stage of LHD project, to suppress initial construction cost.

RELIABILITY TEST OF QUENCH PROTECTION SYSTEM

This section describe the reliability test of quench protection system. Figure 2 shows the detail of OV quench protection circuit. In this test, a load coil, which has enough inductance and low resistance, is required to keep output current while protection sequence is running. For this purpose, a liquid nitrogen cooled copper coil is built and used as a dummy load coil shown in figure.
In this figure, VCB is an ac vacuum circuit breaker and F is a relatively small power fuse with a current rating that is about 3% of the coils. From DS1 to DS3 are disconnectors that have no ability

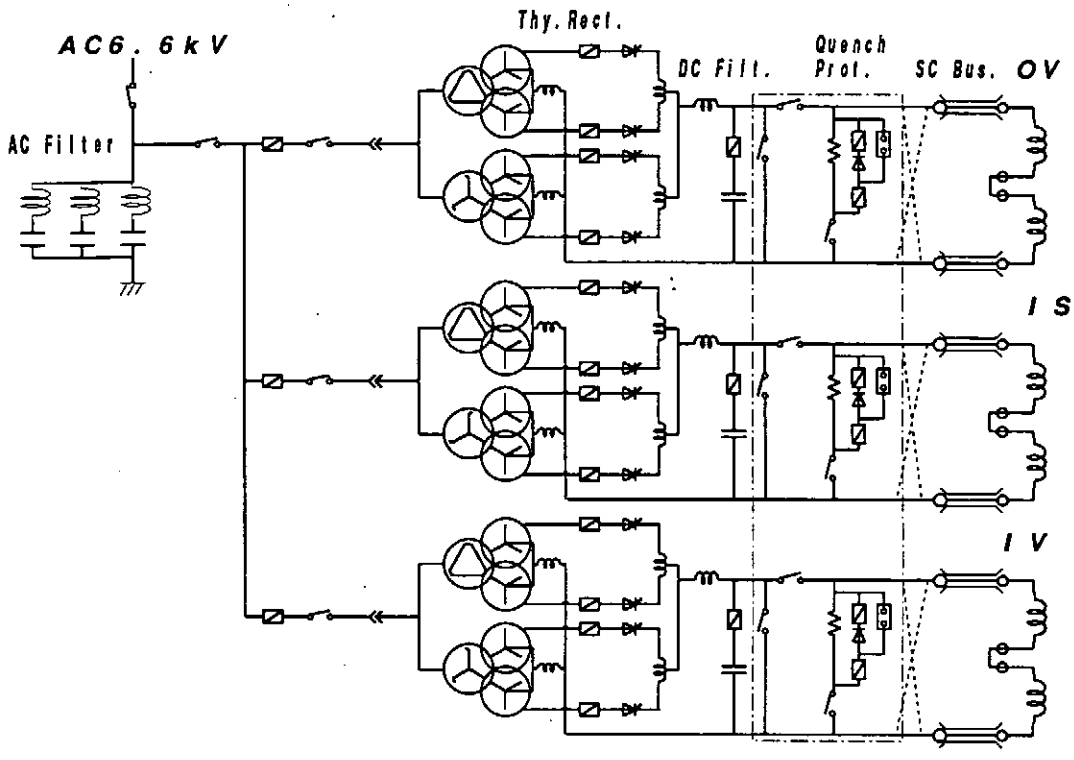

Figure 1: Circuit Diagram of Power Supplies for LHD Superconducting Poloidal Field Coils

Table 1: Coil Currents for LHD Operation in Phase II. [kA]

	1-0	1-A	1-B	1-C	1-D
HI,HM,HO	17.3				
OV	-27.2	-30.3	-24.2	-26.1	-28.3
IS	-6.9	7.5	-21.3	-9.0	-4.6
IV	14.3	8.3	20.2	10.8	17.8

	2a	2b	3a	3b	4a	4b
HI,HM,HO	17.3					
OV	-25.7	-28.8	-28.8	-25.7	-27.8	-26.6
IS	-7.8	-5.8	-1.0	-12.6	-8.5	-5.1
IV	12.8	15.8	9.1	19.6	11.5	17.2

Table 2: Rating of Power Supplies for Stead State Operation.

	HO−HI	OV	IS	IV
DC Voltage	45V	33V	33V	33V
DC Current	17.3kA	31.3kA	21.7kA	20.9kA
		(23.5kA*)	(16.3kA*)	(15.7kA*)

(*) indicates the output current for 3 T operation in the phase I.

Accuracies for all Power supplies	
Current measurement error	0.03% of reading value + 4.5A
Current control error	0.04% of set value + 6A

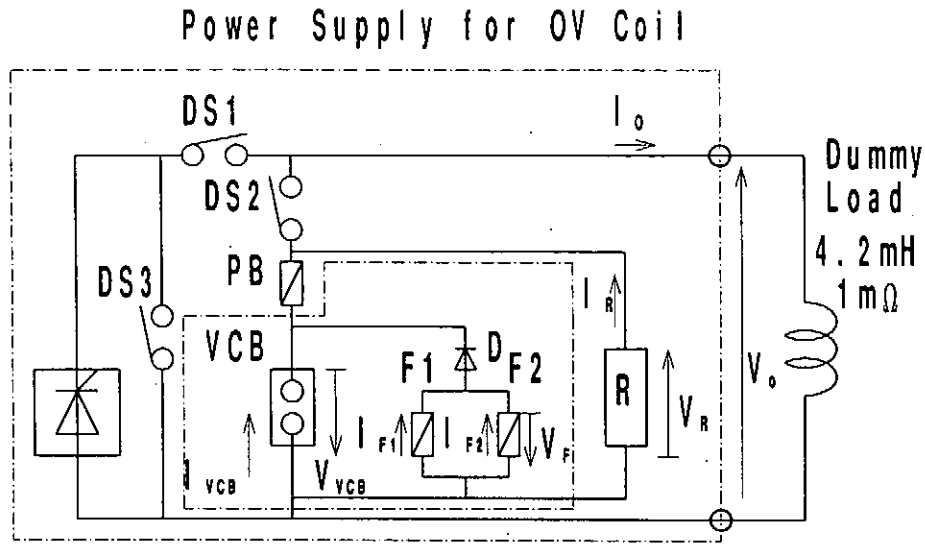

Figure 2: Diagram of Test Circuit for Quench Protection

to break the current. R is a dump resistor. The diode serial connected to the fuse blocks the current by dropping forward before VCB opens to avoid preheating of the power fuse. In the figure, PB is a backup pyro-breaker that is triggered and forces commutation to the external resistors if the previous sequence fails.
In the beginning of the experiments, a trouble, that a rush current flows through DS2 when it closes, is found out. To suppress this rush current, modification quench protection sequence is done. At the same time arcing contacts are installed in DS2. After these correction, no rush current is observed. Figure 3 shows one of current and voltage waveforms in quench protection. In this figure, the protection sequence is as follows:

1. After quench is detected, the protection circuit waits for one second to remove plasma.
2. The dc power supplies turns its output voltage to 0V and DS2 close
3. The dc power supplies generate negative voltage. With this operation, the current flowing in power supplies is transferred to DS2 and VCB.
4. After a short time, the power supply current through DS1 becomes zero; then DS1 opens.
5. VCB opens and the main current is commutated to the power fuse with low voltage.
6. The power fuse melts and opens, then all currents commutate to the dump resistor. At this step, the terminal voltage rises to 2 or 3 kV, but it stays within the rating of the power fuse.

This figure shows the above sequence is finished within 520 milliseconds after quench protection signal and it satisfies a request that opening delay must be less than 1 second.
The experiments are done with operation currents of 3.7kA, 10kA, 17kA and 22kA. We made 50 shots of operation tests for each operation current without failure. Figure 4 shows melt-down time of power fuses versus operation current. In this figure, a solid line is typical characteristic and two broken line show maximum and minimum value. Dots in figure show the test results. All dots are in the aria between minimum and maximum value. With these experiments, the reliability of quench protection system used in OV power supply is confirmed.

CONCLUSION

This paper shows the outline of power supplies and reliability test In the reliability test, total of 200 shots are finished in several operation current without any failure.

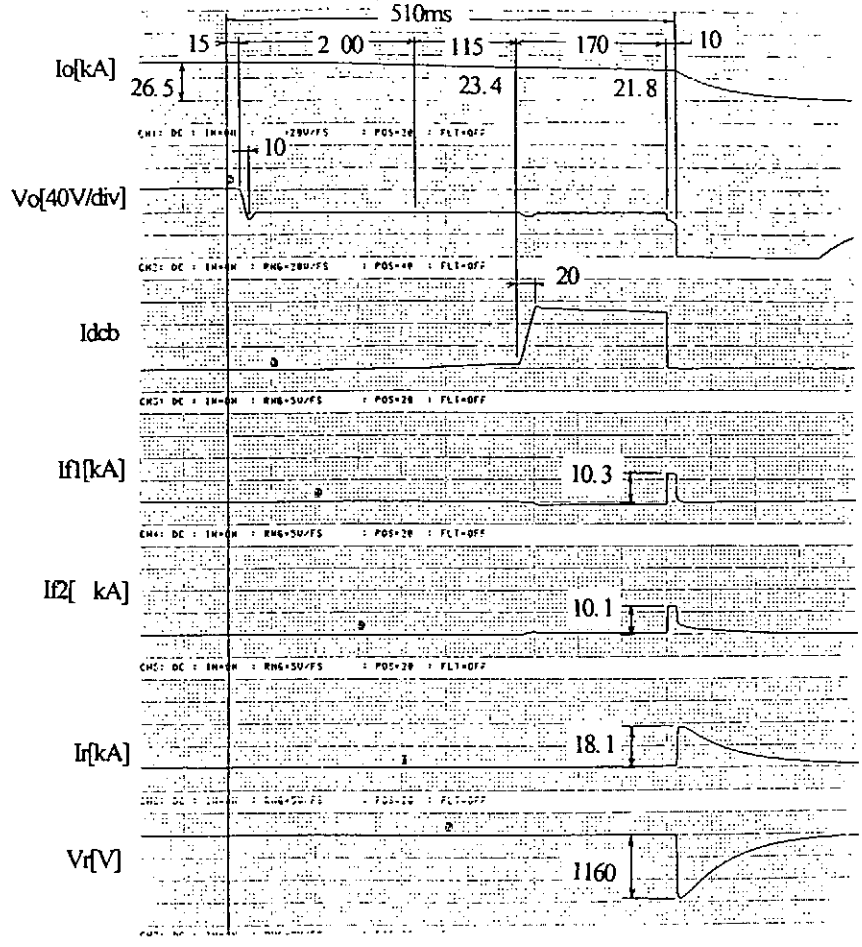

Figure 3: Experimental Waveforms of Coil Current and Voltage

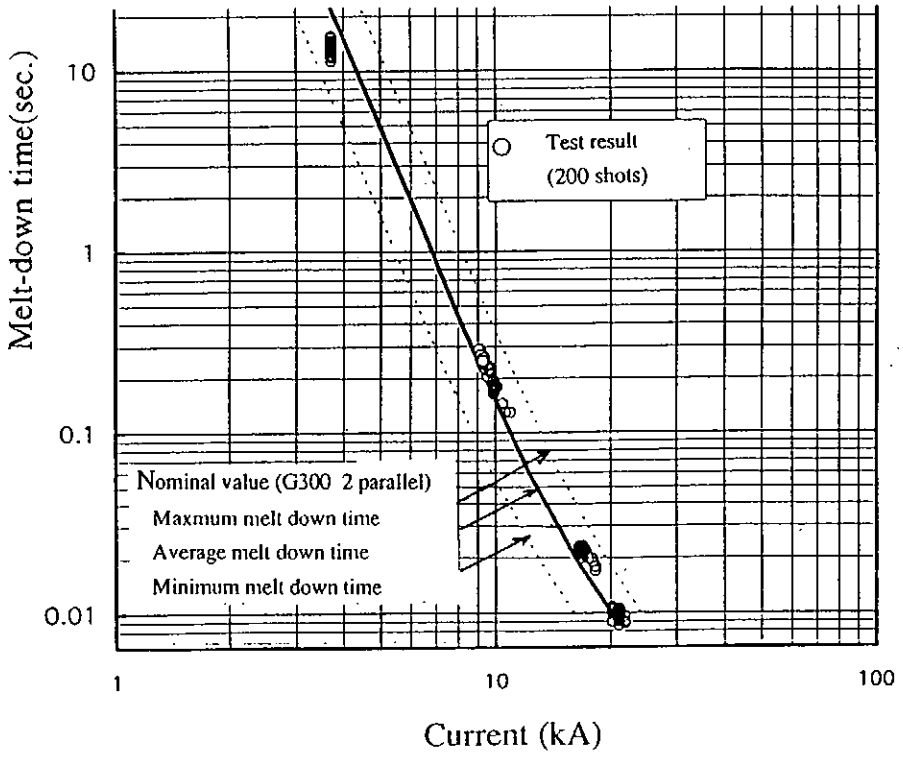

Figure 4: Melt-down Time of Power Fuse vs Operating Current

Current Control System for Superconducting Coils of LHD

H. Chikaraishi, S. Yamada, T. Inoue, S. Tanahasi, O. Motojima, J. Yamamoto,
T. Ise*, H. Yoneda**, Y. Murakami***,Y. Hourai****,T. Haga****

National Institute for Fusion Science, Nagoya 464-01, Japan
*Osaka University, Suita, Osaka 565, Japan, **Fukui University of Technology, Fukui 910, Japan
***NEC,Minatoku, Tokyo 101, Japan, ****Kobe Steel Ltd.,Kobe 651, Japan

This paper introduce a coil current control system of the LHD. The main part of this system consists of two VME based real time computers and a risc based work station which are connected by optical fiber link. In this computer system, a coil current controller for steady state operation of LHD which based on a state variable control theory is installed. Also advanced current control scheme, which are now developing for dynamic current control in phase II operation of LHD, are introduced

INTRODUCTION

The Large Helical Device (LHD) has 12 superconducting coils that generate 4T of magnetic field at a plasma center and its stored energy becomes over 1.6GJ. A power system using six power supplies drive these coils and make required magnetic configuration. In this system, a computer system, that consists of three risc cpus linked using optical data link, controls each power supplies to feed require coil current with small current error.
Following sections introduce this computer control system and coil current control design. At first, a structure of computer control system is described. Next, a current control design that is for steady state operation of LHD is introduced. Finally, advanced control schemes, that are for dynamic current control required in LHD phase II operation and are under developing, are introduced.

COMPUTER SYSTEM FOR DC POWER SUPPLIES

Figure 1 shows the structure of the computer control subsystem for the steady state power supplies. This computer system has a hierarchy shown in the figure. The bottom level consists of controllers in thyristor rectifier unit. Next level is two VME bus computers with real time OS. The top level is an engineering work station with Unix. This machine works as an interface with other control systems such as a plasma experiment control system, temporary data storage and a total system diagnostic. A reflective memory set using an optical fiber links these three computers and it realize the data transfer in real time. Two terminals shown in figure 1 are the remote controllers connected with LAN in the building. Also, this system has a power system simulator. This simulator has same numerical model used in design of control system. The simulator runs in real time and generate simulated coil currents. With comparison the actual coil currents and simulated value, check and refine of numerical model becomes possible.

CURRENT CONTROL DESIGN

This section describes about current control scheme. The required performances to the regulator are as follows:

1 Current control error in steady state is less than 0.04%.
2 Settling time to the 1% off control error is less than 1 second
3 Load condition changes in following situation.
- Low resistance plasma exists in a vacuum chamber.

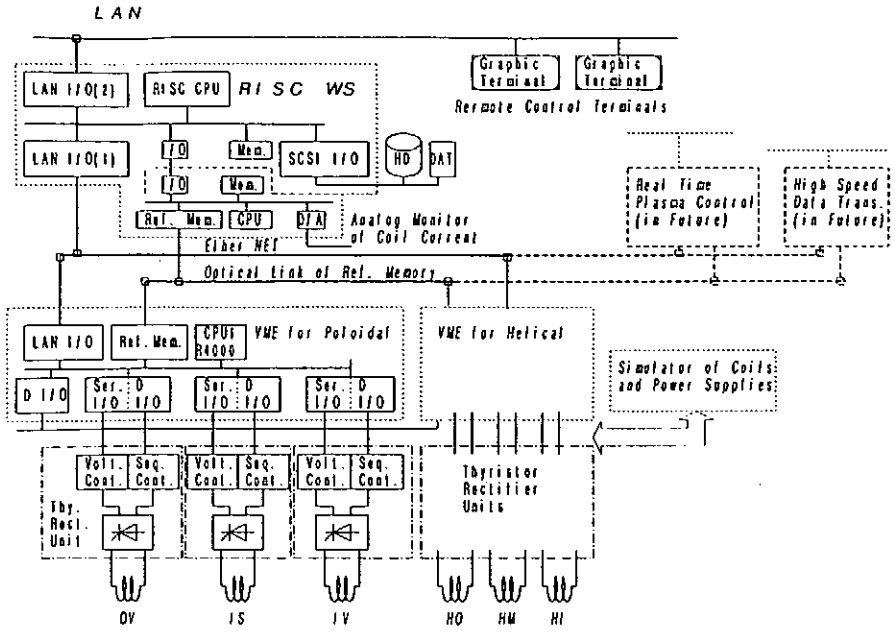

Figure 1: Structure of Computer Control Sub-system for LHD Power system.

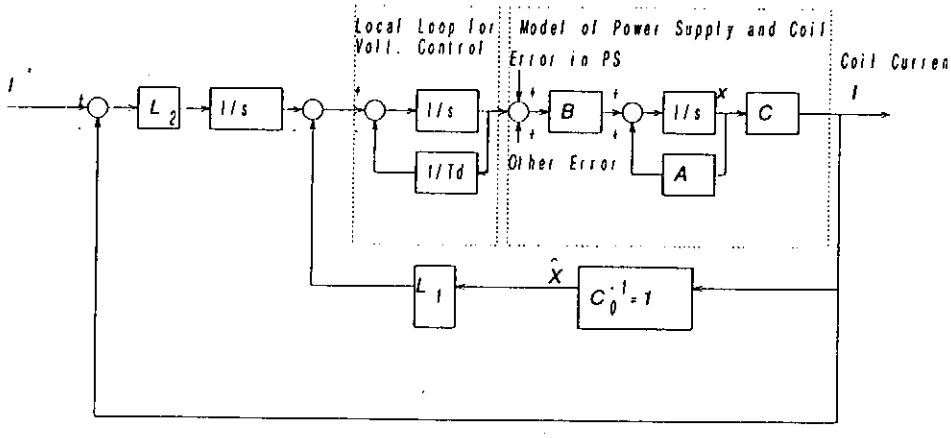

Figure 2: Block Diagram of Coil Current Control System

- No plasma in a vacuum chamber.

Because of magnetically coupling between coils and structures, classical control design like as a PID control cannot satisfy abouve requirements. Therefore the current regulator design should be based on a state variable control theory which is one of modern control design method.
In the LHD coil system, the plant model is as follows;

$$\begin{bmatrix} V_c \\ 0 \end{bmatrix} = s \begin{bmatrix} L_{cc} & L_{cs} \\ L_{sc} & L_{ss} \end{bmatrix} \begin{bmatrix} I_c \\ I_s \end{bmatrix} + \begin{bmatrix} R_c & 0 \\ 0 & R_s \end{bmatrix} \begin{bmatrix} I_c \\ I_s \end{bmatrix}, \quad [I] = \begin{bmatrix} 1 & 0 \end{bmatrix} \begin{bmatrix} I_c \\ I_s \end{bmatrix}$$

where V_c:coil terminal voltage, I_c, I_s:coil and structure currents, $L_{cc}, L_{cs}, L_{sc}, L_{ss}$: Inductance of coils and structures, R_c, R_s:Resistance of coils and structures, I: observed coil current.
Here, actual coil terminal voltage delays in voltage control miner loop and dc passive filter like as $V_c = \frac{1}{1+s\tau} V_c^*$, where τ: delay time constant, V_c^*: voltage reference.
For this plant, a basic current control scheme using state variables is as follows;

$$\left[V_c^* \right] = \frac{1}{s} \left[L_2 \right] \left(\left[I_c^* \right] - \left[I_c \right] \right) + \left[L_1 \right] \left(\left[I_c^* \right] - \left[I_c \right] \right)$$

In the above equation, I_s is not used because it cannot be observed directory.
Figure 2 shows a whole block diagram of coil current regulator.
The main part of this current regulator is installed in the VME machines in figure 1. In this control loop, required control period is less than 20ms because the shortest characteristic time constant of

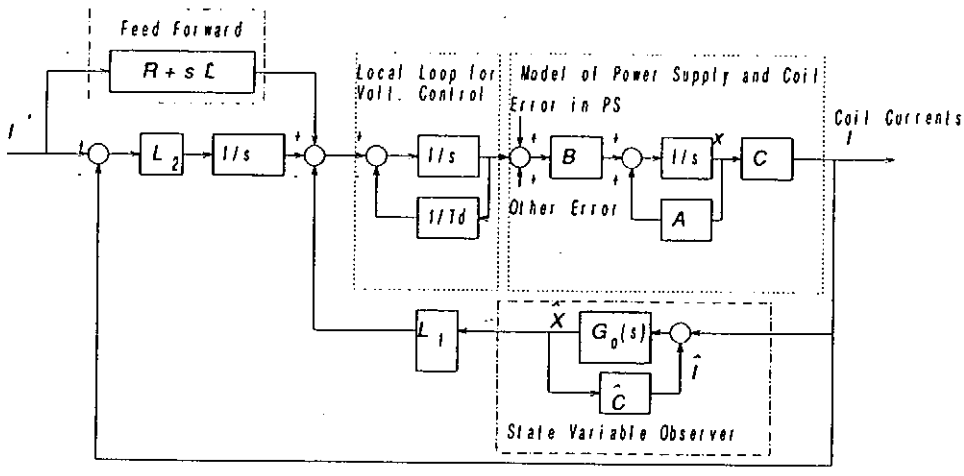

Figure 3: Block Diagram of Coil Current Control System using State valiable observer

the load is about 0.5s and we need more than 10 control steps between this time. The number of state variables is 10 that includes 6 coil currents, 3 currents in structure and a plasma current. As a result, the regulator routine must perform about 200 multiplies and accumulation in one control period with two cpus. We estimated the actual time to perform this regulator with test program. The result shows that the cpu needs only 118 μ s for calculation and 10.8ms for data communication with 3 rectifier units.

ADVANCED CONTROL SCHEME

In phase II operation of LHD, high voltage power supplies drive the coils because faster response of coil current is required. In this case, current control scheme menshoned above is not sufficient because it uses only coil currents as state valuables. For this reason, two new control schemes are under investigation. One is a controller using state valuable observer and feed forward, and the other is H_∞ control scheme.

State Variable Observer

Figure 3 shows a diagram of current regulator that uses state variate observer and feed forward. Inside of the doted line is the observer that estimates state valuables, which cannot be estimated from output signal directory, and current regulator uses all of the state variables to control coil currents. The feedforward term forecast necessary output voltages for power supplies from current references.

H_∞ Controller

H_∞ Control is one of design method of state variable based controller that using a H_∞ norm in frequency domain s. Figure 4 shows a generic diagram of H_∞ control, where $P(s)$ and $K(s)$ are plant characteristics and controller gain. W_1 and W_2 are evaluate functions and they indicate maximum tracking error and system robustness. In the H_∞ control , a control gain $K(s)$ must be designed to satisfy following equation,

$$\left\| \begin{array}{c} W_1/(1+K(s)P(s)) \\ W_2P(s)K(s)/(1+K(s)P(s)) \end{array} \right\|_\infty < 1$$

For the LHD control system, W_1 and W_2 are selected as shown in figure 5. With these function, $K(s)$ is designed using MATLAB code and coil currents are simulated. Figure 6 shows a simulation result of coil current. It is clear that the coil currents are controlled independently using H_∞ control.

CONCLUSION

This paper introduces a coil current control system for the LHD. This system is just under constructing and some numerical simulations for presented control scheme are done. Each simulation results shows that these control schemes satisfy the requirements for current control design.

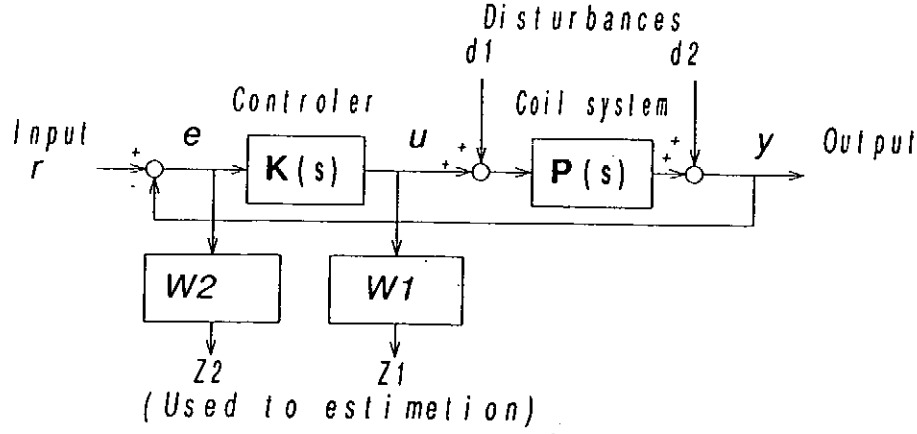

Figure 4: Generic Block Diagram of H_∞ control

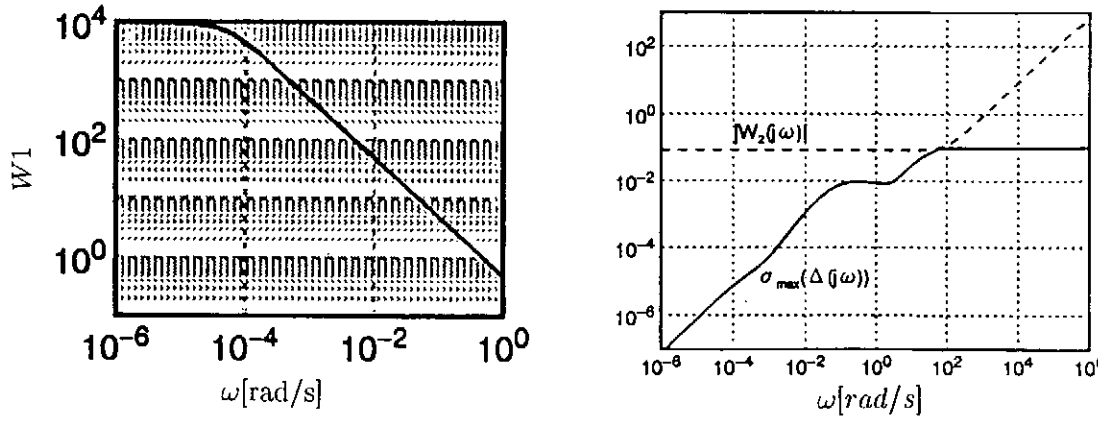

(a) Function W_1 (b) Function W_2

Figure 5: Weight Function W_1 and W_2 for LHD Current Control

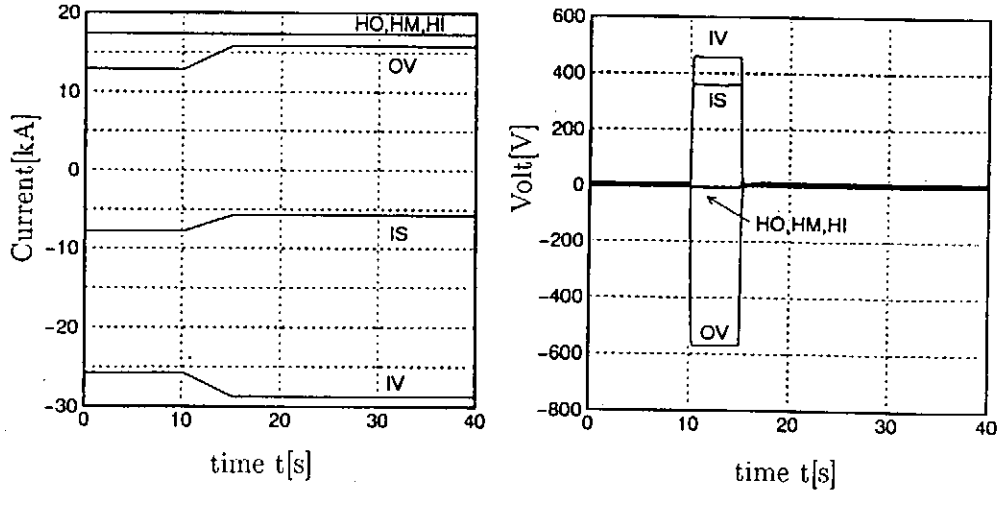

(a)Coil Currents (b)Terminal Voltage

Figure 6: Simulation Result of Current Control using H_∞ Scheme

MECHANICAL TEST RESULTS FOR COIL PACKS SIMULATING SUPERCONDUCTING COILS IN LHD

H. Tamura, A. Nishimura, S. Imagawa, T. Mito, K. Takahata, J. Yamamoto,
K. Asano,* T. Tamaki,* K. Nakanishi,* S. Suzuki,**
T. Yamamoto,** T. Yamakoshi,** K. Nakamoto**
National Institute for Fusion Science, Oroshi-cho, Toki-shi, Japan
*Hitachi Ltd., Hitachi-shi, Japan
**Toshiba Corporation, Tsurumi-ku, Kanagawa, Japan

ABSTRACT

The helical coil in the LHD is a pool-boiling-type superconducting coil and the poloidal coils are forced-flow-type coil. These coils may show different mechanical behaviors since their types of conductor, insulating method and coil structure are different. To simulate these superconducting coils, some mechanical tests of coil packs have been carried out at the liquid helium temperature and the mechanical behaviors of them were evaluated with their rigidity.

INTRODUCTION

Concerning the development of superconducting coils for fusion reactors, it is important to clarify the mechanical behavior and rigidity of the coil at the liquid helium temperature. The Large Helical Device[1] has one pair of superconducting helical coils and three pairs of superconducting poloidal coils. The helical coil is a pool-boiling-type superconducting coil and the poloidal coils are forced-flow-type coils. These coils may show different mechanical behavior since their internal structure and winding method are different. Insulators in the coils are subjected to a large electromagnetic force of about 10 MN/m under a condition of 18 kA current flow and 4 T at a plasma center in the case of helical coil. To simulate these superconducting coils, some mechanical tests of coil packs were carried out at the liquid helium temperature[2,3] by using 10 MN cryogenic testing machine with a servo control system[4].

HELICAL COIL PACK

Sample

The insulators in the helical coil have variable area ratio against the conductor's surface to ensure the helium flow paths in a high magnetic field area and to reinforce a mechanical strength in a high electromagnetic forced area[5]. We chose two typical insulator's ratio for the coil packs. Figure 1 shows a configuration and dimension of the helical coil pack sample I-4. This sample simulates fourth layer of I-block in the helical coil. Another sample simulates fifth layer of M-block (sample M-5). Each coil pack has a 6 layers x 6

turns structure of a superconductor with 200 mm long. The differences between them are a dimension of the insulator (11mm and 16 mm trapezoid cross section for I-4 and 28 mm and 33 mm for M-5) and its adhering pitch (52 mm for I-4 and 58 mm for M-5). A piled up structure was constructed in SUS304 case that had enough rigidity compare with a coil section. A displacement was measured between compressive rod and SUS304 case by using four clip type displacement gage and a compressive load was converted from pressure gage in a servo system.

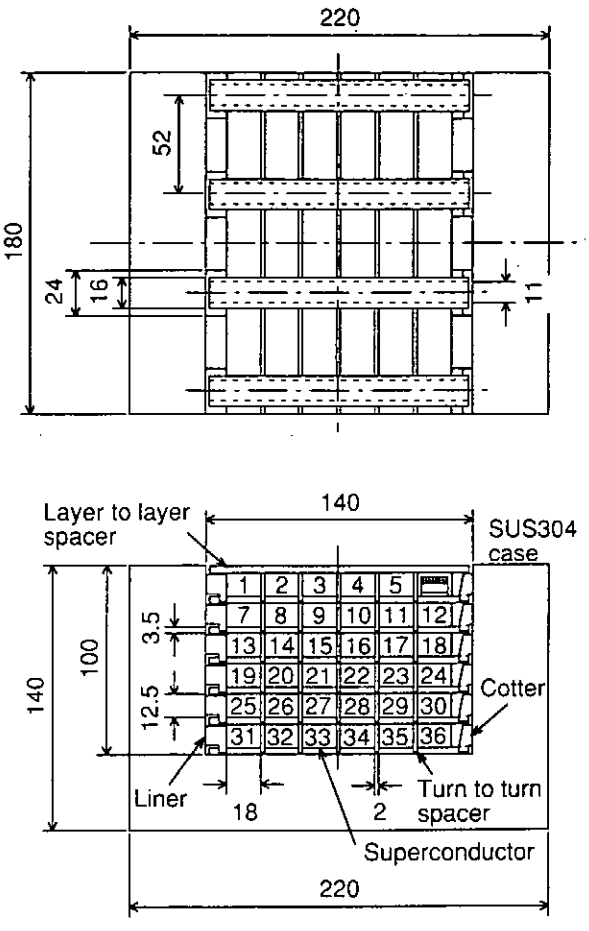

Figure 1 Dimension of helical coil pack

Results

Figure 2 shows the results of experiment of coil packs. Large hysteresis and nonlinearity were observed in curves especially in the first cycle of compression. An apparent compressive rigidity was approximately 30 GPa at the beginning of unloading process when the layer to layer insulator was subjected compressive stress of 100 MPa. Nonlinearity has been understood that the effect of surface touch problem in the coil pack. It is rather difficult to place the conductors and the insulators with an ideal accuracy because it was wound by pile up method, and residual gaps are generated between the insulator and the superconductor. Evaluation of this nonlinear behavior and stress distribution in the cross section of the coil

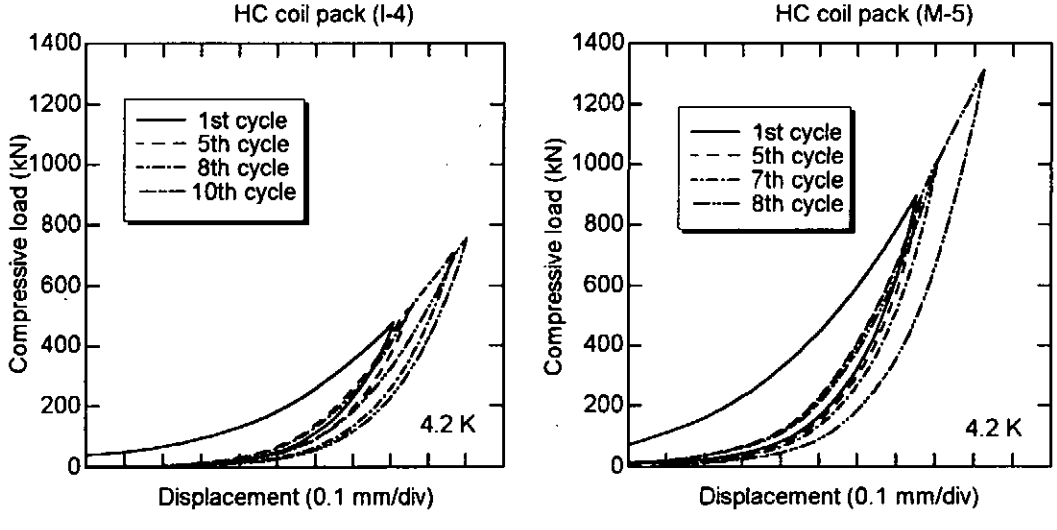

Figure 2 Load vs. Displacement curves of the helical coil pack.

pack have been attempted using finite element analysis with assumption of a gap between conductor and insulator[6]. It is difficult to estimate an apparent rigidity absolutely, but it is possible to estimate a change of rigidity and global displacement.

POLOIDAL COIL PACK

Sample

We carried out two coil packs simulating the inner vertical (IV) poloidal coils in LHD. The coil packs were made of conduits that have been used in the superconductor for IV coil. The material of this conduit SUS316L with 3 mm thick. We assumed that the effect of the superconducting strand in the conduit was small for cross sectional compression. Figure 3 shows the dimension of poloidal coil pack. Two samples were prepared to evaluate a rigidity for a radial and vertical direction (Z direction sample and R direction sample, respectively).

Results

Load versus displacement curves of the poloidal coil pack for z direction compression. Each curve was shifted to displacement direction ease to see (0 for 1st cycle, +0.05 mm for 3rd cycle and +0.1 mm for 5th cycle). They originally along the similar loading and unloading paths. Even though some hysteresis and nonlinearity were observed, they were very small in comparison with that of helical coil. This is assumed there are no effect of gaps in poloidal coils since it was cured with GFRP and epoxy resin after wound the conductor. Apparent compressive rigidity for each sample was measured on the

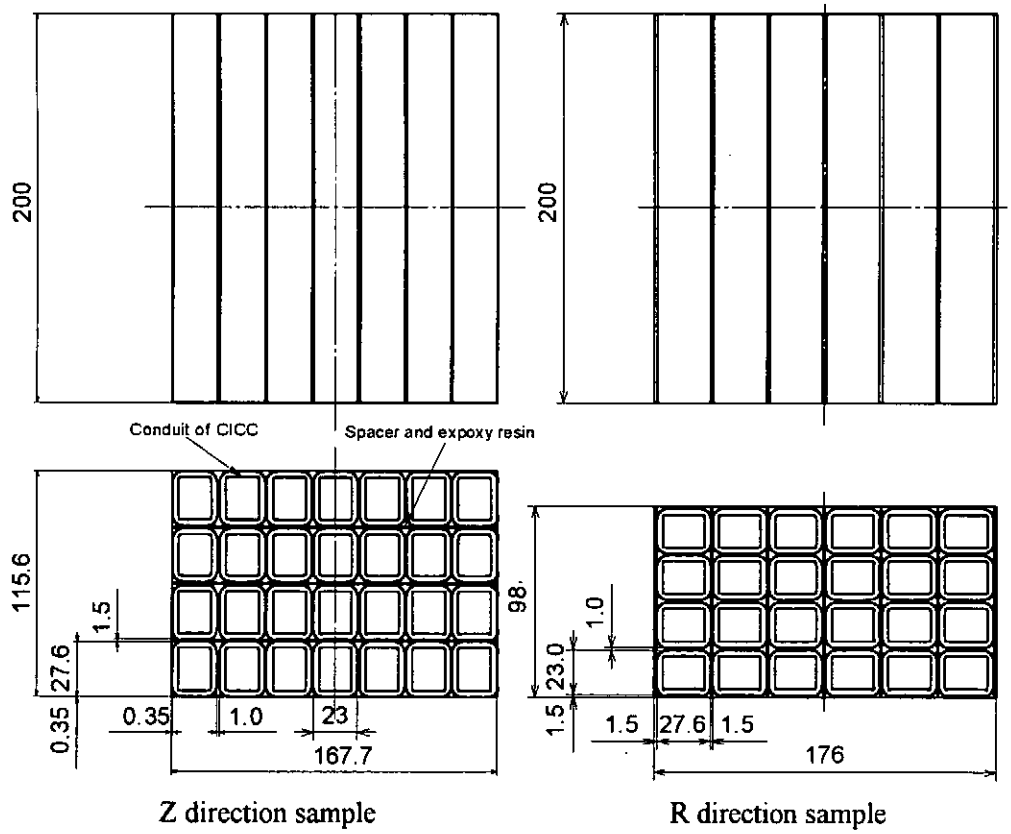

Z direction sample R direction sample

Figure 3 Dimension of poloidal coil pack.

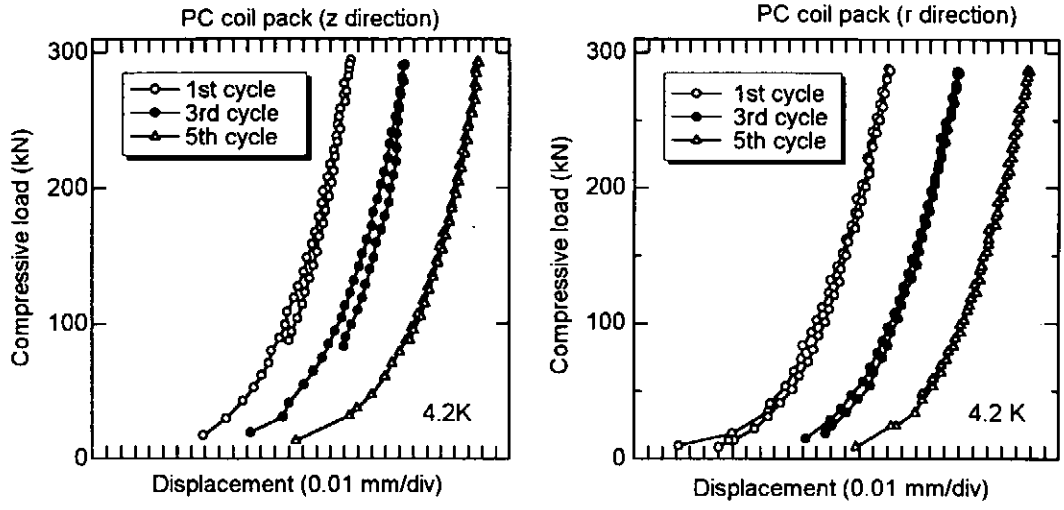

Figure 4 Load vs. Displacement curves of poloidal coil pack. Each curve was shifted for ease to see (+0.05 mm for 3rd cycle and +0.1 mm for 5th cycle).

unloading process from the maximum compressive load in the 5th cycle. Each rigidity was 22.7 GPa and 16.0 GPa, respectively.

CONCLUSIONS

In this report, the experimental results of compressive rigidity for coil pack simulating helical and poloidal coil in LHD was presented. Both coil pack show nonlinear behavior especially in an initial compressive or a low compressive load. The maximum apparent rigidity for helical coil pack and poloidal coil pack are approximately 30 GPa and 16 to 23 GPa, respectively. In the case of helical coil pack, it is difficult to estimate an apparent rigidity absolutely, but it is possible to estimate a change of rigidity and global displacement.

REFERENCES

1 Motojima, O., et al., Physics and engineering design studies on the Large Helical Device, Fusion Engineering and Design, (1993) 20 3-14

2 Nishimura, A. et al., Experimental Rigidity Evaluation of Conduit Pack for Forced-Flow Superconducting Coil, Advances in Cryogenic Engineering, (1994) Vol. 40 1413-1420

3 Nishimura, A. et al., Deformation behavior of coil pack for helical coil in Large Helical Device, ICEC16 (1996) Kitakyushu, Japan PS3-e2-39

4 Nishimura, A., et al., Rigidity tests of a superconducting coil at 4.2 K simulated for the helical coil on the LHD program, Fusion Engineering and Design, (1993) 20 211-216

5 Imagawa, S., et al., Construction of Helical Coil Winding Machine for LHD and On-site Winding, IEEE Transaction on Magnetic (1996) to be published

6 Tamura, H., et al., Deformation analysis for coil pack simulating large scale pool-boiling superconducting coil, ICEC16 (1996) Kitakyushu, Japan PS3-e2-38

Fracture Toughness of Structural Material for LHD

A. Nishimura, H. Tamura, S. Imagawa, and J. Yamamoto
National Institute for Fusion Science. 322-6 Oroshi, Toki, Gifu 509-52 Japan

ABSTRACT

Several fracture toughness tests have been carried out to characterize and confirm a structural reliability of Large Helical Device. A material used for a supporting structure of helical and poloidal coils is an austenitic stainless steel (SUS316). This material has a yield stress of over 620 MPa and a fracture toughness of over 300 MPa$\sqrt{m}$ at 4.2 K. In this paper, an effect of a magnetic field on the toughness, the toughness of a weld joint which has a natural crack at weld root, and the toughness of a full size thickness specimen will be summarized.

INTRODUCTION

Since a coil can or a support structure of the Large Helical Device (LHD) will experience a high magnetic field and these cryogenic structures will be assembled by welding, several fracture toughness data of base metals and weld joints were investigated

The materials used for this test series are the same stainless steels (SUS316) as those used for a lower support shell of LHD. Two kinds of plates were prepared. One was a 75 mm thick plate used for a rib structure of the support shell and the other plate was about 110 mm thick for the support shell structure. The chemical composition of the tested steel in mass % is Fe-0.04C-0.61Si-0.81Mn-0.025P-0.001S-11.23Ni-16.64Cr-2.27Mo-0.73N. Table 1 lists the 295-K and 4-K tensile properties. Butt welded joints were fabricated by TIG/MAG multiple-pass welding. Although a total welding passes were different depending on the plate thickness, the first pass was welded by TIG welding and a partial welding was performed to simulate an actual weld joint in LHD construction. Welding conditions for these test specimens were almost same as the normal ones applied for LHD construction. In the case of a base metal specimen, a fatigue pre-crack was induced according to ASTM E 813-89, but in the weld joint specimen, a crack started from a natural crack at a weld root. There were no post-weld heat treatments before testing, since LHD is too large to perform PWHT.

Table 1 Tensile properties of SUS316 tested.

Test Temp. (K)	E (GPa)	YS (MPa)	UTS (MPa)	EL (%)	RA (%)
295	198	254	564	69	---
4	202	621	1642	46	41

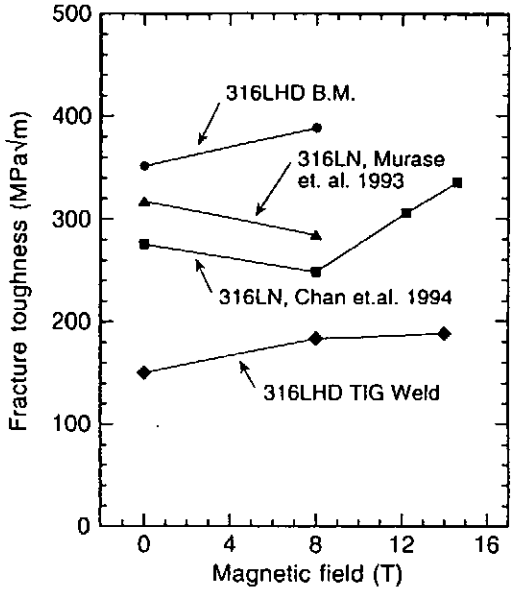

Figure 1 Effect of magnetic field on fracture toughness of SUS316 and TIG weld joint.

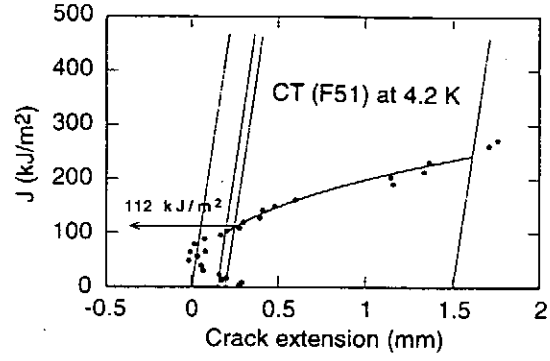

Figure 2 J-Δa curve of weld joint CT specimen.

Major interests are (1) an effect of a magnetic field on the fracture toughness at 4 K, (2) the fracture toughness of the weld joint which has the natural crack at the weld root and (3) the fracture toughness of a full size thickness specimen especially under bending. Some important results will be summarized in this paper.

EFFECT OF MAGNETIC FIELD ON FRACTURE TOUGHNESS

The effect of magnetic field on the fracture toughness is shown in Fig. 1 [1]. The tests were carried out in liquid helium using conventional compact tension specimens with 35.6 mm wide (W) and 12.7 mm thick (B). In this figure, the published data [2,3] are also presented. It is difficult to note a general tendency of the magnetic effect on the fracture toughness. However, SUS316 base metal and the weld joint for LHD showed that the toughness increased slightly in high magnetic field.

The fracture resistance is considered to be determined by a balance between a stress relaxation at the crack tip (induced by the martensitic transformation) and a lower stress intensity required for fracture of the fresh martensite and austenite. The SUS316 base metal used in this study will behave well in that the martensitic transformation is very localized around the crack tip and not expanded much, so the amount of martensite (or the transformation rate) accelerated by the magnetic field will be very small.

FRACTURE TOUGHNESS OF PARTIALLY WELDED JOINT

For the TIG/MAG joint specimens, many large pop-ins were observed on the load-displacement curve. The first large pop-in tends to occur around the maximum load, and the load decreases rapidly when a large pop-in happens in tests using stroke or cross head control.

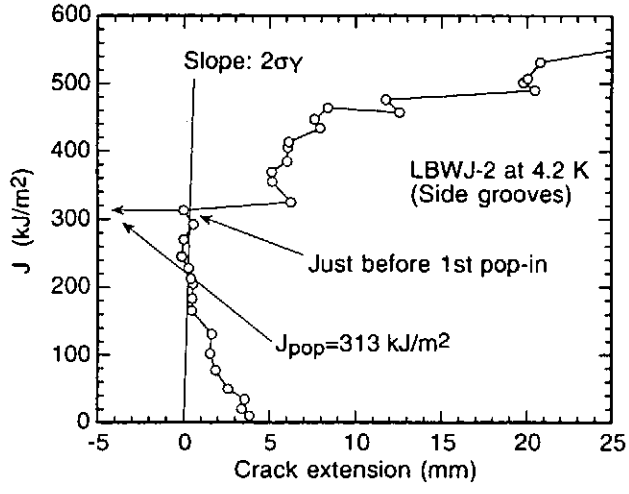

Figure 3 J-R curve of large bend bar (Weld joint).

Crack growth resistance curves are shown in Figs. 2 and 3. In both specimens, large crack extensions are associated with the first large pop-ins. In the case of CT specimen, a J-test evaluation according to ASTM E 813-89 could be applied, since the sudden crack extension at the first large pop-in was less than 1 mm. However, in the case of a large bend bar, it was not possible to apply ASTM E 813-89, for the crack extension at the first instability was over 5 mm. In this case, K_{max} was adopted as the critical toughness instead of J_{Ic}. This reason will be discussed later.

FRACTURE TOUGHNESS OF FULL SIZE SPECIMEN UNDER BENDING

The resistance curve data of the base metal bend bar is shown in Fig. 4. The J-Δa plot shows an anomalous "back-up", but there is a relatively steep blunting line and a well-defined knee point. The measured critical J value is 1528 kJ/m^2 and valid in terms of the specimen size requirements ($B>25(J_Q/\sigma_Y)$). Results of CT specimen at 4.2 K showed a small "back-up" at lower loads and gave the toughness J_{Ic} of 592 kJ/m^2, and this was much lower than that obtained with the bend bar.

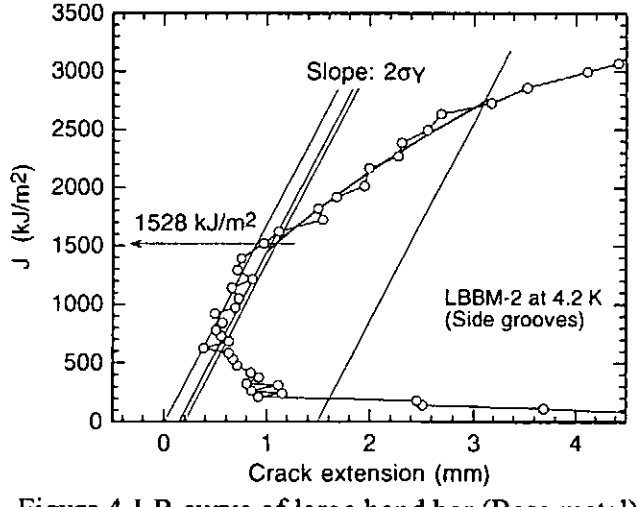

Figure 4 J-R curve of large bend bar (Base metal).

The "back-up" behavior and the larger critical toughness obtained with the bend bar were addressed with a wedge effect model [4]. A careful attention should be paid for the first instability observed in the weld joint [5]. In stroke control, running cracks in laboratory tests are periodically arrested because the applied load decreases with crack extension. However, the electro-magnetic forces applied to the magnet structure will remain constant throughout the operation of the device; they will not decrease or otherwise depend on the mechanical response of the structure. In magnet service, therefore, cracks running in the welds at 4 K will not be arrested, and catastrophic failure should be anticipated at the first instability if the critical stress intensity factor is exceeded. So, the lower critical value, such as K_{max}, should be defined and applied on the design of main cryogenic structures.

GENERAL REMARKS

Some results of the fracture toughness were presented. General remarks are as follows:
(1) It is difficult to note the general tendency of the effect of the magnetic field on the toughness, but SUS316 and the weld joint for LHD showed good results even at 14 T.
(2) The fracture toughness of SUS316 base metal and the weld joint were investigated using the CT specimen and the large bend bar with thick section.
(3) The "back-up" behavior was observed in both types of specimens and the bend bar gave larger toughness than CT specimen.
(4) The first large pop-in happened at the maximum load in the weld joint. This large crack extension behavior should be noted especially in magnet service.

ACKNOWLEDGMENTS

Authors wish to express our thanks to Dr. Iiyoshi, Director General of NIFS, and Professor O. Motojima for their continuous encouragement. Also, we would like to thank the LHD construction group for useful discussions and their help.

REFERENCES

1 Nishimura, A. et. al. Fracture Toughness of Partially Welded Joints of SUS316 in High Magnetic Field at 4 K ICMC 1995 Columbus, Ohio, USA (1995) WE-Y1-5
2 Chan, J. W. et. al. Cryogenic Fracture Behavior of 316LN in Magnetic Fields up to 14.6 T Adv. Cryo. Eng. (1994) 40 1215-1221
3 Murase, S. et. al. Effects of a High Magnetic Field on the Fracture Toughness at 4.2 K for Austenitic Stainless Steels Fusion Eng. Des. (1993) 20 451-454
4 Nishimura, A. et. al. Fracture Toughness of SUS316 and Weld Joint at Cryogenic Temperature ICMC 1996 Kitakyushu, Japan (1996) OC1-1
5 Nishimura, A. et. al. Fracture Toughness of Partially Welded Joints of SUS316 Stainless Steel at 4 K by Large Bend-Bar Tests MT-14 Tampere, Finland (1995) E-86

Heat Transfer Measurement for the Stability Analyses of the Helical Coil Superconductor

A. Iwamoto, T. Mito, K. Takahata, N. Yanagi, and J. Yamamoto
National Institute for Fusion Science
322-6 Oroshi, Toki, Gifu 509-52, Japan

ABSTRACT

Heat transfer of liquid helium was measured to analyze the stability of the helical coil superconductor for the Large Helical Device(LHD). Dependence of heat transfer from a prototype superconductor to liquid helium on surface orientation and cooling channel width was investigated. A sample was a copper block with 18 x 18 mm and 72 mm long. Sample orientation of the prototype superconductor was changed from 0°(horizontal) to 90°(vertical) at the interval of 15°. The copper block was surrounded by four stainless steel plates to make up a cooling channel. The cooling channel width was either 2 or 3 mm, furthermore measurements were conducted without a channel. Dependence of heat transfer from a copper plate on surface treatment was also investigated. The copper plate was 18 mm wide, 76 mm long and 7.5 mm thickness. Only one surface was exposed to LHe as heat transfer surface. The surface treatment, oxidation, of the copper plate was changed from 0% to 100% on the surface area. Heat fluxes of a partially oxidized surfaces were estimated, using heat fluxes of the 0% and 100% oxidized surfaces and a rule of mixture on surface treatment area.

INTRODUCTION

The LHD is under construction in National Institute for Fusion Science (NIFS)[1]. A pool boiling superconductor is applied to the helical coil[2]. Usually, according to Maddock's equal area theorem, the stability of the large sized superconductor have been analyzed. In the analysis, the heat transfer characteristics decides the stability of the superconductor. For the reliable stability analysis, the heat transfer characteristics have to be investigated. In the helical coil, conductor orientation varies according to the winding position, and the surface is oxidized to improve the heat transfer characteristics. To analyze the stability of the helical coil, the effect of the surface orientation and the surface treatment must be estimated. The surface treatment may peel off in the winding. In this study, the heat transfer of liquid helium for the stability analyses was measured as a function of surface orientation, channel width and the area fraction of surface treatment.

EXPERIMENT

The samples were a copper plate and a prototype superconductor. Dependence on the surface treatment was estimated, using the copper plate, and heat transfer from the prototype superconductor was measured as changing surface orientation and channel width. Temperature difference between the surface and the liquid helium was measured using AuFe-Chromel thermocouple.

The copper plate was 18 mm wide, 76 mm long and 7.5 mm thickness. Dependence of the heat transfer on surface treatment was investigated at 90°(vertical). The schematic illustration is shown in Fig.1. The samples were treated surfaces of polished Cu and oxidized Cu. The area fraction of the surface treatment was changed from 0 % to 100 %(Fig.2). The roughness of the polished Cu surface was less than 10 μm. The sample was covered with an FRP holder, except for the heat transfer surface (18 x 76 mm).

The prototype superconductor was a polished copper block with 72 mm long and 18 x 18 mm cross section. The schematic illustration is shown in Fig.3. Dependence of the heat transfer on channel width and sample orientation was investigated. The surface roughness was less than 10 μm. The sample orientation was changed form 0° (horizontal) to 90° (vertical). The copper block was surrounded by four stainless steel plates to make up a cooling channel. The channel width was 2, 3 mm or open.

RESULTS AND DISCUSSIONS

Dependence of the heat transfer on surface treatment

Figure 4 shows the dependence of the critical and the minimum heat fluxes(CHFs and MHFs) on surface treatment. Oxidation of the entire heat transfer surface improves the CHFs and the MHFs compared with those of the entire polished surface. It appears that the critical and the minimum heat fluxes change discontinuously as a function of the area fraction of the oxidized surface. The critical heat flux suddenly changes at around 75%

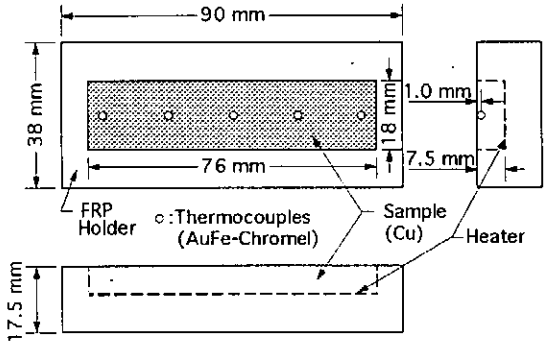

Fig. 1 Schematic illustration of the copper plate

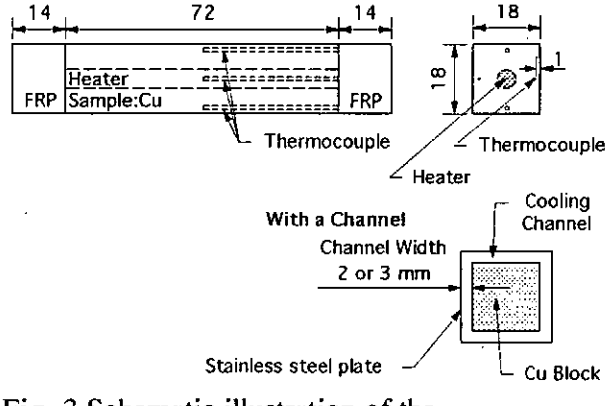

Fig. 3 Schematic illustration of the prototype superconductor

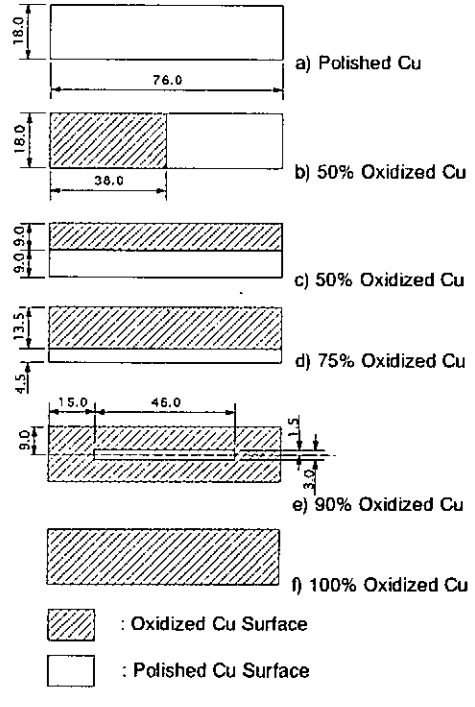

Fig. 2 Various surface treatments

Table 1. Summary of heat transfer characteristics (at bath temperature of 4.2 K).

Angle	Critical Heat Flux (W/cm^2) (at T_1 K)	Minimum Heat Flux (W/cm^2) (at T_2 K)	Boiling Curve Nucleate $T < T_1$		Transition $T_1 < T < T_2$		Film $T_2 < T$	
			a	b	a	b	a	b
Polished Cu Sample								
90°	0.484 (at 4.60 K)	0.108 (at 5.71 K)	1.20	-5.06	-0.340	2.05	0.0368	-0.102
100% Oxidized Cu Sample								
90°	0.648 (at 5.33 K)	0.243 (at 9.58 K)	0.573	-2.41	-0.0951	1.16	0.0318	-0.0617

oxidation. Between 0 and 50% oxidation, the minimum heat flux does also. The oxidation drives the critical and the minimum heat fluxes to improve.

Heat is transferred to the liquid helium with contributions from the polished and the oxidized regions proportional to their area fractions. We approximate the heat transfer curve for each case as $HF(T)=aT+b$, then calculate the total heat transfer for a partially oxidized sample using Table 1 and a rule of mixtures, Eq.(1):

$$HF_{POS}(T) = HF_{Oxidized}(T) \cdot x + HF_{Polished}(T) \cdot (1 - x) \qquad (1)$$

In this expression, $HF_{POS}(T)$, $HF_{Oxidized}(T)$, and $HF_{Polished}(T)$ are the heat fluxes of the partially oxidized, 100% oxidized, and 100% polished Cu samples at T K, and x is some area fraction of oxidation. The effect of thermal conductivity in the copper block are neglected in such calculations. We calculate the critical and the minimum heat fluxes at 90° using Eq.(1)(Fig.3). The calculated results are almost agree with those of the measurements.

Dependence on surface orientation and channel width

Table 2 summarizes the heat transfer of the prototype superconductor. The heat transfer curve for each case was approximated as $HF(T)=aT+b$. Figure 5 shows the dependence of the critical and the minimum heat fluxes on sample orientation and channel width. The critical heat fluxes depended on the sample orientation and increased as the sample orientation increased from 0° to 45° and decreased from 45° to 90°. The CHFs had a peak at 45°. The CHFs were significantly affected by the channel width and were improved as increasing the channel width. The channel width of more than 3 mm makes the heat transfer be as same as that without a channel. It is assumed that a narrow cooling channel prevented liquid helium from being supplied to the heat transfer surface. On the other hand, the minimum heat fluxes were less dependent on the surface orientation as well as the channel width than the critical heat fluxes. According to these experimental results, it is thought that the stability of a pool boiling superconducting magnet with more than 3 mm channel width is as same as that of its superconductor.

CONCLUSION

To analyze the stability of the helical coil superconductor, the heat transfer was measured, using the copper plate and the prototype superconductor. The dependence of the heat transfer characteristics on surface orientation, channel width and the area fraction of surface treatment was investigated. According to the data obtained from measurements, it

is thought that more than 3 mm of the channel width and more than 75% of the surface treatment make the superconducting magnets stable. The measured results were applied to the stability analyses of the superconductor for the helical coil.

REFERENCES

[1] Motojima, O., et al., Physics and engineering design studies on the Large Helical Device Fusion Engineering and Design (1993) 20 3-14

[2] Yanagi, N., et al., Experimental observation of anomalous magneto-resistivity in 10 - 20 class aluminum-stabilized superconductors for the Large Helical Device Advances in Cryogenic Engineering (1994) 40 459-468

Table 2 The heat transfer of the prototype superconductor (at bath temperature of 4.2 K)

Angle	Critical Heat Flux (W/cm^2) (at T_1 K)	Minimum Heat Flux (W/cm^2) (at T_2 K)	Boiling Curve Nucleate $T < T_1$ a	b	Transition $T_1 < T < T_2$ a	b	Film $T_2 < T$ a	b
Channel Width 2 mm								
0°	0.279 (at 4.69 K)	0.0574 (at 5.67 K)	0.569	-2.39	-0.227	1.35	0.0139	-0.0210
30°	0.359 (at 4.85 K)	0.0674 (at 5.82 K)	0.552	-2.32	-0.300	1.81	0.0211	-0.0556
60°	0.383 (at 4.77 K)	0.0674 (at 5.74 K)	0.672	-2.82	-0.324	1.93	0.0233	-0.0663
90°	0.366 (at 4.85 K)	0.0664 (at 5.82 K)	0.562	-2.36	-0.307	1.86	0.0241	-0.0738
Channel Width 3 mm								
0°	0.338 (at 4.77 K)	0.0622 (at 5.74 K)	0.594	-2.49	-0.283	1.69	0.0164	-0.0320
30°	0.476 (at 4.61 K)	0.0687 (at 5.74 K)	1.17	-4.91	-0.359	2.13	0.0214	-0.0540
60°	0.494 (at 4.61 K)	0.0686 (at 5.74 K)	1.22	-5.11	-0.375	2.22	0.0237	-0.0678
90°	0.447 (at 4.61 K)	0.0655 (at 5.74 K)	1.10	-4.62	-0.336	2.00	0.0243	-0.0737
Without a Channel								
0°	0.449 (at 4.69 K)	0.0558 (at 5.82 K)	0.920	-3.86	-0.346	2.07	0.0187	-0.0529
30°	0.509 (at 4.69 K)	0.0643 (at 5.82 K)	1.04	-4.38	-0.391	2.34	0.0236	-0.0731
60°	0.508 (at 4.69 K)	0.0658 (at 5.66 K)	1.04	-4.38	-0.454	2.64	0.0256	-0.0791
90°	0.467 (at 4.68 K)	0.0658 (at 5.82 K)	0.960	-4.03	-0.354	2.13	0.0275	-0.0942

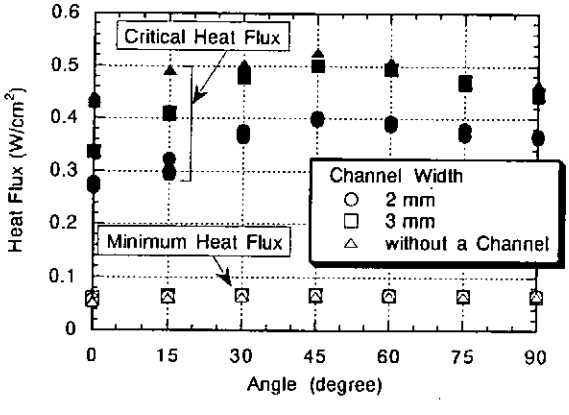

Fig. 4 Dependence of the critical and the minimum heat fluxes on surface treatment

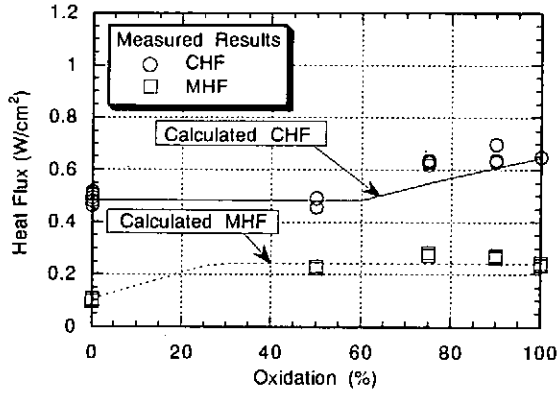

Fig. 5 Dependence of the critical and the minimum heat fluxes on sample orientation and channel width

Design and Experiments on Component Hardwares for LHD Cryogenic System

Sadao Satoh, Toshiyuki Mito, Shuichi Yamada, Junya Yamamoto,
Osamu Motojima and LHD Group

National Institute for Fusion Science, Nagoya 464-01, Japan

The Large Helical Device (LHD) is a heliotron fusion experimental device in which magnetic fields are controlled exclusively by superconducting magnet : a pair of helical coils and three pairs of poloidal coils. The refrigerator for the 3 Tesla experiments (phase I) has already been constructed and is being put to trial operations without LHD magnets. Its current status is reported elsewhere [1,2]. On the other hand, construction of other key cryogenic components have progressed as well. The paper reviews their design and heat load measurements obtained in NIFS experiments. Developments on some new technologies are also described. The results are encouraging and are expected to contribute to the operation of LHD cryogenic system significantly.

INTRODUCTION

Because a cryogenic system requires comparatively a long construction time and some machine training period before a whole superconducting system is put into operation, the cryogenic heat load of LHD has to be estimated with some uncertainty in the beginning of its construction. The design work for the cryogenic system was initially made by the study group on "Cooling and Refrigeration Technology of Superconducting Magnets of LHD" in which nearly 60 scientists, engineers and researchers from universities and industries discussed on the design of LHD cryogenic system. About 115 various proposals were inspected through 20 meetings held during a two year period preceding the start of LHD construction. The sum of the heat loads is shown in pevious papers [1,2] and it becomes the basis of the capacity of the refrigerator / liquefier for LHD. In parallel with the construction progress, a real and revised heat load became clear by the improved designs and actual scale bench test at NIFS. Several examples are reviewed below.

HEAT LOAD MEASUREMENTS ON KEY COMPONENTS

Joule Heat at Conductor Joints

The conductor joints of Cable-in-Conduit-Conductors for the poloidal coils are bonded by a solid state bonding method [3]. The purpose is to obtain a joint resistance less than 10^{-9} Ω per a soldered joint and a contact area as small as possible. 486 NbTi strands were taken out from a conduit end, their Cu matrix was removed, groups of filaments were mutually arranged, and pressure and heat were applied in a vacuum chamber. They demonstrated a twice higher quench current than operation current at a rated bias field and at 4.2 K. A total of 42 joints of three poloidal coil pairs were fabricated by this technique. No measurable resistance was obtained. Similarly, a joint soldering method was applied to the aluminum-stabilized composite superconductor of the helical coils. It's Cu sheath removed, the inside NbTi composite strands were mutually laid in parallel and soldered with a superconducting spacer bar standing

in-between [4]. The resistance was measured as 0.7 nΩ at 9 T, which is 0.21 W / joint at a rated 17.3kA and a total of 6.7 W was calculated for 32 joints of the helical coils. This is one sixth smaller than originally assumed.

Conduction to Superconducting Bus-line

To reduce the load of the power supply system and the steps of on-site assembling, 9 pairs of prefabricated, flexible superconducting bus-lines were adopted for LHD [5]. A pair of SC cables consisting each of 9 NbTi / Cu, Al stabilized compacted strands, is inserted into the center corrugated tube which is assembled coaxially with other 4 corrugated tubes of 220 mm outermost diameter and 50 m length. The rated current is 31.3 kA at 1 T, 4.2 K and the critical current is 180 kA. A full scale model of 20 m length 4 corrugated tube assembly, was put to an excitation test [8]. Because the construction has no radiation heat shield except vacuum insulation, 4.55 W/m at 5 K heat load into the return cold gas was obtained from the model experiment.

To reduce the heat load on the 5 K level, a 80 K helium gas channel will be added for the SC bus-lines of LHD as mentioned above. This leads to a 3 W / m load at 80 K and 0.3 W / m at 5 K. SC wires are embedded in the flexible cable joints which connect each two ends of the bus-line to the coil or the current lead. 2 W / joint were obtained and 144 watt is required for 72 joints of 9 paires. Additional 650 L/h liquid helium is evaporated and heated up to 300 K through the gas cooling type current leads.

Transfer Tubes

Cryogenic transfer tubes are grouped according to their destination and each group is enclosed in a 80 K radiation heat shielded, vacuum insulated transfer tube line, TRT 1 to TRT 3. Their design descriptions may be referred to [6]. During the combined runs of the refrigerator with the dummy heat load cryostat [7], measurements were made of the heat leak into TRT 2 (5 lines-550mmØX50m) and TRT 3 (6 lines-650mmØX68m) altogether. As shown in Figure 1, the measured value for the radiation heat load was about 1450±50 W between 40 and 45 K. Because the size, length and number of contained tubes, partitions, bayonet joints and junction boxes attached are different in the two transfer tubes, 8.5 W/m^2 of the heat flux was calculated by averaging the heat load with the total internal shield surface area of two tubes. The figure may not be claimed as excellent, but still a fair amount of heat load is saved from the original design. Measurement of the heat leak at the 4.5 K level failed mainly due to an inadequate comparison of temperature readings from two different types of sensors.

Heat Isolation Columns

10 heat isolation columns support a full assembly of the cryogenic part of LHD. They are the super-conducting coils and their magnetic force support structure. The overall weight is about 800 ton. The column stand upright on the base plate of the LHD cryostat at room temperature and support the 4.5 K cold assembly at its bottom. 8 CFRP square plates of each column can carry 95 ton in compression stress and their double folded shapes with thermal anchor are expected to limit heat load within 3W / column at 4.5 K, whereas a cooling rate of 82 W / column is required at the 80K level which is a 3 times larger heat load than initially estimated.

Supercritical Helium Circulation Pump

Recently, a supercritical helium (SHe) circulation pump has been appreciated in the usage of cooling CCIC type SC magnets for its compact size and comparatively robust performance. Cooling and excitation tests with a centrifugal type supercritical pump were made on one of the poloidal coils for LHD, the inner vertical coil IV-L [8]. Inside the pump cryostat there is a liquid helium dewar containing an aluminum brazed plate-fin heat exchanger which precools the SHe to 4.5K. Nearly 2 m above the top plate of the cryostat a 50 g/s pump is mounted, which is surrounded by a 40 mm thick iron magnetic shield [9]. The arrangement limitation would force the pump to run under a magnetic field of 1000 Gauss unless the magnetic shield is adopted.

At the excitation test, the pump ran at a speed of 55000 rpm without any problem thanks to the magnetic shield, under which the attached Hall effect sensor detected no magnetic field strength of importance. Figure 2 shows the hydraulic performance of the SHe pump. The adiabetic efficiency of the pump was measured to be 63 % at maximum.

1200 cycle on-off Endurance Test on three Bonnet-less Cryogenic Valves in Liquid Helium

Cryogenic valves with a long extended bonnet is commonly used with the benefit of maintainability and demerits of large size and inherent heat leaks. Three different designs of plug position and seat material combination were put to endurance test both in liquid nitrogen and helium for 1200 cycle open and close activation [10]. The mass leaks through the valve seat under the closing position were compared before and after the endurance run, but no change was observed for neither of the three valves. The heat loads carried in by actuating helium gas at room temperature were compared among the three designs, the normally closed type showing a higher heat leak.

The bonnet-less cryogenic valves provide the possibilitiy for a switching usage, where actuator helium gas is not necessary for normal operation and/or when it is beneficial to put a valve directly at a local position in a piping system. A possible application for LHD is the switching and balancing of the flow to the magnetic force support structure, where the valves are needed to be active for the period of the initial cool down from ambient temperature.

REMARKS AND ACKNOWLEDGMENT

The current status in the construction of certain cryogenic components for LHD was described especially in the aspect of thermal performances. The construction is not completed until all of the superconducting magnets are assembled and connected to the refrigerator, that is in the end of 1997.

The authors acknowledge Dr. A. Iiyoshi for his leadership in promoting LHD construction. We are also indebted to scientists, engineers and researchers from universities, institutes and industries who joined to the NIFS Study Group on "Cooling and Refrigeration Technology of Superconducting Magnets of LHD" for their discussions and cooperation in the design of LHD cryogenic system.

REFERENCES

1 Satoh, S. et.al. Construction of a 10kW Class Helium Cryogenic System for the large Helical Device Cryogenics (1994) 34, 95-98

2 Satoh, S. et.al. Construction and Commissioning Tests of a 10-kW-Class Helium Refrigerator

for the Large Helical Device Proceeding WE-B1-3 CEC/ICMC (1995) or to be published 41 Advances in Cryogenic Engineering
3 Hanawa, S. et.al. Development of a Superconducting Joint Technique between CIC Conductors for Poloidal Coil of Large Helical Device (LHD) 5 .2 IEEE Trans. Appl. Supercond. (1995) 757-760
4 Yanagi, N. et.al. Development, Fabricacation, Testing and Joints of Aluminum Stabilized Superconductors for the Helical Coils of LHD PS3-e2-37 ICEC16/ICMC Kitakyushu (1996)
5 Yamada, S. et.al. Superconducting Current Feeder System for the Large Helical Device B72 MT-14 Tampere (1995)
6 Matsuda, H. et.al. The Constituent Hardware of the Large Helium Refrigeration Plants for LHD PS1-e1-08 ICEC16/ICMC Kitakyushu (1996)
7 Satoh, S. et. al. Construction report of 10-kW-Class Helium Refrigerator for LHD PS1-e1-10 ICEC16/ICMC Kitakyushu (1996)
8 Mito, T. et.al. Test Facilities of the Experiments on a Single Inner Vertical Coil (EXSIV) for the Large Helical Device PS3-e2-28 ICEC16/ICMC Kitakyushu (1996)
9 Miyake, A. et.al. Development of a Supercritical Helium Circulation Unit for Testing SC Magnets (in Japanese) 35 .4 Ishikawajima-Harima Engineering Review (1995)
10 Daido, K. et.al. Characterization of Bonnetless Cryogenic Valves PS2-e1-26 ICEC16/ICMC Kitakyushu (1996)

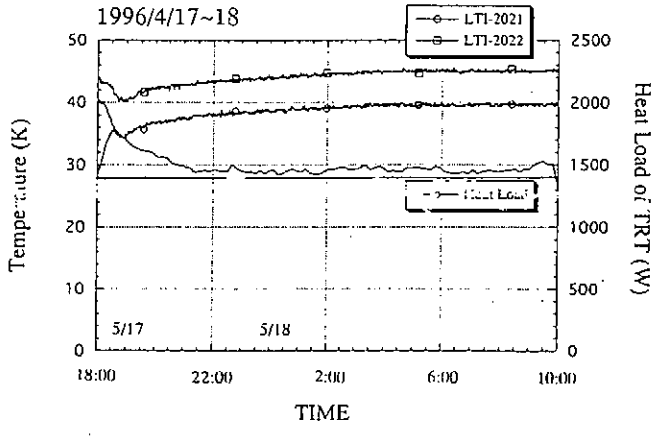

Figure 1 Heat load to radiation shield measured at transfer tubes TRT 2 and TRT 3 altogether.

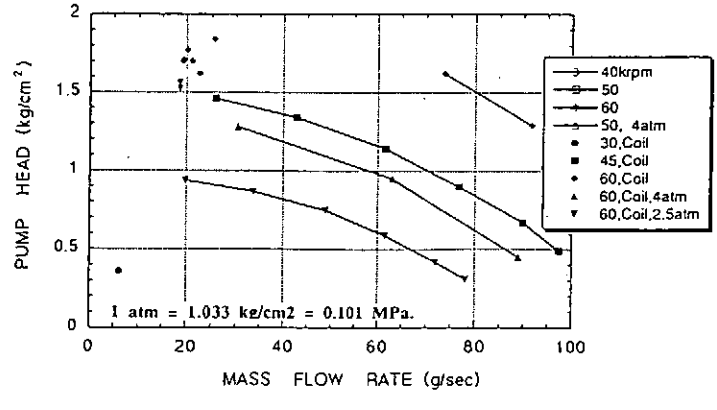

Figure 2 Hydrauric performance of SHe pump

DESIGN OF CENTRAL CONTROL SYSTEM FOR LARGE HELICAL DEVICE

H.Yamada, K.Y.Watanabe, K.Yamazaki, S.Yamaguchi, K.Nishimura,
Y.Taniguchi, H.Ogawa, N.Yamamoto, S.Sakakibara, M.Shoji, O.Motojima
National Institute for Fusion Science, Toki-shi, Gifu 509-52, Japan

ABSTRACT

Design of central control system for large helical device has been continued. The central control system consists of a central programmable logic controller, a torus supervision monitoring system, a timing system, a protective interlock, and the server computer with databases providing man-machine interface environment. Composition of conservative hard-wired logic control with a programmable logic controller and the man-machine interface system with a client/server system fulfills requirements of reliability, flexibility and extensibility.

INTRODUCTION

The large helical device (LHD) [1] is a superconducting toroidal facility with a mission to steady-state operation of high temperature plasmas. The major radius, the minor radius of plasmas, and the designed toroidal field are 3.9m, 0.65m, and 4T, respectively. While LHD is a plasma physics experimental device, it has a specific feature of a large-scale plant due to a steady-state capability and cryogenic systems. The control system of LHD [2] is required to cooperate a number of plant component devices/facilities (sub-systems) as well as manage flexible plasma experiments. Also safety protection against all expected occasions and easy extension for up-grade are key issues. The control system of LHD should be, therefore, reliable, flexible and extensible. Composition of conservative hard-wired logic control with a programmable logic controller and the man-machine interface (MMIF) system with a client/server system fulfills these requirements complementarily (see Fig. 1). The central control system has been designed to operate LHD safely without help of the MMIF system and hard-wired logic has priority over information transmitted through LAN, however, the MMIF system greatly facilitates procedures of experimental set-up, supervision of facility condition and sequence control. It also contributes to prevent operational human errors and consequent accidents.

COMPOSITION OF CENTRAL CONTROL SYSTEM

The central control system consists of a central programmable logic controller (PLC), a torus supervision monitoring system, a timing system, a protective interlock, and the server computer with databases providing man-machine interface environment. The facilities composing LHD are arranged into 50 sub-systems, ex. a vacuum pumping unit,

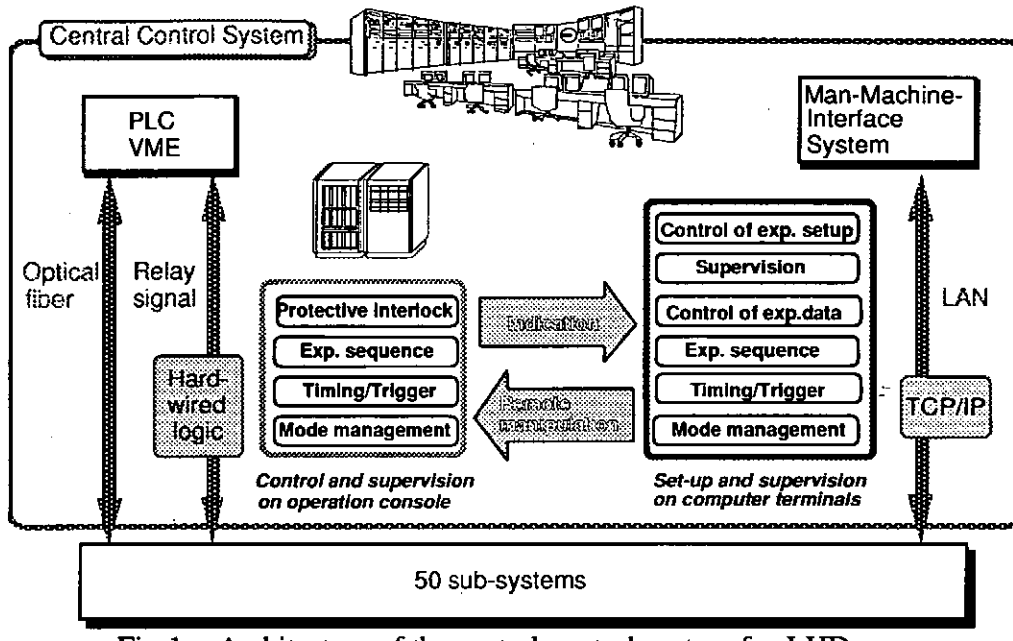

Fig.1 Architecture of the central control system for LHD

a cryogenic unit, a power supply for helical coils, an ECH heating unit, etc. Major sub-systems have their own control computers and can be operated independently and protect themselves. It should be noted that the central control system do not dictate a device control layer of a sub-system directly except for the protective interlock for an event of quench. The operation of LHD is managed in the framework of operational modes. Transition from a mode to a mode and the process of the operation is controlled by the central PLC which judges consistency with hard wired logic. Figure 2 shows the structure of operational modes and an experimental sequence. The timing system with a VME unit controls the process of plasma discharges precisely.

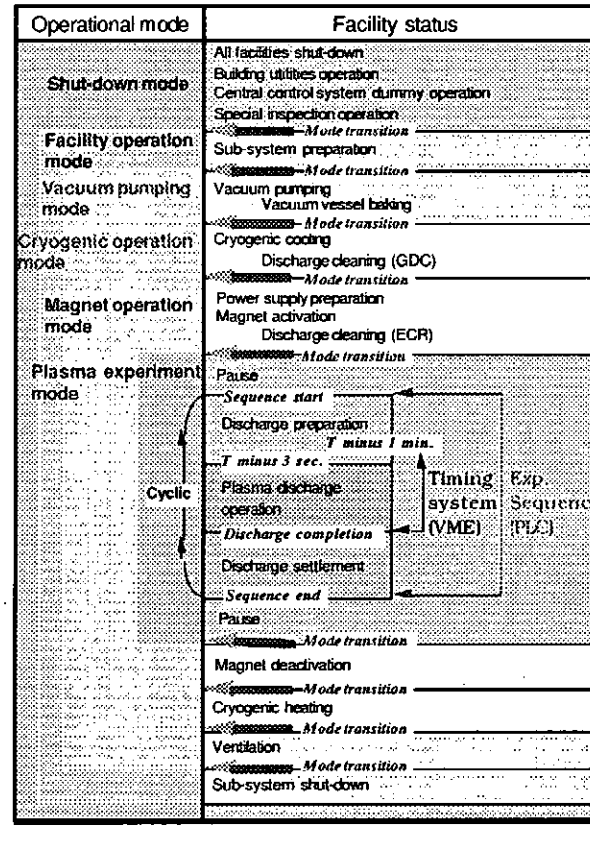

Fig.2 Structure of operational modes and experimental sequence.

MAN-MACHINE-INTERFACE SYSTEM

A man-machine-interface (MMIF) system which is a primary component of the central control system for LHD has been specified. The MMIF system, here, involves a variety

of intelligent functions needed in the LHD experiments as well as a scheme of graphical user interface in a narrow sense. The MMIF system provides a variety of information transmission through LAN. While LHD is a plasma physics experimental device, it has a specific feature of a large-scale plant due to a steady-state capability and cryogenic systems. The control system of LHD is, therefore, required to cooperate a number of component devices/facilities and should be reliable, flexible and extensible. Composition of conservative hard-wired logic control with a programmable logic controller and the MMIF system with a client/server system fulfills these requirements complementarily. The central control system has been designed to operate LHD safely without help of the MMIF system and hard-wired logic has priority over information transmitted through LAN, however, the MMIF system greatly facilitates procedures of experimental set-up, supervision of facility condition and sequence control. It also contributes to prevent operational human errors and consequent accidents. Major functions of the MMIF system are (1) Control of experimental sequence, (2) Conduction of experimental set-up on component devices/facilities, (3) Supervision of status of component devices/facilities. The architecture of platform of the MMIF system is shown in Fig.3. The protocol between the server machine and the sub-systems is limited to TCP/IP, since a variety of computers are utilized for the sub-systems. An experimental information LAN is protected by a firewall from attacks from the backbone network. All manipulation and indication are conducted in human friendly graphical environment on client terminals (a presentation layer). A server manages information between client terminals and control computers for component devices/facilities with a relational database (a transmission and data house layer). It should be here noted that the MMIF system does not dictate directly a device control layer of each control system for component. Examination on a prototype has been continued intensively to demonstrate performance capability and usefulness of the planned MMIF system. Both hirdwares and softwares have been selected from industry standards. Since compatibility in combination of softwares (OS, GUI, RDMS, etc.) determines performance and required labor in development, comparative studies in a prototype are of importance before the start of coding of a real application program.

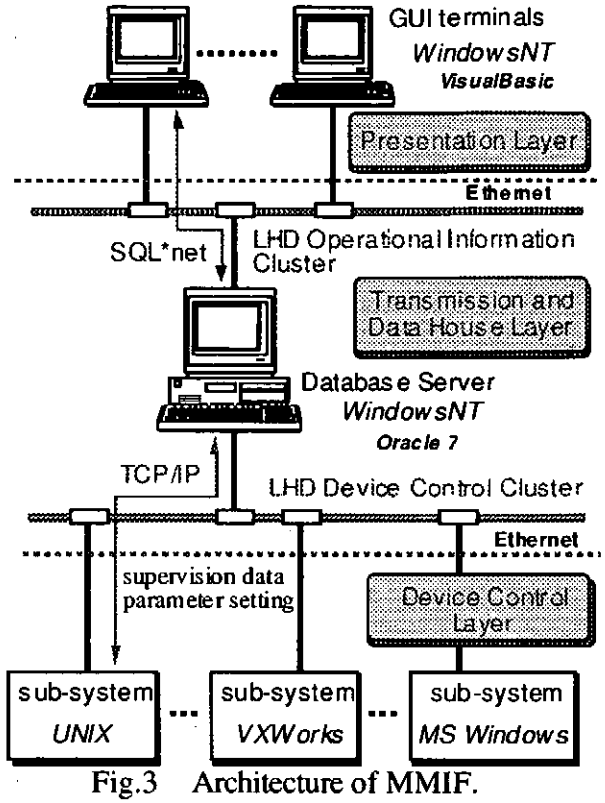

Fig.3 Architecture of MMIF.

LHD EXPERIMENTAL LAN

The LHD operation LAN is one component of the LHD experimental LAN, on which

the information of LHD experiment is transmitted. The LHD experimental LAN consists of three sub-networks (clusters), i.e., operation, analysis and plasma data acquisition clusters. The LHD experimental LAN is designed based on a concept that the data with different purposes are transmitted on a independent cluster in order to transmit the network data reliably and safely, and to control network traffic. The LHD operation cluster composes an operational information LAN, torus device and peripheral devices control LAN's. Information exchange for operation and discharge condition, management of the sequence of experiments and plasma discharges are conducted on these LAN's. In 1995 fiscal year, a backbone part of the LHD operation cluster LAN consisting of FDDI, FDDI-switch, CDDI, Ethernet and Ethernet-switch system has been constructed in the LHD main building and buildings supporting the LHD experiment except for the LHD control building. As concerns the protocol routing and packet bridging, routers in torus device and peripheral devices control LAN's permit only TCP/IP routing and prevent no other protocol packets in order to keep reliability and security of network. On the other hand, in the operational information LAN, various network terminals comparing with the devices operation LANs exist. Therefore NetBEUI and AppleTalk protocol in addition to TCP/IP are applied in the network. In order to keep security of the whole LHD operation LAN clusters, the firewall system which controls security in the level of network application software carefully is employed on the upper network stream side. The test run of these network system from view point of keeping security and traffic control has been started. The rest of LHD operation LAN will be completed another year after the completion of the LHD control building in 1996 fiscal year.

CONCLUSION

Reliable protection of superconducting coils and flexibility for plasma physics experiments are simultaneously prerequisite to the central control system for LHD. The central control system for LHD is based on composition of conservative hard-wired logic and information transmission by client/server system with LAN. Safety interlock, mode transition and experimental sequence are conducted by a programmable logic controller with hird-wired logic. Timing and trigger are provided by a VME system through optical fibers. A man-machine-interface system serves operators for preventing errors with efficient, visual, and comprehensible operation. The LHD operation LAN cluster was designed to guarantee safe and reliable transmission of the LHD experimental information and data of device operation. A part of the LHD operational LAN is completed in the middle of this May. The LAN consists of FDDI switches and Ethernet system. Test run has been started and construct the rest of LHD operational LAN will be completed another year. Fabrication of the central control system has been started and will be completed by the end of 1997.

REFERENCES

[1] O.Motojima et al., Fusion Engr. and Design 20 (1993) 3.
[2] K.Yamazaki et al., Nucl. Instr. and Meth. in Phys. Res. A 352 (1994) 43.

CRYOGENIC CONTROL SYSTEM FOR LHD

T. Mito, S. Satoh, R. Maekawa, S. Yamada, K. Takahata, A. Iwamoto,
H. Yamada, K. Watanabe, T. Baba, S. Moriuchi, T. Oba, H. Sekiguchi,
K. Murai, J. Yamamoto, O. Motojima, LHD Group,
(National Institute for Fusion Science, Oroshi, Toki, Gifu 509-52, Japan)
K. Iimura and K. Nakamura
(Nippon Sanso Corporation, Tsukagoshi, Sawai-ku, Kawasaki 210, Japan)

ABSTRUCT

We have been constructing the cryogenic control system for the Large Helical Device (LHD). The development of a new control system, which is highly flexible and expandable concerning both hardware and software, is crucial for the cryogenic system of the LHD because of fairly complicated cooling schemes. The cryogenic control system consists of workstations, VME (Versa Module Europe) controllers, Local Area Networks (LAN), operating graphic consoles, peripherals and signal terminals. The control system is composed as a duplex system which significantly improves the reliable operation with fault diagnoses of each component. Primarily, the overall control system can be expandable, using standard hardware and operating software. Furthermore the software tool packages are being developed based upon them, which provide us more flexible and easy construction of a control program. These software tool packages have the function of system configuration, easy making of graphic control panels, reporting and programming sequence and loop control.

INTRODUCTION

The Large Helical Device (LHD) is a fully superconducting heliotron type fusion experimental device under construction at the National Institute for Fusion Science (NIFS). The superconducting coils for the LHD consists of two helical coils and three pairs of poloidal coils. The helical coils are cooled by the pool boiling of liquid helium. The poloidal coils are cooled by the forced flow of supercritical helium.

CRYOGENIC SYSTEM FOR THE LHD

The cryogenic system consists of the helium refrigerator/liquefier, the superconducting helical and poloidal coils and the peripheral equipment, such as superconducting bus-lines, control-valve-boxes and cryogenic transfer-lines. The flow diagram of the LHD cryogenic system is shown in Figure 1. The engineering design and construction of the helium refrigerator/liquefier was started in 1992 and was completed at the end of 1994 [1,2]. We have been conducting test operations of the helium refrigerator/liquefier with a dummy heat load to gather data on cooling characteristics of a large-scale cryogenic system. The cooling scheme of the LHD is fairly complicated. It is necessary to construct automatic control system for a safe and reliable operation of the cryogenic system. The control system for the cryogenic system has two features; one is highly reliable system such as a large-scale chemical plant, the other is very delicate and sensitive system such as a laboratory instrument. The development of a new control system, which is highly flexible and expandable concerning both hardware and software, is crucial for the LHD cryogenic system.

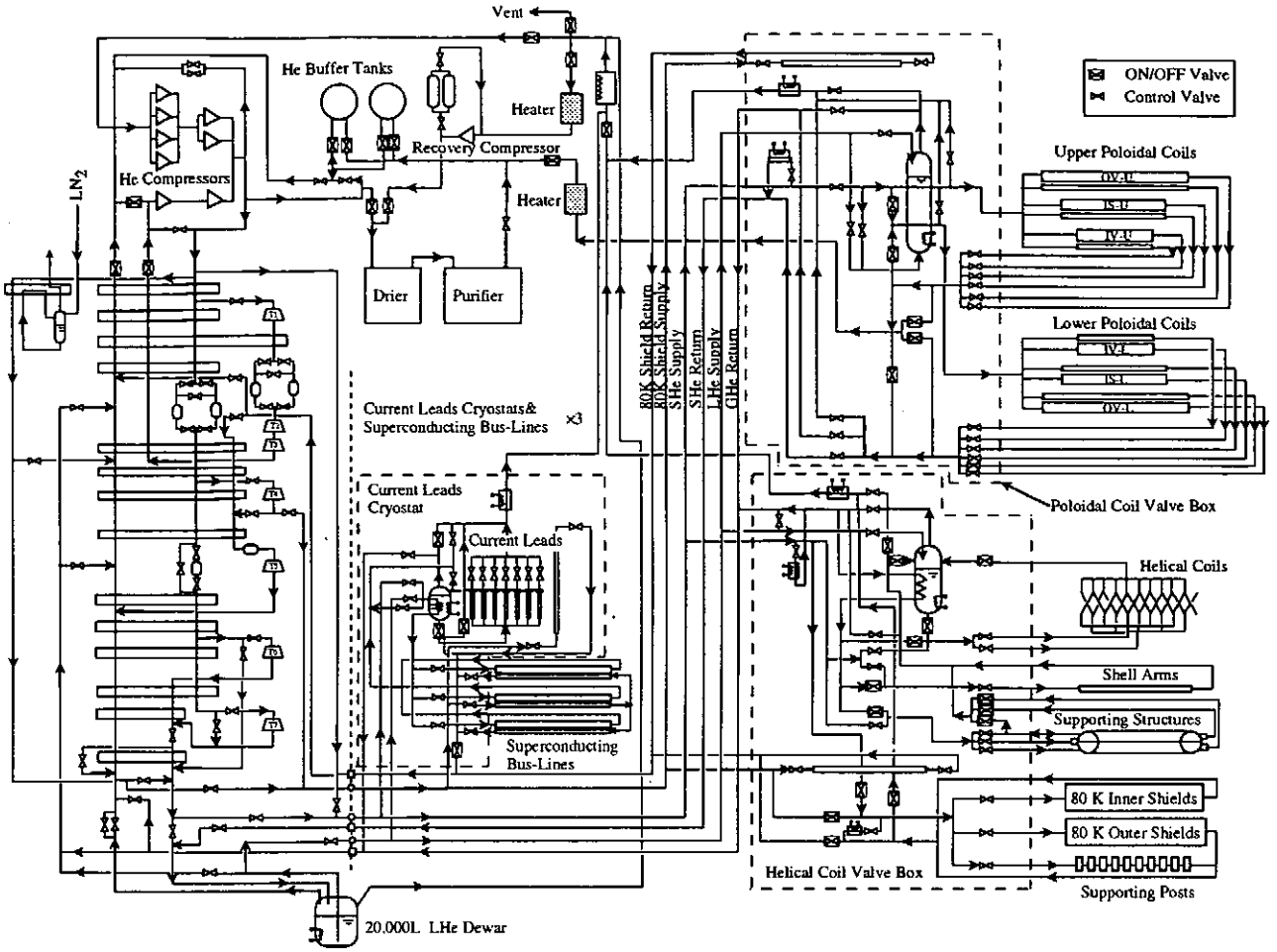

Figure 1. Flow diagram of the LHD cryogenic system

CRYOGENIC CONTROL SYSTEM

System configuration

Figure 2 shows the system configuration of the cryogenic control system. The cryogenic control system consists of workstations, VME (Versa Module Europe) controllers, Local Area Networks (LAN), operating graphic consoles, peripherals and signal terminals.

The work stations are used for making and debugging control programs for VME controllers. Usually, the programming environment of a VME controller is not user-friendly. We can construct control programs easily with the aid of the work stations. The control programs made by the work station are down loaded to the VME controllers and are executed on the VME controllers.

The VME controllers are the main control parts of this control system in which the real-time control programs are running. The VME controllers consists of CPU boards, analogue input/output boards, digital input/output board, network communication boards and reflective memory boards. These boards perform their duties; 1) data acquisition from various sensors of the cryogenic system such as pressure gauges, flow meters, temperature sensors, level meters, etc., 2) data conversion from voltage signals to engineering values and execution of sequential and loop control programs, 3) control operation for control valves, ON/OFF valves, heaters, compressors, etc., 4) communication with the work station and the operating graphic consoles, 5) equalization of control data between the VME controllers.

The LAN connects each component of the control system for data communication, remote operation, file transmission, data output to the printers, etc. The optical duplex link type LAN, which is compatible with Ethernet, is used for high reliability because the LAN is a lifeline of

this control system. TCP/IP and UDP/IP, which are world standard like Ethernet, are used as protocol. They are versatile communication protocol not only for a work station but also for a personal computer, and are utilized in various fields. These features make it easy to integrate this cryogenic control system to the other system such as the central control system.

The operating graphic consoles are man-machine interface hardware by which we can operate and monitor the cryogenic system. Same function could be done by a work station. However the refreshing speed of a display is not so fast as that of the operating graphic console. The operating graphic console, which is an exclusive machine for the plant operation, consists of CRT, keyboards and CPU board computers supporting VME bus communication. The peripherals are a hard-copy for the operating graphic consoles, a line printer for alarm and event logging, laser printers for data output and X-terminals and personal computers for monitoring and data management. The signal terminals are sets of signal conditioners and relay terminals to unify level and kind of input/output signals.

The control system is based on what is called 'open system'. The operating system of workstations and VME controllers are the UNIX and the Vxworks, respectively. Primarily, the overall control system can be expandable, using standard hardware and operating software.

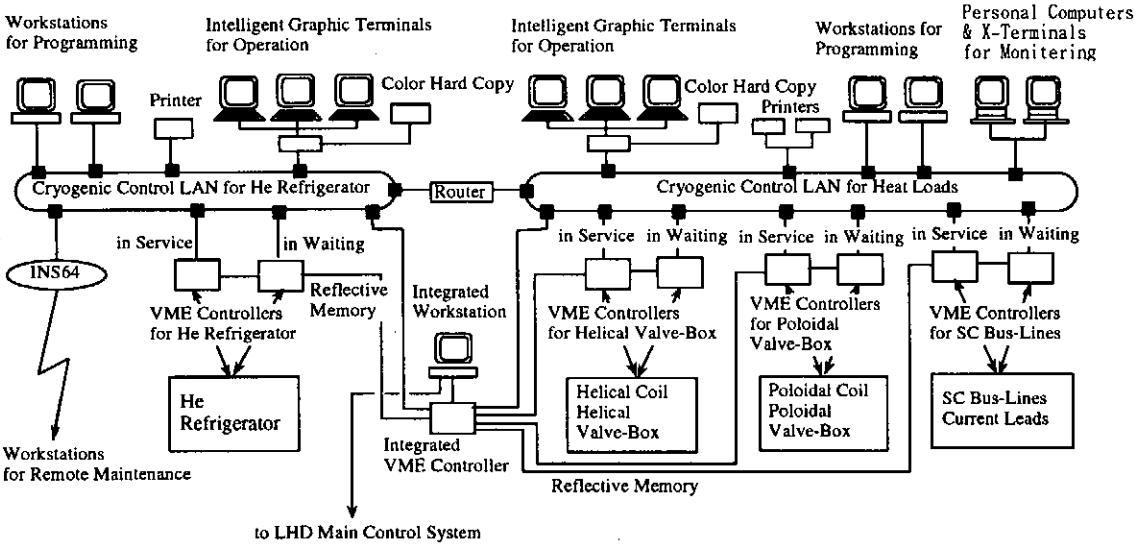

Figure 2. Cryogenic control system for the LHD.

Redundancy system

The control system is composed as a duplex system which significantly improves the reliable operation with fault diagnoses of each component. The VME controllers are used as a pair of one in service and the other in waiting. Two VME controllers in service and in waiting are identical in both hardware and software configuration. In case the VME controller in service has trouble, the service is instantly switched over to the VME controller in waiting.

The work stations are also duplicated and can be switched over from the master work station to the back-up work station when there are any failures. The LAN is duplex and link type, which is protected from the interruption of communication even when the lines are down out in two positions at the same time.

Figure 3 shows typical case of the failures. Usually, the master work station communicates with the VME controller in service as shown in Figure 3a. There are failures on the master work station and the VME controller in service and two lines of the LAN are also cut off. The work station is switched over to the back-up one, the VME is switched to one in waiting and the LAN continues its communication with loop back as shown in Figure 3b.

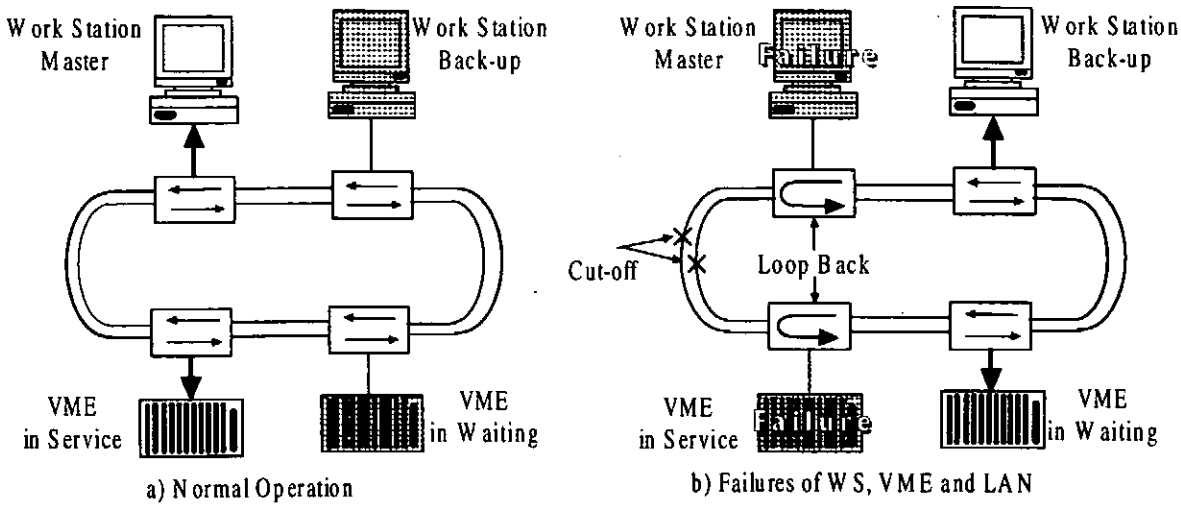

Figure 3. Duplex control system; a) in normal operation, b) in failure.

Software configuration

Furthermore the software tool packages are being developed based upon the hardware and software configuration mentioned above, which provide us more flexible and easy construction of a control program. These software tool packages have the function of system configuration, easy making of graphic control panels, reporting and programming sequential control and loop control. The development of the control program can be done on the work station with no disturbance on the actual real-time control of the VME controller. The completed program is down loaded to the VME controller from the work station. In case of the modification of the control program on the VME controllers, however, there is no necessity to stop the running program on the VME controllers. This is important feature for the cryogenic system because the cryogenic system cannot be reset to the initial state easily. Therefore we can revise the control programs continuing the operation of the cryogenic system.

CONCLUSION

The development of a new control system is crucial for the cryogenic system because of fairly complicated cooling scheme of the LHD. The control system must be highly reliable and flexible to handle a delicate cryogenic system. The control system is based on open system and consists of work stations, VME controllers, LAN and operating graphic consoles, etc. The control system is composed as a duplex system which significantly improves the reliable operation with fault diagnoses of each component. The fault diagnoses of the VME controllers are now limited to the CPU and communication boards. However we will extend them to every board including analogue input/output boards and digital input/output boards. Based on above cryogenic control system, the overall operating scenario of the cryogenic control system; such as, a cool-down, a steady-state operation, a warm-up, a power failure and a coil quench, are being considered to develop a fully automatic control program for the LHD cryogenic system.

REFERENCES

1. Satoh, S. et al. Construction of a 10 kW Class Helium Cryogenic System for the Large Helical Device Cryogenics (1994) 34 95-98.
2. Satoh, S. et al. Construction and Commissioning Tests of a 10 kW Class Helium Refrigerator for the Large Helical Device presented at CEC/ICMC 1995 to be published in 41 Advances in Cryogenic Engineering.

Test operation of the Helium Refrigeration System with a Dummy Heat Load Apparatus

R. Maekawa, T. Mito, S. Yamada, S. Satoh, A. Iwamoto, T. Baba, S. Moriuchi, K. Ohba, H. Sekiguchi, I. Ohtake, H. Yamada, J. Yamamoto, O. Motojima and LHD Group
National Institute for Fusion Science, Toki, Gifu 509-52, JAPAN

K. Chida and T. Fukano
Nippon Sanso Corp., 6-2 Kojima, Kawasaki, Kanagawa 210, JAPAN

ABSTRACT

A dummy heat load experimental apparatus has been developed to establish a full-automatic operating scenario of the helium refrigeration system for the Large Helical Device (LHD). The apparatus primarily consists of a forced-flow low temperature helium line, a liquid helium supply line and a liquid helium bath. The design philosophy of apparatus is to simulate two dominant cooling schemes of the LHD: pool-boiling and a forced-flow supercritical helium. Mass flow rates can be controlled by control valves adjusted with electro-pneumatic actuators. A process control computer system was used for data acquisition, valve control and a PID control of liquid helium in the bath. Experiment were conducted under steady state condition with heat inputs from two heaters which induce unbalanced operating condition to the refrigeration system.

INTRODUCTION

The National Institute for Fusion Science is developing a large heliotron/torsatron type experimental fusion apparatus, Large Helical Device (LHD), to study currentless, steady state toroidal plasmas. The LHD has two types of superconducting coils; a pair of pool-boiling helical coils and three sets of forced-flow poloidal coils. Reliable and safe operation of superconducting coils is essential to provide successful operation of the LHD. A 10 kW class helium refrigerator/liquefier has been developed to satisfy all refrigeration requirements for the LHD. Various design aspects of the refrigeration system and the test operation results have been reported.[1] However, it is still essential for the refrigeration system to test its capability under variable heat inputs. The present paper will describe a test operation of the system with a dummy load apparatus.

EXPERIMENTAL DESCRIPTION

1. EXPERIMENTAL APPARATUS

A dummy heat load experimental apparatus is developed to test a refrigeration system of the LHD. As shown in Figure 1, the apparatus consists of a supercritical helium (SHe) line, a liquid helium (LHe) filling line, a gaseous helium (GHe) return line. Each line is connected to the refrigeration system via a joint box. Approximately 40 m long 0.55 m diameter transfer line (TRT-2) attached the joint box with a cold box of the refrigeration system. The SHe line is connected to an outlet of the turbine #6 and #7, while the LHe-fill line is connected to the 20,000 liter liquid helium reservoir. The GHe return line eventually reaches at a suction side of compressors. The apparatus was mounted to a 3m long, 200 mm diameter cryostat which has a liquid nitrogen shield. Fig. 2 shows flow diagram of a cold box of the refrigeration system as well as a dummy-load apparatus.

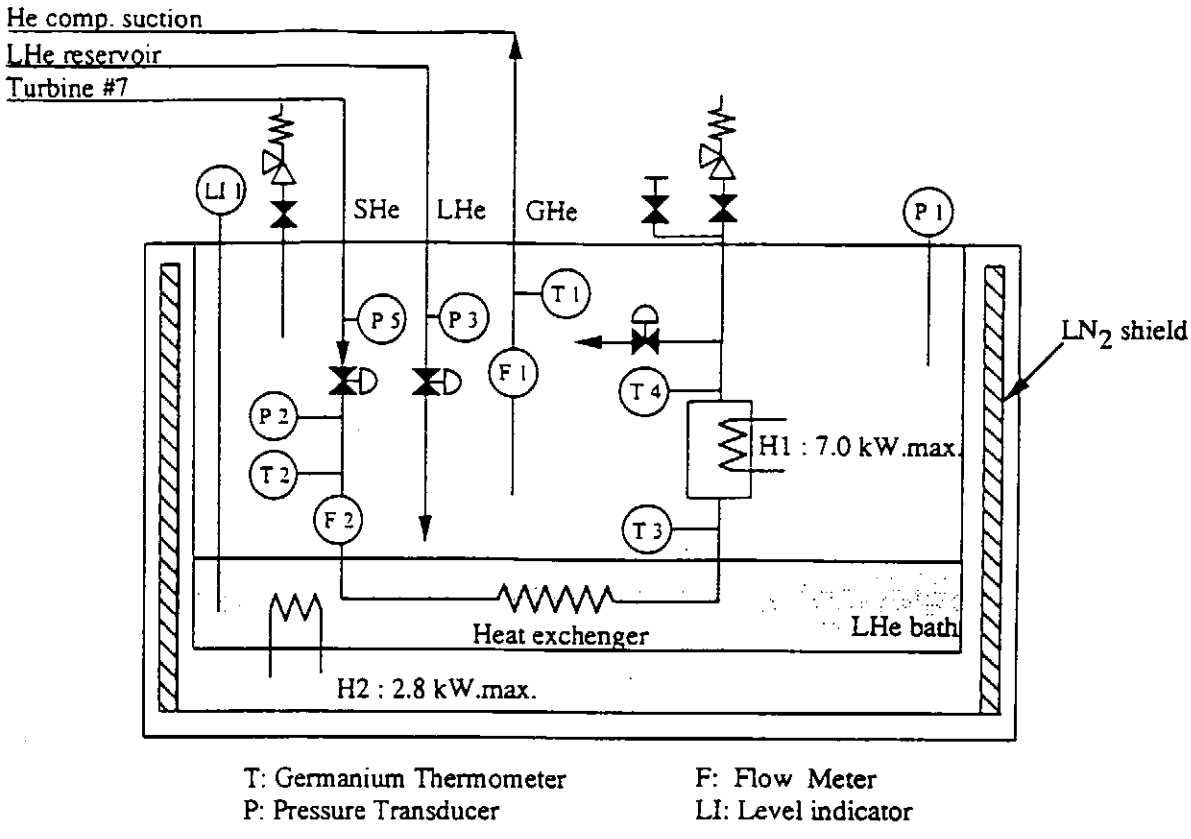

Figure 1. Dummy load experimental apparatus.

Two orifice flow meters are used to measure mass flow rates of supercritical helium and gaseous helium, respectively. Germanium resistance thermometers (GRTs) and absolute pressure transducers are used to estimate thermophysical properties of low temperature helium. Since all apparatus is in just above the atmospheric pressure environment, thermometry of fluids is crucial. To avoid any influence from surrounding, a 4.7 mm diameter hole was drilled through the line and a copper tube was silver soldered in it. A GRT was placed in the copper tube with crycon grease to ensure thermal contact between them. Leads wires of the GRT were wound around the line and fixed with a Teflon tape for an additional heat sink as well as protection. Both differential and absolute pressure transducers are located at room temperature, 0.32 mm stainless steel capillary tube connect between transducers and lines. A bath pressure is used to estimate properties of the helium gas. A 2.8 kW heater was also immersed in the liquid helium bath for a heat load.

A process control computer system, CENTUM, was used to control electro-pneumatic actuators and heaters as well as for data acquisition system. CENTUM basically consists of a operator's console, a field console station. Both process control commands and data acquisition performed from the console to the apparatus via the control station or vise versa. One of the versatile feature of CENTUM is ability set up various PID controls with corresponding sequence program. Two types of PID controls were used to adjust LHe level in the bath as well as to regulate mass flow rate of SHe with a control valve. Communications from CENTUM to the apparatus is performed with one second period. Therefore, the process operation/data acquisition can be considered as continuous.

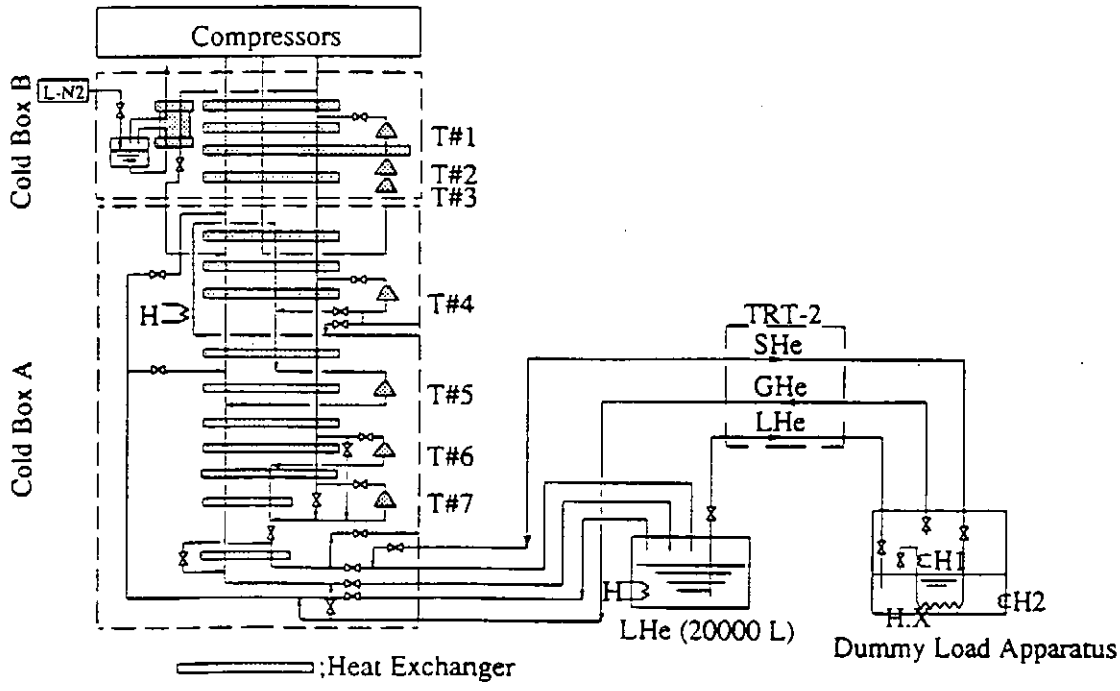

Figure 2. Schematic of a flow diagram.

2. EXPERIMENTAL PROCEDURE

Primarily two types of refrigeration scenario can be established with the apparatus; precooling mode and steady state mode. For a precooling mode, simulating precooling of poloidal coils, supercritical helium is the only refrigerant to the apparatus so that no liquid helium is in the bath. The experiment was focused on 15K level refrigeration condition since turbines have to provide maximum work to maintain the condition. The heat input to the supercritical helium line was set at 7.0 kW. For steady-state mode, a total heat input to the refrigeration system is approximately 1/3 of the LHD under steady state operating condition. Thus, the mode requires approximately 1/3 of total refrigeration capacity. Mass flow rates of liquid helium and supercritical helium are set at about 120 g/s and 100 g/s, respectively. Heat inputs are 1.3 kW for the bath and 1.6 kW for the supercritical helium line. In this case, mass flow rate of gaseous helium return is balanced with those of liquid helium and supercritical helium.

RESULTS AND DISCUSSION

Figure 3 shows a result of dummy heat load experiment conducted on March 28, 1996. Three types of refrigeration schemes were tested and maintained until the steady-state condition was established. N.H. denotes no heat input to the LHe bath. This mode was operated to confirm overall system. Following the N.H. operation, two refrigeration modes were simulated. For S.S mode, mass flow rates of gas helium were not fully stabilized since the LHe level in the bath was controlled under a PID-control coupled with a heater #2 (H2). The fluctuation in the mass flow rate is proportional to the heater power. Absolute pressures of LHe and GHe lines are also plotted, which was stabilized after 20 min. of operation. The PID-control was then turned-off to proceed the E.H (extra-heat-input) mode. The system reached at steady state condition after 5 min. Any fluctuation of the system was not observed. The mode was maintained about 10 min. because of time constrain.

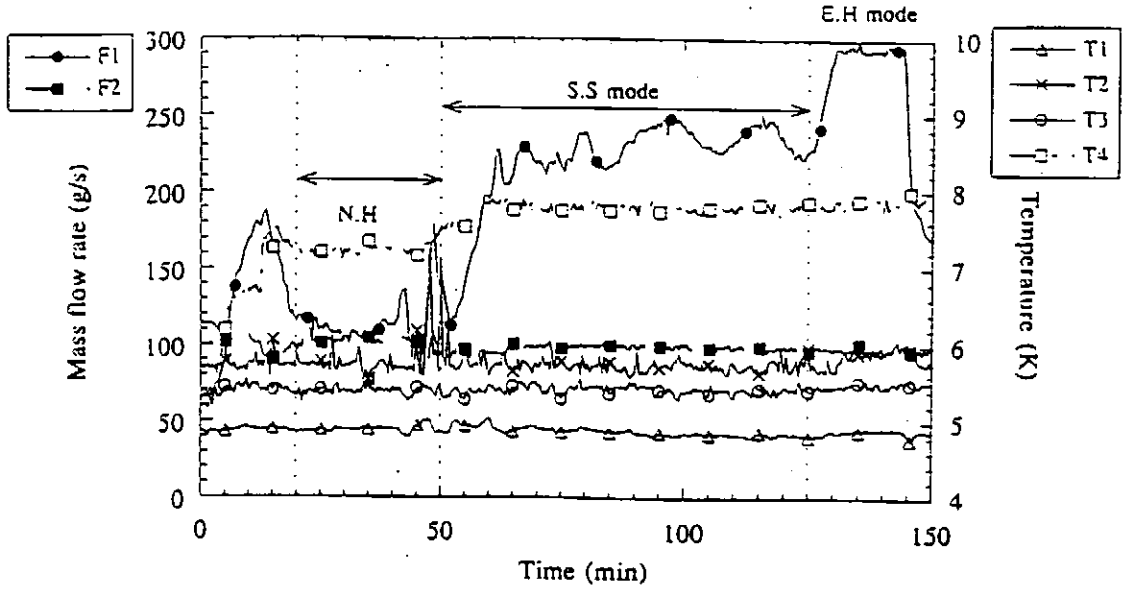

Figure 3. Experimental result of two refrigeration modes.

CONCLUSION

The helium refrigeration system was operated with three refrigeration modes under steady-state condition. It was confirmed that the refrigeration system maintain reliable operation with a dummy load apparatus. However, the system was not fully satisfied its full-automatic operating mode. In other words, control valves of the refrigerator/liquefier are required some adjustment by an operator while operating with various refrigeration modes. Additional experiments are still necessary to establish full-automatic condition of the refrigeration system.

REFERENCE

1. S. Sato *et al.* "A 10kW class helium refrigeration system for the LHD", presented at CEC in Columbus, 1996.

Quench Analysis for the Helical Coils of the Large Helical Device

N. Yanagi*, S. Imagawa*, S. Takács*,**, H. Chikaraishi*, T. Mito*,
K. Takahata*, T. Satow*, J. Yamamoto*, O. Motojima*and LHD Group

*National Institute for Fusion Science, Toki, Gifu 509-52, Japan
**Institute of Electrical Engineering, Slovak Academy of Sciences, 842 39 Bratislava, Slovakia

ABSTRACT
The discharging process after a quench is analyzed for the helical coils of the Large Helical Device. The heat generation due to the AC losses during the field decay as well as due to the joule heating of the propagating normal zones is calculated using the measured time constants for the coupling currents and the normal resistivity of the superconductor. The consumption of the liquid helium is evaluated and the temperature rise of the coil windings is examined after the total amount of the liquid helium is lost from the helical coil cans.

INTRODUCTION

The Large Helical Device (LHD) is a toroidal fusion experimental device which is now under construction with all superconducting coil systems [1]. The two helical coils have the major radius of 3.9 m and the average minor radius of 0.975 m with the poloidal pole number 2 and the toroidal pitch number 10. A schematic bird's-eye view of the helical coils is shown in Fig. 1.

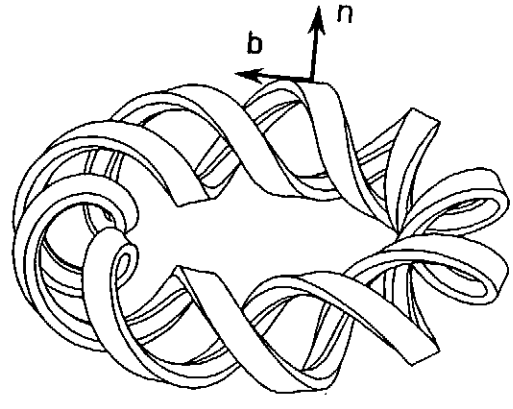

Figure 1 Schematic bird's-eye view of the helical coils. The normal and the binormal directions to the coil windings are shown by the arrows.

The pool cooled helical coils will be immersed in the liquid helium of 4.4 K in the Phase I operation condition of LHD and will generate a heliotron magnetic configuration with the central toroidal field of 3 T. Composite-type superconductors with NbTi/Cu compacted strands and pure aluminum and copper stabilizers are used with the nominal current of 13.0 kA [2]. Superfluid helium will be later utilized in the Phase II operation condition at the reduced temperature of 1.8 K in order to raise the field up to 4 T with the nominal current of 17.3 kA. The on-site winding process of the helical coils (900 turns, 35 km) has been successfully completed in May, 1996.
Since the helical coils will possess a large amount of magnetic stored energy (up to 1.6 GJ in the Phase II operation mode), it is very important to extract their energy quickly and safely in case of a quench. In this report, the heat release and the temperature rise of the winding conductors are analyzed during the discharging process after a quench of the helical coils by taking account of the AC losses due to the field decay as well as the joule heating in the propagating normal zones.

ANALYSIS PROCEDURE

In the present analysis, once a normal zone is initiated, it is assumed to propagate along the conductor with a velocity of 100 m/sec. This value is much larger than the experimentally measured propagation velocity of the normal zones since the superconductor satisfies the full stabilization condition. However, this may correspond to a rough simulation including turn-to-turn and/or layer-to-layer propagations of the normal zones, which might occur in the real helical coils with tight cooling channels. The experimentally measured normal resistivity of the conductor is used to give the temperature dependent joule heating power.
One of the characteristic features of the pool-cooled helical coil windings, being optimized for DC operations, is their fairly large AC losses [3] during the field decay due to the strong inter-strand coupling in the superconducting cables. Since the evaluation of the precise AC loss power is rather difficult for the helical coils which have complicated structures, here we restrict ourselves to a simple calculation which deals only with the volume averaged power density within the whole conductors, expressed as [4]

$$\langle P_{AC} \rangle (t) = \alpha(T_{cond}) \frac{2}{\mu_0} \left\{ \tau_n \langle B_n \rangle^2 \left(\frac{e^{-t/\tau_n} - e^{-t/\tau_0}}{\tau_0 - \tau_n} \right)^2 + \tau_b \langle B_b \rangle^2 \left(\frac{e^{-t/\tau_b} - e^{-t/\tau_0}}{\tau_0 - \tau_b} \right)^2 \right\} \quad (1)$$

where B_n and B_b denote the magnetic field before the discharge, defined in a plane perpendicular to the winding direction of the helical coil; B_n is parallel to the minor radial direction and B_b is perpendicular to B_n, as indicated in Fig. 1. In Eq. (1), τ_0 is the time constant for an exponential field decay and τ_n and τ_b are the time constants for the

coupling currents in the superconductor which have been experimentally measured for short samples [4]. Since the AC loss power must be drastically reduced when the conductors become normal, the coefficient $\alpha(T_{cond})$ is assumed to be 1.0 for T_{cond} < 10 K and 0.1 for > 10 K, where T_{cond} is the temperature of the superconductor.
In the early stage of a discharge, the consumption of the liquid helium is taken into account for dissipating the heat generation in the windings. If the total liquid helium is lost from the helical coil cans, the released energy will be dissipated by raising the temperature of the coil windings as well as of the surrounding helium gas. The temperature rise of the windings is calculated by solving the time-dependent power balance equation in which the rate of the enthalpy increase of the conductor should be balanced with the power density of the released heat due to the AC losses and to the joule heating. After the coil temperature exceeds the sharing temperature for the transport current, the whole conductors are assumed to have transitions into the normal state, and the temperature rise becomes rapid due to the strong joule heating.

RESULTS OF THE ANALYSIS

The discharging of the helical coils will be conducted using a specially developed circuit with fuses and dump resistors [5], which provides the time constants of τ_0 = 20 s and/or 300 s for the exponential current decays. The 20-s discharge will be mainly used in case of a quench whereas the 300-s discharge will be used for the fast ramp down during the power fault with reduced AC loss generation. After a quench is detected, one second has to be waited in order to extinguish the high temperature plasma confined in the vacuum vessel for preventing the generation of runaway electrons accelerated by the loop voltage.

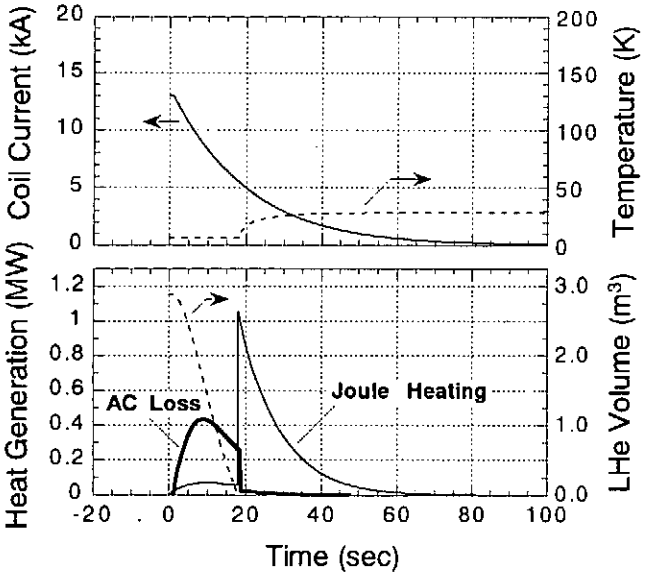

Figure 2 Temporal evolution of the discharging process of the helical coil windings with τ_0 = 20 s after a quench. The coil current, the conductor temperature, the power generation and the volume of the liquid helium left in the helical coil cans are shown.

Figure 2 shows the numerically calculated temporal evolution of a discharging process of the helical coil windings with τ_0 = 20 s after a normal transition from the transport current of 13.0 kA in the 3 T operation mode. The parameters used here are B_n = 3.4 T, B_b = 3.8 T, τ_n = 4.34 s and τ_b = 0.47 s. In this case, the total amount of the liquid helium contained in the helical coil cans (~ 2.9 m^3) is lost in 20 s due to the large AC loss, and the vaporized helium gas should be released from the safety valves. Thereafter, the whole windings have transitions into the normal state and the conductor temperature reaches up to ~ 30 K at the end of the discharge.
It should be noted that in case of the discharge with τ_0 = 300 s without a quench, about 10 % of the total liquid helium is vaporized, which can be recovered with the normal operation of the refrigeration system.

CONCLUSION

The discharging process after a quench is analyzed for the helical coils of the Large Helical Device by taking account of the heat generation due to the AC loss and the joule heating. A simple numerical calculation with a volume averaged heat generation shows that the total amount of the liquid helium will be vaporized during the discharge with the time constant of 20 s and the coil temperature will reach up to 30 K in the Phase I operation of LHD.
More precise calculations will have to be carried out by taking into account the three dimensional structures of the helical coils, the heat transfer from the conductor surface to the liquid helium and the temperature dependence of the critical currents in the coils.

ACKNOWLEDGMENTS

The authors appreciate the fruitful discussions with many staffs in the LHD group.

REFERENCES

1 Motojima, O., Akaishi, K., Fujii, K., et al., Physics and engineering design studies on the Large Helical Device, Fusion Eng. Des. (1993) 20 3-14
2 Yanagi, N., Mito, T., Imagawa, S., et al., Development, fabrication, testing and joints of aluminum stabilized superconductors for the helical coils of LHD, ICEC16 (1996) PS3-e2-37
3 Sumiyoshi, F., Kawabata, S., Fukushima, K., et al., Transverse-field losses in aluminum-stabilized superconducting conductors, IEEE Trans. Mag. (1994) 30 2491-2494
4 Wilson, M. N., Superconducting Magnets, Oxford University Press (1983)
5 Yanagi, N., Takács, S., Mito, T., et al., Measurement of time constants for coupling losses in the LHD superconductors, ICEC16 (1996) PS3-e2-24
6 Tanahashi, S., Satoh, T., Morimoto, S., et al., Design study of power supplies for LHD superconducting magnets, Fusion Eng. Des. (1993) 20 107-111

Operations Experience in Cryogenic Measurement Techniques and Process Control During Testing S.C. Magnets at the FZK TOSKA Facility

M. Süßer
Forschungszentrum Karlsruhe, Institut für Technische Physik, Postfach 3640, D-76021 Karlsruhe, Germany

ABSTRACT

This paper gives a description of operations experience gained during the testing of the POLO coil at FZK/ITP Karlsruhe. For the first time, supercritically cooled current leads were successfully operated for more than 4000 hours. A proposal to optimize the mass flow for the current leads is discussed and experience with two phase cooling circuits is presented.

INTRODUCTION

During the last decade, useful investigations in connection with large s.c. fusion magnets have been carried out in the FZK TOSKA facility. Reliable cryogenic measurements devices and techniques for process control, especially for the operation of the isothermal two-phase forced-flow-cooling loop of the FZK Poloidal Field Coil (POLO) [1] and for cooling the 30 kA/23 kV current leads were needed. For the first time, forced-flow-cooled current leads connected to a s.c. magnet were successfully operated up to 24 kA.

OPERATIONS EXPERIENCE WITH SUPERCRITICALLY COOLED CURRENT LEADS

The cooling power consumed by the current leads (c.l.) makes up a great portion of the overall cooling power needed for a superconducting magnet system. It is an indispensible task to reduce the power consumption to a minimum, without an impact on the safety and reliability of the system. In comparison to a bath cooling system with a self-regulating cooling mode, the mass flow through the c.l. has to be adjusted by a control system responding to various input parameters (e.g. current, temperature). Since a Nb_3Sn-insert is used in the lower part of the FZK c.l., much

more care must also be taken regarding the superconducting state of the insert.

Figure 1 shows the design parameters of the c.l. [2] used during the test of the POLO coil.

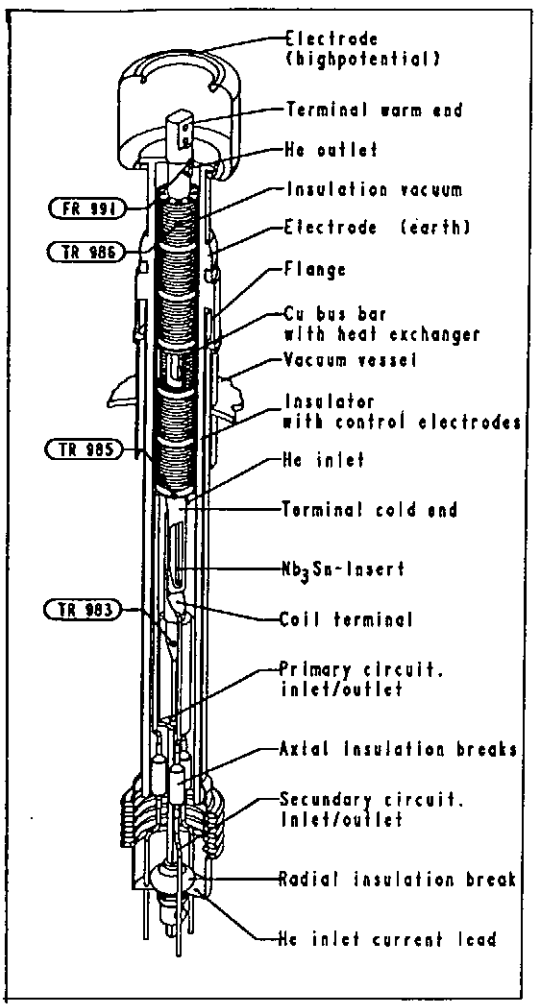

Figure 1 Current lead

Table 1: Main parameters of the current lead

Maximum current	30 kA
Nominal insulation voltage	23 kV
Helium mass flow rate for zero current	0.3 g/s
Helium mass flow rate for 15 - 30 kA	0.055 - 0.63 g/skA
Total length	2.77 m
Heat exchanger length	2.05 m
Conductor cross section	38.5 cm^2
Residual resistivity ratio of Cu-conductor	5

Figures 2 - 3 show the mass flow through the heat exchanger and the temperature in the lower part of the c.l. during 24 kA operation. The chosen mass flow was higher than the nominal flow. The reasons were: safety margin against temperature fluctuations during the fast ramping of the coil (Fig. 3), occasionally unexpected temperature fluctuations of about 2 - 3 K during stable current operation (TR 985), the temperature uncertainty at the end of the Nb_3Sn-insert, lack of optimization of the mass flow control parameters, temperature rise in the top of the c.l.

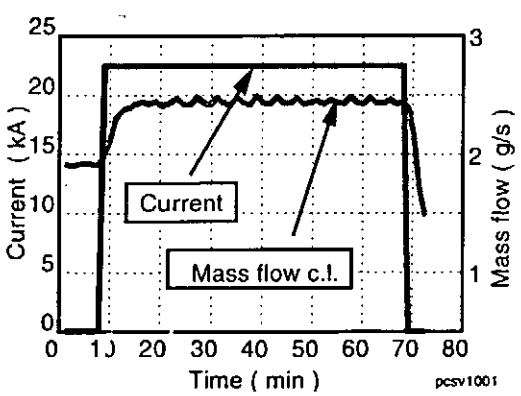

Figure 2 Current and mass flow

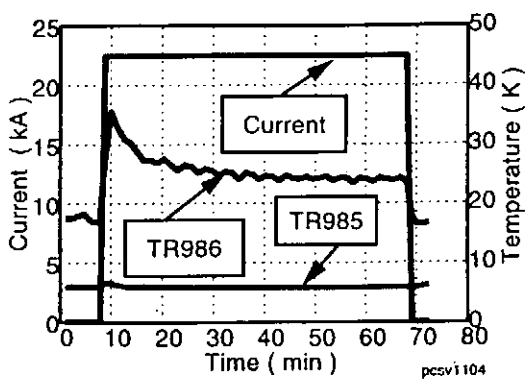

Figure 3 Current and temperature TR 985, TR 986

For safe and economical operation of supercritically cooled c.l. it seems to be necessary to take the following parameters into account:

- level of electrical current
- temperature and temperature variations of the coolant at various locations along the c.l., e.g. entrance of the c.l., copper conductor at the entrance of the heat exchanger and at the top and bottom of the Nb_3Sn-insert.
- voltage drop and voltage variations across the Nb_3-Sn-insert and the copper conductor
- pressure drop and pressure oscillations.

The above mentioned statement necessitates the use of a finely tuned system which adapts the mass flow to the operation parameter (current) and the control parameters (temperature, voltage drop, etc.). This needs a more sophisticated system, for example, a fuzzy controller, to satisfy these requirements.

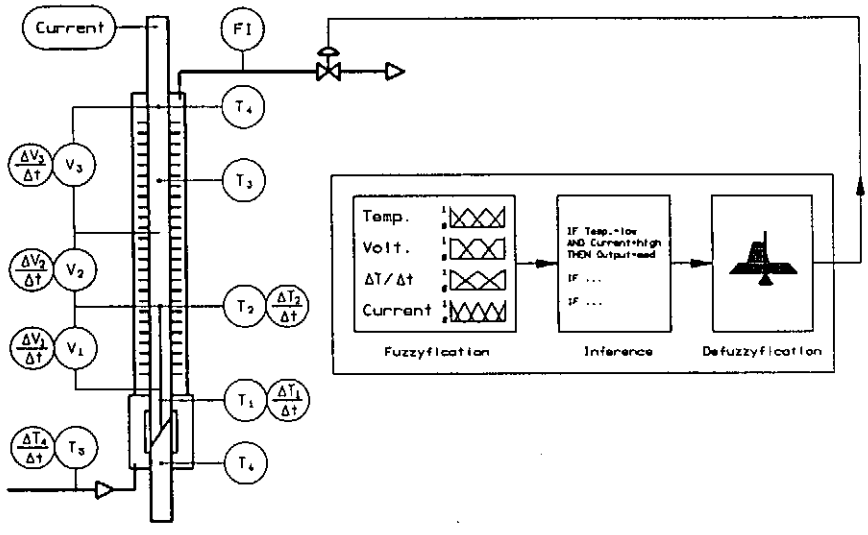

Figure 4 Fuzzy controller system

EXPERIENCE WITH THE TWO PHASE FLOW SYSTEM

The unique feature of the cryogenic cooling system (Fig. 5) for the POLO coil is the use of a dual cooling system. The two phase helium in the center tube removes the heat at constant temperature, while stagnant supercritical helium in the annular space surrounding the cable guarantees well defined heat transfer conditions for good stabilization against sudden, short heat pulses. The two phase flow was controlled by the controllers FIC820, FIC840, FIC860, FIC880 installed at the entrance to each pancake. To detect the vapor content at the outlet of each pancake, a measurement system [3] was installed. The optimized mass flow to insure the stability of each pancake was about 2 g/s and the pressure drop about 5 - 10 mbar over a length of 140 m.

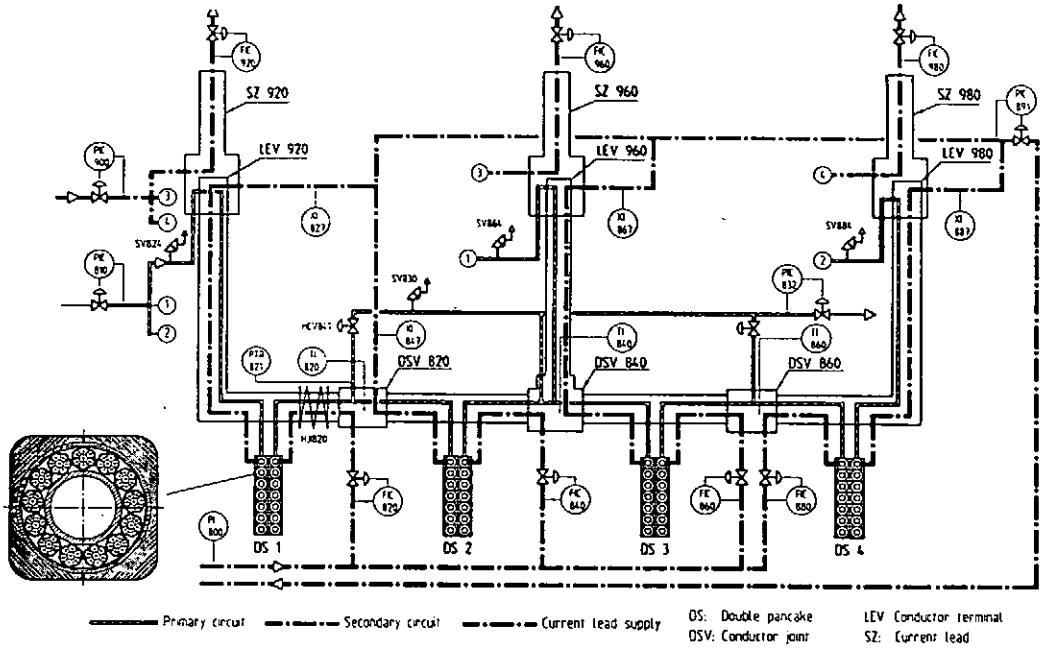

Figure 5 The cooling circuits of the POLO-coil

Very large pressure fluctuations in the two-phase cooling circuits occured sometimes, particularily during operation with the piston pump. The trigger for these fluctuactions could be: a change of the operation by throttling the mass flow control valve (Fig. 6), charging of the supercritical cooling circuit, or changing the mass flow through the current leads (Fig. 7).

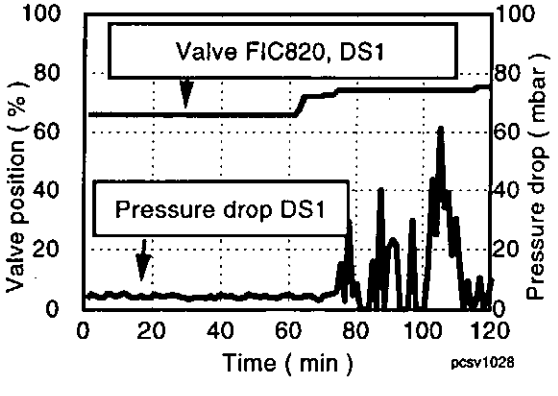

Figure 6 Pressure fluctuation caused by change of control valve position

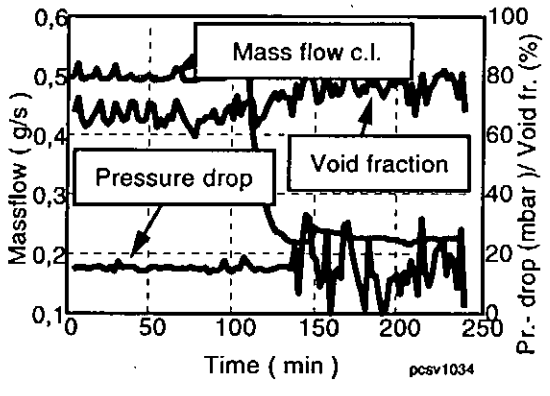

Figure 7 Pressure fluctuation DS1 caused by changing the mass flow through the current leads

REFERENCES

1 Herz, A. et al., The operation experience with the POLO coil dual cooling system (two phase-supercritical He), ICEC 16

2 Heller, R. et al., Test of a forced-flow cooled 30 kA/23 kA current lead for the POLO model coil, IEEE Transactions on magnetics (1994) 30 No. 4

3 Katheder, H. and Süßer, M., Measurement device with cold oscillator for measuring vapour content in helium two phase flow, Cryogenics (1991)

Construction and Operation of 10 kW Class Helium Refrigerator for LHD

Sadao Satoh, Toshiyuki Mito, Shuichi Yamada, Akifumi Iwamoto,
Ryuuji Maekawa, Sadatomo Moriuchi, Tomosumi Baba, Kouki Ooba,
Haruo Sekiguchi, Junya Yamamoto, Osamu Motojima and LHD Group

National Institute for Fusion Science,Nagoya 464-01,Japan

A 10 kW class helium refrigerator has been constructed for LHD at National Institute for Fusion Science. In the previous papers, the authors have reported about its design, shop test results on its key components and on-site performance measurement. During the last twelve months between 1995 and 1996, the refrigerator has been put to the training operations without connecting to any of the superconducting magnets of LHD. As one of its series report, the paper reviews on significant events and major observations which were experienced during that period and makes a brief discussion about several interesting topics on preliminary base.

INTRODUCTION

The Large Helical Device (LHD) is a heliotron fusion experimental device in which magnetic fields are controlled exclusively by superconducting magnets: a pair of helical coils and three pairs of poloidal coils. The helium refrigerator in the LHD cryogenic system has a design capacity of 5700 W refrigeration at 4.4 K, plus 650 L/h liquefaction and 20600 W refrigeration between 40 and 80 K. This combined capacity amounts to be the largest refrigerator ever made in Japan. The contract was signed in July 1992 and the construction at the site (Toki-city, Japan) was completed at the end of FY 1994. Subsequently a series of commissioning runs was made and various performances were obtained with a stand-alone mode of the refrigerator. In the previous papers [1,2], the authors have reported about its design, shop test results on some key components and the on-site refrigerator performance measurement. During the last twelve months between 1995 and 1996, the refrigerator is connected to a "dummy" heat load simulator which can partially simulate LHD heat load and so far four stand-alone runs and two combined runs with dummy heat load have been performed. Every run contains liquefaction and gas recovering back into gas strages and therefore each run took more than one hundred continual operation hours. The paper reviews several significant events experienced and major observations during the period and makes a brief discussion about several interesting topics on preliminary base.

Table 1 Operation Record of LHD Refrigerator (March 1995-April 1996)

Date	Calender	Date	Calender
14-March-1995	Application for Official's	2~6-Oct.-'95	Manual Operation By NIFS
	COMPLETION INSPECTION	8-Nov.-'95	3 Turbine Operation By Vender
24-March-'95	COMPLETION INSPECTION	22-Jan.~9-Feb.-'96	C Box SAFETY INSPECTION
23-April -'95	Manual Operation,	19~23-Feb.-'96	Sift Organizing and Job Training
	Capacity Measurement	26~27-Feb.-'96	Auto. Switch Ope.Test from Master
22~26-May -'95	Automatic Operation		to Slave VME
12~18-June-'95	Tuning Operation		Connect Dummy Heater Cryostat
19~23-June-'95	Operator Training Operation	25~29-March-'96	#1 Combined Ope. with Dummy
4-Aug.-'95	Compressors Turning for 24 Hr	15~19-April-'96	#2 Combined Ope. with Dummy
27-Sep.-'95	C.E. SAFETY INSPECTION		

CONSTRUCTION AND OPERATION RECORD

A refrigerator operation calender is shown in Table 1. In Japan, there is a national code and standard for equipments producing and handling high pressure gas. It is required for any equipment to be inspected by officials and the equipment user must obtain a permission before starting his operation management. Therefore, a date of COMPLETION INSPECTION, March 24th 1995, indicates a completion of hardware construction. Before that date each of the helium compressors was accumulated 95 hours of running time. One month later the first refrigerator operation was made by manual control for 4 days. Automatic control operation was made for 5 days and emergency shut-down from full refrigeration run was also confirmed by the NIFS witnesses. Those were basically the manufactures trial and tuning runs. A commissioning run to confirm the rated capacity was made for 12 days from June 12th. The run of the latter week was dedicated to the hands-on training and demonstration to the NIFS operators. After one day compressor turning run and the first annual and official inspection for safety and security control were made, the first refrigeration run only by owner's operator was made for 5 days beginning from 2 October. However, supervising engineers were chartered from the manufacturer. One day turbine turning was conducted in November for load re-tuning of No.1 turbine brake circuit. Up to now the refrigerator ran as a stand-alone mode of operation which means a run with a mere combination of refrigerator and a 20000 liter liquid helium storage that has a built-in electrical heater. The accumulated compressor running hour was close to 770 h.

In the meantime a "dummy" heat load simulator was constructed and connected to one end of the transfer tube, TRT-2, which contains 5 cryogenic lines inside of 550 mm dia., 50 m long, vacuum insulated and radiation heat shielded duct. The purpose of the dummy heater is to give the refrigerator the various patterns of heat load with the different time constant and the different amount of heat input. By the combined operation of the dummy heat load with the refrigerator, one can quickly and easily simulate LHD cryogenic operation at least in its substantial aspects and therefore collect a data-base of the refrigerator, so that many algorythms can be established for the computer controlled operation of the LHD cryogenic system. After a second annual and voluntary inspection of equipments was made for safety and security, a first combined operation was planned as a trial run for one week in February 1996. However, a computer software defect, and also a simple ill-manipulation of the control system interrupted the refrigerator

operation. As will be shown later this event posed the most significant defect in the design concept of the cryogenic control system though no apparent damage to the hardware resulted. The last two runs in March and April 1996 are also a combined operation, during which a well known and a rather unfavourable phenomenon of density wave originated instability was observed between the dummy load and the refrigerator. In the following section this observation will be briefly discussed on preliminary base. The total operation time is 1055 h at present.

EVENTS AND OBSERVATIONS

Considering its short run time, it might be natural that except protection trips only one emergency shut-down is counted for runs during past twelve months after the construction. Two insufficient control system design forced the operator to pull the shut-down button. One was the external intervention to the engineering workstation through the ISDN line between the manufacturer and the operator. Although these EWS does not directory control operation, they receive operation data every few seconds from VME which are the controller. A manufacture's unintended close-off on his EWS made the NIFS VME to keep on straging the huge data without overwriting until the occupied terminals brought about a down of the DP-1000 which is the CRT at the operator terminal during a refrigeration run. The other was due to the insufficient computer program proof inspection before loading on the VME. Switching algorithm from master VME to slave VME sent a conflicting instruction to the control valves in the event of switch operation. These substantial deficiencies in design concept were promptly removed and the program has been revised.

At a combined run with the dummy heat load, an instability in pressures and temperature was observed. In Figure 1, a typical pattern of pressure oscillation is shown with the behavior of automatic pressure control JT expansion valve. Here, the pressure oscillation in the dummy cryostat (noted by × symbols) seems to precede one cycle ahead and to lead other oscillation (other symbols) in the refrigerator. Flow rate and turbine speed also showed similar pattern. This phenomenon might be defined as density wave originated system instability. As shown in the flow diagram attached in the figure,

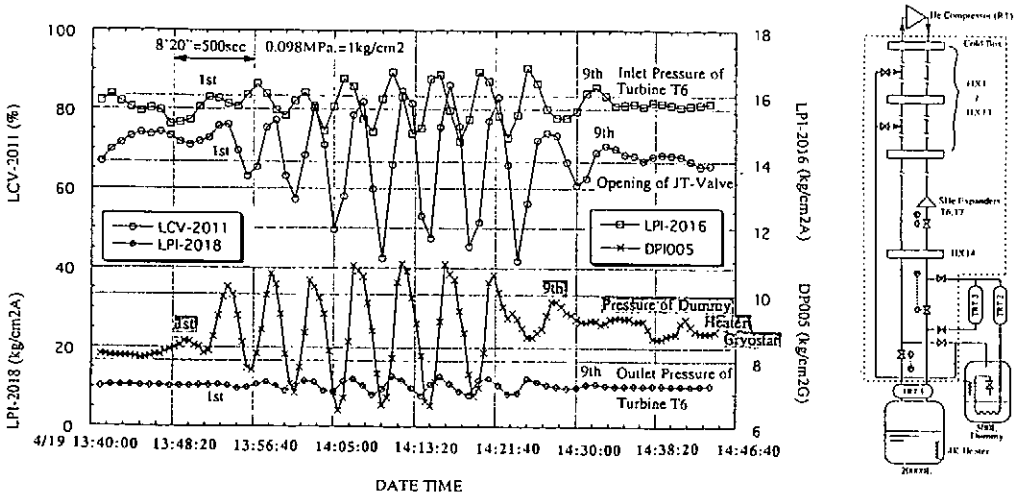

Figure 1 Example of Instability in Cold Box and Dummy Heater Cryostat

supercritical helium is divided into two flows at the outlet of cold-box of the refrigerator. Through JT valve one goes into a liquid helium storage which has a level control electrical heater. The other flows into the dummy load cryostat which has the precooling heat exchanger HX-D immersed in liquid helium. The cycle time of oscillation can be read as 4 to 5 minutes, which roughly corresponds to the time necessary for the supercritical helium to flow down the transfer tube TRT-2 and refrecting-back as the saturated vapour via. liquid heat exchanger HX-D. Any thermal disturbance in the supercritical helium originating at the dividing point which is also the outlet of heat exchanger HX-14 of the cold-box, could be converted into an increased amount of the vapour at the dummy load HX-D and retured to the heat exchanger HX-14. This composes a feedback loop and nearly the same model with which Tamada and Tomiyama showed theoretically that such instability could be possible [3]. The thermal disturbance is inferentially to originate from a hot line of other transfer tube, TRT-3, which is again connected to the same dividing point. It was observed that an activation of built-in heater to LHe strage suppresses the instability. Furthermore, any of such phenomena was not observed when the heat exchanger HX-D of dummy heater cryostat is not filled with liquid helium. The former may be attributed to a much larger cold bunch from the LHe storage (4.4K cold return corresponding to 6 to 8 kW heater input) which might dissipate the smaller negative feedback from the dummy heat load. However, before this presumptions are confirmed a more detailed investigation is necessary through coming runs. In addition, it should be noted that the observation above is an extreme example caused partly by insufficient tuning of controls and the unskilled initial operation as well. The same authors are reporting its stable operations on the same system [4].

REMARKS AND ACKNOWLEDGEMENT

The current status in the construction of the refrigerator of LHD was shown especially in its operational aspect. The construction is not completed until all of the superconducting magnet will be connected that is in the end of 1997.

The authors acknowledge Dr. A. Iiyoshi for his leadership in promoting LHD construction and to the NIPPON SANSO Co.,Ltd. for their assistance in operation of the LHD refrigerator.

REFERENCES

1 Satoh, S. et.al. Construction of a 10kW Class Helium Cryogenic System for the large Helical Device Cryogenics (1994) 34 95-98

2 Satoh, S. et.al. Construction and Commissioning Tests of a 10-kW-Class Helium Refrigerator for the Large Helical Device Proceeding WE-B1-3 CEC/ICMC (1995) or to be published in 41 Advances in Cryogenic Engineering

3 Tamada, N. and Tomiyama, S. Temperature Oscillation Caused by Coupling of Heat Exchangers (in Japanese) Cryogenic Engineering (Japan) 13 4 (1978) 198-204

4 Maekawa,R. et.al. Study of the Optimum Operating Condition of the Helium Refrigerator with a Dummy Load Appratus for the Large Helical Device PS1-e1-13 ICEC16 /ICMC Kitakyusyu (1996)

Cooling and Excitation Tests of a Single Inner Vertical Poloidal Coil

K. Takahata*, T. Mito*, T. Satow*, A. Nishimura*, S. Yamada*, H. Chikaraishi*, N. Yanagi*, A. Iwamoto*, R. Maekawa*, S. Imagawa*, H. Tamura*, S. Yamaguchi*, S. Satoh*, S. Tanahashi*, K. Yamazaki*, J. Yamamoto*, O. Motojima*, EXSIV Group*, T. Kai**, K. Nakamoto**, T. Yoshida**, Y. Wachi** and M. Ono**
*National Institute for Fusion Science, Oroshi, Toki, Gifu 509-52, Japan
**Toshiba Corporation, Chiyoda-ku, Tokyo 100, Japan

ABSTRACT

The second Experiments on a Single Inner Vertical coil (EXSIV) for the Large Helical Device were carried out to confirm the performance. The coil is one of poloidal coils for the Large Helical Device (LHD) and consists of a forced-flow Nb-Ti cable-in-conduit conductor (CICC). After a cooldown for 250 hours, the superconducting transition of the whole coil was confirmed. Then, the coil was successfully energized up to the specified current, 20.8 kA. In this experiments, we gathered many useful data, such as pressure drop, displacement, voltage of joints, acoustic emission (AE) and so on. In this paper, these data will be introduced.

INTRODUCTION

Poloidal coil system of the Large Helical Device (LHD) consists of three pairs of circular solenoids. Inner Vertical (IV) coils with an average diameter of 3.6 m and Inner shaping (IS) coils with a diameter of 5.6 m have been fabricated. Outer Vertical (OV) coils with a diameter of 11.1 m are now under fabrication inside the experimental hall as scheduled. A lower OV coil has just been completed. Three coils have been installed into a lower part of the LHD supporting shell since April of 1996.

We performed cooldown and excitation tests of an IV coil using test facilities at the cryogenics and superconductivity laboratories of NIFS. The main purpose of this experiment is to confirm the designed performance before installing the coils in the LHD cryostat. The first experiment were performed from February 1 to March 1 of 1995. The coil was cooled down to the superconducting state for 23 days [1]. However, blocks of the inlet filter resulted in instability of the cooling system, and the excitation up to the specified current of 20.8 kA was suspended. A new filter system was then developed and the capacity of the cooling system was increased. The second experiment was performed from November 13 to December 8 of 1995. The peripheral devices, such as a centrifugal pump and a superconducting bus line, could be operated smoothly, and the coil was successfully energized up to the specified current, 20.8 kA. In this paper, the obtained data during the cooldown and excitations will be described.

Table 1. Specifications of the conductor and coil

Conductor		Coil	
Type	Cable-in-conduit	Inner/Outer radii (m)	1.6/2.1
Superconducting material	Nb-Ti	Height (m)	0.46
Conduit dimension (mm)	23.0×27.6	Total weight (tons)	16
thickness (mm)	3.0	Number of pancakes	16
Void fraction	0.38	Number of turns	240
Strand diameter (mm)	0.76	Operating current (kA)	20.8
Number of strands	486	Maximum field (T)	5.2
Nb-Ti:Cu	1:2.7	Stored energy (MJ)	68

CONDUCTOR AND COIL

The specifications are listed in Table 1. The conductor is a Nb-Ti cable-in-conduit type. The number of strands is 486 and the void fraction is approximately 0.38. The surface of strands are uncoated, which affects the overall current distribution and improves the stability margin. The coil consists of eight double-pancakes. The coolant flows in parallel from the inner turns to the outer turns. Seven conductor joints are arranged outside and become the outlets of the coolant. The length of a path is 170 m on average. The total weight is 16 tons including the stainless steel covers. The operating current and the maximum field are 20.8 kA and 5.2 T, respectively.

TEST PROCEDURE

The coil was set on ten cryogenic supporting posts in a single-coil-testing cryostat and connected to the test facilities at the cryogenics and superconductivity laboratories of NIFS. The capacity of the helium refrigerator is 600 W at 4.4 K or 250 l/h. The inlet gas temperature was controlled by mixing cool (~80 K) and hot (~280 K) gases from the cold box. The temperature difference between inlet and outlet was then kept less than 50 K. When the coil became 100 K, the turbine cooling started, and the coil was cooled with gas of 10~20 K. After the initial cooling, the steady cooling was carried out with the supercritical helium centrifugal pump. The specified mass flow rate was 50 g/s, and the inlet pressure was about 0.9 MPa.

We measured the inlet and outlet temperatures, pressures and mass flow rate. The voltage taps were attached to measure the resistance of each pancake coil and joint. The displacement of the coil was measured in the radial direction during the cooldown and excitations. Four displacement meters were installed inside the cryostat wall and attached to the outside surface of the coil. Measured angles are 46, 134, 226 and 314 degrees when the angle of the feeders is zero. The pressure drop between inlet and outlet was measured during cooldown and steady cooling. The pressure drop was then transformed into the friction factor by Darcy's equation. Acoustic emission (AE) sensors were attached onto the coil surface.

RESULTS AND DISCUSSION

Figure 1 shows the linked cooldown curves after omitting the suspended time. The temperature difference between inlet and outlet was successfully controlled to less than 50 K before the coil became 100K. The average coil temperature was calculated from the coil resistance. The coil temperature agrees well with the outlet temperature. This indicated that the heat was exchanged almost completely between the coil and helium. Figure 2 shows the displacement during the cooldown. It was found that the coil contracted uniformly by about 6 mm. This value is the same as calculated one.

The friction factors during the cooldown and steady cooling are shown in Fig. 3 as a function of Reynolds number. The open and closed circles indicate the data for the first and the second cooldowns, respectively. The open triangles indicate the data for the previous R&D coil named "IVS" [2], of which path length is 35 m. Both conductors have almost the same configuration. The pressure drop characteristics of both coils agree well in spite of the difference of the path length. The friction factor of both coils is larger than the Hagen-Poiseuille and Blasius equations for the smooth pipe when the Reynolds number exceeds 50. On the other hand, the Katheder's formula [3], which is a general correlation of many different conductors, agrees with the experimental data.

We energized the coil over 10 kA eight times, including three fast discharge tests. During the tests, the coil has not quenched even once. The voltage of a joint was about 3 μV. This corresponds to the heat generation of 0.06 W, which is negligible for conductor stability. Figure 4 shows the radial displacement of the coil during the excitations. N_{ex} in the figure indicates the excitation number. The coil expanded by 0.7 mm at the maximum current. The rigidity of the coil are now under calculation. After the second excitation, the same hysteresis was observed. The acoustic emissions were observed mainly in the first excitation, and then decreased after the second excitation. These confirmed that the coil is mechanically stable.

CONCLUSION

The single cooldown and excitation tests of an IV coil for the LHD were performed. A summary of the results is shown below.

(1) Total cooldown time was about 250 hours, not counting suspended time.
(2) The coil contracted uniformly by the design value, about 6 mm.
(3) The relationship between the friction factor and the Reynolds number in the cooldown agrees well with the results obtained as the R&D coil previously tested and Katheder's formula.
(4) The coil was successfully energized up to the specified current, 20.8 kA.
(5) The heat generation of a joint was 0.06 W at 20.8 kA, which is negligible for conductor stability.
(6) The radial displacement and acoustic emission suggested that the coil is mechanically stable.

REFERENCES

1. Takahata, K. et al., Cooldown performance of an inner vertical field coil for the Large Helical Device, presented at MT-14, Tampere, Finland, June 11-16, 1995
2. Takahata, K. et al., Stability tests of the Nb-Ti cable-in-conduit superconductor with bare strands for demonstration of the Large Helical Device poloidal field coils IEEE Transactions on Magnetics (1994) 30 1705-1709
3. Katheder, H., Optimum thermohydraulic operation regime for cable in conduit superconductors (CICS) Cryogenics (1994) 34 595-598

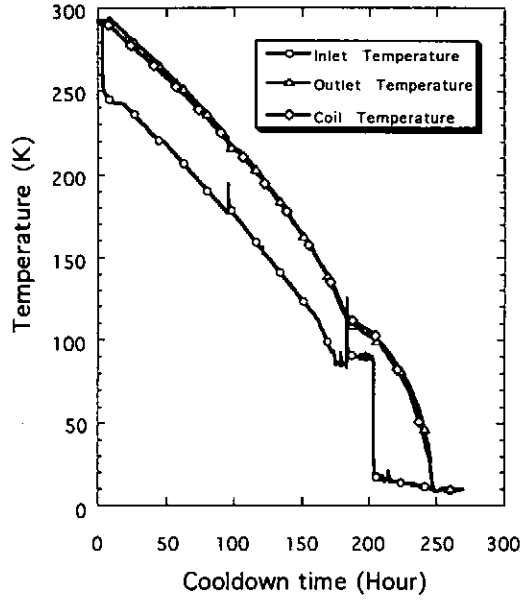

Figure 1 Cooldown curves

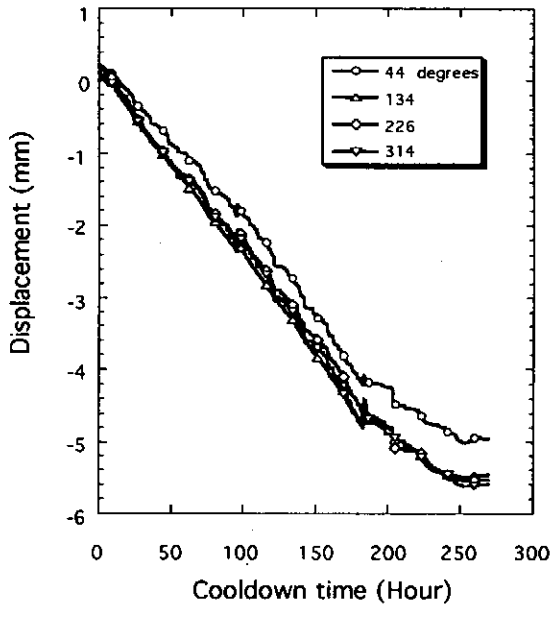

Figure 2 Displacement during the cooldown

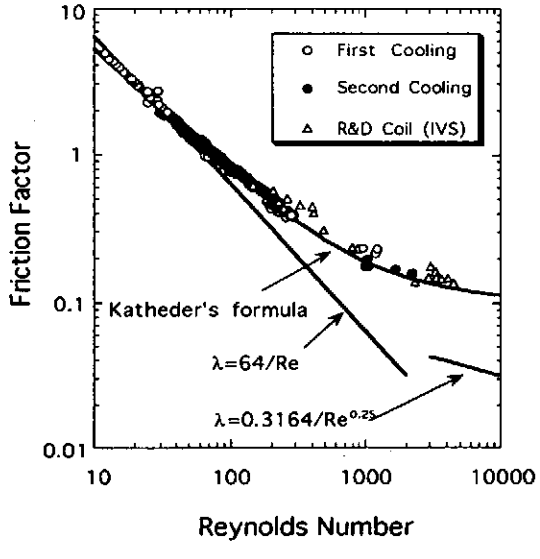

Figure 3 Friction factor versus Reynolds number

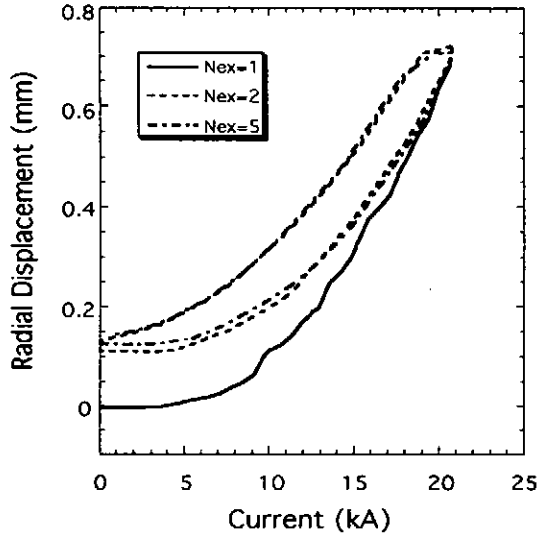

Figure 4 Displacement during the excitations

Cryogenic Mechanical Test Facilities and Test Results

A. Nishimura, H. Tamura, S. Imagawa, T. Mito, K. Takahata, N. Yanagi, S. Yamada, J. Yamamoto, and O. Motojima
National Institute for Fusion Science. 322-6 Oroshi, Toki, Gifu 509-52 Japan

ABSTRACT

A large capacity mechanical test facility and a normal mechanical test machine were installed in Cryogenics and Superconductivity Laboratories in National Institute for Fusion Science to characterize a deformation behavior of a large scale superconducting coil in liquid helium and investigate cryogenic mechanical properties of structural materials for Large Helical Device. Some mechanical tests have been carried out using these test facilities. This report will give the outlines of these test facilities and some typical test results.

INTRODUCTION

In order to evaluate deformation properties of large superconducting magnets and investigate mechanical properties of cryogenic structural materials, a large capacity mechanical test machine was planed and installed in National Institute for Fusion Science together with a normal mechanical test machine [1, 2].

The normal mechanical test machine is Instron Universal Testing Instrument, type 4507, with a capacity of 200 kN. This machine is a screw driven type. A special cryostat has fabricated at the same time, and 10 tensile specimens on a turret disk are able to be cool down simultaneously. A compressive test of one helical coil conductor and a tensile test of a cryogenic structural material have been performed.

The large capacity mechanical test facility was named 10 MN cryogenic mechanical testing machine. Since a maximum electro-magnetic force of around 10 MN/m would act on one helical coil of LHD, the capacity of this machine was determined to be 10 MN in compressive to perform an actual size coil test. This machine has the largest load capacity in the world for cryogenic service.

In this report, this 10 MN cryogenic mechanical test machine system will be addressed and some test results using this machine will be presented.

10 MN CRYOGENIC TESTING MACHINE

A height of the large testing machine is about 8.5 m and an outer size in one plane is about 4.8 m square including a working stage. It has a large cryostat of which size is about 2.3 m high, 1.6 m outer diameter, and 1.3 m inner diameter. A sample attachment is described in Fig. 2. A support bed with a 350 mm maximum thickness is located in the cryostat and this bed is supported by 4 tie rods connected to the actuator. A main

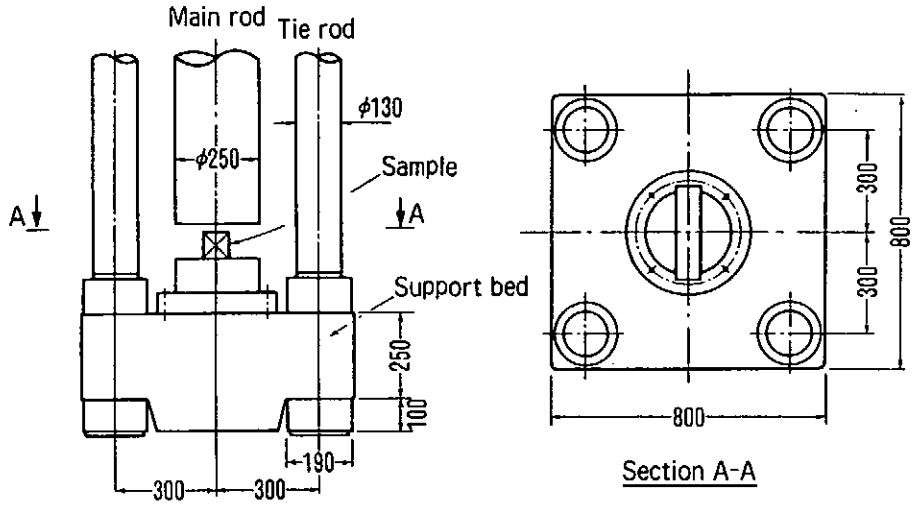

Figure 1 Shape and dimensions of sample bed.

rod of 250 mm diameter comes into the cryostat and presses a specimen placed on the support bed. The flatness and the parallelism of the bottom surfaces of the main rod and the support jig have been checked by a pressure indication sheet (Fuji Film Prescale). A coil pack was placed on a special jig bolted to the support bed, and a rigidity test was carried out in liquid helium. This main rod has a joint inside the cryostat. By changing a lower part of the main rod, three-point bending test could be performed. The tensile load capacity of this machine is reduced to about 2 MN because of this connection joint.

A hydraulic servo-control system was adopted to carry out a load control or a ram stroke control test and an actuator was placed at the top of this test machine. Both tests can be controlled by a personal computer and the data are stored in a hard disk. Repeatability of this system is ± 1 % for an indicated load range.

CRYOGENIC SYSTEM

A cryogenic system was designed and installed for supplying a liquid helium, a cold helium gas, and/or a supercritical helium to all test facilities in Cryogenics and Superconductivity Laboratories [3]. It has a refrigeration capacity of 600 W at 4.4 K or a liquefying capacity of 250 l/h. Cold helium lines for supplying and returning, a liquid helium line and a warm recovery line are connected to the cryostat.

After setting up the test sample, the cryostat is purified for one day. Then, it is cooled down and a liquid helium of over 1.5 m^3 is stored in the cryostat. It needs two days to cool down and fill the liquid helium in the cryostat. A normal evaporation rate in the cryostat is about 12.6 l/h at steady state.

TEST RESULTS

Some rigidity tests of a poloidal coil pack and a helical coil pack were carried out and the deformation behaviors of these coil packs were investigated [4-6]. Results of helical

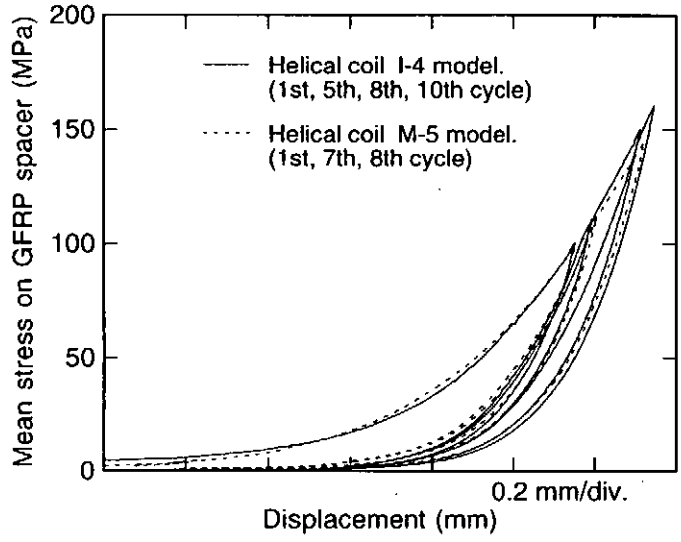

Figure 2 Stress-displacement curves of helical coil packs.

coil pack tests are shown in Fig. 2, for example. All of these test results showed an obvious non-linear behavior on the first loading process in a stress-displacement curve, and hysteresis curves were observed in sequential load cycles. Rigidity of each coil pack was measured at the maximum design load and it was noticed that coil rigidity would be changeable by an effect of a change in a contacting area between a conductor and a spacer together with that between a main rod and a coil pack [7].

A series of a fracture toughness test using a large bend bar specimen with 87.5 mm thick, 175 mm wide, and 700 mm span was carried out in liquid helium [8]. SUS316 base metal and weld joint specimens were tested according to ASTM E 813-89. As shown in Fig. 3, a large negative crack growth region was observed, and higher toughness than that of a conventional compact tension specimen was obtained. These behaviors were addressed with a wedge effect model [9], and the results presented an importance of the fracture toughness test with a full size specimen.

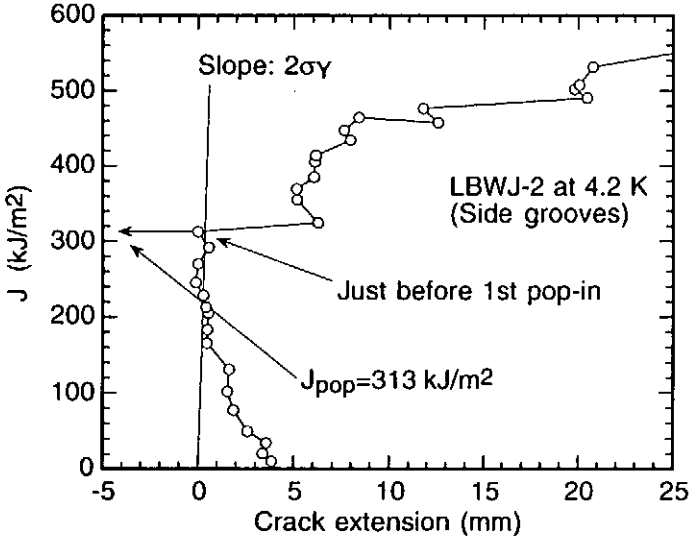

Figure 3 One example of J-R curve of large bend bar. (Partially welded joint)

GENERAL REMARKS

Cryogenic mechanical test facilities in NIFS and some test results were described in this paper. General remarks are as follows:
(1) 10 MN cryogenic mechanical testing machine was designed and installed in Cryogenics and superconductivity Laboratories in 1990, together with 600 W at 4.4 K refrigeration system. This large capacity testing machine with a hydraulic servo-control system is working on well.
(2) Several coil pack tests simulating for helical coils and poloidal field coils were carried out in liquid helium and rigidity of these coils was investigated.
(3) Also, large bend bar tests of SUS 316 base metal and weld joint were performed and the fracture toughness of a thick section plate and weldment was measured.
(4) These test results are very useful and helpful for a design and a construction of Large Helical Device and other large superconducting magnet systems.

ACKNOWLEDGMENTS

Authors wish to express our thanks to Dr. Iiyoshi, Director General of NIFS, for his continuous encouragement. Also, we would like to thank the LHD construction group for useful discussions and their help.

REFERENCES

1 Nishimura, A. et. al. Cryogenic 10 MN Mechanical Testing System for Superconducting Coil ICMC 1991 Huntsvill, Alabama, USA (1991) AP-28
2 Nishimura, A. et. al. Rigidity Tests of A Superconducting Coil at 4.2K Simulated for the Helical Coil on the LHD Program Fusion Engineering and Design (1993) 20 211-216
3 Yamamoto, J. et. al. Superconducting Test Facility of NIFS for the Large Helical Device Fusion Engineering and Design (1993) 20 147-151
4 Nishimura, A. et. al. Cryogenic Compressive Deformation Properties of Superconducting Coil Packs Simulated for Helical Coils on LHD Program Cryogenics, (1992) 32 376-379
5 Nishimura, A. et. al. Effect of GFRP Spacer on Local Deformation of Large Superconductor in Coil Pack IEEE Trans. Mag. (1994) 30 1887-1890
6 Nishimura, A. et. al. Experimental Rigidity Evaluation of Conduit Pack for Forced Flow Superconducting Coil Advances in Cryogenic Engineering (1994) 40 1413-1420
7 Nishimura, A. et. al. Deformation Behavior of Coil Pack for Helical Coil in Large Helical Device ICEC-16 Kitakyushu, Japan (1996) PS3-e2-39
8 Nishimura, A. et. al. Fracture Toughness of Partially Welded Joints of SUS316 Stainless Steel at 4 K by Large Bend-Bar Tests MT-14 Tampere, Finland (1995) E-86
9 Nishimura, A. et. al. Fracture Toughness of SUS316 and Weld Joint at Cryogenic Temperature ICMC 1996 Kitakyushu, Japan (1996) OC1-1

Research Work on Large Scale Cryogenic System at SWIP

Li Huanxing Pu Men
Southwestern Institute of Physics, P.O.Box 432, Chengdu, 610041 Sichuan, China

ABSTRACT
In this paper we describe the basic research work in cryogenic technology of the large scale cryogenic system from a few aspects, which are in the fusion research, in the conceptual design of a tokamak fusion reactor, in other application and so on, near three decades at SWIP. This work will be fundamental to establish large scale cryogenic systems for the future fusion device and superconducting magnet.

INTRODUCTION

Southwestern Institute of Physics(SWIP), which is an institute of controlled nuclear fusion research, has established tens fusion research devices, such as the steady state superconducting mirror machine, the HL-1 and the HL-1M tokamak,etc.. On these devices a great many of experiments and research work of the fusion engineering and the plasma physics have been carried out. SWIP is the largest base of the fusion research in China, and has the scientific research ranks of the controlled nuclear fusion theory, engineering and experiment .

We have studied a series of cryogenic engineering problems in fusion technology and set up a lot of cryogenic laboratories (e.g., the superconducting magnet lab, the cryogenic mechanics property of structure materials lab, the heat conductivity and the specific heat of solid materials lab, the helium properties and the cooling method of superconducting magnet lab, low temperature measurement lab, etc.), and have a group of qualified scientists and technicians in cryogenic and superconducting technology in order to build up the superconducting mirror machine and the future superconducting tokamak fusion reactor.

Here we first present the research work of cryogenic technology in the mirror machine, then describe some of cryogenic systems for the HL-1 tokamak(e.g., ECRH and pellet injection) and other application (e.g., Wiggler system and VSM_3 magnetometer), finally discuss research project of cryogenic and superconducting magnet system in the conceptual design of a tokamak fusion reactor. Our research work and project will be fundamental to establish large scale cryogenic systems for the future fusion device and the superconducting magnet.

RESEARCH WORK OF CRYOGENIC ON MIRROR MACHINE

Our cryogenic research work started from building up the steady state superconducting

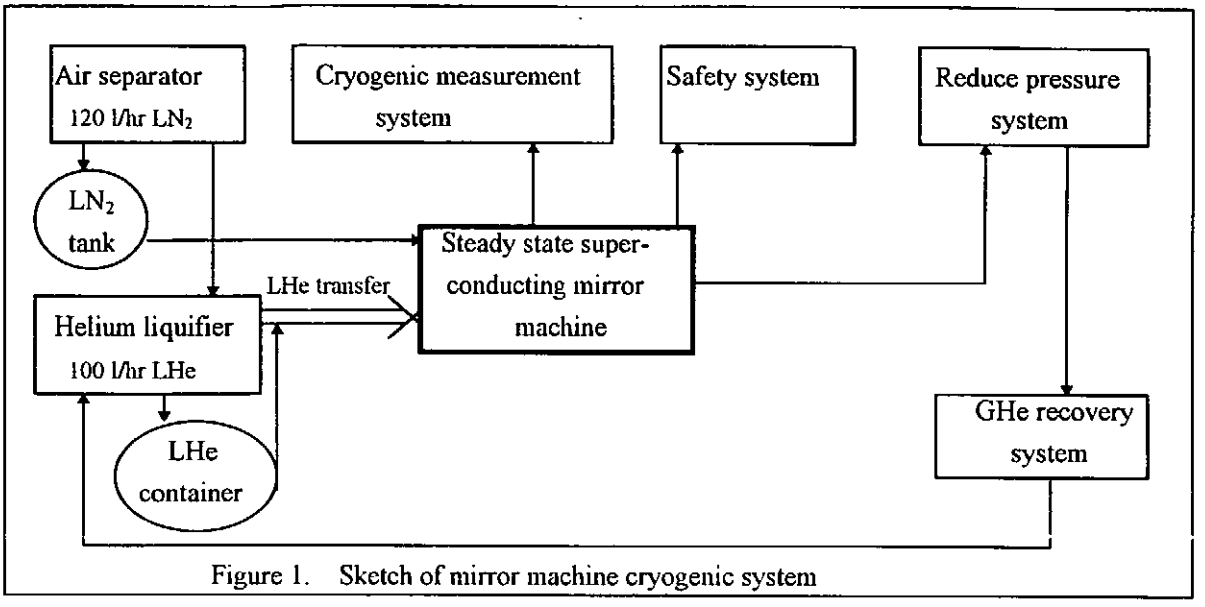

Figure 1. Sketch of mirror machine cryogenic system

mirror machine. We studied a series of cryogenic technology problems to be solved in the mirror machine and decided on the design plan and the parameter of cryogenic system of the mirror machine according to superconductor property and research condition at that time. Cryogenic system sketch is shown in figure 1.

Required coolant of the machine is 2200 l LN_2, 3205 l LHe (include the cryostat requires 880 l LN_2, 735 l LHe) during cooling down. The cryogenic system and the super-conducting magnet operate steady. The liquefaction devices of coolant are a set of 100 l/hr helium liquifier, which is developed by us combining with cryogenic equipment factory at home, and two sets of air separator of 120 l/hr LN_2. The store capacity of coolant is 4500 l LHe and 15000 l LN_2.

We developed total length 53.4 m of LHe transfer line to transfer continually for mirror machine. The line consists of the standard main line, two LHe entrances connected with LHe container and controlled by inlet valve, five branch pipes connected with the cryostat and adjustment by valves. Its insulation way is high vacuum and LN_2 shield. In operation at pressure about 30 kPa the transfer ability, efficiency and pressure difference are separately 150 l/hr, about 87% and 8 kPa.

The cryostat of mirror machine consists of a 4.2K container and two reduce pressure containers that can be cooled down 1.8K, uses insulation way of high vacuum and LN_2 shield . Its LHe quality is controlled by liquid level indicator. It can be full of 400 l LHe. All kinds of cryogenic thermometers (e.g., AuFe-NiCr thermocouple; Ge, RhFe and Pt resistance thermometers, etc.) and LHe level indicators (e.g., capacitor model, superconductor model, etc.) are developed all by ourselves in the system.

SOME OF BASIC RESEARCH WORK

We have made a great many of basic research work in cryogenic technology near three decades. They are mainly as following:

- Heat transfer properties of the superfluid helium and the supercritical helium;

- Mechanics properties of structure materials at low temperature;
- Heat conductivity of solid materials at the range of 4.2 ~ 20 K;
- Specific heat of solid materials at low temperature;
- Research and development of insulation property of cryogenic system;
- Safety of cryogenic system for superconducting magnet; [1]
- Low temperature measuring technology;
- Research and development of the cryosorption pump and the G-M refrigerator.

APPLICATION OF CRYOGENIC TECHNOLOGY

Application on the HL-1 tokamak

Electron cyclotron resonance heating (ECRH) is a subject of fusion research. Heating device is a large power gyrotron. It requires a uniform field of a few tesla in millimeter wave band. We developed not only a superconducting magnet but also a cryogenic cryostat with room channel to give coordination of gyrotron. The cryostat uses high vacuum and multilayer as insulation, and can make continually experiment for gyrotron. This system with the gyrotron attained better result in plasma preionization experiment on the HL-1 tokamak.[2]

Pellet injection is an advanced technology of feed fuel of fusion experiment at present. According to program a pellet injection system has been built up at SWIP, and a pellet injection experiment has been carried out successfully at the HL-1 tokamak in 1992. The single shot H_2 or D_2 pellet has a cylindrical shape with diameter of 1.1 mm, length range from 1.1 to 2.4 mm, and a speed of 300-500 m/s. In the experiment it was observed obviously to increase in the electron density of 100% and the energy confinement time of 40% owing to the pellet injection. The target of the next step is a multishot pellet injection system capable of injecting pellet at a speed of 3 km/s and 1-10 shots/s[3]. It is the one of the plans to freeze into pellet in magnetic refrigeration.

Application of cryogenic technology in other field

Superconducting Wiggler magnet system is a part of the Hefei Synchrotron Radiation Accelerator. The magnet to consist of SC coils and yoke has an external form of cuboid of 348 mm length, 334 mm width, 288 mm height. The cryostat consists of a LHe container of 500 mm diameter and 512 mm length, a case of 642 mm diameter and 962 mm length and a LN_2 jacket between the container and the case to reduce heat radiation. The LHe container with the magnet is fixed to the case by four hanging and four pulling rods. The beam tube along the magnetic axis is an operation channel of Wiggler system for the accelerator, and is also the one of difficult points in design. It has an oval cross section of 40 mm major axis and 20 mm minor axis, and a gap of 8.5 mm with the magnet pole core, 5T field strength at its axis center. Its cross section is shown figure 2. [4]

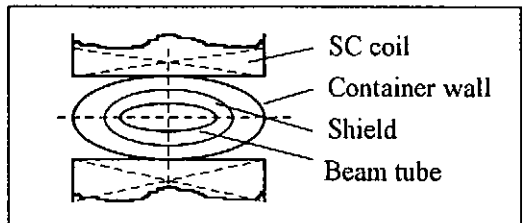

Figure 2. cross section of beam tube

VSM_3 variable temperature vibrating sample magnetometer is a kind of device for measuring magnetic properties(e.g., magnetic moment, intensity of magnetization, magnetic susceptibility, etc.) under the range of 0 ~ 7 T and of 4.2 K ~ 300K. According to work experience of many years we have formed ripe method of design and development of cryostat for middle-small size superconducting magnet system. The design program are:
1) setting technical targets; 2) structure design; 3) calculation and verification of strength and rigidity; 4) considering overall plan included machine technique, leak check, operating pressure and safety pressure, etc. ; 5) adjusting design; 6) heat transfer calculation and analysis; 7) determining total design.
The cryostat for VSM_3 uses high vacuum multilayer and LN_2 jacket as insulation, and is put a center dewar of variable temperature as sample chamber along its central axis. In the experiment its LHe evaporation capacity is 0.18 l/hr at zero field or closed operation of superconducting magnet.[5]

PROJECT IN CONCEPTUAL DESIGN OF A TOKAMAK FUSION REACTOR

Now our research work is mainly around large scale cryogenic and superconducting magnet system in the conceptual design of a tokamak fusion reactor. We have investigated this aspect at international advance through the research and the technical references.We also have analyzed preliminary cooling and stability issues of conductor[6], structure material and insulation issues in cryogenic system, protection during quench, etc.. We take further steps to calculate and analyze the cryogenic system and the magnetic field, stress and heat transfer of D shape magnet by ANSYS Program, and to give in better design plan of the superconducting magnet and the cryogenic system in the future fusion reactor.

REFERENCES

[1] Zhu, X.W. and Pu, M. Safety of cryostat for middle-small superconducting magnet, CRYOGENIC (CN11-3478/V) (1995) 5 5-10

[2] Zhu, X.W. and Pu,M. Development & application of a superconducting magnet for gyrotron with 4 mm wave length, CHINESE JOURNAL OF LOW TEMPERATURE PHYSICS (1989) 3 243-247

[3] Huang, J.H. Fusion reactor design and technology program in China, Fusion Engineering and Design (1994) 25 35-47

[4] Zhu, X.W. and Pu, M. Cryostat of superconducting wiggler magnet system for synchrotron radiation accelerator, CHINA NUCLEAR SCIENCE & TECHNOLOGY REPORT (1994) CNIC-00824, SIP-0070

[5] Pu, M. and Zhu, X.W. Cryostat for VSM_3 variable temperature vibrating sample magnetometer CRYOGENIC (CN11-3478/V) (1993 Special) 249-252

[6] Pu, M. and Li, H.X. Feature and design of superconductor for tokamak fusion reactor, SWIP Research Report (1995)

Cryogenics of the K500 Superconducting Cyclotron at VEC Centre Calcutta

Narayan Bhattacharya
Variable Energy Cyclotron Centre
1/AF Bidhan Nagar,
Calcutta - 700 064, India

ABSTRACT

A superconducting cyclotron of K 500 is being fabricated at VECC, DAE, Calcutta for research in nuclear physics with heavy ions. It has a peak magnetic field of 5.5 T at 800 A. It has an iron core of 100 t and iron hills and valleys for shaping the magnetic field in the median plane. The superconducting (~3.5 km) cable of 2.8 x 5.0 mm dimension, has been made cryogenically and adiabatically stable by embedding the 500 filaments, NbTi wire (filament dia <40μm) into a OFHC copper substrate. The cryostat, made of SS 316L, has a liquid helium volume of 300 l and the evaporation rate is 15 l/hr. The copper LN_2 shield of the cryostat is cooled by a closed circuit LN_2 supply and the evaporation rate is 2 l/hr. The cyclotron vacuum chamber is evacuated to 1 x 10^{-7} torr with the help of 3 cryopumps cooled with 4.2 K LHe.

INTRODUCTION

A superconducting cyclotron is being built at VECC, Calcutta. The main advantage of building a superconducting cyclotron is that the running cost will be minimum. Also, since the cyclotron magnet will be very compact owing to the high magnetic field, the building to house the cyclotron will be much smaller compared to a room temperature cyclotron. The vacuum volume will also be much smaller and the cooling water requirement will be minimum. So even if the initial investment is slightly higher, there will be overall saving in running the cyclotron over a period of fifteen to twenty years.

SUPERCONDUCTING COIL

In the cyclotron, only the coil, made of NbTi, will be housed in a cryostat filled with liquid helium at 4.2K. Other components like the iron yoke, radio frequency cavities, ion source etc. are all kept at room temperature. The parameters of the superconducting coil are given in Table-1. Similar cyclotrons are operating at Michigan State University and Texas A&M University, U.S.A. for the last ten years. One cyclotron at Milan, Italy and another cyclotron AGOR at Groningen, The Netherlands, have been commissioned last year. Since the stability of the coil depends on the diameter of the filaments, we have chosen a filament of diameter < 40μ m and increased the number of filaments from 54 to 500 to keep the overall diameter of the superconducting wire same as that of Texas A&M i.e., 1.3 mm. The superconducting wire is embedded in a copper matrix to make the coil cryogenically stable . A perspective view of the superconducting magnet with the cryostat is shown in figures 1 and 2 and the cross section of the wire is shown in Fig. 3.

CRYOSTAT

In Fig.2, the details of the vertical and horizontal supports are shown. There are six vertical supports and three horizontal supports to hold the superconducting coil in position and to restrain any motion of the coil, because of the force generated by energising the coil.
Fig.4 gives the dimensions and weights of the different components of the cryostat. It may be mentioned that the vacuum chamber is made of AISI 1010 carbon steel and the helium chamber is made of SS 316L. Since AISI 1010 carbon steel has poor degassing property, both Texas A&M and MSU have done electroless nickel plating on the inside surface of the vacuum chamber. Nickel plating over such a huge volume and surface of the vacuum chamber is very cumbersome and expensive, because of this reason, in the case of AGOR, they have used SS 304 for the vacuum chamber. Since carbon steel vacuum chamber forms a part of the return path for the magnetic field, changing the carbon steel with SS 304 involves a detailed analysis of the magnetic field in the median plane.
The LN_2 shield consists of a copper cylinder which is in thermal contact with a closed cycle LN_2 supply and the LN_2 consumption is about 2 litre/hour. It may be mentioned that in the case of Milan and AGOR the LN_2 shield is made of aluminium and stainless steel respectively. In fact SS has poor thermal and electrical conductivity than those of aluminium and copper. So from the point of eddy current generation in the LN_2 shield, during the energisation of the coil, aluminium is more suitable than both copper and SS.
The material used in the link for the vertical support is glass epoxy rather than SS. This is because the better performance so far as strength to thermal conductivity ratio in the case of glass epoxy compared to SS. The clevis pin in the cold end is at liquid helium temperature and hence a special alloy A286 with 26% nickel is being used. The horizontal support links are prestressed before the coils are energised and when the coils are energised they experience outer forces so that the tension on the supports are reduced in the maximum current level . It is interesting to note that both Texas A&M and MSU have used ring rolled forgings for the vacuum chamber of the cryostat. In our country, to procure ring rolled forging will be expensive and since there are at least five to six welding joints, there is no point to use seamless ring rolled forgings.
From the cool down curve of the cryostat, it can be seen that the total cool down takes about seven to eight days and the helium refrigerator must be capable of producing continuous refrigeration from 300 K to 4.2 K through various stages.

REFRIGERATION REQUIREMENT

The details of the heat leak into the cryostat through conduction, convection and radiation and the total liquification rate required from the refrigerator is given in Table-2.

CONCLUSION

Successful completion of such a big superconducting magnet and its cryogenic transfer line and its trouble-free operation of such a big helium liquifier/refrigerator shall boost the application of superconducting magnet in other areas like MRI & Tokamak magnets & will encourage Indian industries to venture in this high technology area.

Table 1

SUPERCONDUCTING MAGNET PARAMETERS

Conductor	
NbTi,500 filaments with one turn in < 12.7 cm.	
soft soldered into copper stabilizer.	
Overall copper to superconducting ratio :	20 : 1
Overall Dimensions :	0.28 cm x 0.5 cm
Short Sample Ic @ 4.2 K, 5.5 Tasla	1030 A
Conductor Current Density	5800 A/cm
Coil	
1.32 4 m. ID x 1.80 m. OD	
Number of Turns :	
Short Coil : 36 Layers	1092 turns
Long Coil : 36 Layers	2250 turns
4 Coils, Total Turns	6684 turns
4 Coils, Total Length	35 Kms
Design Current :	800 A
Inductance :	13.6 H
Short Coils :	27.6 H
Mutual :	13.8 H
Stored Energy (with Iron)	22 MJ
Magnet Yoke	
Nominal Weight :	100 tonnes
Size :	3.048 m x 2.1844 m.
Material :	Forged 1020 Steel

Table 2

REFRIGERATION REQUIRMENTS

Heat leak from the supports	1.0 watt
Radiation	1.0 watt
Plumbing and instrumentation	3.3 watts
Total	5.3 watts
5.3 watts = 5.3/0.64 = 8.3 l/h	
Transfer loss is 20%. Hence 8.3 x 1.2	10.0 l/h
Current lead loss at 800 Amps	1.2 l/h
Heat load from median plane penetration	2.0 i/l
Miscellaneous	1.8 1/h
Total	15.0 l/h
Refrigeration load at 4.2 K (taking 10 l/h = 38 watts)	57 watts
Cryopumping load for three pumps (20 watts per cryo-pump)	60 watts
Total	117 watts

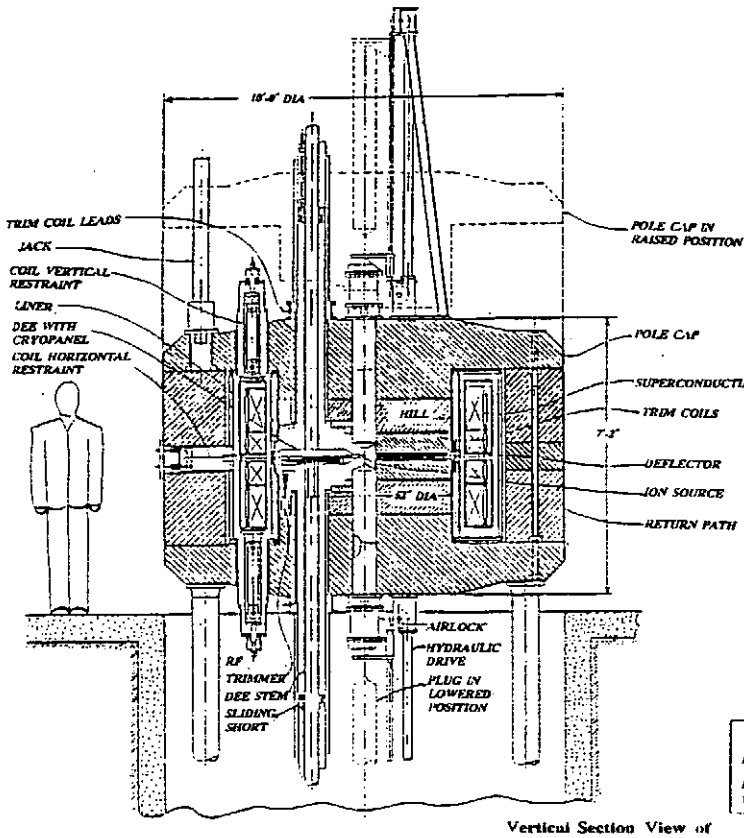

Vertical Section View of the 500 MeV Cyclotron.

FIG. 1

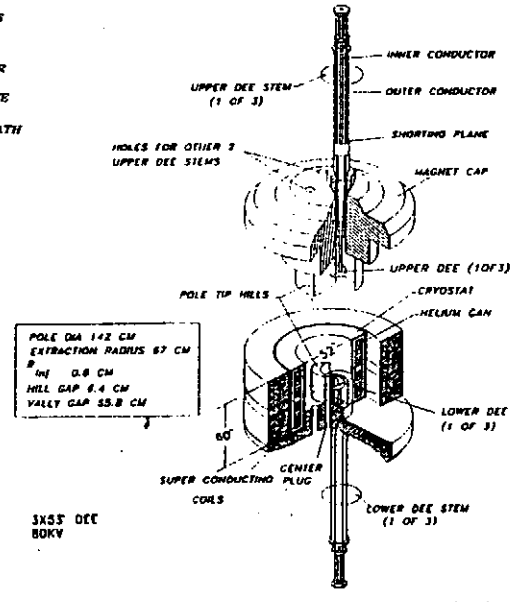

CROSS SECTIONAL VIEW OF K-500 SUPERCONDUCTING CYCLOTRON FOR VECC

FIG 2.

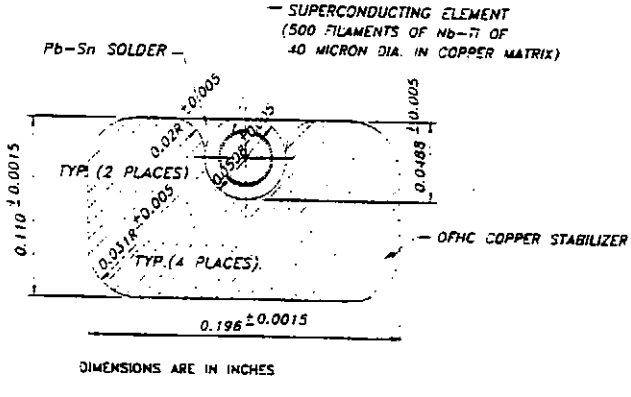

CONDUCTOR CROSS SECTION

FIG 3.

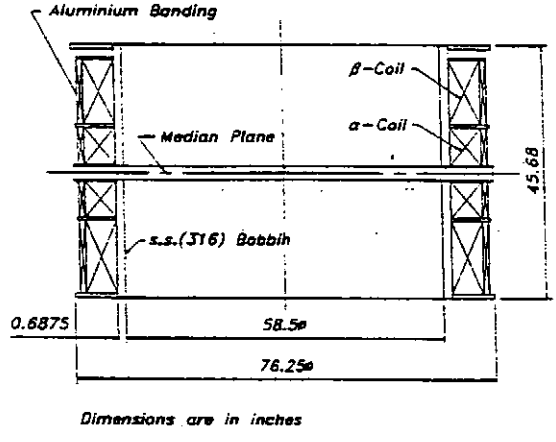

CROSS SECTIONAL VIEW OF COIL AND BOBBIN

FIG. 4.

Design of Superfluid-cooled Cryostat for 1 GHz NMR Spectrometer

A. Sato*, T. Kiyoshi*, H. Wada*, H. Maeda*, S. Itoh** and Y. Kawate**
* National Research Institute for Metals, 1-2-1 Sengen, Tsukuba 305, Japan
** Kobe Steel, Ltd., Electronics Research Laboratory, 1-5-5 Takatsukadai, Nishi-ku, Kobe 651-22, Japan

ABSTRACT

The basic design of one gigahertz NMR spectrometer is being carried forward. A magnetic field of more than 23.5 T for this spectrometer will be achieved by the superfluid cooling technology. The superfluid helium cryostat for an outer superconducting magnet with a cold bore of about 150 mm was designed. Some technical points have become clear. Safety of the cryostat involving a magnet with a huge stored energy of 50 MJ has been checked. The amount of cryogen in the magnet vessel should be less than 100 L. The consumption rate of 708 cc/hr has been estimated.

INTRODUCTION

Tsukuba Magnet Laboratory (TML) of National Research Institute for Metals has started the second Multi-core research project for the development of a one gigahertz NMR spectrometer. A magnetic field of more than 23.5 T for this spectrometer is a challenging target, but will be achieved, using a newly developed oxide superconducting coil in a backup field of 21.1 T.

The cryogenic system consists of two sections: one is a 4 K pool boiling part for the oxide superconducting insert coil, and the other is a superfluid helium cryostat for an outer superconducting magnet with a field over 21 T in a cold bore of about 150 mm. Superfluid cooling is one of the key technologies necessary to achieve a high field of more than 21 T in such a large bore, effectively increasing the critical current for superconducting wire.

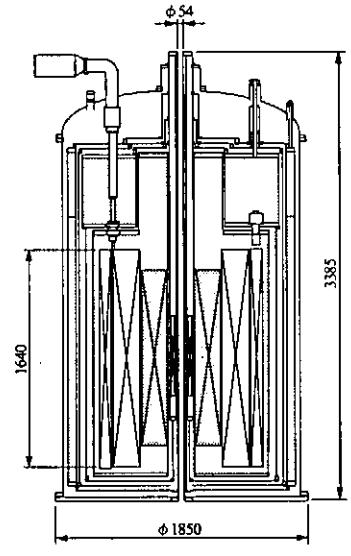

Figure 1 Overview of the 1 GHz NMR cryostat

The magnet design is being carried out for several types. The final design will depend on superconducting wire development status in the coming few years. We took the following magnet size for granted in the cryostat design. The magnet size was supposed to be 1200 mm in diameter and 1500 mm in height. The total weight of the magnet will be 8 tons. The magnet has a peculiarity in its superconducting joints; inner Nb_3Sn coils have superconducting joints 400 mm above the upper surface of the coils as shown in Figure 2.

This paper will describe a basic cryostat design for this magnet, and point out problems to be solved for the superfluid helium cryogenic system for an NMR spectrometer.

BASIC DESIGN OF CRYOSTAT

Pressurized superfluid helium cooling has been adopted to achieve long term operation and cryogen reduction in a magnet cryostat, resulting in cryostat compactness and safety insurance in case of a magnet quench.

A helium I vessel that supplies coolant to the heat exchanger for cooling helium II is located in the doughnut space around Nb_3Sn superconducting joints as shown in Figures 1 and 2. The helium I vessel capacity is 650 L. Power leads will be removed after energizing the magnet and current transfer to the Persistent Current Switch (PCS). The PCS will be situated in the helium I vessel, preventing heat loss in the helium II vessel during the energizing process, whereas protection resistance and diode will be located in the helium II vessel.

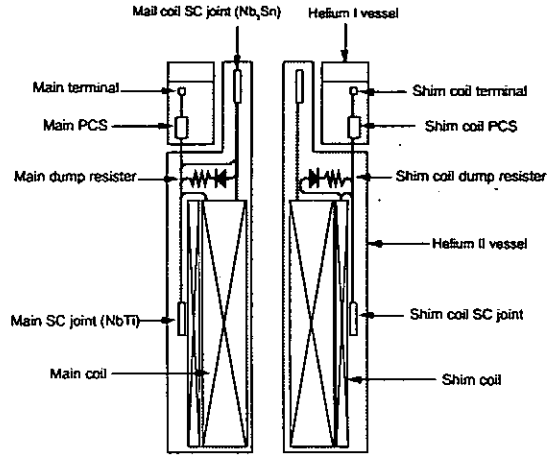

Figure 2 Arrangement of the NMR magnet, the superconducting joints and the helium I vessel.

The superfluid helium acts as a superconductivity stabilizer especially for bare superconducting wire because of its excellent heat transfer characteristics. In our case, however, all of the coils are impregnated solenoid, so the magnet is almost in an adiabatic condition in the superfluid helium. The superfluid helium thus acts as only a temperature stabilizer.

The amount of helium II coolant is a kind of trade-off between temperature stabilization and cryostat security. In this design, a helium II vessel coolant capacity of less than 100 L has been selected. The heat capacity of 100 L superfluid helium at 1.8 K is 43.4 kJ/K, so an accidental decrease of cooling power of one Watt would increase the superfluid bath temperature by only 1.38 mK/min. It means that the heat capacity is large enough for temperature stabilization.

100 L of coolant is very small compared with the volume of the magnet. Reduction of the coolant amount in the helium II vessel to less than 100 L will be achieved by filling some compound in the magnet vessel.

SAFETY ANALYSIS IN CASE OF QUENCH

In the case of a quench the magnet will release its storage energy of about 50 MJ. The storage energy will be consumed as Joule heat loss in the magnet, and the magnet temperature will increase up to about 80 K in a few seconds. The superfluid helium around the magnet will begin to increase its temperature and will then evaporate at saturated temperature in the closed helium II vessel. The only exit of evaporated gas is a cold safety valve connecting to the helium I vessel. The flow rate will achieve to a maximum value of 340 L/s in the case where release pressure is 0.14 MPa. Therefore the maximum flow rate through the cold safety valve is estimated to be 4.3 m/s when the valve diameter is 50 mm. All of the liquid coolant inside the magnet vessel will be changed to gas in 1.6 seconds if helium II coolant is 80 L under film boiling assumption, and the release flow rate will decrease to 267 L/s. In this estimate, a cold safety valve of diameter of 50 mm has suffi-

cient capacity for the relief valve.

For redundancy, in case of an accident with the cold safety valve, a rupture disk that will release high pressure gas to adiabatic vacuum space and a drop-off valve on the outer shell of the cryostat will be fitted.

THERMAL DESIGN

The superfluid heat exchanger in the magnet vessel cools down the helium under conditions of atmospheric pressure. The superfluid heat exchanger is exhausted by a 200 L/min vacuum pump in a steady state at 1.8 K. An alternative vacuum pump is used when maintenance is required. An auxiliary pump with an exhausting rate of 6000 L/min will be used in the precooling process from 4 K to 1.8 K, resulting in a reduction of cooling time to half a day.

Coolant supplied from the helium I vessel through the Joule-Tomson (JT) valve flows in a mist state through the heat exchanger, and evaporates on the inner surface of the heat exchanger to cool down the outside helium in the magnet vessel.

Temperature differences between pressurized helium and saturated helium in the heat exchanger are controlled by the JT valve in a certain value to keep the magnet temperature steady. The stable controllability of the temperature difference control method has been confirmed by the authors [1,2].

There are three types of thermal radiation shield including Gas Cooled Shield (GCS). The 80 K- shield is cooled by liquid nitrogen, and the 4 K-shield for the 1.8 K magnet vessel is cooled by helium I. The magnet vessel is supported directly from the outer vessel by an FRP supporting rods thermally-anchored at 4 K and 80 K and the intermediate GCS temperature, respectively, considering mechanical stiffness.

Thermal flows for the cryostat are shown in Figure 3. An example of the thermal balance calculation result is summarized in Table 1. Total consumption rate of liquid helium has been calulated to be 708 cc/hr. Liquid helium is mainly consumed in the insert Dewar that is designed so as to exchange an oxide superconducting magnet.

We plan to supply liquid helium at the rate of one 500 L Dewar every month. The consumption rate almost satisfies this specification.

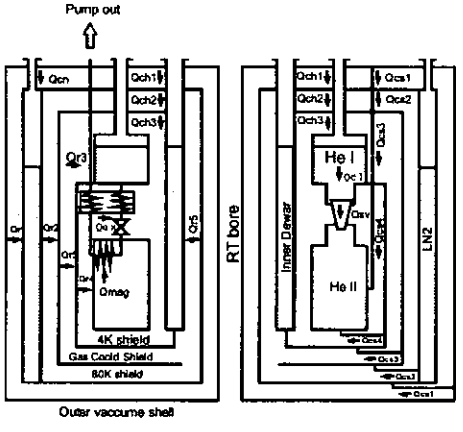

Qch Conduction through neck tube (helium)
Qcn Conduction through neck tube (nitrogen)
Qcs Conduction throuh supporting rod
Qcl Conduction in liquid helium
Qr Radiation
Qsv Super-leak of liquid helium

Figure 3 Thermal flow model for calculation.

PROBLEMS IN LIQUID HELIUM SUPPLY SYSTEM

The liquid helium supply will seriously affect the temperature distribution in the helium I vessel, especially in the bottom part of the vessel where lambda point superfluid helium layer is formed in a steady state. Any temperature increase around the communication

Table 1 An example of the thermal balance calculation result, where OVC and GCS are the Outer Vacuum Can and the Gas Cooled Shield, respectively; LN_2 means thermal shield of liquid nitrogen or the stage of 77K; He I and He II also represent its temperature stage.

Heat Flow Path	OVC ~ LN_2	LN_2 ~ GCS	LN_2 ~ He I	GCS ~ He I	He I ~ He II
Radiation	50.6	0.997	8.45×10^{-3}	0.0190	7.53×10^{-6}
Supporting Rods	2.04	0.162		0.133	2.99×10^{-3}
Neck tube (He)	0.519	0.045		0.0164	
Neck tube (N_2)	0.229				
Insert Dewar	8.20	0.593		0.216	
Feedtrough				9.12×10^{-3}	5.76×10^{-3}
Communication Channels					0.112
Total	61.6	1.80	8.45×10^{-3}	0.394	0.121

(in Watt)

Liquid helium supplied to the superfluid heat exchanger	5.75×10^{-3} g/s 166 cc/hr @ 4.2 K; 1 atm
Exhausting rate from the superfluid heat exchanger	90.8 L/min @ 300 K
Boil-off rate of liquid helium (Helium I vessel)	184 cc/hr
Boil-off rate of liquid helium (Insert Dewar)	359 cc/hr
Total consumption rate of liquid helium	708 cc/hr @ 4.2 K; 1 atm
Total consumption rate of liquid nitrogen	1450 cc/hr @ 77 K; 1 atm

channel such as the safety valve will induce an effective cooling power decrease. Any temperature change would affect the persistent current of the superconducting magnet with many superconducting joints and induce a magnet quench in the worst case. Therefore one of the key technologies necessary for a stable long term operation of an NMR spectrometer is a reliable liquid helium supply system. A detailed design of the liquid helium supply line exit and the helium I vessel structure will be carried out in the next stage, avoiding disturbance around the communication channel.

SUMMARY

In this basic design some technical points have become clear. The amount of cryogen in the magnet vessel is designed to be less than 100 L, which will ensure cryostat insurance in the case of a magnet quench. Safety of the cryostat involving a magnet with a huge stored energy of 50 MJ has been checked. Precooling of the magnet in the restricted space is a remaining problem. The estimated consumption rate of 708 cc/hr for liquid helium will allow the monthly supply system by one 500 L helium Dewar. We will continue the cryostat design and research and development works to obtain design data.

REFERENCES

1 Watanabe, K., Noto, K., Muto, Y., Maeda, H., Sato, A., Suzuki, E., and Uchiyama Y., Research and Development for Pressurized He II Cooled Superconducting Magnets Sci. Rep. RITU (1986) A-33 297 - 306

2 Noto, K., Watanabe, K., , Muto, Y., Sato, A., Horigami, O., Ogiwara, H., Nakamura, S., Suzuki, E., NbTiHf-High Field Superconducting Magnet in 1.8 K-pressurized Liquid He II Proc. ICEC-10 (1984, Helsinki) 181 - 184

NUMERICAL SIMULATION OF BASIC CRYOGENIC SYSTEMS

M. Kauschke, H. Quack
Technische Universität Dresden
Institut für Energiemaschinen und Maschinenlabor
Lehrstuhl für Kälte- und Kryotechnik
01062 Dresden, Germany

Abstract

The key for an optimum design of cryogenic refrigerators is previous knowledge of the problems, which may appear by scaling up test facilities to a larger system. Therefore the development of simulation tools for cryogenic systems is forced.
However, the simulation algorithm have to be sensitive to cryogenic components, which react fast onto changes in working conditions as well as to components with an large inertia. In respect of having the possibility of varying several parameter the calculation time have to be reasonable. Our attempt of creating a suitable simulation tool is presented.

Introduction

For the development of new cryogenic refrigerators it is helpful to use numerical simulation before the technical drawings for the components are made. These numerical simulations give insights into the behaviour of the system and thus allow for study of certain transient phenomena which may cause instability. For the simulation it is necessary to assemble a mathematic model of the system. The assumptions made by deriving this set of equations should be investigated carefully. The underlying physical laws are derived from mass- and energy balances for every component such as compressor, heat exchanger, throttle valve, expansion machines etc.
They lead to a set of partial and ordinary differential equations in combination with algebraic equations. For the numerical simulation a solution for this set have to be found for consecutive time steps. For running the simulation on off-the-shelf mainframe computers the slow and the fast components have to be identified in the system. A modification of the components with large inertia only every x-th timesteps will help to save CPU time. This way of using different stepsizes in time and distance for different components is possible.

Three types of equations and their solution

The system can be described by the equations for the energy and the mass balance, which include partial and ordinary differential as well as algebraic equations:

mass balance: $$\left.\frac{\partial}{\partial t}M\right|_{i,j} = \left.\frac{\partial}{\partial x}\dot{m}\right|_{i,j} dx$$

energy balance : $$\left.\frac{\partial}{\partial t}(Mh)\right|_{i,j} = -\left.\frac{\partial}{\partial x}(\dot{m}h)\right|_{i,j} dx - (kA)_{i,j}(T_{i,j} - T_w)$$

Every component of the system is divided into a number of single elements. For every element the relevant equations are assembled. The length of an element within each component depends on the velocity of the fluid. The reference distance is the one which allows the fluid to pass through it during the timestep given. In practice to get stable results, the actual length must be about half of this distance. This holds true for the numerical solution using explicit solving algorithms. The tool we used, utilises the method of lines method to modify the partial differential equations into ordinary ones. Once this has been achieved, the differential algebraic equation (DAE) system is solved by using a readily available DAE-solver [1], [2]. There is an advantage of not evaluating certain elements of the mathematical system every time the DAE is doing an iteration loop to find the solution for a particular time step.
We can identify certain elements of the system which change relatively little when subjected to high gradients at the inlet. By calculating the output of those slow changing elements every x-th time step, considerable savings can be made with no loss in model accuracy. This algorithm is shown in figure 1.

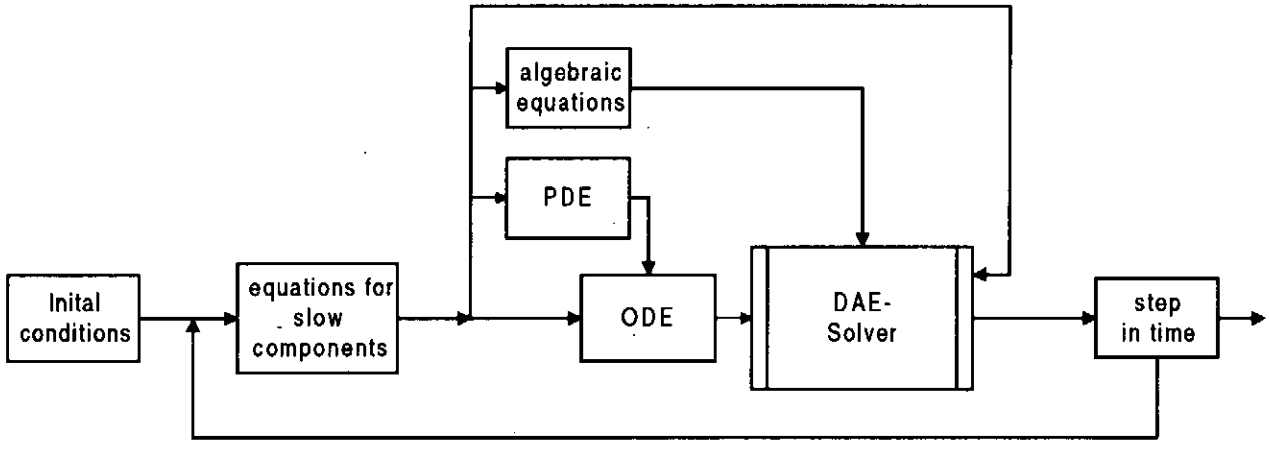

Figure 1: flow diagram of the simulation algorithm

Heat exchanger material and fluid properties

The properties of the refrigerant (helium) and the heat exchanger material have to be evaluated at each point in time and space. To handle this effectively, explicit equations for all the needed property routines for helium in both one and two phase area have been assembled.
We subdivided the p-T plane into several domains and used interpolation methods to get equations for entropy, enthalpy, specific volume and mass fraction of vapour. The output of these equations compare reasonably well compared to the NIST equation of state [3], with typical errors being in the order of one percent.
From the data given by Klipping [4], we formulated algebraic equations for the thermal properties of aluminium and stainless steel.

The temperature profile during the cool down of Joule-Thomson heat exchanger is shown. On the cold end the high pressure stream is expanded and the liquid phase separated, when appearing. The mass accumulation in the exchanger is considered.

The temperature versus the time-distance plan is shown in figure 2 and 3. The extension of the heat exchanger is depict in x-direction. The y-direction is representing the time and the vertical axis the temperature. The difference between both figures is the viewpoint onto the exchanger. Figure 2 shows the profile from the warm, figure 3 from the cold end.

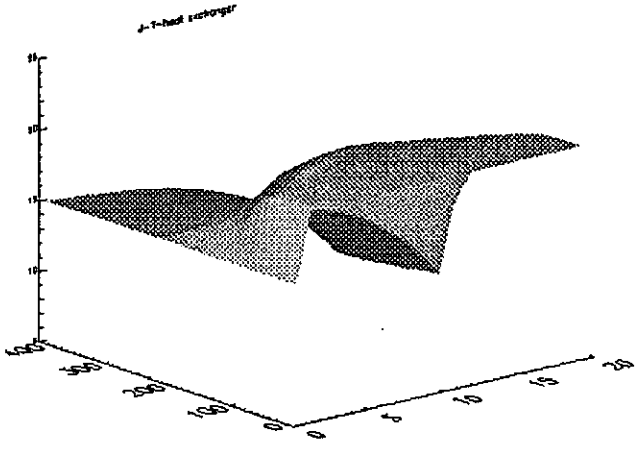

Figure 2: temperature profile of the high pressure stream, seen from the warm end

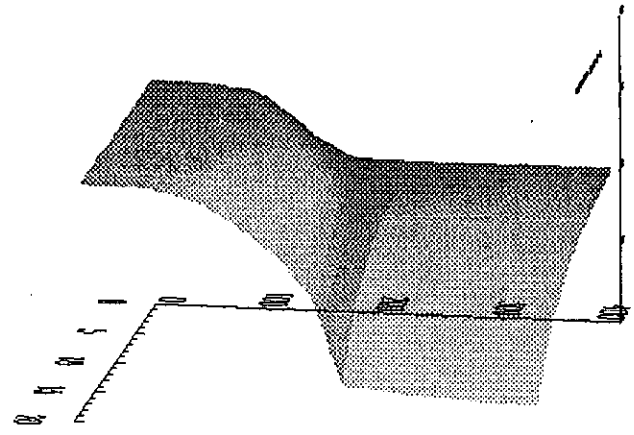

Figure 3: temperature profile of the high pressure stream, seen from the cold end

Acknowledgements

The authors acknowledge the support of DESY (Deutsches Elektronen-Synchrotron) for funding this research project.

References

[1] C.A. Silebi, W. E. Schiesser, Dynamic Modelling of Transport Process Systems, Academic Press Inc., San Diego (1992)

[2] Petzold, L.: Computing and Mathematics Research Division, Lawrence Livermore National Laboratory

[3] NIST Standard Reference Database 12 (Helium), National Institute of Standards and Technology, (1992)

[4] Klipping, I. In: Handbuch der Kryotechnik Grundlagen, Entwicklungsstand, Anwendungen und Entwicklungstendenzen, VDI Bildungswerk, (1981)

DESIGN CONSIDERATIONS FOR VERY LARGE HELIUM REFRIGERATION SYSTEM

Andres Kündig, Karl Löhlein, Bruno Ziegler
Linde Kryotechnik AG, Dättlikonerstr. 5, 8422 Pfungen, Switzerland

ABSTRACT

Future fusion reactors will require very large cryogenic refrigerators to cool their superconducting magnet systems.

The total capacity required is roughly 5 times above the largest cryogenic system presently existing. For redundancy reasons however the capacity will be provided by several parallel plants. The step from today's state of technology to future needs therefore is moderate.

The paper presents a draft design of a 150 kW / 4.5 K Helium refrigeration system and compares it to today's state of technology.

Development needs are identified, which on one hand result from the high capacity and on the other hand are based on weaknesses of today's technology.

INTRODUCTION

As a supplier of cryogenic plants we are looking forward to the challenge of developing very large cryogenic cooling systems for fusion and there are several questions we ask ourselves in this context.

- Are we in a position to build such a system and to accept the corresponding responsibilities?
- How would such a plant look like?
- What might and what must be improved in the present design?

DESIGN BASE

The following assumptions were used for the design of the cryogenic plant:

- The thermal contact between refrigeration system and magnet system is accomplished by a closed pumped helium loop. The supply temperature of the loop is 4.5 K.
- The refrigeration system provides 150 kW refrigeration at 4.4 K.
- The refrigeration system is able to provide a part or all of its capacity as liquefaction.
- The system is designed for very high availability.
- Maintenance can be done without interruption of operation.
- The efficiency of the system is good.

AVAILABILITY AND MAINTENANCE CONSIDERATIONS

There are several approaches to fulfil the demanding requirements with regards to system availability and maintainability. Basically redundancy has to be provided for all kind of machinery and components based on their individual availability and their maintenance requirements. Operational problems of cryogenic systems in long term continuous operation are very often caused by impurities. This fact supports redundant plants rather than redundant machines only.

There is another aspect supporting the idea of redundant plants. Machinery and other components proven for this specific application are typically much smaller than required. This means that a lot of equipment has to be switched in parallel anyway.

Nitrogen precooling was chosen for several reasons:

- it provides a temperature lock at 80 K which is very helpful to keep gas purity high and thereby to improve availability,
- it reduces investment costs for the helium refrigerators and
- it offers a very high degree of availability and maintainability, if it is combined with liquid nitrogen from external sources.

BASIC PLANT CONCEPT

Based on the above our concept foresees five or six parallel helium refrigerators with one nitrogen refrigerator for precooling purposes.

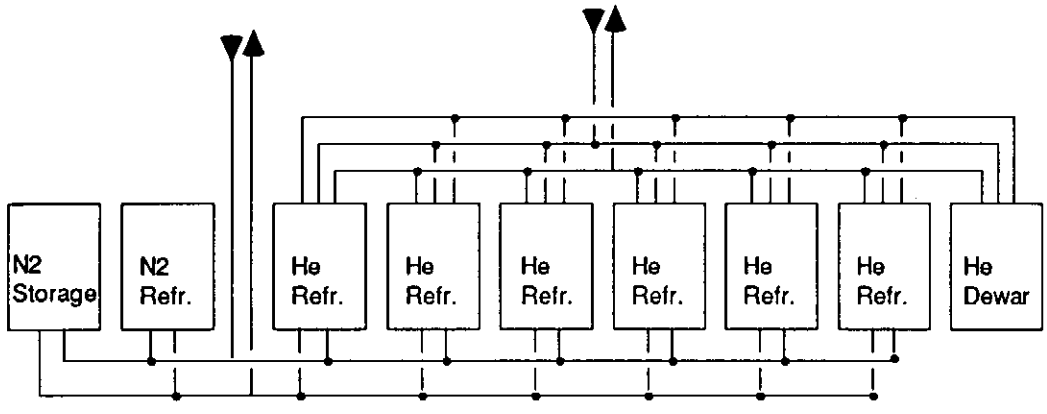

Figure 1 Refrigeration system arrangement

SAMPLE PROCESS FOR HELIUM REFRIGERATORS

We have designed a sample process with a refrigeration capacity of 30 kW at 4.4 K shown in Figure 2.

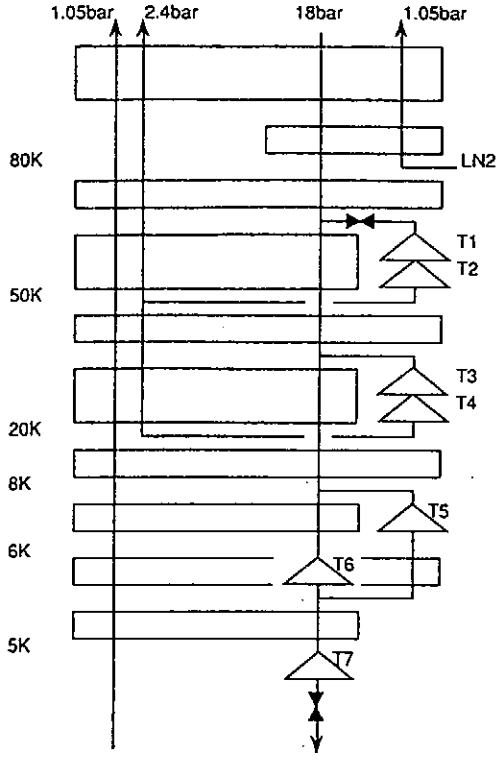

Figure 2 Sample process for 30 kW refrigeration at 4.4. K

The process is based on a total of 5 expansions for which 7 turbines are used. An overview on key process data is given in Table 1, the key components are described below.

		refrigeration	liquefaction
refrigeration at 4.4 K	[kW]	30	0
liquefaction at 4.4 K	[l/h]	0	7650
no. of turbines in operation	[ ]	5	7
liquid nitrogen consumption	[l/h]	132	936
power input He compressors	[kW]	6110	5670
power input nitrogen liquefier	[kW]	161	1150
power input total	[kW]	6271	6820
specific power input	[W/W]	209	

Table 1 Key process data for a 30 kW, 4.4 K refrigerator

In order to identify inefficiencies of the process an exergy balance is given in Table 2 for the two operating modes.

source of inefficiency		refrigeration	liquefaction
Electrical motors	%	5	5
Helium compressors	%	42	36
Nitrogen compressors	%	1	5
Heatexchangers	%	12	13
Turbines (expansion)	%	6	7
Turbines (brakes)	%	1	2
Throttling	%	-	3
Nitrogen coldbox	%	1	3
Product	%	32	26

Table2 Exergy balance of the process

Compressors: Presently oil lubricated screw compressors are considered, which offer very high availability and moderate maintenance requirements. The compression system consists of 4 machines in the first stage and 4 machines in the second stage.

Heatexchangers: Aluminum plate fin heatexchangers would be used. The total volume of the heatexchangers would be in the range of $30m^3$, the total transfer surface approximately 50 $000m^2$.

Expansions turbines: The design is based on existing turbines of the Linde TGL series with the exception of turbine 7, which in our present design is an oil bearing turbine.

Coldbox: A split design is proposed using a perlite insulated coldbox for the 300 to 80 K temperature range and a vacuum insulated coldbox for the 80 K to 4 K range.

AREAS OF IMPROVEMENTS

Helium compression

As shown in Table 2 today's design is based on rather inefficient gas compression. Reciprocation compressors would increase efficiency but also investment cost. A turbocompressor system could increase efficiency, keep gas contamination low and also reduce space requirements.

Turbines

Gas bearing turbines are prefered. Based on our present product range we would require a larger bearing system to handle the very low speed of turbine 7.

Coldbox design

The split coldbox concept leaves some flexibility with regards to higher capacity per plant.

Participants list of ***Cryogenic Systems***

for Large Scale Superconducting Applications

(NIFS symposium and JSPS-DFG Seminar)

on May 27-29, 1996 at Ceratopia-Toki and NIFS in Toki, Japan.

AKIYAMA, Yoshitane

Advanced Technology Lab.
Maekawa MFG.Co.,Ltd.
2000 Tatsuzawa, Moriya-machi,
Kitasooma-gun, Ibaraki, 302-01, Japan

phone 81-297-48-1364
fax 81-297-48-5170

AOYAMA, Takeo

Space & Cryogenic Equipment Dept.
Nippon Sanso Corporation
6-2 Kojima-cho, Kawasaki-ku,
Kawasaki-shi, 210, Japan

phone 81-44-288-6939
fax 81-44-299-4109

ASAKURA, Hajime

General Machinerty Dep.
Ishikawajima-Harima Heavy Industries Co.,Ltd.
3-2-16, Toyosu, Koto-ku,
Japan

phone 81-3-3534-2441
fax 81-3-3534-2333

BHATTACHARYA, Narayan

Department of Atomic Energy, Cryogenics Group
Variable Energy Cyclotron Center
1/AF Bidhannagar
Calcutta-700064, India

phone 91-33-3371230
fax 91-33-3346871
narayan@veccal.ernet.in

BI, Yanfang

Cryogenics Department
Institute of Plasma Physics, Academia Sinica
P.O.Box 1126
Hefei 230031, P.R.China

phone 86-551-5591-374
fax 86-551-5591-310
yfbi@ipv64a.hfcas.ac.cn

CHIKARAISHI, Hirotaka

NIFS
322-6, Oroshi-cho, Toki,
Gifu, 509-52 , Japan

phone 81-572-57-4777
fax 81-572-57-4765
hchikara@nifs.ac.jp

EJIRI, Shinichiro

Space & Cryogenic Equipment Dept.
Nippon Sanso Corporation
15-21, Tsubaki-cho, Nakamura-ku,
Nagoya, 453, Japan

phone 81-52-453-0264
fax 81-52-452-4614

FUJIWARA, Masami

NIFS
Furo-cho, Chikusa-ku, Nagoya,
464-01, Japan

phone 81-52-789-4228
fax 81-52-789-4201

GEYNISMAN, Michael

Accelerator/Cryogenics
Fermi National Accelerator Laboratory
Kirk and Pine Streets
P.O.Box 500, MS 313, Batavia, IL, USA

phone 1-708-840-2191
fax 1-708-840-4322
hope@fnal.gov

GISTAU-BAGUER, Guy

L'AIR LIQUIDE
BP 15
38360 Sassenage, France

phone 33-7643-6036
fax 33-7643-6131

GRAVIL, Bernard

Departement de Recherche sur la Fuion Controlee
C.E.A., Direction des sciences de la matiere
Centre d'Etudes de Cadarache
13108 Saint Paul lez Durance, CEDEX, France

phone 33-42-25-4570
fax 33-42-25-2661
gravil@drfc.cad.cea.fr

HABERSTROH, Christoph

Institut F. Energiemaschinen U. Maschinenlabor
Technische Universitaet Dresden
Lehrstuhl F. Kaelte- U. Kryotechnik
01062 Dresden Germany

phone 49-351-4633406
fax 49-351-4637247
chris@memkn1.mw.tu-dresden.de

HARUYAMA, Tomiyoshi

KEK National Laboratory for High Energy Physics
1-1, Oho, Tsukuba, Ibaraki,
305, Japan

phone 81-298-64-5344
fax 81-298-64-2580
haruyama@kekvax.kek.jp

HASEGAWA, Toshio

Cryogenic Div.
Aishin Seiki Co., Ltd.
2-1, Asahi-cho, Kariya,
Aichi, 448, Japan

phone 81-566-24-8860
fax 81-566-24-8859

HASHIMOTO, Naomi

Electric Power Research & Development Center
Chubu Electric Power Co., Inc.
20-1, Kitasekiyama, Ohdaka-cho,
Midori-ku, Nagoya, 459, Japan

phone 81-52-624-2180
fax 81-623-5117
nhashi@rdbgw.rd.chuden.co.jp

HIRABAYASHI, Hiromi

Cryogenics and Superconductivity Laboratories
NIFS
322-6, Oroshi-cho, Toki,
Gifu, 509-52 , Japan

phone 81-572-57-4777
fax 81-572-57-7465
yamada@scsun2b.nifs.ac.jp

HIRANO, Naoki

Electric Power Research & Development Center
Chubu Electric Power Co., Inc.
20-1, Kitasekiyama, Ohdaka-cho,
Midori-ku, Nagoya, 459, Japan

phone 81-52-624-9094
fax 81-623-5117
hirano@rdbgw.rd.chuden.co.jp

HOFMANN, Albert

Institute fue Technische Physik
Forschungszentrum Karlsruhe
Postfach 3640, D-76021,
Karlsruhe, Germany

phone 49-7247-823527
fax 49-7247-822849

HOLDENER, Fridolin

Cryogenics
WEKA AG
Schuerlistrasse 8
CH-8344 Baeretswil, Switzerland

phone 41-1-939-2959
fax 41-1-939-2963

HONDA, Tadaaki

Superconducting Magnet Laboratory
Japan Atomic Energy Research Institute
801-1 Mukaiyama, Naka-machi,
Naka-gun, Ibaraki 311-01, Japan

phone 81-29-270-7572
fax 81-29-270-7579
honda@naka.jaeri.go.jp

HORLITZ, Gerhard

MKS
Deutsches Elektronen-Synchrotron, DESY
Notkestrasse 85
22607 Hamburg Germany

phone 49-40-8998-3829
fax 49-40-8998-2858

HOSOYAMA, Kenji

National Lab. for High Energy Physics
1-1 Oho, Tsukuba-shi,
Ibaraki, 305, Japan

phone 81-298-64-5734
fax 81-298-64-5735
hosoyama@kekvax.kek.jp

ICHIKAWA, Tatsumi

Engineering Department
Super-GM
Umeda UN Bldg., 5-14-10
Nishi-tenma, Kita-ku, Osaka, 530, Japan

phone 81-6-361-1051
fax 81-6-361-1437
ldm04314@niftyserve.or.jp

IIYOSHI, Atsuo

NIFS
Furo-cho, Chikusa-ku, Nagoya,
464-01, Japan

phone 81-52-789-4501
fax 81-52-789-4200

IMAGAWA, Shinsaku

NIFS
322-6, Oroshi-cho, Toki,
Gifu, 509-52 , Japan

phone 81-572-57-5618
fax 81-572-57-5600
imagawa@nifs.ac.jp

ISHIWATA, Kiyoshi

Space & Cryogenic Equipment Dep.
Nippon Sanso Corp.
6-2, Kojima-cho, Kawasaki-ku, Kawasaki,
210 Japan

phone 81-44-288-6940
fax 81-44-299-4109

ITO, Satoshi

Kobe Steel, Ltd.
1-5-5, Takatsukadai, Nishi-ku,
Kobe, 651-22, Japan

phone 81-78-992-5653
fax 81-78-992-5650
aa16911@giken.kobelco.co.jp

ITOH, Satoshi

Research Institute for Applied Mechanics
Kyushu University
87, Kasuga,
816 Japan

phone 81-92-574-2578
fax 81-92-573-6899
itoh@triam.kyushu-u.ac.jp

IWAMOTO, Akifumi

NIFS
322-6, Oroshi-cho, Toki,
Gifu, 509-52 , Japan

phone 81-572-57-4777
fax 81-572-57-7465
iwamoto@nifs.ac.jp

JIA, Lin Xiang

Alternating Gradient Synchrotron Department
Brookhaven National Laboratory
BLDG. No. 911A,
Upton, New York, 11793, USA

phone 1-516-344-3977
fax 1-516-344-5954
jia@bnldag.bnl.gov

KATADA, Minoru

Nippon Sanso Corporation
6-2 Kojima-cho, Kawasaki-ku,
Kawasaki-shiÂ@210, Japan

phone 81-44-288-6973
fax 81-44-288-2680

KATO, Takashi

Superconducting Magnet Laboratory
Japan Atomic Energy Research Institute
801-1, Mukaiyama, Naka-machi,
Naka-gun, Ibaraki, 311-01, Japan

phone 81-29-270-7572
fax 81-29-270-7579
kato@naka.jaeri.go.jp

KATO, Yudai

NIFS
322-6, Oroshi-cho, Toki,
Gifu, 509-52 , Japan

phone 81-572-57-5634
fax 81-572-57-5600

KAUSCHKE, Marion

Lehrstuhl F. Kaelte- U. Kryotechnik
Technische Universitaet Dresden
TU Dresden
01062 Dresden Germany

phone 49-351-463-2815
fax 49-351-463-7247
marion@memkn1.mw.tu-dresden.de

KIMURA, Nobuhiro

Engineering Research & Scientific Support Centers
National Laboratory for High Energy Physics
1-1 Oho, Tsukuba-shi,
Ibaraki 305, Japan

phone 81-298-64-5461
fax 81-298-64-3209
kimuran@kekvax.kek.jp

KIYOSHI, Tsukasa

Tsukuba Magnet Laboratories
National Research Institute for Metals
3-13 Sakura, Tsukuba,
Ibaraki 305, Japan

phone 81-298-53-1187
fax 81-298-53-1199
kiyoshit@nrim.go.jp

KOMAREK, Peter

Institute fue Technische Physik
Forschungszentrum Karlsruhe
P.O.Box 36 40
76021 Karlsruhe, Germany

phone 49-7247-82-3500
fax 49-7247-82-2849
peter komarek@ccmailgw.fzk.de

LEBRUN, Philippe

LHC Division
CERN
CH-1211
Geneva 23 Switzerland

phone 41-22-767-5778
fax 41-22-767-8666
philippe.lebrun@cern.ch

LEHMANN, Wolfgang

Institute fue Technische Physik
Forschungszentrum Karlsruhe
Postfach 3640, D-76021,
Karlsruhe, Germany

phone 49-7247-923520
fax 49-7247-822849

LIERL, Holger

MKS1
Deutsches Elektronen-Synchrotron, DESY
Notkestrasse 85
D 22607 Hamburg Germany

phone 49-40-8998-3959
fax 49-40-8998-2858

MAEKAWA, Ryuji

NIFS
322-6, Oroshi-cho, Toki,
Gifu, 509-52, Japan

phone 81-572-57-4777
fax 81-572-57-7465

MASUDA, Yoshihiko

Space & Cryogenic Equipment Dept.
Nippon Sanso Corporation
6-2 Kojima-cho, Kawasaki-ku,
Kawasaki-shi 210, Japan

phone 81-44-288-4063
fax 81-44-299-4109

MITO, Toshiyuki

NIFS
322-6, Oroshi-cho, Toki,
Gifu, 509-52, Japan

phone 81-572-57-4777
fax 81-572-57-7465

MIYAKE, Akihiro

Advanced Technology Engineering Dept.
Ishikawajima-Harima Heavy Industries Co.,Ltd.
2-16 Toyosu, 3-chome, Koto-ku,
Tokyo, 135, Japan

phone 81-3-3534-2968
fax 81-3-3534-3104
miyake-a@plant.ty.ihi.co.jp

MORI, Mikio

Advanced Technology Engineering Dept.
Ishikawajima-Harima Heavy Industries Co.,Ltd.
2-16 Toyosu, 3-chome, Koto-ku,
Tokyo, 135, Japan

phone 81-3-3534-2968
fax 81-3-3534-3104
mori-m@plant.ty.ihi.co.jp

MOTOJIMA, Osamu

NIFS
322-6, Oroshi-cho, Toki,
Gifu, 509-52, Japan

phone 81-572-57-5601
fax 81-572-57-5600

MURAKAMI, Yoshishige

Fukui Institute of Technology

phone
fax

NAGAMI, Masakazu

Plant & Machinery Div.
Nippon Sanso Corporation
6-2 Kojima-cho, Kawasaki-ku,
Kawasaki-shi, 210, Japan

phone 81-44-288-2492
fax 81-44-288-2727
m-nagami@pl.sanso.co.jp

NAKASHIMA, Hiroshi

Maglev System Development Department
Railway Technical Research Institute
2-8-38, Hikari-cho, Kokubunji-shi,
Tokyo, 185, Japan

phone 81-425-73-7491
fax 81-425-73-7352
nakasima@magcgol.rtri.or.jp

NISHIDA, Kazuhiko

Engineering & Machinery Div.
Kobe Steel, Ltd.
1-6-14 Edobori, Nishi-ku,
Osaka, 550, Japan

phone 81-6-444-6126
fax 81-6-444-7684

NISHIMURA, Arata

NIFS
322-6, Oroshi-cho, Toki,
Gifu, 509-52, Japan

phone 81-572-57-4777
fax 81-572-57-7465

OBERT, Wolfgang

JET Joint Undertaking
Abingdon, OXON,
OX14 3EA, UK

phone 44-1235-464628
fax 44-1235-464626
wo@jet.uk

OGINO, Osamu

Nuclear Fusion Development Dept.
Mitsubishi Electric Corporation
1-13-14, Namaze-cho, Nishinomiya,
669-11, Japan

phone 81-797-84-1485
fax 81-797-84-1485

OHUCHI, Norihito

Accelerator Department
KEK National Laboratory for High Energy Physics
1-1 Oho, Tsukuba-shi,
Ibaraki, 305, Japan

phone 81-298-64-5243
fax 81-298-64-3182
ohuchi@kekvax.kek.jp

OKAMURA, Tetsuji

Dept. of Energy Sciences
Tokyo Institute of Technology
4259 Nagatsuta, Midori-ku,
Yokohama, 226, Japan

phone 81-45-924-5664
fax 81-45-921-1318
tokamura@es.titech.ac.jp

PFOTENHAUER, John M.

Mechanical Enjineering
University of Wisconsin-Madison
1500 Engineering Dr.
Madison, WI 53706 USA

phone 1-608-263-4082
fax 1-608-263-1087
pfot@engr.wisc.edu

QUACK, Hans

Institut F. Energiemaschinen U. Maschinenlabor
Technische Universitaet Dresden
Lehrstuhl F. Kaelte- U. Kryotechnik
01062 Dresden Germany

phone 49-351-4632548
fax 49-351-4637247
quack@memkn1.mw.tu-dresden.de

REHAK, Margareta

RHIC
Brookhaven National Laboratory
Upton, WY, 11973-5000, USA

phone 1-516-344-4708
fax
rossum@bnl

ROUSSET, Bernard

DRFNC/SBT
C.E.A
CEA-6, 17 avenue des Martyrs
38054, Grenoble, Cedex 9, France

phone 33-76-88-5959
fax 33-79-88-5084
rousset@drfmc.ceng.cea.fr

RUEHLICH, Ingo

Technische Universitaet Dresden
Lehrstuhl F. Kaelte- U. Kryotechnik
01062 Dresden Germany

phone 49-351-4634048
fax 49-351-4637247
ingo@memkn1.mw.tn-dresden.de

SAJI, Nobuyoshi

General Machinerty Dep.
Ishikawajima-Harima Heavy Industries Co.,Ltd.
3-2-16, Toyosu, Koto-ku,
Japan

phone 81-3-3534-2416
fax 81-3-3534-2333

SAKAMOTO, Mizuki

Research Institute for Applied Mechanics
Kyushu University
87, Kasuga,
816 Japan

phone
fax

SARKAR, Biswanath

Magnet and Cryosystem
Institute for Plasma Research
Near Indira Bridge, Bhat,
Gandhinagar-382424, India

phone 91-7864690/7864023
fax 91-79-7864310
sarkar@plasma.ernet.in

SATO, Akio

Tsukuba Magnet Laboratory
National Research Institute for Metals
3-13, Sakura,
Tsukuba, 305, Japan

phone 81-298-53-1189
fax 81-298-53-1202
asat@nrim.go.jp

SATOH, Sadao

Dep. of Large Helical Device
NIFS
Furo-cho, Chikusa-ku,
Nagoya 464-01, Japan

phone 81-52-789-4544
fax 81-52-789-4248
ssatoh@scsun2b.nifs.ac.jp

SATOW, Takashi

NIFS
322-6, Oroshi-cho, Toki,
Gifu, 509-52, Japan

phone 81-572-57-5612
fax 81-572-57-5600

SCHAUER, Felix

Experimental Plasma Physics 2
Max-Planck-Institut fue Plasmaphysik
Boltzmannstr. 2
D-85748 Garching, Germany

phone 49-89-3299-1781
fax 49-89-3299-2579
Schauer@ipp.mpg.de

SENN, Armin-E.

Sales 8 Projects
Linde Kryotechnik AG
Daettlikonerstr.5, P.O.Box
CH-8422 Pfungen, Switzerland

phone 41-52-304-0518
fax 41-52-304-0550

SEO, Kazutaka

Mitsubishi Electirc Corporation
8-1-1, Tsukaguchi-Honmachi, Amagasaki,
Japan

phone 81-6-497-7127
fax 81-6-497-7288
seo@ele.crl.melco.co.jp

SHIMIZU, Noriyuki

Dept. of Electrical Engineering
Nagoya University
Furo-cho, Chikusa-ku,
Nagoya 464-01, Japan

phone 81-52-789-3633
fax 81-52-789-3161
shimizu@nuee.nagoya-u.ac.jp

SHINTOMI, Takakazu

Cryogenics Center
National Lab. for High Energy Physics
1-1 Oho, Tsukuba,
Ibaraki 305, Japan

phone 81-298-64-5452
fax 81-298-64-4051
shintomi@kekvax.kek.jp

SMITH, Kevin

Special Projects
Oxford Instruments
Unit 14 Oakfields Industrial Estate,
Eynsham, Witney, Oxon, OX8 1TH, UK

phone 44-1865-883988
fax 44-1865-883891
kevin.smith@oxinst.co.uk

SUESSER, Manfred

Institut fue Technische Physik
Forschungszentrum Karlsruhe
P.B.3640
D-76021 Karlsruhe, Germany

phone 49-7247-823930
fax 49-7247-822849

TACHIKAWA, Kyoji

Faculty of Engineering
Tokai University
1117 Kitakaname, Hiratsuka,
Kanagawa, 259-12, Japan

phone 81-463-58-1211
fax 81-463-58-1812
tacsuper@keyaki.cc.u-tokai.ac.jp

TAKAHATA, Kazuya

NIFS
322-6, Oroshi-cho, Toki,
Gifu, 509-52 , Japan

phone 81-572-57-4777
fax 81-572-57-7465
takahata@nifs.ac.jp

TAKAI, Yoshiaki

Department of Energy Engineering & Science
Nagoya University
Furo-cho, Chikusa-ku
Nagoya 464-01, Japan

phone 81-52-789-3159
fax 81-52-789-3441
takai@nuee.nagoya-u.ac.jp

TAKEO, Masakatsu

Fac. of Engineering
Kyushu University
6-10-1, Hakozaki, Higashi-ku,
Fukuoka, 812, Japan

phone 81-92-642-4024
fax 81-92-632-2438
takeo@ees.kyushu-u.ac.jp

TAKIZAWA, Hiroshi

Space & Cryogenic Equipment Div.
Nippon Sanso Corporation
15-21 Tsubaki-cho, Nakamura-ku,
Nagoya 453 Japan

phone 81-52-453-0263
fax 81-52-452-4614

TAMURA, Hitoshi

NIFS
322-6, Oroshi-cho, Toki,
Gifu, 509-52 , Japan

phone 81-572-57-5619
fax 81-572-57-5600
tamura@nifs.ac.jp

TANAHASHI, Shugo

NIFS
322-6, Oroshi-cho, Toki,
Gifu, 509-52 , Japan

phone 81-572-57-5606
fax 81-572-57-5600
tanahasi@roprint.nifs.ac.jp

TANEDA, Masanobu

Japan Atomic Energy Research Institute
801-1 Mukaiyama, Naka-machi,
Naka-gun, Ibaraki, 311-01, Japan

phone 81-29-270-7572
fax 81-29-270-7579
taneda@scml.naka.jaeri.go.jp

UEDA, Sei

Faculty of Engineering
Tohoku University
Aramaki-aza-Aoba, Aoba-ku,
Sendai, 980-77, Japan

phone 81-22-217-7342
fax 81-22-217-7374
ueda@msws.material.tohoku.ac.jp

UEDE, Toshio

Engineering Department, Nuclear Power Division
Fuji Electric Co., Ltd.
1-1 Tanabeshinndenn, Kawasaki-ku,
Kawasaki, Japan

phone 81-44-329-2188
fax 81-44-329-2176
ueda@ksk.fujielectric.co.jp

VANSCIVER, Steven W.

National High Magnetic Field Laboratory
Florida State University
1800 E. Paul Dirac Drive
Tallahassee, FL 32310, USA

phone 1-904-644-0998
fax 1-904-644-0867
vnsciver@magnet.fsu.edu

Vysotsky, Vitaly

Electronics Engineering
Kyushu University
6-10-1, Hakozaki, Higashi-ku
Fukuoka 812, Japan

phone 81-92-641-3909
fax 81-92-632-2438
vysotsky@pfc.mit.edu

WACHI, Yoshihiro

Heavy Apparatus Eng. Lab.
Toshiba Corporation
2-4 Suehiro-cho, Tsurumi-ku,
Yokohama 230, Japan

phone 81-45-510-6696
fax 81-45-500-1427
000092060051@tkoi.tg-mail.toshiba.co.jp

WATANABE, Kiyomasa

NIFS
322-6, Oroshi-cho, Toki,
Gifu, 509-52, Japan

phone 81-572-57-5616
fax 81-572-57-5600

WATANABE, Yukio

Energy & Machinery Division
Kobe Steel, Ltd.
1-6-14 Edobori, Nishi-ku,
Osaka, 550, Japan

phone 81-6-444-7646
fax 81-6-444-7684
yuki.watanabe@enginet.kobelco.co.jp

WOLFF, Siegfried

MKS
DESY
Notkestrasse 85
22603 Hamburg, Germany

phone 49-40-89983409
fax 49-40-89982858
swolff@desy.de

YAMADA, Hiroshi

NIFS
322-6, Oroshi-cho, Toki,
Gifu, 509-52, Japan

phone 81-572-57-5615
fax 81-572-57-5600

YAMADA, Shuichi

Cryogenics and Superconductivity Laboratories
NIFS
322-6, Oroshi-cho, Toki,
Gifu, 509-52 , Japan

phone 81-572-57-4777
fax 81-572-57-7465
yamada@scsun2b.nifs.ac.jp

YAMAMOTO, Junya

NIFS
322-6, Oroshi-cho, Toki,
Gifu, 509-52, Japan

phone 81-572-57-4777
fax 81-572-57-4765

YAMAMOTO, Toru

Machinery & Equipment Dept.
Toshiba Corporation
2-4 Suehiro-cho, Tsurumi-ku,
Yokohama-shi, 230, Japan

phone 81-45-510-5881
fax 81-45-500-1412
tooru@kaiki.keihin.toshiba.co.jp

YAMASHITA, Yasuhiro

Machinery & Equipment Dept.
Toshiba Corporation
2-4 Suehiro-cho, Tsurumi-ku,
Yokohama-shi, 230, Japan

phone 81-45-510-6014
fax 81-45-500-2551
000068682925@tkol.tg-mail.toshiba.co.jp

YANAGI, Hideharu

Advanced Technology Lab.
Mayekawa MFG. Co., Ltd.
2000 Tatsuzawa, Moriya-machi,
Kitasooma-gun, Ibaraki, 302-01, Japan

phone 81-297-48-1364
fax 81-297-48-5170

YANAGI, Nagato

NIFS
322-6, Oroshi-cho, Toki,
Gifu, 509-52 , Japan

phone 81-572-57-4777
fax 81-572-57-4765
yanagi@nifs.ac.jp

ZIEGLER, Bruno O.

Linde Kryotechnik AG
Daettlikonerstr. 5, P.O. Box
CH-8422 Pfungen Switzerland

phone 41-52-304-0512
fax 41-52-304-0550

Publication List of NIFS-PROC Series

NIFS-PROC-1 *U.S.-Japan on Comparison of Theoretical and Experimental Transport in Toroidal Systems Oct. 23-27, 1989*, Mar. 1990

NIFS-PROC-2 *Structures in Confined Plasmas –Proceedings of Workshop of US-Japan Joint Institute for Fusion Theory Program–* ; Mar. 1990

NIFS-PROC-3 *Proceedings of the First International Toki Conference on Plasma Physics and Controlled Nuclear Fusion –Next Generation Experiments in Helical Systems– Dec. 4-7, 1989* Mar. 1990

NIFS-PROC-4 *Plasma Spectroscopy and Atomic Processes –Proceedings of the Workshop at Data & Planning Center in NIFS–*; Sep. 1990

NIFS-PROC-5 *Symposium on Development of Intensed Pulsed Particle Beams and Its Applications February 20 1990*; Oct. 1990

NIFS-PROC-6 *Proceedings of the Second International TOKI Conference on Plasma Physics and Controlled Nuclear Fusion , Nonlinear Phenomena in Fusion Plasmas -Theory and Computer Simulation-;* Apr. 1991

NIFS-PROC-7 *Proceedings of Workshop on Emissions from Heavy Current Carrying High Density Plasma and Diagnostics;* May 1991

NIFS-PROC-8 *Symposium on Development and Applications of Intense Pulsed Particle Beams, December 6 - 7, 1990*; June 1991

NIFS-PROC-9 *X-ray Radiation from Hot Dense Plasmas and Atomic Processes*; Oct. 1991

NIFS-PROC-10 *U.S.-Japan Workshop on "RF Heating and Current Drive in Confinement Systems Tokamaks" Nov. 18-21, 1991*, Jan. 1992

NIFS-PROC-11 *Plasma-Based and Novel Accelerators (Proceedings of Workshop on Plasma-Based and Novel Accelerators) Nagoya, Japan, Dec. 1991*; May 1992

NIFS-PROC-12 *Proceedings of Japan-U.S. Workshop P-196 on High Heat Flux Components and Plasma Surface Interactions for Next Devices*; Mar. 1993

NIFS-PROC-13 『NIFS シンポジウム
「核燃焼プラズマの研究を考える－現状と今後の取り組み方」
1992年7月15日、核融合科学研究所』

1993 年 7 月
NIFS Symposium
"Toward the Research of Fusion Burning Plasmas -Present Status and Future strategy-", 1992 July 15, National Institute for Fusion Science; July 1993 (in Japanese)

NIFS-PROC-14 *Physics and Application of High Density Z-pinches,* July 1993

NIFS-PROC-15 岡本正雄、講義「プラズマ物理の基礎」
平成 5 年度　総合大学院大学
1994 年 2 月
M. Okamoto,
"Lecture Note on the Bases of Plasma Pysics"
Graduate University for Advanced Studies
Feb. 1994 (in Japanese)

NIFS-PROC-16 代表者　河合良信
平成 5 年度　核融合科学研究所共同研究
研究会報告書
「プラズマ中のカオス現象」
"Interdisciplinary Graduate School of Engineering Sciences"
Report of the meeting on Chaotic Phenomena in Plasma
Apr. 1994 (in Japanese)

NIFS-PROC-17 平成 5 年度 NIFS シンオジウム報告書
「核融合炉開発研究のアセスメント」
平成 5 年 11 月 29 日-30 日　於　核融合科学研究所
"Assessment of Fusion Reactor Development"
Proceedings of NIFS Symposium held on November 29-30, 1993 at National Insitute for Fusion Science" Apr. 1994
(in Japanese)

NIFS-PROC-18 *"Physics of High Energy Density Plasmas Produced by Pulsed Power"* June 1994

NIFS-PROC-19 K. Morita, N. Noda (Ed.),
"*Proceedings of 2nd International Workshop on Tritium Effects in Plasma Facing Components at Nagoya University, Symposion Hall, May 19-20, 1994",* Aug. 1994

NIFS-PROC-20 研究代表者　阿部　勝憲　（東北大学・工学部）
所内世話人　野田信明
平成 6 年度　核融合科学研究所共同研究［研究会］
「金属系高熱流束材料の開発と評価」成果報告書
K. Abe and N. Noda (Eds.),
"Research and Development of Metallic Materials for Plasma Facing and High Heat Flux Components" Nov. 1994
(in Japanese)

NIFS-PROC-21 世話人：森田　健治（名大工学部）、金子　敏明（岡山理科大学理学部）
「境界プラズマと炉壁との相互作用に関する基礎過程の研究」
研究会報告
K. Morita (Nagoya Univ.), T. Kaneko (Okayama Univ. Science)(Eds.)
NIFS Joint Meeting "Plasma-Divertor Interactions" and "Fundamentals of Boundary Plasma-Wall Interactions" January 6-7, 1995 National Institute for Fusion Science
Mar. 1995 (in Japanese)

NIFS-PROC-22 代表者　河合　良信
プラズマ中のカオス現象
Y. Kawai,
Report of the Meeting on Chaotic Phenomena in Plasma, 1994
Apr. 1995 (in Japanese)

NIFS-PROC-23 K. Yatsui (Ed.),
New Applications of Pulsed, High-Energy Density Plasmas;
June 1995

NIFS-PROC-24 T. Kuroda and M. Sasao (Eds.),
Proceedings of the Symposium on Negative Ion Sources and Their Applications, NIFS, Dec. 26-27, 1994 , Aug. 1995

NIFS-PROC-25 岡本　正雄
新古典輸送概論（講義録）
M. Okamoto,
An Introduction to the Neoclassical Transport Theory (Lecture note), Nov. 1995 (in Japanese)

NIFS-PROC-26 Shozo Ishii (Ed.),
Physics, Diagnostics, and Application of Pulsed High Energy Density Plasma as an Extreme State; May 1996

NIFS-PROC-27 代表者　河合　良信
プラズマ中のカオスとその周辺非線形現象
Y. Kawai ,
Report of the Meeting on Chaotic Phenomena in Plasmas and Beyond, 1995, Sep. 1996 (in Japanese)

NIFS-PROC-28 T. Mito (Ed.),
Proceedings of the Symposium on Cryogenic Systems for Large Scale Superconducting Applications, Sep. 1996